Mosquito-borne viruses on the rise: the role of vectors, viromes and vaccines S.R. Abbo 2022

Mosquito-borne viruses on the rise

The role of vectors, viromes and vaccines

Sandra R. Abbo

Propositions

1. The Asian bush mosquito poses a risk to public health in the Netherlands. (this thesis)

2. Viral dark matter can be illuminated. (this thesis)

3. Humanity will not beat the dinosaurs by surviving more than 160 million years.

4. Narnaviruses underscore that each rule in biology comes with exceptions.

5. Serving non-vegetarian food at conferences about saving the planet is counteractive.

6. Standardized tests are crucial to determine the future level of secondary education for primary school children.

Propositions belonging to the thesis entitled

Mosquito-borne viruses on the rise
The role of vectors, viromes and vaccines

Sandra R. Abbo
Wageningen, 17 May 2022

Mosquito-borne viruses on the rise

The role of vectors, viromes and vaccines

Sandra R. Abbo

Thesis committee

Promotors

Prof. Dr M.M. van Oers
Professor of Virology
Wageningen University & Research

Dr G.P. Pijlman
Associate professor at the Laboratory of Virology
Wageningen University & Research

Co-promotor

Dr C.J.M. Koenraadt
Associate professor at the Laboratory of Entomology
Wageningen University & Research

Other members

Prof. Dr M. Srinivas, Wageningen University & Research
Prof. Dr J.M. Smit, University Medical Center Groningen
Dr M.A.H. Braks, National Institute for Public Health and the Environment, Bilthoven
Dr L. Delang, Rega Institute for Medical Research, KU Leuven, Belgium

This research was conducted under the auspices of the Graduate School Production Ecology & Resource Conservation.

Mosquito-borne viruses on the rise

The role of vectors, viromes and vaccines

Sandra R. Abbo

Thesis
submitted in fulfilment of the requirements for the degree of doctor
at Wageningen University
by the authority of the Rector Magnificus,
Prof. Dr A.P.J. Mol,
in the presence of the
Thesis Committee appointed by the Academic Board
to be defended in public
on Tuesday 17 May 2022
at 1:30 p.m. in the Omnia Auditorium of Wageningen University.

Sandra R. Abbo
Mosquito-borne viruses on the rise: the role of vectors, viromes and vaccines

224 pages

PhD thesis, Wageningen University, Wageningen, the Netherlands (2022)
With references, summaries in English and Dutch

ISBN 978-94-6447-132-8
DOI https://doi.org/10.18174/565720

Table of contents

Chapter 1 **General introduction**

Sandra R. Abbo[1]

[1]Laboratory of Virology, Wageningen University & Research, Wageningen, the Netherlands

Vector-borne diseases: an increasing public health threat

Vector-borne diseases are caused by bacteria, protozoans, nematodes or viruses, and are responsible for more than 700,000 estimated human deaths each year (1). These illnesses are transmitted to humans by arthropod vectors such as bloodsucking mosquitoes, ticks, triatomine bugs, blackflies and sandflies (2). The most prevalent vector-borne disease is the parasitic infection malaria, which is transmitted to humans by mosquitoes, and accounts for more than 400,000 deaths annually (1). Of the causative agents of vector-borne diseases, viruses carried by arthropods, also referred to as arthropod-borne (arbo)viruses, are also becoming increasingly important. Arboviruses are typically transmitted in enzootic cycles between invertebrate vectors and vertebrate animals. Humans often become infected by arboviruses only accidentally when an infected arthropod vector feeds on a human host. Some arboviruses, however, have adapted to urban transmission cycles in which humans serve as amplifying host. Urban arbovirus transmission can result in major disease outbreaks (3, 4). Arbovirus infections in humans cause febrile illness accompanied by encephalitis, arthritis or haemorrhage, and can ultimately even result in death (4). The mosquito-borne dengue virus (DENV) causes an estimated 40,000 deaths per year and more than 3.9 billion people worldwide are at risk of acquiring a DENV infection (1). Yellow fever virus (YFV), also transmitted by mosquitoes, accounts for an estimated 200,000 cases and 30,000 deaths each year, despite the availability of a highly effective vaccine (5). Other well-known arboviruses of medical importance include Japanese encephalitis virus (JEV), West Nile virus (WNV), chikungunya virus (CHIKV), Rift Valley fever virus, Crimean-Congo haemorrhagic fever virus and tick-borne encephalitis virus (TBEV). Due to climate change and globalisation, which favour the invasion of new areas by arthropod vectors, many medically relevant arboviruses have become increasingly widespread in recent years (6, 7). Moreover, new or previously hidden arboviruses continuously emerge and some of these cause sudden, unexpected disease outbreaks at unprecedented scale.

Emerging arboviruses

Three arboviruses that were discovered halfway the twentieth century but remained obscure until they suddenly emerged about half a century later, are the mosquito-borne Zika virus (ZIKV), Usutu virus (USUV) and Mayaro virus (MAYV). ZIKV, first discovered in Uganda in 1947 (8), emerged in 2007 in the Pacific to suddenly erupt as a large outbreak of human disease in Central and South America in 2015 and 2016 (9). USUV, first isolated in South Africa in 1959, spread throughout Europe in the past two decades, and causes high mortality in birds as well as rare neurological complications in humans (10, 11). The tropical MAYV, often referred to as ‘the next

Zika', was discovered in Trinidad in 1954 (12, 13), induces debilitating arthritic disease in humans and is currently spreading in Central and South America (14).

The rapid emergence and spread of these three previously hidden arboviruses called for an in-depth analysis of the possible mosquito vectors capable of transmitting these viruses, as well as for the development of effective countermeasures to confine and prevent outbreaks of these arboviral diseases worldwide. This thesis focuses on the effectiveness of potential mosquito vectors to transmit ZIKV and USUV in order to assess the risk of viral disease outbreaks. Moreover, as no licensed antivirals or vaccines are available against ZIKV and MAYV, whilst these viruses cause high disease burden in humans, strategies to develop efficacious vaccines against both these viruses are also included.

Zika virus

During a study on YFV in Uganda in 1947, a hitherto unknown virus was discovered in a caged rhesus monkey in the canopy of the Zika forest and named 'Zika virus' (8) (Fig. 1). In 1948, *Aedes africanus* mosquitoes collected in the same forest also tested positive for ZIKV (8). Six years later, in 1954, the first human ZIKV isolate was obtained from a 10-year-old female from Nigeria (9, 15). In tropical Africa, ZIKV was found to be maintained in sylvatic cycles between forest-dwelling mosquitoes and non-human primates (Fig. 2A). Serological surveys in humans during the 1950s suggest that ZIKV was not only endemic in Africa but also circulated in various countries in Asia (9), although no clear evidence of sylvatic cycles in Asia has been presented so far (16). For many decades, ZIKV infections in humans were only reported very sporadically and remained limited to Africa and Asia. However, from 2007 till 2015, ZIKV crossed the Pacific and caused epidemics in Yap State, New Caledonia, the Cook Islands, French Polynesia, Vanuatu, the Solomon Islands, Samoa, Fiji and Easter Island (9). After arrival in Brazil, ZIKV initiated a large outbreak in 2015 (17-19). The virus established urban transmission cycles between humans and yellow fever mosquitoes (*Aedes aegypti*) (Fig. 2A), and quickly spread through Central and South America (20). Historically, ZIKV disease in humans only resulted in a mild and self-limiting febrile illness. However, during the outbreak in the Americas, ZIKV infection led to unexpectedly severe illnesses. The virus was found to be associated with Guillain-Barré syndrome, an auto-immune disease causing muscle weakness and paralysis. The most alarming characteristic of ZIKV disease in the Americas was the ability of the virus to cause severe congenital microcephaly (21). The virus was capable of transmitting vertically from mother to fetus during pregnancy, which could result in congenital malformations and also fetal demise. As very little was known about the virus and its associated diseases, ZIKV was declared a Public Health Emergency of International Concern by the World Health

Organisation in February 2016 (22). Currently, ZIKV is still present in tropical regions around the world (Fig. 1). Strikingly, three cases of locally acquired ZIKV infection were reported in southern France in 2019, which were likely caused by bites from the invasive Asian tiger mosquito *Aedes albopictus* (23), thus illustrating the risk of further spread of ZIKV into temperate areas.

Usutu virus

USUV, named after the Usutu River in Swaziland, was first isolated from *Culex* mosquitoes in South Africa in 1959 (10) (Fig. 1). During the next decades, USUV was occasionally detected in mosquitoes and birds in Africa. A small number of human cases was also reported, but these infections were not associated with severe disease (10, 24). In 2001, USUV emerged in Austria, where a sudden die-off of common blackbirds, great grey owls and barn swallows led to the discovery of USUV as the causative agent (10). Retrospective analysis of archived bird tissues identified the presence of USUV in Italy back in 1996, thus suggesting silent circulation of the virus in Europe for multiple years (25). In the summer of 2016, widespread USUV outbreaks were reported among birds in western European countries including Germany, France, Belgium and the Netherlands (26). USUV is mainly transmitted between avian hosts and mosquitoes (Fig. 2B). Humans and other mammals can also be infected via mosquito bites but are considered dead-end hosts as their low level of viraemia does not allow for virus transmission via a next mosquito bite (27) (Fig. 2B). USUV detection in blood donors is common (28, 29), and most human infections seem asymptomatic or only show benign disease symptoms. Importantly however, in Europe rare but severe neuroinvasive disease in humans has been found associated with USUV infection (11, 27), indicating the need for further studies on the exact role of the virus in human illness (27). In Africa, USUV has mainly been detected in *Culex* mosquito species such as *Culex neavei*, *Culex perfuscus*, *Culex univitattus* and *Culex quinquefasciatus* but also in several other species including *Aedes minutus* and *Coquillettidia azurites (24)*. In Europe, the common house mosquito *Culex pipiens* is considered the main vector for USUV (30, 31), although the potential role of other mosquito species still remains to be investigated.

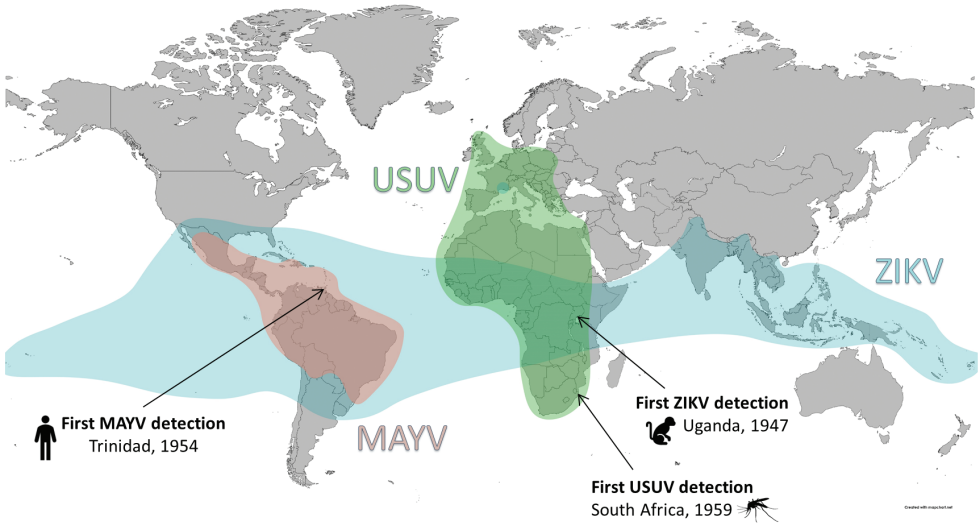

Figure 1. Discovery and geographic distribution of MAYV, ZIKV and USUV. Map created using MapChart.

Mayaro virus

MAYV is transmitted in an enzootic cycle between non-human primates and forest-inhabiting mosquitoes in Central and South America (Fig. 1; Fig. 2A). Humans can also become infected by the virus, which can result in severe, chronic arthritic disease and even death (32, 33). MAYV was first identified in diseased forest workers in Mayaro County, Trinidad in 1954 (12, 13) (Fig. 1). After its initial discovery, the virus has most frequently been observed in Brazil (14), especially around the Amazon basin, where the virus has been detected in humans, monkeys and mosquitoes (34, 35). The forest-dwelling mosquito *Haemagogus janthinomys* is thought to be the main vector of MAYV (35). This likely explains the observation that MAYV infections in humans can usually be linked to residence in tropical rainforests, as was also the case for imported MAYV infections in travellers returning from MAYV endemic areas to the United States (36) and Europe (37, 38). Notably, however, no link to tropical forests was reported when MAYV was detected in an 8-year-old boy with febrile illness in Haiti in 2015 (39). This boy lived in a rural/semi-rural area (39), and moreover, no wild non-human primates are native to Haiti (40). This suggests that MAYV could have been sustained via a transmission cycle involving urban mosquito species and alternative vertebrate reservoir hosts, potentially humans. Mounting evidence has shown that MAYV can be transmitted by the urban mosquito species *Ae. aegypti* and *Ae. albopictus* (41-44), which are the main vectors for ZIKV, CHIKV and DENV worldwide. These findings imply that MAYV could have the

ability to adapt to urban transmission cycles with humans as amplifying host (Fig. 2A), which may potentially result in uncontrollable outbreaks of human disease. It is therefore important to increase awareness for this virus, and to start preparing for possible future outbreaks by the development of effective vaccines (33).

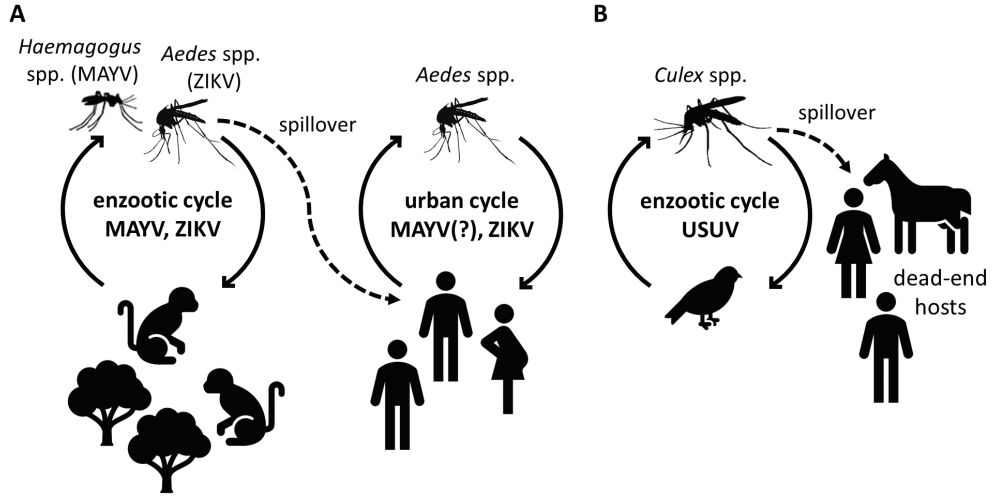

Figure 2. Transmission cycles of MAYV, ZIKV, and USUV. (A) MAYV and ZIKV are transmitted between non-human primates and forest-dwelling mosquitoes in an enzootic jungle cycle. Spillover from the enzootic cycle can occur when an infected mosquito feeds on a human host. Urban cycles can then arise where humans serve as main amplifying host. **(B)** USUV cycles between avian reservoir hosts and mosquitoes of the *Culex* genus. Humans and horses occasionally get infected by USUV but do not develop sufficient viral titers to infect a next blood feeding mosquito and are therefore referred to as dead-end hosts. Mosquito drawings adapted from (45).

Molecular biology of flaviviruses

ZIKV and USUV belong to the genus *Flavivirus* in the family *Flaviviridae*. Other important members of the genus *Flavivirus* are DENV, YFV, JEV, WNV and TBEV. Flaviviruses possess a positive-sense, single-stranded, 5' capped RNA genome of ~11 kilobase pairs (kb) in length. The viral genomic RNA contains a single open reading frame (ORF) that is translated into a polyprotein that is cleaved into three structural and seven non-structural proteins (46) (Fig. 3). The ORF is flanked by highly structured 5' and 3' untranslated regions (UTRs) that have important functions in virus replication (47, 48). The viral RNA is not poly-adenylated. The non-structural proteins (NS1, NS2A, NS2B, NS3, NS4A, NS4B, NS5) are involved in replication of the viral genomic RNA, viral polyprotein processing and evasion of host innate immune responses (46, 49). The structural proteins consist of the capsid (C) protein, the precursor membrane (prM) protein and the envelope (E) glycoprotein, which

together build a spherical virus particle of ~50 nm in diameter (50). The C proteins are on the inside of the virion and form the nucleocapsid that protects the viral genomic RNA, whereas the prM and E proteins face the outside and span the host-derived lipid membrane (Fig. 3).

Entry of flaviviruses in either mosquito or mammalian cells occurs via receptor-mediated endocytosis. The E protein binds a cellular receptor, after which clathrin-dependent endocytosis takes place. After acidification of the endosome, the E proteins on the surface of the virion reorganize from a dimeric, pre-fusion conformation into a trimeric conformation to expose the fusion loops (51). After fusion of the viral membrane with the endosomal membrane, the viral nucleocapsid is released into the cytosol (50, 52, 53). The viral genomic RNA dissociates from the C proteins, and is subsequently translated and replicated. After viral genome replication and translation of viral structural proteins, immature progeny particles arise by enveloping the nucleoprotein complex (consisting of viral RNA and C proteins) into endoplasmic reticulum (ER) membrane containing prM and E proteins. These immature, spiky virions bud into the ER lumen and travel via the trans-Golgi network to the cell surface. During this process, the E proteins undergo pH-dependent conformational changes, which result in rearrangement of the 60 E trimers present on the surface of the virion into 90 E dimers. Subsequently, pr is cleaved off from M by the cellular protease furin. The cleaved pr peptide is dissociated from the M protein when neutral pH is reached in the extracellular milieu. Cleavage and dissociation of pr results in smooth, maturated, infectious particles. When the pr peptide is not cleaved off, the E proteins revert to the immature, spiky, trimeric arrangement during entry into the extracellular environment of neutral pH (54). Interestingly however, complete maturation of all 60 E trimers is not required for infectivity, and partially maturated particles with heterogeneous E protein arrangements and residual pr peptides are frequently observed (50, 55). In this case, the mature part of the virion most likely accommodates cell binding, and processing of residual prM may occur within the cell after entry, ultimately resulting in initiation of membrane fusion (55).

Molecular biology of alphaviruses

MAYV is closely related to CHIKV, and both viruses are members of the genus *Alphavirus* in the family *Togaviridae*. The 5' capped, positive-sense, single-stranded alphavirus RNA genome of ~12 kb in length is poly-adenylated and comprises two ORFs (Fig. 3). The first ORF is translated into a polyprotein that is proteolytically cleaved into four non-structural proteins (nsP1-nsP4), which are responsible for viral RNA replication, modulation of host immune responses, general host shut-off and polyprotein cleavage. The second ORF is translated from a subgenomic messenger RNA and codes for a polyprotein containing the structural proteins: the C protein,

and the envelope proteins E2 and E1 with their associated proteins E3 and 6K (56). In the cytoplasm, the C proteins are autocatalytically cleaved off from the structural polyproteins and form nucleocapsids containing the newly synthesized viral genomic RNA. The remaining envelope protein cassettes (E3-E2-6K-E1) are translocated to the ER, where host-mediated proteolytic cleavage results in E3-E2 (also named precursor E2 (pE2)), 6K and E1. Heterodimers of pE2 and E1 are formed in the ER, and host furin subsequently cleaves E3 from E2 in the Golgi apparatus (57). Mature spikes, consisting of trimeric E2-E1 heterodimers, are displayed at the cell membrane, where they are taken along by the nucleocapsid during budding. The resulting alphavirus virion is ~70 nm in diameter and contains 80 propeller-shaped spikes, which enable cell receptor binding and subsequent receptor-mediated endocytosis. Upon exposure to low pH in the endosome, the E2 and E1 proteins undergo conformational changes leading to E1 homotrimer formation and membrane fusion (58).

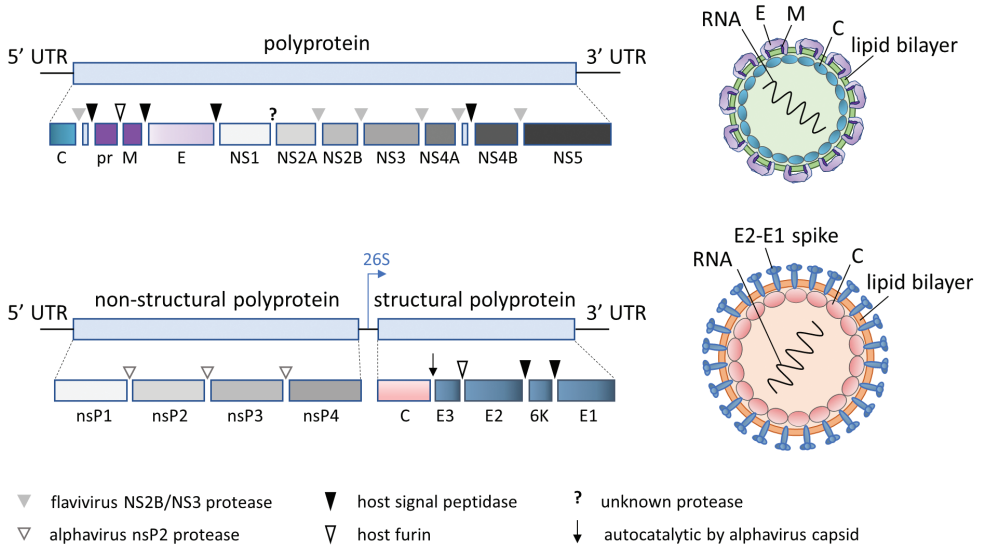

Figure 3. Genome organisation and virion structure of flaviviruses and alphaviruses. Top: schematic representation of flavivirus genome and virion. Flaviviruses produce a single polyprotein containing the structural proteins (C, prM, E) and the non-structural proteins (NS1-NS5). Cleavage sites of host and viral proteases are indicated. Flavivirus particles contain the viral genomic RNA, a host-derived lipid membrane, C proteins, M proteins and E dimers. **Bottom:** schematic representation of alphavirus genome and virion. Alphaviruses code for two polyproteins: a non-structural polyprotein consisting of nsP1-nsP4 and a structural polyprotein consisting of C, E3, E2, 6K and E1. Cleavage sites of host and viral proteases are indicated. The blue arrow shows the location of the 26S promoter responsible for the production of subgenomic messenger RNAs. Alphavirus particles consist of viral genomic RNA, a host-derived lipid membrane, C proteins and trimeric spikes of E2-E1 heterodimers.

Mosquito vectors

Arboviruses actively replicate in their vertebrate hosts and arthropod vectors, and both processes are essential to sustain viral transmission cycles. Mosquito-borne arboviruses such as ZIKV, USUV and MAYV therefore depend on the presence of vertebrate hosts as well as competent mosquito vectors for their emergence and spread. Out of the >3,500 mosquito species described, only a limited number of species are competent vectors for arboviruses, and insight into the ability of mosquito species to successfully transmit arboviruses helps to assess the risk of viral outbreaks among humans and other vertebrates.

An arbovirus is taken up by a female mosquito during ingestion of a blood meal from an infected vertebrate host (Fig. 4.1). The virus travels through the mosquito foregut and ultimately ends up in the midgut (Fig. 4.2). The virus subsequently replicates and spreads within the midgut epithelium and escapes from the midgut epithelial cells (Fig. 4.3) to end up in the body of the mosquito. Next, the virus disseminates through the mosquito body via the haemolymph. It amplifies in secondary tissues, and infects the salivary gland epithelial cells (Fig. 4.4), to finally end up in the salivary glands, where the virus enters the salivary ducts for transmission to the next host (59, 60) (Fig. 4.5). During this entire process, the virus needs to overcome four barriers to enable successful transmission to the next host: the midgut infection barrier, the midgut escape barrier, the salivary gland infection barrier, and the salivary gland escape barrier (59, 61). The effectiveness of a virus to pass these barriers can vary for different arboviruses and mosquito species; it is determined by antiviral immune responses of the mosquito such as RNA interference and by the capacity of the virus to bind to, replicate in and release itself from the cells of the various tissues (59).

Overall, the ability of a mosquito vector to transmit a certain virus is defined as the vector competence (62), which has been studied for many virus-vector combinations (60, 63, 64). The vector competence of a mosquito species is mainly described based on two parameters: the percentage of virus-infected mosquitoes (the infection rate) and the percentage of mosquitoes with virus presence in their saliva (the transmission rate). In addition, a third parameter that is often determined is the percentage of mosquitoes in which virus disseminates from the midgut into other body parts (the dissemination rate).

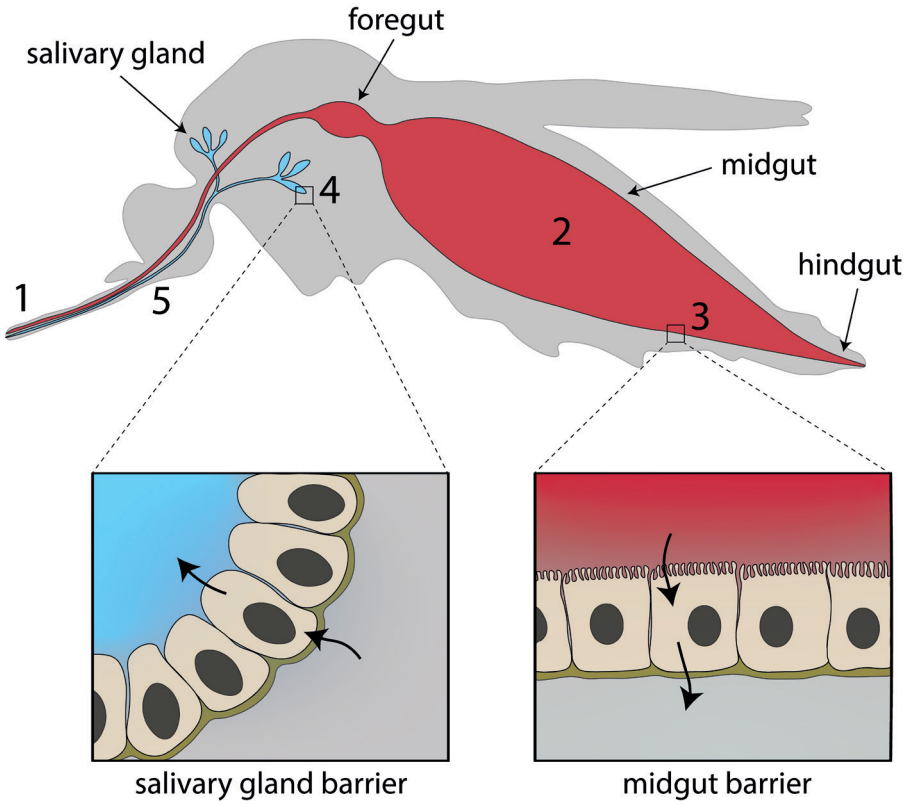

Figure 4. Schematic overview of arbovirus infection and dissemination in the mosquito vector. (1) The virus enters the mosquito via a blood meal from a viraemic vertebrate host. **(2)** The virus ends up in the mosquito midgut. **(3)** After entering the midgut, the virus crosses the midgut barrier to reach the haemocoel. The midgut barrier consists of a layer of midgut epithelial cells with associated antiviral immune responses. **(4)** The virus then disseminates towards the salivary glands, where it needs to cross a layer of salivary glands cells (the salivary gland barrier). **(5)** Virus particles accumulate in the saliva of the mosquito, and will be transmitted during blood feeding on a next vertebrate host.

The risk of mosquito-borne arbovirus transmission in a particular location is however not only determined by the vector competence of the mosquito species present. It also depends on population density, life span, and feeding behaviour of the mosquito vector, as well as the time from virus ingestion to virus transmission (extrinsic incubation period). Together, all these factors contribute to the vectorial capacity of a mosquito population (65).

In recent years, it has become apparent that the mosquito virome (i.e. the total spectrum of viruses present in a mosquito) can also influence arbovirus infection in mosquitoes (66-68). Next-generation sequencing methods have revealed the presence

of highly diverse and abundant virus species associated with mosquitoes (69-71), and the exact composition of these viral communities as well as their potential effects on arbovirus transmission are still largely unknown for most mosquito vector species.

Vaccine development against arboviruses

Besides vector control, vaccination has proven to be an effective strategy to combat arboviral diseases in humans. The live-attenuated 17D vaccine against YFV is considered one of the most effective and safe vaccines produced to date (72). The vaccine provides lifelong immunity after a single shot in most humans, and although it was developed in the 1930s by passaging wild-type YFV in chicken and mouse tissues, the vaccine is still used today to protect humans against YFV infection across the globe. Notwithstanding the long history of the vaccine, the molecular mechanism behind the attenuation of the YFV 17D vaccine strain is still enigmatic (72), but the lack of viral diversity within the YFV 17D vaccine strain compared to the parental wild-type YFV Asibi strain that consists of diverse quasispecies, is thought to play an important role (73). Despite the outstanding success of the YFV 17D vaccine, the development and use of novel live-attenuated vaccines in general have been greatly limited by adverse side-effects in immunocompromised individuals as well as by the risk of reversion to virulence (74). Nowadays, newly developed live-attenuated vaccines are only considered acceptable for human use when the molecular mechanism of attenuation is well understood and the potential for reversion to virulence has been excluded (75).

Two other arbovirus vaccines with proven success for human use are the inactivated vaccines against JEV (76) and TBEV (77). For DENV, however, despite more than 30 years of research, an efficacious and safe vaccine is still lacking. DENV vaccine development has been challenging due to difficulties associated with achieving balanced immune responses against all four serotypes of the virus in a single vaccine and limited understanding of the immune response a vaccine would have to trigger in order to protect from future viral disease (i.e. correlates of protection) (78, 79). Although inactivated, live-attenuated, DNA, and subunit vaccine candidates against DENV have all been developed over the past decennia, only a few live-attenuated DENV vaccines have entered phase III clinical trials (79). One of these, named Dengvaxia, was licensed for human use in 2015 and incorporated into public health programs in the Philippines and Brazil. However, it became clear that the vaccine poses an increased risk of severe DENV illness in persons seronegative for DENV at first vaccination. It is hypothesized that the vaccine acts as a mild, ‘primary’ DENV infection in naive individuals, and that a subsequent ‘secondary’ infection by wild-type DENV can then induce severe illness (80). The underlying molecular mechanisms however are not yet entirely

understood, but antibody-dependent enhancement (ADE) is thought to play a role (81). The theory of ADE states that at specific concentrations, antibodies induced by a primary DENV infection do not protect against subsequent infection with a distinct DENV serotype, but instead facilitate virus entry in target immune cells, in this way resulting in severe DENV disease. Indeed, it has recently been confirmed that humans with pre-existing antibodies against DENV within a certain narrow concentration range have the highest risk of developing severe DENV disease upon subsequent DENV infection (82). These findings could therefore hint towards a possible role of ADE during 'secondary' DENV infections after vaccination, possibly linked to unbalanced vaccine performance against the distinct DENV serotypes (81, 83). The increased risk of developing severe DENV illness for individuals seronegative at first vaccination led to termination of the vaccination program in the Philippines, and a distrust of vaccines in general arose within the country, with the re-emergence of measles virus as a consequence (84). In persons seropositive for DENV at first vaccination, the vaccine however has proven beneficial, and the World Health Organisation currently recommends pre-vaccination screening to ensure that only seropositive individuals will receive the DENV vaccine (79). However, this would require large-scale implementation of diagnostic testing, which will be challenging to achieve, especially in low-income countries where DENV is most prevalent.

For other arboviruses such as CHIKV, MAYV and ZIKV, no vaccines are currently commercially available for human use. In recent decennia, advances in recombinant DNA technology and protein expression methods have opened up new opportunities for vaccine development, and next-generation virus-like particle (VLP) vaccines have proven effective against arboviral diseases during preclinical testing in animals and phase 1 clinical trials in humans. These vaccines possess the effectiveness of an inactivated vaccine combined with the safety profile and ease of upscaling of a subunit vaccine (85) (Fig. 5). VLPs are structurally identical to wild-type virus, but do not contain genetic material (Fig. 5). The repetitive pattern of epitopes present on the surface of the VLPs triggers potent immune responses, whereas the lack of a viral genome excludes replication and thus reversion to virulence. Importantly, in contrast to the production of pathogenic viruses for the formulation of inactivated vaccines, for which facilities with a high biosafety level are needed, VLPs can be produced on a low biosafety level at low cost using similar methods as for subunit vaccines (85). CHIKV VLP vaccines have provided promising results and a CHIKV VLP produced in 293F human cells has recently successfully completed phase 2 clinical trials (86), indicating the potential of VLP vaccines to contribute to the prevention of arboviral disease in humans.

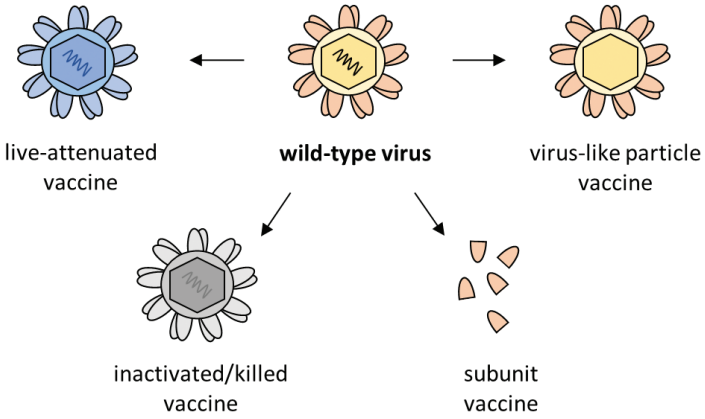

Figure 5. Principle of live-attenuated, inactivated/killed, subunit and virus-like particle vaccines. Live-attenuated vaccines can replicate but show reduced virulence compared to wild-type virus. Inactivated vaccines are produced by treating wild-type virus with heat, chemicals or radiation to destroy the ability to cause disease. Subunit vaccines only consist of a fragment of the virus and are therefore unable to cause disease. Virus-like particles are structurally identical to wild-type virus, but do not contain a viral genome and are therefore unable to replicate.

Outline of the thesis

Large outbreaks of arboviral disease often take the world by surprise. Obscure arboviruses, discovered decades ago, can suddenly spread into new areas leading to a significant public health burden (87). This phenomenon results in an urgent need to study such emerging arboviruses, as very limited knowledge is normally available at the onset of arboviral epidemics. ZIKV, USUV and MAYV are three previously hidden arboviruses that have been on the rise in recent years. This thesis specifically aims to determine the vector competence of Dutch indigenous and exotic mosquito species for ZIKV and USUV to assess the risks of viral outbreaks for the Netherlands. In addition, as ZIKV and MAYV induce severe disease in humans and have the potential to invade new areas whilst no commercial vaccines are available to prevent human disease, this thesis also describes the development and characterization of VLP vaccines against both these viruses.

Studying the arthropod vectors involved in arbovirus transmission helps to direct vector control strategies, but also to assess the risk of viral spread into new regions. When ZIKV emerged into the Americas in 2015, little was known about the diversity of competent mosquito vectors, and large collaborative efforts were established to study the role of a range of mosquito species in ZIKV transmission. Within the multidisciplinary and multinational ZIKAlliance consortium, funded by the European Union, multiple research partners came together to study the vector competence of European mosquito species to assess the risk of mosquito-borne

ZIKV outbreaks for Europe. At the same time, the ZikaRisk program, funded by the Dutch government through ZonMw, focused on the vector competence of Dutch indigenous and invasive mosquito species for ZIKV. In this thesis, we contribute to the objectives of ZIKAlliance and ZikaRisk by investigating whether or not mosquito species present in the Netherlands are capable of transmitting ZIKV.

The invasive Asian bush mosquito *Aedes japonicus* has recently established a large population in Lelystad, the Netherlands (88), and is currently expanding its territories. In **Chapter 2**, we determine the vector competence of this exotic mosquito for ZIKV. Moreover, as USUV emerged in the Netherlands in 2016, we also tested whether *Ae. japonicus* could potentially be involved in USUV transmission.

The common house mosquito *Cx. pipiens*, which is indigenous to the Netherlands and abundantly present throughout the country, can efficiently transmit USUV and WNV (31). However, at the time of ZIKV emergence in the Americas, it was unknown whether this mosquito species could transmit ZIKV. In **Chapter 3**, we therefore assess the ability of *Cx. pipiens* biotypes *pipiens* and *molestus* from the Netherlands to transmit ZIKV.

In the research field of vector competence studies, differences in experimental design among laboratories have proven to complicate meta-analysis of large data sets, and to prevent drawing of firm conclusions in some cases. Many factors within the experimental methods of a vector competence study can vary, and may as such affect the outcome of the study. An important component that is highly variable among vector competence studies is the source of blood used to feed the mosquitoes an artificial infectious blood meal to introduce the virus (89). Little is known about the effect of blood origin on the experimental outcome, and we therefore analyse the effect of blood source on the vector competence of *Cx. pipiens* mosquitoes for USUV in **Chapter 4**.

Since recent studies have shown that the virome present in mosquito vectors has the potential to affect mosquito vector competence for arboviruses, we analyse the virome of *Ae. japonicus* populations from France and the Netherlands using a small RNA-based metagenomic approach in **Chapter 5**.

As ZIKV continues to threaten public health in tropical regions and also has the potential to spread into new areas, a vaccine is needed to prevent infections in humans. In **Chapter 6**, we develop two VLP vaccine variants against ZIKV using insect cells, and test the immunogenicity and protective ability of the candidate vaccines in mice. An arbovirus currently on the rise is MAYV, which is spreading in the Americas. To prepare for future outbreaks of MAYV, we produce and test a VLP vaccine against MAYV in **Chapter 7**.

In Chapter 2 and 3, we observed that both biotypes of *Cx. pipiens* were unable to transmit ZIKV, whereas multiple *Aedes* species readily transmitted

the virus. As the molecular determinants underlying the vector competence of mosquitoes for arboviruses are still largely unknown, we initiate the search for the mechanism(s) underlying the specific restriction of ZIKV in *Cx. pipiens* mosquitoes in **Chapter 8**. Moreover, this chapter also discusses the results from this thesis in view of the existing knowledge. Factors influencing the risk of arboviral outbreaks in the Netherlands are discussed, as well as the consequences of the discovery of mosquito viromes for vector competence studies and arbovirus control strategies. In addition, the feasibility of a ZIKV vaccine is addressed.

Chapter 2 **The invasive Asian bush mosquito *Aedes japonicus* found in the Netherlands can experimentally transmit Zika virus and Usutu virus**

Sandra R. Abbo[1], Tessa M. Visser[2,*], Haidong Wang[1,*], Giel P. Göertz[1], Jelke J. Fros[1], Marleen H.C. Abma-Henkens[1], Corinne Geertsema[1], Chantal B.F. Vogels[2,#a], Marion P.G. Koopmans[3], Chantal B.E.M. Reusken[3,#b], Sonja Hall-Mendelin[4], Roy A. Hall[5], Monique M. van Oers[1], Constantianus J.M. Koenraadt[2], Gorben P. Pijlman[1]

[1]Laboratory of Virology, Wageningen University & Research, Wageningen, the Netherlands
[2]Laboratory of Entomology, Wageningen University & Research, Wageningen, the Netherlands
[3]Department of Viroscience, Erasmus Medical Center, Rotterdam, the Netherlands
[4]Public Health Virology, Forensic and Scientific Services, Department of Health, Coopers Plains, Australia
[5]School of Chemistry and Molecular Biosciences, University of Queensland, St. Lucia, Australia
[#a]Current address: Epidemiology of Microbial Diseases, Yale School of Public Health, New Haven, USA
[#b]Current address: Centre for Infectious Disease Control, National Institute for Public Health and the Environment, Bilthoven, the Netherlands

*These authors contributed equally to this work.

A slightly modified version of this work has been published in PLOS Neglected Tropical Diseases (2020), 14, e0008217.

Abstract

The Asian bush mosquito *Aedes japonicus* is invading Europe and was first discovered in Lelystad, the Netherlands in 2013, where it has established a permanent population. In this study, we investigated the vector competence of *Ae. japonicus* from the Netherlands for the emerging Zika virus (ZIKV) and zoonotic Usutu virus (USUV). ZIKV causes severe congenital microcephaly and Guillain-Barré syndrome in humans. USUV is closely related to West Nile virus, has recently spread throughout Europe and is causing mass mortality of birds. USUV infection in humans can result in clinical manifestations ranging from mild disease to severe neurological impairments. In our study, field-collected *Ae. japonicus* females received an infectious blood meal with ZIKV or USUV by droplet feeding. After 14 days at 28°C, 3% of the ZIKV-blood fed mosquitoes and 13% of the USUV-blood fed mosquitoes showed virus-positive saliva, indicating that *Ae. japonicus* can transmit both viruses. To investigate the effect of the mosquito midgut barrier on virus transmission, female mosquitoes were intrathoracically injected with ZIKV or USUV. Of the injected mosquitoes, 96% (ZIKV) and 88% (USUV) showed virus-positive saliva after 14 days at 28°C. This indicates that ZIKV and USUV can efficiently replicate in *Ae. japonicus* but that a strong midgut barrier is normally restricting virus dissemination. Small RNA deep sequencing of orally infected mosquitoes confirmed active replication of ZIKV and USUV, as demonstrated by potent small interfering RNA responses against both viruses. Additionally, *de novo* small RNA assembly revealed the presence of a novel narnavirus in *Ae. japonicus*. Given that *Ae. japonicus* can experimentally transmit arthropod-borne viruses (arboviruses) like ZIKV and USUV and is currently expanding its territories, we should consider this mosquito as a potential vector for arboviral diseases in Europe.

Introduction

Unexpected infectious disease outbreaks are increasingly common. Many of these are viral diseases transmitted between vertebrate hosts by arthropod vectors such as mosquitoes, ticks and sandflies. The prevalence of these arthropod-borne viruses (arboviruses) is illustrated by numerous recent outbreaks, fuelled by man-made changes to ecological landscapes in which invertebrate vectors and viruses thrive (9). In this study we investigate the risk of transmission of the pathogenic flaviviruses Zika virus (ZIKV) and Usutu virus (USUV) by the invasive Asian bush mosquito *Aedes japonicus.*

ZIKV is a mosquito-borne pathogen that was first discovered in the Zika forest of Uganda in a captive, sentinel rhesus monkey in 1947 and in *Aedes africanus* mosquitoes in 1948. Since then, it spread via Asia and the Pacific islands to densely

populated regions in the Americas (9, 17). Historically, ZIKV was considered to cause only mild disease with headache, fever, rash, joint pain and muscle pain. However, after its introduction in South America and the start of a large outbreak in humans in 2015, the virus generated worldwide attention due to its severe clinical symptoms, fast spread, and long-term persistence. ZIKV infections in humans caused unexpectedly severe diseases including congenital microcephaly and Guillain-Barré syndrome (21). ZIKV quickly spread across Central and South America, where the virus established urban transmission cycles involving humans and mosquitoes. The main mosquito vector for ZIKV is the yellow fever mosquito *Aedes aegypti*, but ZIKV transmission by other *Aedes* species, including the Asian tiger mosquito *Aedes albopictus*, has also been reported (64).

USUV was first isolated from mosquitoes in South Africa in 1959 (10), and emerged on the European continent in Italy in 1996 (25). The first European USUV outbreak became apparent in Austria in 2001 after a sudden mass mortality of birds (10). Since then, widespread USUV outbreaks in birds have been reported in many European countries, including the Netherlands in 2016 (90). USUV is primarily transmitted between birds and mosquitoes. The common house mosquito *Culex pipiens* is thought to be an important vector for USUV in Europe (30, 31). In the past years, an increasing number of clinical human USUV infections has been reported while the presence of USUV RNA in donations from healthy blood donors raised concerns for blood safety (29, 91). Symptoms of USUV infection in humans include fever and rash. In addition, USUV has also been linked to human cases of encephalitis (91), underlining the need for awareness of this virus.

The emergence and spread of arboviruses such as ZIKV and USUV are determined by the presence of mosquitoes that can transmit these viruses from one vertebrate host to the next. *Ae. japonicus*, belonging to the same genus as the ZIKV vector *Ae. aegypti*, has recently received attention due to its potential role in arbovirus transmission (63, 92). This mosquito can transmit multiple flaviviruses of the *Flaviviridae* family including West Nile virus (WNV), Japanese encephalitis virus (JEV), dengue virus and Saint Louis encephalitis virus, but also viruses from other virus families including eastern equine encephalitis virus and chikungunya virus (family *Togaviridae*, genus *Alphavirus*), and La Crosse virus (family *Peribunyaviridae*, genus *Orthobunyavirus*) (92).

Ae. japonicus is native to Korea, Japan and southern China, and was first detected outside this area in the 1990s. Multiple incursions occurred in New Zealand, however the first established populations outside the native area were reported in eastern states of the USA (92). *Ae. japonicus* is currently present in more than 30 states of the USA and, since 2001, also in Canada. In 2000, *Ae. japonicus* was detected for the first time in France, where it was eradicated shortly thereafter (92).

Since this first interception in Europe, permanent *Ae. japonicus* populations have been reported in eleven European countries (93). In the Netherlands, this mosquito was first discovered in 2013, when a female mosquito collected during routine mosquito surveillance in the municipality of Lelystad in 2012, was morphologically and genetically identified as *Ae. japonicus*. After extensive surveillance in Lelystad in 2013, the presence of a large *Ae. japonicus* population was confirmed (88). In 2015, a mosquito control program was implemented in Lelystad in an attempt to reduce the population size (94).

Ae. japonicus is a container-dwelling mosquito, which can colonize diverse natural and man-made habitats. It is an opportunistic feeder; the mosquito feeds on both avian and mammalian hosts, including humans, making it a potential bridge vector for bird-borne zoonotic arboviruses. Importantly, *Ae. japonicus* is tolerant to relatively low temperatures, which allows it to successfully expand to regions with a temperate climate (92).

Considering the invasive nature of *Ae. japonicus* and its ability to transmit many different arboviruses (92), it is of prime importance to study the potential role of this mosquito in the transmission cycles of newly emerging arboviruses such as ZIKV and USUV. In this study, we determined the vector competence of *Ae. japonicus* for ZIKV and USUV. We show that field-collected *Ae. japonicus* mosquitoes from the Netherlands can experimentally transmit ZIKV and USUV, and therefore, that *Ae. japonicus* could be a potential vector for these arboviruses in Europe. We also found that ZIKV and USUV can efficiently replicate in *Ae. japonicus*, but that a mosquito midgut barrier is limiting ZIKV and USUV dissemination. To investigate the effect of mosquito immune responses on virus replication, we studied RNA interference (RNAi) responses against ZIKV and USUV in *Ae. japonicus*. The detection of ZIKV- and USUV-derived small interfering RNAs (siRNAs), which are 21 nucleotide (nt) sized RNA products from viral double-stranded RNA (dsRNA) cleavage by the endoribonuclease Dicer-2 (95, 96), confirmed active replication of both viruses in *Ae. japonicus*. We also investigated whether natural virus infections were present in *Ae. japonicus* since these infections could potentially interfere with the vector competence studies. Using *de novo* small RNA assembly, we discovered a novel narnavirus (family *Narnaviridae*; genus *Narnavirus*) in *Ae. japonicus*.

Methods

Mosquito collection and rearing

Ae. japonicus eggs, larvae and adults were collected in Lelystad, the Netherlands (52°31’42.6”N, 5°28’00.6”E), during August 2017 and July, August and September 2018. Mosquitoes were collected on public and private land. Private land was only accessed when permission was given by the owners to conduct the work on their land.

Eggs were collected with oviposition traps (Fig. 1A). Each trap consisted of a black plastic flower pot (Elho, Tilburg, the Netherlands) which contained approximately 3.5 litre tap water, hay, and a floating Styrofoam block (length: 6 cm, width: 6 cm, height: 1.5 cm). The Styrofoam blocks were collected and replaced every two weeks. Eggs were found on the sides of the Styrofoam blocks, just above the water surface. Larvae were collected from aboveground water reservoirs in local rain barrels using nets (Fig. 1B). Adult females (Fig. 1C) were collected by performing human landing catches. During human landing catches, the collector him-/herself acted as bait for mosquitoes. The collector waited for a mosquito to land on him-/herself, and before the mosquito could bite, the mosquito was captured with the use of a mouth aspirator. During the periods of human landing catches in Lelystad, there were no notifications of arbovirus circulation in the area.

The collected *Ae. japonicus* larvae and eggs were reared in the laboratory at 26°C, 12:12 light:dark period and 70% relative humidity. Eggs on Styrofoam blocks were hatched in tap water with Liquifry No. 1 (Interpet Ltd., Dorking, UK). A maximum number of 100 eggs was added per plastic tray containing 1.5 litre tap water. Larvae were fed with Tetramin baby fish food (Tetra, Melle, Germany) every 2-3 days. Adults were kept in Bugdorm cages (30 x 30 x 30 cm; MegaView Science Co., Ltd., Taichung, Taiwan) and received a 6% glucose solution as a food source. Adult mosquitoes obtained with human landing catches and adults reared from collected larvae and eggs were pooled and used for experiments. Of the adult mosquitoes used for experiments, 60% originated from field-collected eggs, 35% originated from field-collected larvae and 5% was captured by human landing catches.

Ae. aegypti mosquitoes (positive control; Rockefeller strain, obtained from Bayer AG, Monheim, Germany) were reared at 27°C with 12:12 light:dark period and 70% relative humidity. Adults were kept in Bugdorm cages (MegaView Science Co., Ltd.) and were provided with 6% glucose solution as a food source. The colony was supplied with human whole blood (from 10 ml tubes coated with lithium heparin; Sanquin Blood Supply Foundation, Nijmegen, the Netherlands) through Parafilm (Heathrow Scientific, Vernon Hills, IL, USA) by the Hemotek PS5 feeder (Discovery Workshops, Lancashire, UK).

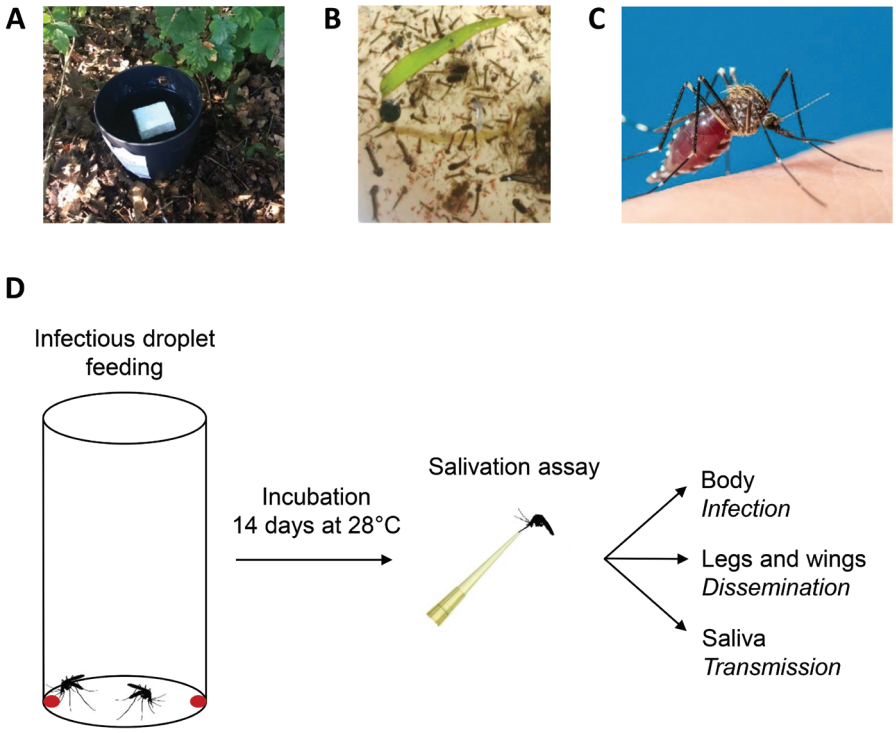

Figure 1. *Ae. japonicus* mosquito collection and the infectious droplet feeding experiment. **(A)** Mosquito eggs were collected using oviposition traps. **(B)** Mosquito larvae were collected from local rain barrels. **(C)** An adult female mosquito, which was captured during human landing catches. **(D)** Infectious droplet feeding and subsequent salivation assays were performed to determine the vector competence of *Ae. japonicus* females for ZIKV and USUV.

Cells and viruses

African green monkey kidney Vero E6 cells were cultured as a monolayer in Dulbecco's Modified Eagle Medium (DMEM; Gibco, Carlsbad, CA, USA) supplemented with 10% fetal bovine serum (FBS; Gibco), penicillin (100 U/ml; Sigma-Aldrich, Saint Louis, MO, USA) and streptomycin (100 µg/ml; Sigma-Aldrich) (P/S). Cells were cultured at 37°C and 5% CO_2. Prior to virus infections, Vero cells were seeded in HEPES-buffered DMEM medium (Gibco) supplemented with 10% FBS and P/S. When mosquito lysate or saliva was added to the cells, the HEPES-buffered DMEM growth medium was also supplemented with fungizone (2.5 µg/ml of amphotericin B and 2.1 µg/ml of sodium deoxycholate; Gibco) and gentamycin (50 µg/ml; Gibco). This medium is hereafter named DMEM HEPES complete.

Asian tiger mosquito (*Ae. albopictus)* C6/36 cells were cultured as a monolayer in Leibovitz L-15 medium (Gibco) supplemented with 10% FBS, 1% nonessential amino acids (Gibco) and 2% tryptose phosphate broth (Gibco). Cells

were cultured at 27°C. When mosquito lysate was added to the cells, the Leibovitz L-15 medium was also supplemented with P/S, fungizone (2.5 µg/ml of amphotericin B and 2.1 µg/ml of sodium deoxycholate) and gentamycin (50 µg/ml). This medium is hereafter named Leibovitz L-15 complete.

All procedures involving infectious virus were executed in the biosafety level 3 facility of Wageningen University & Research. Passage 5 and 6 virus stocks of ZIKV, Suriname 2016 (GenBank accession no. KU937936.1; EVAg Ref-SKU 011V-01621; obtained from Erasmus Medical Center, Rotterdam, the Netherlands), and passage 6 virus stocks of USUV, the Netherlands 2016 (GenBank accession no. MH891847.1; EVAg Ref-SKU 011V-02153; obtained from Erasmus Medical Center), were grown on Vero cells. Virus titers were determined by end point dilution assays (EPDAs) on Vero cells.

Infectious droplet feeding

Ae. japonicus and *Ae. aegypti* females received an infectious blood meal with either ZIKV or USUV by droplet feeding (Fig. 1D) as previously described (97). Groups of 20 mosquitoes were transferred to plastic vials with squeeze foam caps (height of vial: 10 cm, diameter of vial: 5 cm; Carl Roth, Karlsruhe, Germany) and starved for one day. The next day, the mosquitoes were orally infected by feeding on infectious blood droplets. Blood meals were prepared by mixing human blood (Sanquin Blood Supply Foundation), 10% FBS and 1.6% fructose with virus stock to a final virus titer of 1.6×10^7 50% tissue culture infectious dose per millilitre ($TCID_{50}$/ml). Viral titers in the blood meal were afterwards verified by EPDA. For droplet feeding, two 50 µl droplets were provided at the bottom of each plastic vial. Mosquitoes were fed at room temperature with the lights on. After 3-4 hours, the mosquitoes were anesthetized with 100% CO_2 (continuous supply) and the fully engorged females were selected. These mosquitoes were maintained in netted buckets at 28°C and 12:12 light:dark period for 14 days. A 6% glucose solution was provided as a food source.

Intrathoracic injection

Ae. japonicus females received a 69 nl ZIKV injection of 4.4×10^3 $TCID_{50}$ (mosquitoes collected in 2018) or 1.0×10^4 $TCID_{50}$ (mosquitoes collected in 2017), or a 69 nl USUV injection of 3.5×10^3 $TCID_{50}$ in the thorax. *Ae. aegypti* females were injected with a 69 nl ZIKV injection of 1.0×10^4 $TCID_{50}$. Mosquitoes were immobilised with 100% CO_2, and injected using a Drummond Nanoject II Auto-Nanoliter Injector (Drummond Scientific, Broomall, PA, USA) with a glass needle. Injected mosquitoes were kept at 28°C and 12:12 light:dark period for 14 days, and received 6% glucose solution as a food source.

Salivation assay

Fourteen days post infection, mosquitoes were anesthetized using 100% CO_2. The legs and wings of each mosquito were removed, collected and stored at -80°C in 1.5 ml SafeSeal micro tubes (Sarstedt, Nümbrecht, Germany) containing 0.5 mm zirconium oxide beads (Next Advance, Averill Park, NY, USA). The mosquito proboscis was inserted into a 200 µl pipet tip containing 5 µl of a 50% FBS and 25% sugar solution in tap water for 45 min to collect mosquito saliva. Afterwards, the mosquito bodies were stored at -80°C in individual 1.5 ml SafeSeal micro tubes (Sarstedt) containing 0.5 mm zirconium oxide beads (Next Advance). Individual mosquito saliva samples were resuspended in 55 µl DMEM HEPES complete and stored at -80°C.

Infectivity assay

Frozen mosquito body samples and samples containing legs and wings were homogenized in a Bullet Blender Storm (Next Advance) at maximum speed for 2 min. The homogenates were centrifuged in an Eppendorf 5424 centrifuge at 14,500 rpm for 1 min. Afterwards, 100 µl of DMEM HEPES complete was added to each body sample, and 60 µl of DMEM HEPES complete to each legs and wings sample. The homogenates in medium were blended again at maximum speed for 2 min, and centrifuged at 14,500 rpm for 2 min. Thirty µl of each mosquito sample (body, legs and wings, saliva) was added to one well of a 96-well plate containing a monolayer of Vero cells in DMEM HEPES complete. After 2 hours incubation at 37°C, the medium of the cells was replaced by 100 µl fresh DMEM HEPES complete. At 6 days post infection, the wells were scored virus-positive or negative based on cytopathic effect (CPE). The number of virus-positive bodies, legs and wings, or salivas was expressed as a percentage of the total number of analysed mosquitoes.

Virus titration

Virus titers in $TCID_{50}$/ml were determined by EPDA on Vero cells. This assay measured the virus dilution at which the virus caused CPE in 50% of the inoculated cell cultures. Based on this information, the $TCID_{50}$/ml could then be calculated (98). Serial tenfold dilutions (10^{-1} till 10^{-9}) of virus were made in DMEM HEPES complete. Detached Vero cells were diluted to 5 x 10^5 cells/ml and added in a 1:1 ratio to the virus dilutions. Of each suspension with diluted virus and Vero cells, 10 µl was added to six wells of a 60-well MicroWell plate (Nunc, Roskilde, Denmark). After 6 days, wells were scored virus-positive or negative based on CPE.

Immunofluorescence assay

Vero cells were fixed with 4% paraformaldehyde in PBS for 1-4 hours. Cells were washed three times with PBS, permeabilised by incubation in PBS with 0.1% SDS

for 10 min, and washed again three times with PBS. Cells were stained with pan-flavivirus α-E (4G2 (99); mouse monoclonal; dilution 1:50) in PBS with 5% FBS at room temperature for 1 hour. Monolayers were then washed three times with PBS, and stained with goat-α-mouse-Alexa Fluor 488 (dilution 1:2000; Invitrogen, Carlsbad, CA, USA) at 37°C for 1 hour. Cells were washed again three times with PBS and visualised using an Axio Observer Z1m inverted microscope (Zeiss, Jena, Germany) with an X-Cite 120 series lamp.

Detection of viral RNA replicative intermediates

Pools of approximately ten *Ae. japonicus* mosquitoes which were not engorged after a blood meal with ZIKV and incubated at 25°C for 14-29 days, were frozen at -80°C. To prevent potential interference of input virus from the blood meal with the subsequent analysis, mosquitoes were processed at least 14 days post bloodmeal. A total of 28 frozen mosquito pools were blended with 0.5 mm zirconium oxide beads (Next Advance) using a Bullet Blender Storm (Next Advance) at maximum speed for 2 min, and afterwards centrifuged in an Eppendorf 5424 centrifuge at 14,500 rpm for 1 min. One ml of Leibovitz L-15 complete was added to each homogenate. Homogenates were blended again at maximum speed for 2 min, and afterwards centrifuged at 14,500 rpm for 2 min. Next, homogenates were filtered through a 0.2 µm filter (VWR International, Radnor, PA, USA), and collected into fresh tubes. Fifty µl of filtered homogenate was inoculated onto four wells with C6/36 cells in a 96-well plate. After incubation at 27°C for 7 days, the presence of viral RNA replicative intermediates was tested by enzyme-linked immunosorbent assay using monoclonal antibodies to viral dsRNA intermediates in cells (MAVRIC) (100). The newly discovered insect-specific flavivirus Binjari virus (101) was used as a positive control. Briefly, medium was removed and cells were fixed and permeabilised on ice for 10 min using 4% paraformaldehyde and 0.5% Triton X in PBS. After removal of the fixative, cells were dried overnight. The next day, cells were blocked with 1% milk powder in PBS with 0.05% TWEEN 20 (PBS-T) at room temperature for 40 min. Monolayers were stained with α-dsRNA (3G1.1 (100); mouse monoclonal; dilution 1:32) in blocking solution at 37°C for 1 hour. Cells were washed four times with PBS-T, and stained with goat-α-mouse-HRP (dilution 1:2000; Dako, Santa Clara, CA, USA) in blocking solution at 37°C for 1 hour. Afterwards, monolayers were washed six times with PBS-T. To prepare the substrate buffer, 0.2 M Na_2HPO_4 was added to 0.1 M citric acid until a pH of 4.2 was reached. 2,2'-azino-bis(3-ethylbenzothiazoline-6-sulfonic acid) (ABTS) and H_2O_2 were mixed with the beforementioned buffer to reach final molar concentrations of 1 mM and 3 mM respectively, and this buffer with substrate was added to the cells. Cells were incubated at room temperature in the dark. After 1 hour, absorbance was measured at 405 nm using a FLUOstar OPTIMA microplate reader (BMG LABTECH, Ortenberg, Germany).

RNA extraction

Total RNA was extracted from cells using TRIzol reagent (Invitrogen) according to manufacturer's instructions. For RNA isolation from mosquito bodies, the bodies were first blended in the Bullet Blender Storm (Next Advance) using 0.5 mm zirconium oxide beads (Next Advance) at maximum speed for 2 min, and afterwards centrifuged in an Eppendorf 5424 centrifuge at 14,500 rpm for 1 min. 100 µl of DMEM HEPES complete was added to each homogenate. Homogenates were again blended at maximum speed for 2 min. After centrifugation at 14,500 rpm for 2 min, the medium was removed and used for infectivity assays. 1 ml of TRIzol reagent was added to the pellet. Pools of 4-6 mosquito homogenates were collected in 1 ml TRIzol reagent. Mosquito total RNA was isolated as described above. An additional 75% ethanol wash was included. RNA yields were determined using a NanoDrop ND-1000 spectrophotometer.

Reverse transcriptase PCR

Reverse transcriptase PCR (RT-PCR) was performed with 100 ng total RNA per reaction using a 2720 Thermal Cycler (Applied Biosystems, Foster City, CA, USA) and the SuperScript III One-Step RT-PCR System with Platinum *Taq* DNA polymerase (Invitrogen) according to manufacturer's instructions. Primers targeting the region coding for ZIKV non-structural protein 1 (NS1) (forward: 5'-GAGACGAGATGCGGTACAGG-3'; reverse: 5'-CGACCGTCAGTTGAACTCCA-3') and the region encoding USUV non-structural protein 5 (NS5) (forward: 5'-GGCTGTAGAGGACCCTCGG-3'; reverse: 5'-GACTGCCTTTCGCTTTGCCA-3') were used at annealing temperatures of 55°C and 60°C, respectively.

Small RNA deep sequencing

Total RNA was extracted from two pools of *Ae. japonicus* mosquitoes that were found virus-positive after blood droplet feeding with either ZIKV or USUV. The pool with ZIKV-infected mosquitoes consisted of six mosquitoes, whereas the pool with USUV-infected mosquitoes contained four mosquitoes. Twenty µl of mosquito total RNA with a concentration of 250 ng/µl was sent to BGI (Shenzhen, Guangdong, China) for small RNA sequencing as previously described (102). Single-end FASTQ reads were generated with an in-house filtering protocol of BGI. Small RNA sequencing libraries have been uploaded to the NCBI sequence read archive (SRA) under BioProject PRJNA545039.

Small RNA analysis

Small RNA analysis was performed using the Galaxy webserver (103). Small RNA sequences were mapped with Bowtie 2 (104) version 2.3.4.2 allowing 1 mismatch

and a seed length of 28. Reads were mapped against the ZIKV, Suriname 2016 genome (GenBank accession no. KU937936.1) or the USUV, the Netherlands 2016 genome (GenBank accession no. MH891847.1). Since the Netherlands 2016 USUV sequence did not have complete sequences of the untranslated regions (UTRs), it was complemented with the 5' UTR sequence of a closely related USUV isolate from the Netherlands (GenBank accession no. KY128482.1) and the 3' UTR sequence of USUV, Italy 2012 (GenBank accession no. KX816650.1). Next, size distribution profiles of the viral small RNAs were made from all mapped reads. The read counts of the size distribution profiles were normalized as percentages of the total number of reads in the library. The 5'-ends of 21 nt sized virus reads were mapped to the viral genome to generate siRNA genome distributions. The number of 21 nt reads per location on the genome was calculated as a percentage of the total number of reads in the library. The 25-30 nt small RNAs derived from ZIKV or USUV were analysed for PIWI-interacting RNA (piRNA) signatures using Weblogo3. Sequence overlaps between the putative piRNAs were analysed using the small RNA signatures tool (105) version 3.1.0 on the mississippi.snv.jussieu.fr Galaxy server using 25-30 nt small RNAs as input. *De novo* assembly from small RNA reads was done as previously described (102).

Results

Collection of *Ae. japonicus* from Lelystad, the Netherlands in the summers of 2017 and 2018

Ae. japonicus mosquitoes were collected from Lelystad, the Netherlands in the summers of 2017 and 2018. In total, 3,130 mosquito eggs were collected in 2017 and 5,435 eggs in 2018. Human landing catches during two days in July 2018 resulted in a total of 17 captured females. In addition, over 60 *Ae. japonicus* females were collected during two days in August and September 2018. These findings confirm that *Ae. japonicus* mosquitoes from Lelystad have an interest to feed on human hosts.

Ae. japonicus from the Netherlands can experimentally transmit ZIKV and USUV

To investigate the vector competence of *Ae. japonicus* for ZIKV and USUV, female mosquitoes received a blood meal with either ZIKV or USUV by droplet feeding (Fig. 1D). As a positive control, ZIKV-competent *Ae. aegypti* mosquitoes (106) were also offered an infectious blood meal containing ZIKV by droplet feeding. This particular method was used because *Ae. japonicus* did not feed on blood meals offered via the Hemotek system, with either a Parafilm membrane or a pig intestine membrane. The percentage of *Ae. japonicus* females that took up a blood meal varied from 1-33% depending on the experiment, whereas the percentage of *Ae. aegypti* females that

engorged a blood meal during droplet feeding was low with feeding percentages of maximum 5%. After 14 days, the presence of virus in the mosquito body, legs and wings, and saliva was determined by infectivity assays on Vero cells. For a subset of the results, these scores based on CPE of Vero cells were confirmed by RT-PCR using primers targeting NS1 (ZIKV) or NS5 (USUV).

The combined results from five (*Ae. japonicus* with ZIKV), three (*Ae. aegypti* with ZIKV) and three (*Ae. japonicus* with USUV) independent experiments are shown in Figure 2. After a blood meal with ZIKV and subsequent incubation at 28°C for 14 days, 10% of the *Ae. japonicus* mosquitoes had virus-positive bodies, 8% had virus-positive legs and wings, and 3% had detectable ZIKV in their saliva (Fig. 2A). For *Ae. aegypti*, 100% of the bodies and legs and wings were ZIKV-positive, and 83% of the mosquitoes showed ZIKV-positive saliva (Fig. 2B), suggesting that *Ae. aegypti* is a more competent vector for ZIKV compared to *Ae. japonicus*. Of the *Ae. japonicus* mosquitoes orally exposed to USUV, 13% had virus-positive bodies, legs and wings, and salivas (Fig. 2C). These results demonstrate that *Ae. japonicus* is able to experimentally transmit ZIKV and USUV.

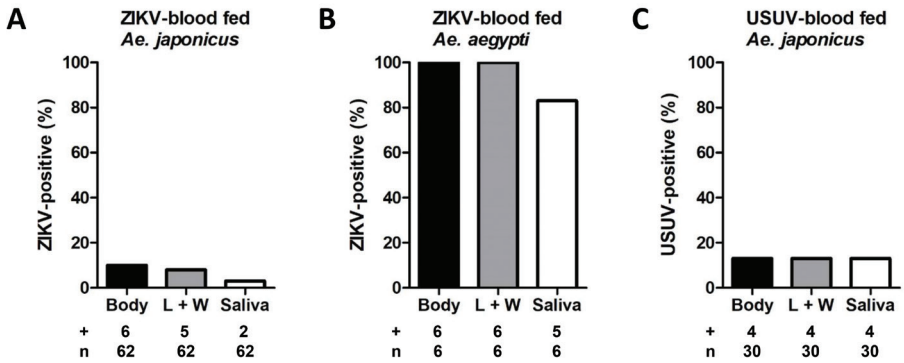

Figure 2. *Ae. japonicus* can experimentally transmit ZIKV and USUV. *Ae. japonicus* mosquitoes received an infectious blood meal with ZIKV or USUV, and were subsequently incubated at 28°C for 14 days. As a positive control, *Ae. aegypti* mosquitoes were offered an infectious blood meal with ZIKV. The percentage of virus-positive bodies, legs and wings (L + W) and salivas out of the total number of mosquitoes tested (number positive (+) / total number tested (n)) was determined for **(A)** ZIKV-blood fed *Ae. japonicus* mosquitoes, **(B)** ZIKV-blood fed *Ae. aegypti* mosquitoes and **(C)** USUV-blood fed *Ae. japonicus* mosquitoes.

Viral titers were determined for the ZIKV- and USUV-positive mosquito bodies, legs and wings, and salivas by EPDA (Fig. 3). For ZIKV-positive *Ae. japonicus* mosquitoes, titers were variable, with median titers of 1.0 x 10^5 $TCID_{50}$/ml in the body, 2.9 x 10^4 $TCID_{50}$/ml in the legs and wings, and 1.5 x 10^3 $TCID_{50}$/ml in the saliva (Fig. 3A). Interestingly, the two *Ae. japonicus* mosquitoes with ZIKV-positive

saliva also showed the highest viral titers in the legs and wings, suggesting that strong virus dissemination is needed for the virus to accumulate in the saliva. ZIKV-positive *Ae. aegypti* mosquitoes showed median viral titers of 6.5 x 10^6 $TCID_{50}$/ml in the body, 6.3 x 10^3 $TCID_{50}$/ml in the legs and wings, and 6.3 x 10^3 $TCID_{50}$/ml in the saliva (Fig. 3B). USUV-positive *Ae. japonicus* mosquitoes showed median viral titers of 2.2 x 10^6 $TCID_{50}$/ml in the body, 7.1 x 10^4 $TCID_{50}$/ml in the legs and wings, and 3.0 x 10^3 $TCID_{50}$/ml in the saliva (Fig. 3C). Thus, *Ae. japonicus* mosquitoes showing fully disseminated ZIKV and USUV infections and also virus-positive salivas were detected.

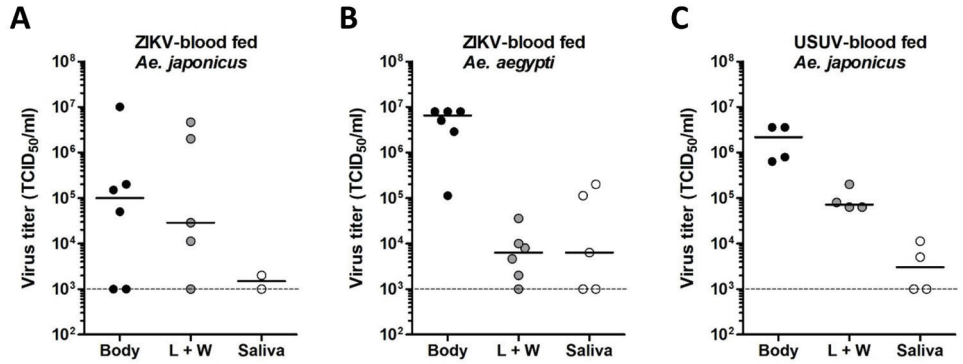

Figure 3. ZIKV and USUV can replicate to high viral titers in *Ae. japonicus* after oral infection. Viral titers of the mosquito bodies, legs and wings (L + W), and salivas were determined by EPDA for **(A)** ZIKV-blood fed *Ae. japonicus* mosquitoes, **(B)** ZIKV-blood fed *Ae. aegypti* mosquitoes, and **(C)** USUV-blood fed *Ae. japonicus* mosquitoes. Data points represent individual mosquitoes infected with either ZIKV or USUV. Lines show the median viral titers. Dashed lines show the detection limit of the EPDA.

No natural flavivirus infections detected in field-collected *Ae. japonicus* mosquitoes

The low ZIKV and USUV transmission reported for *Ae. japonicus* after an infectious blood meal could theoretically be due to a natural flavivirus infection already present in the field-collected mosquitoes that is preventing virus transmission of the newly introduced ZIKV and USUV (67, 107, 108). To exclude potential natural flavivirus infections in *Ae. japonicus* that could have interfered with the vector competence studies, MAVRIC analysis (100) was performed on a total of 228 *Ae. japonicus* females (subdivided over 28 pools). Females that were offered a ZIKV blood meal but did not show engorgement afterwards, were incubated at 25°C for 14-29 days and subsequently analysed using MAVRIC. Out of the 28 pools, 6 were found to be virus-positive, however all of these 6 pools were shown to be RT-PCR positive for ZIKV. This indicated that *Ae. japonicus* mosquitoes could become ZIKV-positive

even though the mosquitoes were not engorged and must have taken up only a very small volume of infectious blood. We conclude that no natural replicating flaviviruses were present in *Ae. japonicus* mosquitoes used in the vector competence assays. Importantly, this experiment also showed that ZIKV can replicate in *Ae. japonicus* at an incubation temperature of 25°C.

A mosquito midgut barrier limits ZIKV and USUV dissemination in *Ae. japonicus*
The vector competence experiments indicated that only 3% of the ZIKV-blood fed *Ae. japonicus* mosquitoes and 13% of the USUV-blood fed *Ae. japonicus* mosquitoes were able to transmit the virus. To investigate whether a mosquito midgut barrier and/or a salivary gland barrier is limiting virus dissemination, *Ae. japonicus* mosquitoes were intrathoracically injected with either ZIKV or USUV to bypass the midgut barrier. *Ae. japonicus* mosquitoes were injected with 4.4 x 10^3 $TCID_{50}$ of ZIKV during four independent experiments or 1.0 x 10^4 $TCID_{50}$ of ZIKV during three independent experiments. As a positive control, *Ae. aegypti* mosquitoes were also injected with ZIKV in three independent experiments. Injections of *Ae. japonicus* with USUV were done in two independent experiments. The injected mosquitoes were incubated at 28°C for 14 days, and afterwards the mosquito bodies, legs and wings, and salivas were checked for the presence of infectious virus by infectivity assays on Vero cells. The inoculated Vero cells were scored based on CPE, and a subset of the results was also validated using RT-PCR with primers against ZIKV NS1 or USUV NS5. In addition, the findings were also confirmed by immunofluorescence assays using 4G2 panflavivirus α-E.

The combined results are shown in Figure 4. Of all injected mosquitoes, 100% showed virus-positive bodies. Moreover, the observed viral dissemination for 100% of the injected *Ae. japonicus* mosquitoes indicated that both ZIKV and USUV can replicate in *Ae. japonicus* and disseminate to the mosquito legs and wings. Very efficient transmission was observed for ZIKV (96% of the analysed mosquitoes showed ZIKV-positive saliva after an injection with 4.4 x 10^3 $TCID_{50}$, and 98% after an injection with 1.0 x 10^4 $TCID_{50}$; Fig. 4A, 4B), indicating that there is no salivary gland barrier against ZIKV present in *Ae. japonicus*. For *Ae. aegypti*, a better salivary gland barrier against ZIKV was observed, as only 72% of the injected mosquitoes showed virus-positive saliva (Fig. 4C), which is in agreement with our earlier studies (106). Additionally, 88% of the USUV-injected *Ae. japonicus* showed USUV accumulation in the saliva (Fig. 4D), which indicated that USUV, like ZIKV, does not encounter a strong salivary gland barrier in *Ae. japonicus*. We thus found that both ZIKV and USUV can efficiently replicate in *Ae. japonicus* after intrathoracic injection. However, only a low percentage of the *Ae. japonicus* mosquitoes became virus-positive after an infectious blood meal with high titer, which shows the

existence of a midgut barrier that strongly limits virus dissemination through the mosquito and lowers virus transmission as a result.

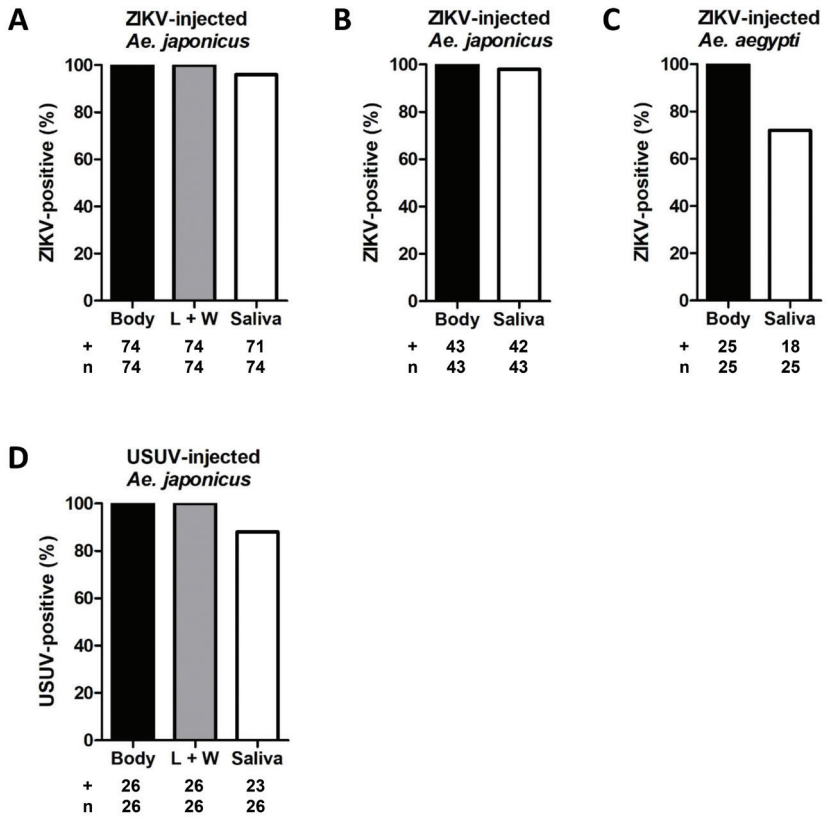

Figure 4. After intrathoracic injection, ZIKV and USUV can fully disseminate in *Ae. japonicus*. *Ae. japonicus* mosquitoes were intrathoracically injected with ZIKV or USUV. *Ae. aegypti* mosquitoes, injected with ZIKV, were included as a positive control. After injection, mosquitoes were incubated at 28°C for 14 days. The percentage of virus-positive bodies, legs and wings (L + W) and salivas out of the total number of mosquitoes tested (number positive (+) / total number tested (n)) was determined for **(A)** *Ae. japonicus* mosquitoes injected with 4.4 x 10^3 $TCID_{50}$ of ZIKV, **(B)** *Ae. japonicus* mosquitoes injected with 1.0 x 10^4 $TCID_{50}$ of ZIKV, **(C)** *Ae. aegypti* mosquitoes injected with ZIKV and **(D)** *Ae. japonicus* mosquitoes injected with USUV.

Viral titers were measured for the ZIKV- and USUV-injected mosquitoes by EPDA (Fig. 5). *Ae. japonicus* mosquitoes injected with 4.4 x 10^3 $TCID_{50}$ of ZIKV reached median viral titers of 9.6 x 10^5 $TCID_{50}$/ml in the body, 4.8 x 10^6 $TCID_{50}$/ml in the legs and wings, and 2.0 x 10^3 $TCID_{50}$/ml in the saliva (Fig. 5A). *Ae. japonicus* mosquitoes injected with 1.0 x 10^4 $TCID_{50}$ of ZIKV showed median viral titers of 1.1 x 10^6 $TCID_{50}$/ml in the body, and 2.9 x 10^3 $TCID_{50}$/ml in the saliva (Fig. 5B). The

median viral titers for ZIKV-injected *Ae. aegypti* mosquitoes were 6.3 x 10^6 $TCID_{50}$/ml in the body, and below the detection limit of 1.0 x 10^3 $TCID_{50}$/ml in the saliva (Fig. 5C). USUV-injected *Ae. japonicus* mosquitoes showed median viral titers of 5.5 x 10^6 $TCID_{50}$/ml in the body, 6.3 x 10^4 $TCID_{50}$/ml in the legs and wings, and 2.3 x 10^3 $TCID_{50}$/ml in the saliva (Fig. 5D). The results show that high median viral titers in bodies and legs and wings were found for both ZIKV- and USUV-injected *Ae. japonicus* mosquitoes. This indicated that both ZIKV and USUV can efficiently replicate in *Ae. japonicus*, which is also supported by the fact that both viruses can easily cross the mosquito salivary gland barrier and induce high viral titers in the saliva.

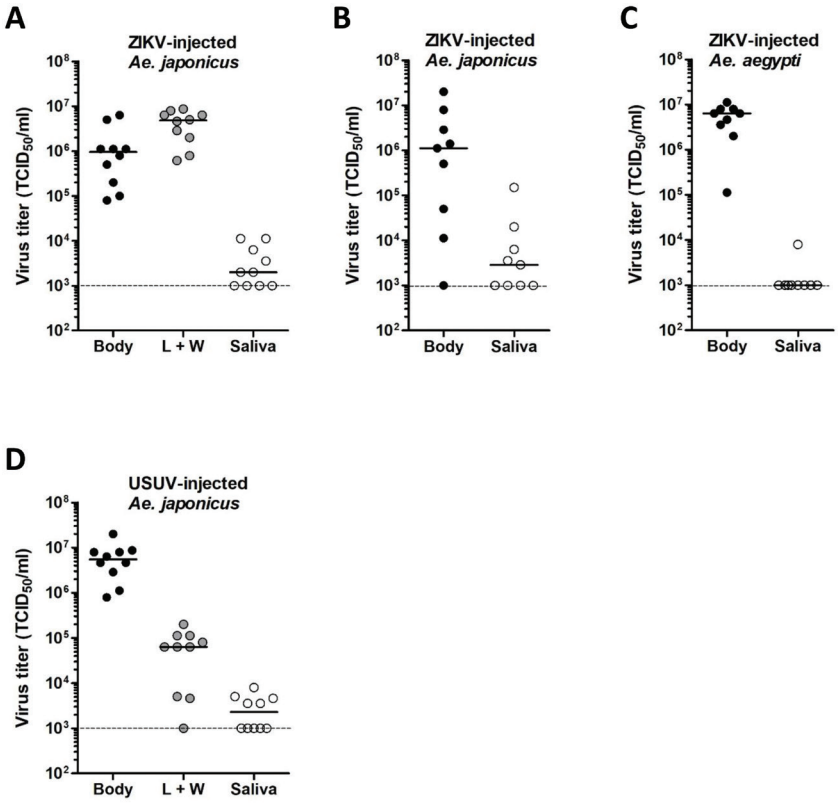

Figure 5. ZIKV and USUV can replicate to high viral titers in *Ae. japonicus* after intrathoracic injection. Viral titers of the mosquito bodies, legs and wings (L + W), and salivas were determined by EPDA for **(A)** *Ae. japonicus* mosquitoes injected with 4.4 x 10^3 $TCID_{50}$ of ZIKV, **(B)** *Ae. japonicus* mosquitoes injected with 1.0 x 10^4 $TCID_{50}$ of ZIKV, **(C)** *Ae. aegypti* mosquitoes injected with ZIKV and **(D)** *Ae. japonicus* mosquitoes injected with USUV. Data points represent individual mosquitoes intrathoracically injected with either ZIKV or USUV. Lines indicate the median viral titers. Dashed lines show the detection limit of the EPDA.

ZIKV and USUV induce strong viral siRNA responses in *Ae. japonicus*

Viral infection in insects induces antiviral responses, of which RNAi is considered to be an important pathway (95). During flavivirus replication in mosquitoes, a viral dsRNA intermediate is formed in viral replication complexes, which is recognized and processed by the RNAi machinery. The endoribonuclease Dicer-2 recognizes and cleaves dsRNA into 21 nt siRNAs (95, 96). In addition to viral siRNAs, the production of 25-30 nt viral piRNAs has been reported for arbovirus-infected *Aedes* species (109, 110). To the best of our knowledge, the small RNA responses of *Ae. japonicus* against arboviral infections have never been studied. Detailed analysis of the small RNA deep sequencing libraries derived from *Ae. japonicus* mosquitoes revealed a high abundance of 21 nt small RNA reads mapping to both the positive-sense and negative-sense viral RNA strands of ZIKV and USUV, which indicates strong small RNA responses against both viruses (Fig. 6). This further confirmed active replication of ZIKV and USUV in *Ae. japonicus*. USUV-infected mosquitoes showed stronger RNAi responses compared to ZIKV-infected mosquitoes, because a higher percentage of the total number of reads mapped to the USUV genome compared to the percentage of the total number of reads that mapped to the ZIKV genome (Fig. 6A, 6B).

For both ZIKV and USUV, 21 nt viral-derived siRNAs were the most abundant group of viral small RNAs (Fig. 6A, 6B). A shoulder of 25-30 nt sized viral small RNAs was also observed, which is in the size range of piRNAs. These small RNAs were analysed for the presence of the characteristic piRNA signature (10 nt overlap and 1U/10A sequence bias) caused by the ping-pong piRNA amplification cycle (109, 110). No such signatures were identified. For ZIKV and USUV, 21 nt viral siRNAs mapped across the entire viral RNA genome on both the positive and negative strand (Fig. 6C, 6D), with a major hot spot of ZIKV siRNAs at the 3' stem-loop (SL) of the ZIKV 3' UTR. Thus, the ZIKV 3' SL is preferentially processed by the RNAi machinery into 21 nt siRNAs.

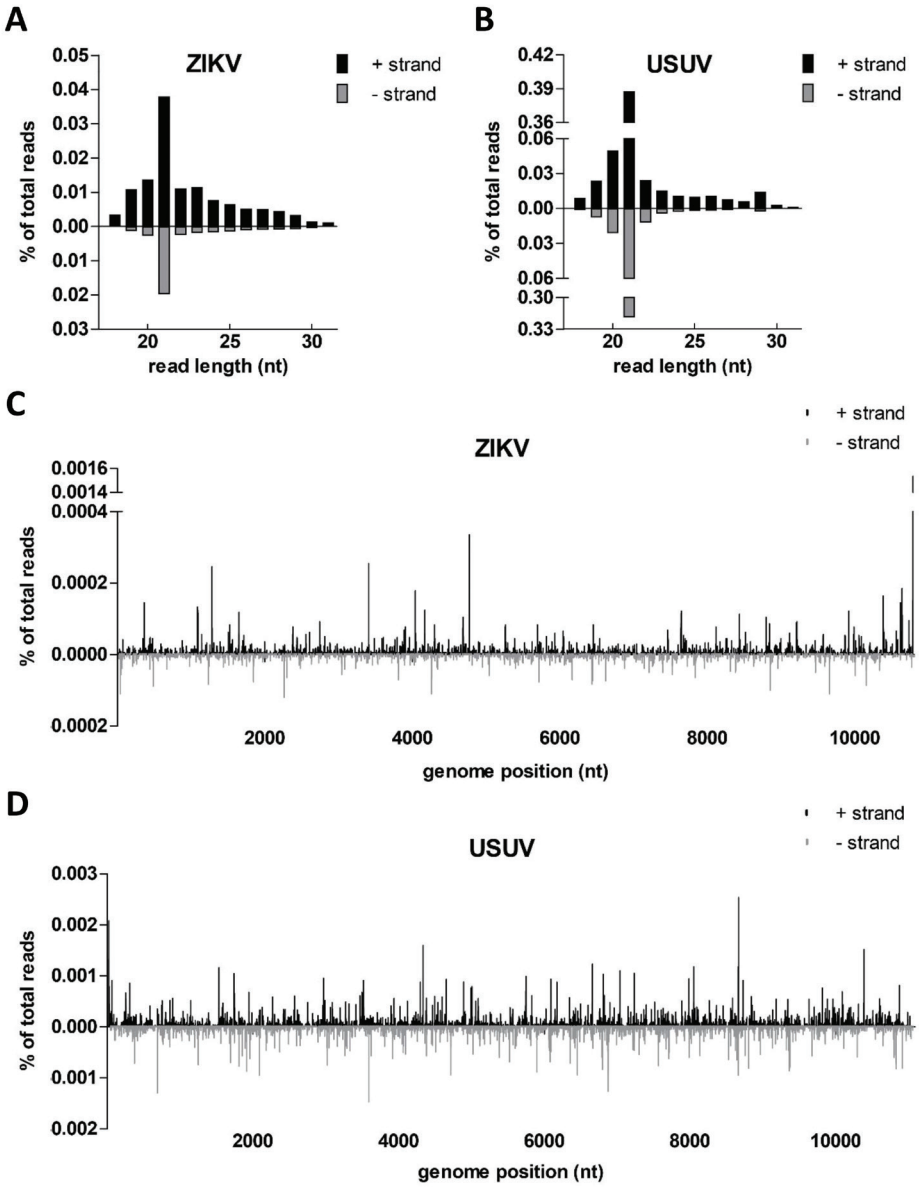

Figure 6. Small RNA sequencing revealed 21 nt siRNA responses against ZIKV and USUV in *Ae. japonicus*. The size distribution profiles of small RNAs that mapped to the genomes of **(A)** ZIKV or **(B)** USUV are indicated. The distribution of 21 nt **(C)** ZIKV-derived or **(D)** USUV-derived siRNAs across the viral genome is shown. Viral reads mapping to the positive-sense viral RNA strand are depicted above the X-axes and presented in black; viral reads mapping to the negative-sense viral RNA strand are depicted below the X-axes and presented in grey. The viral small RNA read counts were normalized against the total library of small RNA reads and are presented as a percentage of the total number of small RNAs in the library.

Discovery of a novel narnavirus in *Ae. japonicus*

De novo assembly of small RNA reads revealed the presence of a novel narnavirus (family *Narnaviridae*; genus *Narnavirus*) in *Ae. japonicus*. This narnavirus was detected in both pools of *Ae. japonicus* mosquitoes which were sent for small RNA sequencing, and was named *Ae. japonicus* narnavirus 1 (AejapNV1). The genome sequence of AejapNV1 was uploaded to GenBank (accession no. MK984721). The ~3 kilobase pair genome of AejapNV1 contains two open reading frames (ORFs). The first ORF, present on the positive-sense viral RNA strand, encodes an RNA-dependent RNA polymerase (RdRp). The second ORF, present on the negative-sense viral RNA strand, codes for a hypothetical protein with no known homology.

Discussion

Ae. japonicus is an invasive mosquito species and a potential vector for a panel of arboviruses, including JEV and WNV (92, 97, 111, 112). Here we show for the first time that field-collected *Ae. japonicus* mosquitoes from the Netherlands can experimentally transmit ZIKV and USUV. So far, no ZIKV- or USUV-positive *Ae. japonicus* mosquitoes have been found in the Netherlands, but a pool of *Ae. japonicus* mosquitoes with disseminated USUV infection has recently been collected from Graz in Austria (113). This finding could suggest a potential role of *Ae. japonicus* in the transmission cycle of USUV in Europe. Currently, there is no evidence of ZIKV transmission by *Ae. japonicus* in the field. Nonetheless, 10% of the *Ae. japonicus* mosquitoes could transmit ZIKV in a laboratory study with *Ae. japonicus* mosquitoes from south-western Germany at 27°C (97), which was slightly higher than the 3% found in our study. Furthermore, the infection rates greatly differed between the German *Ae. japonicus* mosquitoes (67%) (97) and the *Ae. japonicus* mosquitoes from the Netherlands (10%). This might be explained by technical differences between both studies. In the study with *Ae. japonicus* mosquitoes from Germany, the presence of ZIKV in mosquito bodies was determined by quantitative real-time RT-PCR directly on mosquito bodies (97), whereas in our study, mosquito bodies were only considered ZIKV-positive when the inoculation of supernatant from blended bodies on Vero cells resulted in CPE. A real-time RT-PCR assay cannot distinguish viral RNA from infectious virus particles, whereas infectivity assays on Vero cells solely detect infectious virus. The higher infection rate reported for *Ae. japonicus* from Germany could therefore be explained by the (perhaps more sensitive) detection of viral RNA. But it could also be that the RT-PCR detects residual input RNA from the blood meal. The percentage of mosquitoes showing virus dissemination out of the total number of mosquitoes tested was similar for *Ae. japonicus* from Germany (10%) (97) and the Netherlands (8%), which might indeed indicate equal percentages of mosquito bodies with infectious, replicating virus.

RNAi is considered an essential antiviral defence mechanism in insects, including mosquitoes. Here we show that *Ae. japonicus* induces strong small RNA responses against both ZIKV and USUV, with small RNA reads mapping to both the positive and negative viral RNA strands of ZIKV and USUV. RNAi responses against USUV were stronger than the RNAi responses against ZIKV. This could be explained by the fact that the median viral body titer of the analysed USUV-infected mosquitoes was approximately 20-fold higher compared to the median viral body titer of the ZIKV-infected mosquitoes (Fig. 3A, 3C). For ZIKV, only two out of six mosquitoes within the analysed pool showed fully disseminated viral infection including virus accumulation in the mosquito saliva, whereas for the USUV-infected mosquitoes, all four analysed mosquitoes had fully disseminated infections including the presence of virus in the saliva. Thus, a better disseminated USUV infection in *Ae. japonicus* mosquitoes is associated with a stronger RNAi response, probably because there is a higher amount of dsRNA template available for processing into viral siRNAs by Dicer-2.

Of the small RNAs derived from ZIKV or USUV in *Ae. japonicus*, 21 nt siRNAs were most abundant, yet viral piRNAs with characteristic ping-pong signatures were not identified, thus suggesting that siRNA-mediated activity is the major RNAi pathway against these viruses in *Ae. japonicus*. Likewise, 21 nt viral-derived siRNAs were the major group of small RNAs present in ZIKV-infected *Ae. aegypti* and USUV-infected *Cx. pipiens* but no piRNAs were detected in these mosquito species (31, 114). In our study, we identified a major hotspot of 21 nt small RNAs at the 3' UTR of the positive viral RNA strand of ZIKV. This peak, present at the 3' SL, was only observed for ZIKV-infected *Ae. japonicus* mosquitoes but not for USUV-infected *Ae. japonicus* mosquitoes. The position of the peak and the length of the small RNA are identical to a previously described microRNA-like small RNA which is produced from the 3' SL of the 3' UTR of WNV (115). This viral small RNA, named KUN-miR-1, is known to facilitate virus replication in mosquito cells (115). Moreover, a similar viral small RNA hotspot has also been found during WNV infection in *Cx. pipiens* mosquitoes (116). However, an earlier study with a different *Cx. pipiens* colony did not detect this hotspot in USUV-infected mosquitoes (31). This viral small RNA hotspot at the 3' SL of the 3' UTR thus only seems to be present for certain combinations of flaviviruses and mosquito species.

Interestingly, we found AejapNV1 in our *Ae. japonicus* mosquitoes. Classical members of the *Narnavirus* genus infect yeasts and oomycetes and are historically known to only code for an RdRp on the positive-sense viral RNA strand (117). AejapNV1, however, contains a second ORF on the negative-sense viral RNA strand, which encodes a protein of no known homology. This ambisense coding strategy has also been found for other narnaviruses discovered in mosquitoes (69,

118) and for a narnavirus detected in mosquito *Culex tarsalis* CT cells (102), which indicates the existence of a novel group of narnaviruses containing a second ORF. The effect of narnavirus persistent infections on the vector competence of mosquitoes for arboviral diseases such as ZIKV and USUV is currently unknown and remains to be investigated.

In Europe, *Cx. pipiens* is considered the main vector for USUV (30). Out of the *Cx. pipiens* mosquitoes that ingested a blood meal containing USUV, 69% was reported to experimentally transmit USUV (31), which is considerably higher than the percentage of blood fed *Ae. japonicus* mosquitoes that transmitted USUV in our study. Given that *Cx. pipiens* is a competent vector for USUV and that this mosquito is abundantly present in Europe, it likely plays a more important role in USUV outbreaks in Europe than *Ae. japonicus*. In addition, USUV-positive *Ae. albopictus* mosquitoes have also been detected in Europe (30), however the exact role of this invasive mosquito in USUV transmission needs to be studied in more detail.

ZIKV transmission by the primary vector *Ae. aegypti* and the secondary vector *Ae. albopictus* was found to be more efficient than ZIKV transmission by *Ae. japonicus* in our study (106, 119). For *Ae. aegypti* Rockefeller, only a minor mosquito salivary gland barrier is restricting ZIKV transmission whereas a midgut barrier was found to be absent (106). In our study, we found a strong midgut barrier restricting virus dissemination in *Ae. japonicus*, suggesting that there is an intrinsic difference in the midgut of *Ae. aegypti* and *Ae. japonicus*, which strongly affects the vector competence of these mosquitoes for ZIKV. Importantly, the high prevalence of *Ae. albopictus* in Mediterranean Europe (120) received recent attention due to the recognition of three locally acquired human ZIKV cases in the south of France during the summer of 2019, which were likely caused by human-to-human transmission via *Ae. albopictus* mosquitoes (121-123). The fact that *Ae. albopictus* seems to be a competent vector for ZIKV in France, underlines the need to study in more detail whether *Ae. japonicus* could also initiate ZIKV transmission in the Netherlands. In general, arbovirus outbreaks are notoriously hard to predict and not all parameters contributing to the efficiency of a certain mosquito population to transmit an arbovirus are always known in sufficient detail. The efficiency of a vector to transmit a pathogen in the field is often referred to as the vectorial capacity. Besides vector competence, the vectorial capacity of a mosquito species also depends on mosquito population density, mosquito survival, host preference, feeding frequency and behaviour of the mosquito, and environmental conditions (60). A thorough understanding of all these contributing factors is needed to assess the risk of transmission of arboviruses such as ZIKV and USUV by *Ae. japonicus* in the field.

Infectious droplet feeding has proven to be an efficient method to provide a blood meal to field-collected *Ae. japonicus* mosquitoes that do not feed on the

conventional Hemotek feeding system. Inside a vertebrate host or the artificial Hemotek, the blood with virus is usually kept at a temperature ranging from 37°C to 40°C, whereas during infectious droplet feeding, the blood droplets with virus are kept at room temperature. The temperature difference between these ways of infectious blood feeding could potentially have an effect on virus entry in the mosquito midgut cells. Currently, there is no indication that infectious droplet feeding at room temperature positively or negatively influences the vector competence of mosquitoes for ZIKV. Infection and transmission rates of *Ae. aegypti* mosquitoes in our study were similar as reported in previous experiments where *Ae. aegypti* mosquitoes were provided with an infectious blood meal using a Hemotek feeding system (106). Another caveat of our study is that artificial feeding on infectious blood droplets might not reflect feeding on infectious hosts under natural conditions. Artificial feeding of *Ae. aegypti* mosquitoes with ZIKV resulted in lower transmission potential compared to *Ae. aegypti* mosquitoes blood fed on viraemic mice (124). Moreover, it has been suggested that ZIKV transmission by mosquitoes is enhanced after engorgement of a second blood meal (125). *Ae. japonicus* could therefore be a more competent vector for ZIKV and USUV when feeding under natural conditions in the field instead of receiving an artificial infectious blood meal by droplet feeding. Thus, it remains challenging to determine the real risk of ZIKV and USUV transmission by *Ae. japonicus*.

Environmental conditions such as temperature are important determinants of arbovirus transmission by mosquitoes (126, 127). In this study, we found transmission of ZIKV by *Ae. japonicus* at 28°C. Moreover, we also found replicating ZIKV in the bodies of *Ae. japonicus* after oral exposure of these mosquitoes to ZIKV and subsequent incubation at 25°C. This indicates that ZIKV can also infect *Ae. japonicus* at temperatures lower than 28°C, which supports previous findings where after incubation as low as 21°C, the bodies of *Ae. japonicus* mosquitoes tested ZIKV-positive (97). In the same study, ZIKV dissemination but not transmission was reported for mosquitoes kept at 24°C (97). Follow-up studies with high numbers of mosquitoes at temperatures lower than 28°C could give more insight into the true risk of ZIKV and USUV transmission by *Ae. japonicus* in north-western European countries such as the Netherlands, as average summer temperatures in these areas are usually around 18°C (128).

At the moment, we do not have strong indications that *Ae. japonicus* represents a major risk for public health in Europe, as widespread *Ae. japonicus* populations are currently present in e.g. Germany and Austria, and to the best of our knowledge, no arboviral outbreaks have so far been linked to the presence of *Ae. japonicus* in these areas. Nevertheless, we found that *Ae. japonicus* can experimentally transmit ZIKV and USUV at 28°C. This implies that in the case of large, expanding populations of

Ae. japonicus and high environmental temperatures, this mosquito could potentially be involved in future arboviral outbreaks. Thus, we need to consider *Ae. japonicus* as a potential vector for ZIKV and USUV in Europe.

Acknowledgements

The authors thank Linda van Oosten, Marjolein Dijkema, Tessy Hick, Jeroen Kortekaas, Marieke de Swart, Julian Bakker, Tim Möhlmann, Bob Hendrikx, Steffanie Teekema, Frans Jacobs, Anton Bekendam and Arjan Stroo for their help during *Ae. japonicus* collection in the field, Esther Schnettler and Mayke Leggewie for sharing details on the methodology of artificial feeding of mosquitoes via blood droplets, Jody Hobson-Peters for providing Binjari virus and the antibodies 4G2 and 3G1.1, Barry Rockx for his continued interest in the project, and Hans Smid for taking macro photographs of *Ae. japonicus*. This work was financially supported by ZonMw (project: ZikaRisk "Risk of Zika virus introductions for the Netherlands", project no.: 522003001) and by the European Union's Horizon 2020 Research and Innovation Programme through the ZIKAlliance project (grant agreement no. 734548). Roy Hall was supported by a PE&RC Visiting Scientist grant.

Chapter 3 **Forced Zika virus infection of *Culex pipiens* leads to limited virus accumulation in mosquito saliva**

Sandra R. Abbo[1], Chantal B.F. Vogels[2,#], Tessa M. Visser[2], Corinne Geertsema[1], Monique M. van Oers[1], Constantianus J.M. Koenraadt[2], Gorben P. Pijlman[1]

[1]Laboratory of Virology, Wageningen University & Research, Wageningen, the Netherlands
[2]Laboratory of Entomology, Wageningen University & Research, Wageningen, the Netherlands
[#]Current address: Epidemiology of Microbial Diseases, Yale School of Public Health, New Haven, USA

Published in Viruses (2020), 12, 659.

Abstract

Zika virus (ZIKV) is a mosquito-borne pathogen that caused a large outbreak in the Americas in 2015 and 2016. The virus is currently present in tropical areas around the globe, and can cause severe disease in humans including Guillain-Barré syndrome and congenital microcephaly. The tropical yellow fever mosquito *Aedes aegypti* is the main vector in urban transmission cycles of ZIKV. The discovery of ZIKV in wild-caught *Culex* mosquitoes and the ability of *Culex quinquefasciatus* mosquitoes to transmit ZIKV in the laboratory raised the question whether the common house mosquito *Culex pipiens*, which is abundantly present in temperate regions in North America, Asia and Europe, could also be involved in ZIKV transmission. In this study, we investigated the vector competence of *Cx. pipiens* (biotypes *molestus* and *pipiens*) from the Netherlands for ZIKV, using Usutu virus as a control. After an infectious blood meal containing ZIKV, none of the tested mosquitoes accumulated ZIKV in the saliva, although 2% of the *Cx. pipiens pipiens* mosquitoes showed ZIKV-positive bodies. To test the barrier function of the mosquito midgut on virus transmission, ZIKV was forced into *Cx. pipiens* mosquitoes by intrathoracic injection, resulting in 74% (*molestus*) and 78% (*pipiens*) ZIKV-positive bodies. Strikingly, 14% (*molestus*) and 7% (*pipiens*) of the tested mosquitoes accumulated ZIKV in the saliva after injection. This is the first demonstration of ZIKV accumulation in the saliva of *Cx. pipiens* upon forced infection. Nevertheless, a strong midgut barrier restricted virus dissemination in the mosquito after oral exposure and we therefore consider *Cx. pipiens* as a highly inefficient vector for ZIKV.

Introduction

Mosquito-borne viruses are a severe threat to human health (4, 9). Climate change, increased global trade and travel, and the ability of viruses to adapt to new vectors and hosts contribute to the geographic expansion of these mosquito-borne pathogens (4, 9). Zika virus (ZIKV; family *Flaviviridae*, genus *Flavivirus*) was first isolated from a caged, sentinel rhesus monkey in the canopy of the Zika forest in Uganda in 1947 (8, 9). In 1948, the virus was discovered in *Aedes africanus* mosquitoes in the same forest (8, 9), and in 1954 the first human ZIKV isolate was obtained from a Nigerian female (9, 15). Much later, the virus re-emerged in Asia and the Pacific islands, and started a large outbreak in humans in Brazil in 2015 (9, 17, 18). Historically, ZIKV infection results in a mild, self-limiting febrile illness for an estimated 20% of the infected individuals (21). However, during the outbreak in the Americas, ZIKV infections in humans unexpectedly caused severe diseases such as Guillain-Barré syndrome and congenital Zika syndrome including microcephaly (21, 129).

The widespread distribution of the yellow fever mosquito *Aedes aegypti* and the Asian tiger mosquito *Aedes albopictus* in Central and South America (130) may have favoured the rapid emergence of ZIKV across the Western Hemisphere. Field studies and laboratory vector competence experiments have shown that mosquitoes of the *Aedes* genus are the main vectors in both sylvatic and urban transmission cycles of ZIKV (8, 131-137). However, the discovery of ZIKV in field-collected *Culex* mosquitoes (138-141) and the recent demonstration of experimental ZIKV transmission by *Culex quinquefasciatus* (142, 143) have posed the question whether the common house mosquito *Culex pipiens* could also be involved in ZIKV transmission. Since *Cx. pipiens* mosquitoes are abundantly present in temperate regions in North America, Asia and Europe (144, 145), where the ZIKV vectors *Ae. aegypti* and *Ae. albopictus* are less dominant (130, 146), ZIKV transmission by both *Aedes* and *Culex* vectors would greatly increase the human population size at risk for ZIKV infection.

Cx. pipiens can be found in two morphologically indistinguishable biotypes, *pipiens* and *molestus*, which differ in behaviour, physiology and genetic background. The *pipiens* biotype prefers to feed on birds, diapauses during winter and requires a blood meal to lay eggs (147). The *molestus* biotype prefers to bite mammals including humans, remains active during winter, and does not need a blood meal to lay the first batch of eggs (147). *Cx. pipiens* is a competent vector for the flaviviruses West Nile virus (WNV) and Usutu virus (USUV) (31, 128, 145, 148). So far, *Cx. pipiens* has shown to be an incompetent vector for ZIKV during vector competence experiments (119, 149-154), although important positive controls for the competence of the tested mosquitoes and the infectivity of the viruses have not always been included.

The aim of this study was to determine the vector competence of *Cx. pipiens* (biotypes *molestus* and *pipiens*) from the Netherlands for ZIKV. We investigated whether or not *Cx. pipiens* mosquitoes could experimentally transmit ZIKV after an infectious blood meal. We tested high numbers of mosquitoes, and we infected *Cx. pipiens* with USUV and *Ae. aegypti* with ZIKV as positive controls. We also injected ZIKV into the thorax of *Cx. pipiens* mosquitoes to study viral replication dynamics and the barrier function of the mosquito midgut on ZIKV transmission.

Methods

Mosquito rearing

Colonies of *Cx. pipiens molestus* and *Cx. pipiens pipiens* from the Netherlands (148) were maintained at 23°C with 60% relative humidity and a 16:8 light:dark period. Mosquitoes were reared as previously described (148). Egg rafts were placed in trays with tap water and Liquifry No. 1 (Interpet Ltd., Dorking, United Kingdom). Emerged larvae were fed daily with TetraMin baby fish food (Tetra, Melle, Germany). Pupae

were allowed to emerge in 30 cm cubic Bugdorm cages, and adults were provided with a 6% glucose solution.

Ae. aegypti mosquitoes (Rockefeller strain, obtained from Bayer AG, Monheim, Germany) were maintained as described earlier (106). Mosquitoes were reared at 27°C with 70% relative humidity and a 12:12 light:dark period. Adult female mosquitoes laid their eggs on moist filter paper that was placed in a cup containing tap water. The eggs were air-dried for 3-4 days and then placed in trays containing tap water with Liquifry No. 1 (Interpet Ltd.). The larvae were fed with TetraMin baby fish food. Adults were kept in 30 cm cubic Bugdorm cages with access to a 6% glucose solution.

Cells and viruses

African green monkey kidney Vero E6 cells were grown as monolayer in Dulbecco's Modified Eagle Medium (DMEM; Gibco, Carlsbad, CA, USA) supplemented with 10% fetal bovine serum (FBS; Gibco), penicillin (100 U/ml; Sigma-Aldrich, Saint Louis, MO, USA) and streptomycin (100 µg/ml; Sigma-Aldrich) (P/S). Cells were maintained at 37°C and with 5% CO_2. Prior to virus infections, Vero cells were seeded in HEPES-buffered DMEM medium (Gibco) supplemented with 10% FBS and P/S. When mosquito body lysate or saliva was added to the cells, the HEPES-buffered DMEM medium was additionally supplemented with gentamycin (50 µg/ml; Gibco) and fungizone (2.5 µg/ml of amphotericin B and 2.1 µg/ml of sodium deoxycholate; Gibco). This medium will hereafter be named DMEM HEPES complete.

All experiments involving infectious ZIKV and USUV were executed in the biosafety level 3 laboratory of Wageningen University & Research. Passage 5 and 6 virus stocks of ZIKV, Suriname 2016 (GenBank accession no. KU937936.1; EVAg Ref-SKU 011V-01621; obtained from Erasmus Medical Center, Rotterdam, the Netherlands), and passage 6 virus stocks of USUV, the Netherlands 2016 (GenBank accession no. MH891847.1; EVAg Ref-SKU 011V-02153; obtained from Erasmus Medical Center), were grown on Vero cells. Viral titers, expressed as 50% tissue culture infectious dose per millilitre ($TCID_{50}$/ml), were measured using end point dilution assays (EPDAs) on Vero cells in 60-well MicroWell plates (Nunc, Roskilde, Denmark).

Infectious blood meal

Prior to the infectious blood meal, female mosquitoes were starved for one day. Mosquitoes were then orally exposed to ZIKV or USUV by providing them with infectious blood from a Hemotek PS5 feeder (Discovery Workshops, Lancashire, United Kingdom) in a dark room for 1 hour. Infectious blood meals were prepared by mixing virus stock with human blood (Sanquin Blood Supply Foundation, Nijmegen, the Netherlands) to obtain a final virus titer of 1.0×10^7 $TCID_{50}$/ml. *Cx. pipiens*

molestus and *Cx. pipiens pipiens* received ZIKV during four and three independent experiments, respectively. As positive controls, *Ae. aegypti* was infected with ZIKV to test the quality of the virus stock, and *Cx. pipiens molestus* and *Cx. pipiens pipiens* were exposed to USUV to test the competence of the mosquitoes. After the blood meal, mosquitoes were anesthetized using CO_2, and fully engorged females were selected. A small number of engorged females was collected in individual SafeSeal micro tubes (Sarstedt, Nümbrecht, Germany) containing 0.5 mm zirconium oxide beads (Next Advance, Averill Park, NY, USA) to determine the virus titer in the mosquito body directly after engorgement. All other females were incubated at 28°C with access to 6% glucose.

Intrathoracic injection

Female mosquitoes were immobilised with CO_2 prior to intrathoracic injection using a Drummond Nanoject II Auto-Nanoliter Injector (Drummond Scientific, Broomall, PA, USA). *Cx. pipiens molestus* was injected with 1.0 x 10^4 $TCID_{50}$ of ZIKV or 3.5 x 10^3 $TCID_{50}$ of USUV (positive control). *Cx. pipiens pipiens* was injected with decreasing doses of ZIKV containing 1.0 x 10^4, 1.0 x 10^2 or 3.0 x 10^1 $TCID_{50}$ or with 3.5 x 10^3 $TCID_{50}$ of USUV (positive control). *Ae. aegypti* was injected with 1.0 x 10^4 $TCID_{50}$ of ZIKV (positive control). Injected mosquitoes were incubated at 28°C with access to 6% glucose.

Salivation assay

Fourteen days post infection, mosquitoes were immobilised with CO_2 and the legs and wings of each mosquito were removed. Next, mosquito saliva was collected by inserting the mosquito proboscis into a 200 µl pipet tip containing 5 µl of a 50% FBS and 25% sugar solution in sterilised tap water. After 45 minutes, the mosquito bodies were stored at -80°C in individual SafeSeal micro tubes (Sarstedt) containing 0.5 mm zirconium oxide beads (Next Advance). Individual mosquito saliva samples were mixed with 55 µl DMEM HEPES complete and stored at -80°C.

Infectivity assay

Frozen mosquito body samples were homogenized in a Bullet Blender Storm (Next Advance) at maximum speed for 2 min. The body homogenates were centrifuged in an Eppendorf 5424 centrifuge at 14,500 rpm for 1 min. Next, 100 µl of DMEM HEPES complete was added to each body homogenate. The homogenates in medium were blended again at maximum speed for 2 min, and centrifuged at 14,500 rpm for 2 min. Thirty µl of each mosquito body or saliva sample was then added to one well of a 96-well plate containing a monolayer of Vero cells in DMEM HEPES complete. After 2 hours at 37°C, the medium of the cells was replaced by 100 µl fresh DMEM HEPES complete. Six days post infection, the wells were scored virus-

positive or negative based on cytopathic effect (CPE). The number of virus-positive mosquito bodies or salivas was expressed as a percentage of the total number of mosquitoes tested. Viral titers in $TCID_{50}$/ml were measured for mosquito bodies and salivas using EPDAs on Vero cells. After 6 days, wells were scored virus-positive or negative based on CPE.

RNA extraction and reverse transcriptase PCR

Total RNA was isolated from Vero cells using TRIzol reagent (Invitrogen, Carlsbad, CA, USA) according to manufacturer's protocol. RNA yields were measured using a NanoDrop ND-1000 spectrophotometer. Reverse transcriptase PCR (RT-PCR) was done using a 2720 Thermal Cycler (Applied Biosystems, Foster City, CA, USA) and the SuperScript III One-Step RT-PCR System with Platinum *Taq* DNA polymerase (Invitrogen) according to manufacturer's protocol. Per RT-PCR reaction, 100 ng of total RNA was added. Primers targeting the region encoding ZIKV non-structural protein 1 (NS1) (forward: 5'-GAGACGAGATGCGGTACAGG-3'; reverse: 5'-CGACCGTCAGTTGAACTCCA-3') and the region coding for USUV non-structural protein 5 (NS5) (forward: 5'-GGCTGTAGAGGACCCTCGG-3'; reverse: 5'-GACTGCCTTTCGCTTTGCCA-3') were used at annealing temperatures of 55°C and 60°C, respectively.

Mosquito wing length measurement

The right wings of 20 female *Cx. pipiens molestus*, *Cx. pipiens pipiens* and *Ae. aegypti* were removed and mounted on sticky tape on a slide. The wing length was measured from the end of the alula to the top of the wing excluding the fringe scales using ImageFocus software (Euromex Microscopes, Arnhem, the Netherlands) calibrated with a slide graticule of 0.01 mm. The wing length measurements were used as an estimate of body size, as wing length is known to be correlated with body mass (155).

Statistical analysis

The Kolmogorov-Smirnov test was used to determine whether mosquito wing lengths and viral titers of engorged mosquitoes were normally distributed. Differences in wing lengths and differences in viral titers were then tested for significance using an unpaired, two-tailed t-test. All statistical tests were performed using GraphPad Prism 5 (GraphPad Software, San Diego, CA, USA).

Results

No ZIKV transmission by *Cx. pipiens* after an infectious blood meal

To assess the vector competence of *Cx. pipiens molestus* and *Cx. pipiens pipiens* for ZIKV, mosquitoes were offered an infectious blood meal containing

1.0 x 10^7 $TCID_{50}$/ml of ZIKV. As positive controls, *Ae. aegypti* and both *Cx. pipiens* biotypes were infected with 1.0 x 10^7 $TCID_{50}$/ml of ZIKV or USUV, respectively. To investigate the variability in engorgement among individual mosquitoes, viral body titers were determined for a selection of mosquitoes directly after ingestion of an infectious blood meal (Fig. 1A, 1B). *Cx. pipiens* mosquitoes blood fed with ZIKV or USUV showed very similar median viral titers ranging from 4.6 x 10^5 to 6.3 x 10^5 $TCID_{50}$/ml. *Ae. aegypti* mosquitoes blood fed with ZIKV showed significantly lower viral titers compared to the *Cx. pipiens* biotypes blood fed with ZIKV ($p < 0.05$). This can be explained by the fact that *Ae. aegypti* mosquitoes were smaller in size than *Cx. pipiens* mosquitoes. *Ae. aegypti* mosquitoes showed an average wing length (± standard deviation) of 2.60 mm (± 0.18 mm), whereas average wing lengths of 3.34 mm (± 0.32 mm) and 3.65 mm (± 0.24 mm) were measured for *molestus* and *pipiens*, respectively. The measured wing lengths of *Ae. aegypti* were significantly lower compared to the wing lengths of each *Cx. pipiens* biotype ($p < 0.0001$). The smaller size of *Ae. aegypti* mosquitoes likely results in a lower volume of ingested blood containing virus.

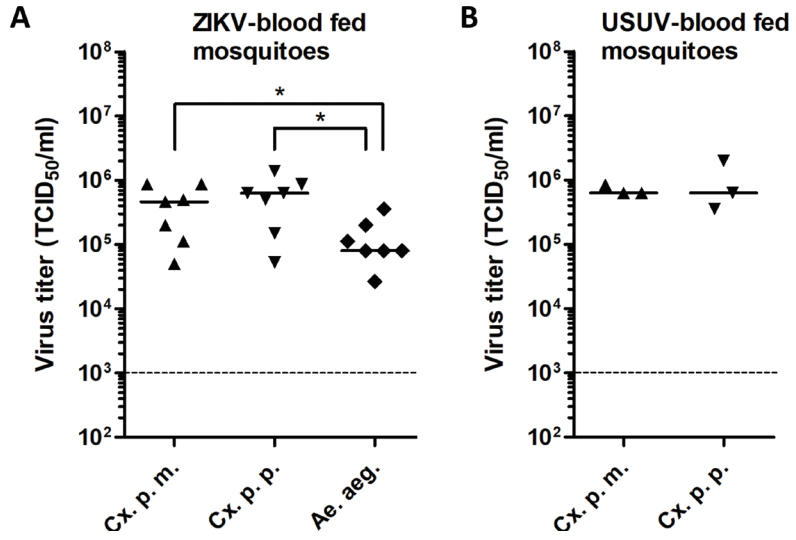

Figure 1. Virus titers in engorged *Cx. pipiens molestus* (Cx. p. m.), *Cx. pipiens pipiens* (Cx. p. p.), and *Ae. aegypti* (Ae. aeg.) mosquitoes immediately after ingestion of a blood meal containing (A) ZIKV or (B) USUV. Data points show individual mosquitoes exposed to ZIKV or USUV. Lines show median virus titers. Dashed lines indicate the detection limit of the EPDA. Asterisks indicate a significant difference ($p < 0.05$, t-test).

After the infectious blood meal, all other engorged mosquitoes were incubated at 28°C for 14 days, and afterwards mosquito bodies and salivas were tested for the presence of virus using infectivity assays on Vero cells. The presence of virus was scored based on CPE, and the presence of viral RNA was also confirmed using RT-PCR for a subset of the results. None of the 55 tested *Cx. pipiens molestus* mosquitoes showed a ZIKV-positive body or saliva (Fig. 2A, 2B). Out of the 133 *Cx. pipiens pipiens* tested, two mosquitoes showed a ZIKV-positive body but no positive saliva (Fig. 2A, 2B). For ZIKV-blood fed *Ae. aegypti* mosquitoes, which served as positive controls, 100% of the tested mosquitoes was infected and 65% showed virus-positive saliva (Fig. 2A, 2B), which corresponds with our previous work (106). In addition, the USUV-blood fed *Cx. pipiens* showed 67% (*molestus*) and 88% (*pipiens*) virus-positive bodies (Fig. 2A), and 31% (*molestus*) and 21% (*pipiens*) virus-positive salivas (Fig. 2B), demonstrating that both *Cx. pipiens* biotypes were competent vectors for USUV. Given that none of the *Cx. pipiens* mosquitoes accumulated ZIKV in the saliva after oral infection, we conclude that *Cx. pipiens* is a highly inefficient vector for ZIKV.

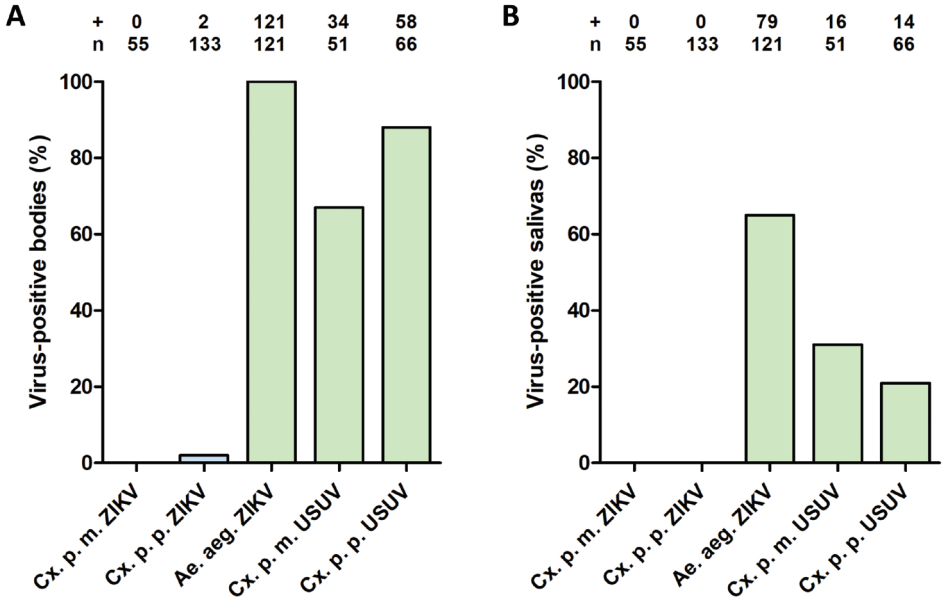

Figure 2. (A) Infection and (B) transmission of ZIKV and USUV after oral exposure to *Cx. pipiens molestus* (Cx. p. m.), *Cx. pipiens pipiens* (Cx. p. p.) and *Ae. aegypti* (Ae. aeg.). After the infectious blood meal, mosquitoes were incubated at 28°C for 14 days. The number of virus-positive mosquito bodies or salivas (indicated by +) is expressed as a percentage of the total number of mosquitoes tested (indicated by n). Experimental groups are depicted in blue; positive controls are depicted in green.

Low ZIKV titers in *Cx. pipiens* after an infectious blood meal

Viral titers of virus-positive bodies and salivas were measured by EPDAs. The two ZIKV-positive *Cx. pipiens pipiens* bodies both had a viral titer of 6.3 x 10^3 $TCID_{50}$/ml (Fig. 3A), whereas the viral body titers of *Ae. aegypti* mosquitoes were very high with a median titer of 1.1 x 10^7 $TCID_{50}$/ml (Fig. 3B). The median viral saliva titer of *Ae. aegypti* was below the detection limit of 1.0 x 10^3 $TCID_{50}$/ml (Fig. 3B). For USUV-blood fed *Cx. pipiens*, the median viral body titers were 8.0 x 10^4 $TCID_{50}$/ml (*molestus*) and 2.9 x 10^5 $TCID_{50}$/ml (*pipiens)*, and the median viral saliva titers were below the detection limit of 1.0 x 10^3 $TCID_{50}$/ml (*molestus*) and 6.3 x 10^3 $TCID_{50}$/ml (*pipiens*) (Fig. 3C, 3D). These results showed that ZIKV had the ability to infect *Cx. pipiens* and replicate in the mosquito with very low efficiency.

Intrathoracic ZIKV injection leads to virus replication in *Cx. pipiens* with limited dissemination to the mosquito saliva

To investigate whether ZIKV was unable to pass the mosquito midgut barrier in *Cx. pipiens*, mosquitoes were injected in the thorax with 1.0 x 10^4 $TCID_{50}$ of ZIKV. As positive controls, *Ae. aegypti* was injected with ZIKV and both *Cx. pipiens* biotypes were injected with USUV. After 14 days at 28°C, mosquito bodies and salivas were analysed for the presence of virus. During infectivity assays, the presence of virus was scored based on CPE and, for a subset of the results, these scores were also confirmed by RT-PCR. High percentages (74% for *molestus* and 78% for *pipiens*) of the injected mosquitoes had ZIKV-positive bodies (Fig. 4A). Interestingly, 14% (*molestus*) and 7% (*pipiens*) of the injected mosquitoes also showed infectious ZIKV in their saliva (Fig. 4B). After injection of *Ae. aegypti* with ZIKV, which served as a positive control experiment, 100% of the injected mosquitoes showed virus-positive bodies (Fig. 4A), whereas 72% of the injected mosquitoes showed virus-positive saliva (Fig. 4B), which is in line with our earlier results (106). As another positive control, both biotypes of *Cx. pipiens* were injected with USUV, which showed that 100% of the tested *Cx. pipiens molestus* and *Cx. pipiens pipiens* had USUV-positive bodies (Fig. 4A), and 94% (*molestus*) and 88% (*pipiens*) of the injected mosquitoes had USUV-positive saliva (Fig. 4B). This indicates that virus dissemination to the saliva in *Cx. pipiens* is more efficient with USUV than with ZIKV.

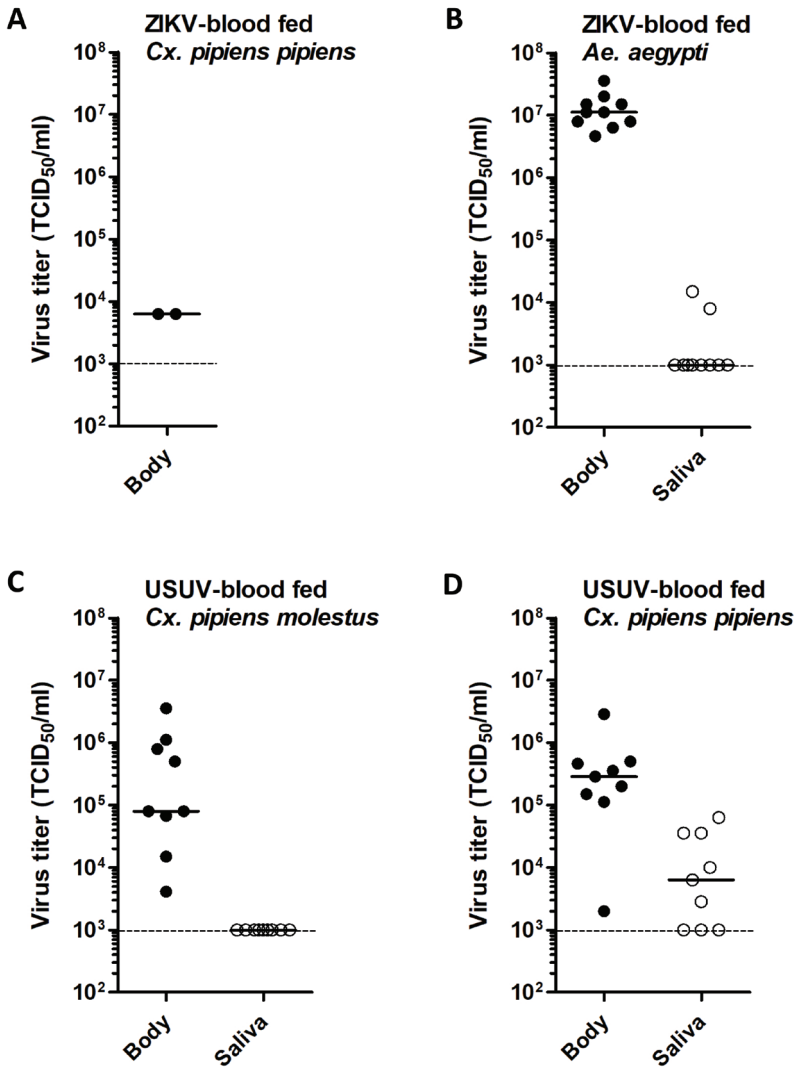

Figure 3. Virus titers in bodies and salivas of *Cx. pipiens molestus*, *Cx. pipiens pipiens*, and *Ae. aegypti* mosquitoes after oral exposure to ZIKV or USUV. After oral exposure, mosquitoes were incubated at 28°C for 14 days. Virus titers were determined by EPDA for **(A)** bodies of ZIKV-blood fed *Cx. pipiens pipiens*, **(B)** bodies and salivas of ZIKV-blood fed *Ae. aegypti*, **(C)** bodies and salivas of USUV-blood fed *Cx. pipiens molestus*, **(D)** bodies and salivas of USUV-blood fed *Cx. pipiens pipiens*. Data points show individual mosquitoes infected with ZIKV or USUV. Lines show median virus titers. Dashed lines indicate the detection limit of the EPDA.

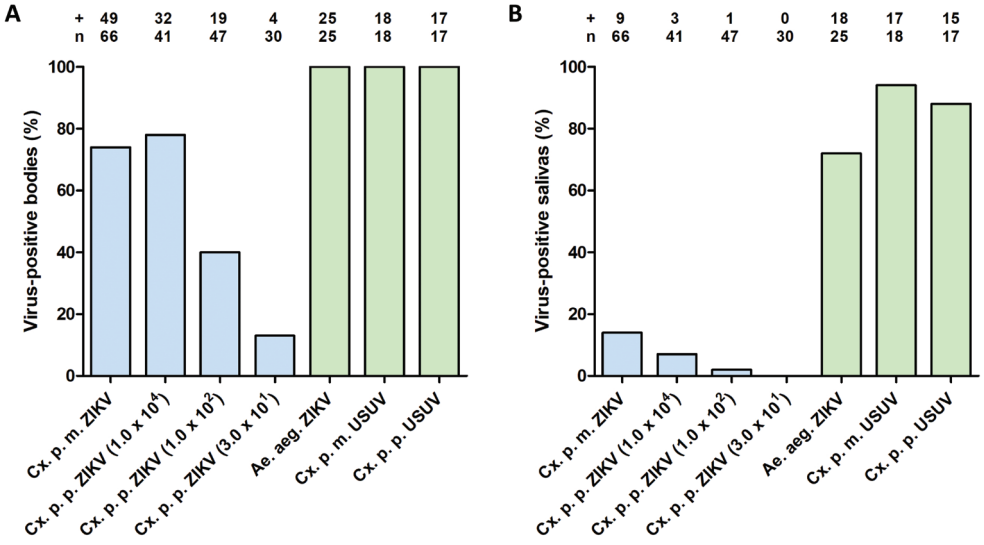

Figure 4. (A) Infection and (B) transmission of ZIKV and USUV after intrathoracic injection in *Cx. pipiens molestus* (Cx. p. m.), *Cx. pipiens pipiens* (Cx. p. p.) and *Ae. aegypti* (Ae. aeg.). *Cx. pipiens pipiens* mosquitoes were injected with three different ZIKV doses as indicated (in $TCID_{50}$). The injected mosquitoes were incubated at 28°C for 14 days. The number of virus-positive mosquito bodies or salivas (indicated by +) is expressed as a percentage of the total number of mosquitoes tested (indicated by n). Experimental groups are depicted in blue; positive controls are depicted in green.

Effect of injected viral dose on ZIKV infection of *Cx. pipiens*

To investigate whether the percentage of ZIKV-positive mosquitoes after intrathoracic injection was affected by the viral dose provided, *Cx. pipiens pipiens* mosquitoes were also injected with lower doses of ZIKV. After 14 days, 40% of the *Cx. pipiens pipiens* mosquitoes injected with 1.0 x 10^2 $TCID_{50}$ of ZIKV showed virus-positive bodies, whereas 2% showed virus-positive salivas (Fig. 4A, 4B), Additionally, when a viral dose of 3.0 x 10^1 $TCID_{50}$ was supplied, 13% of the tested *Cx. pipiens pipiens* mosquitoes showed virus-positive bodies, whereas none of the mosquitoes showed virus-positive saliva (Fig. 4A, 4B). This indicated that the infection and transmission potential of ZIKV-injected *Cx. pipiens pipiens* was dependent on the viral dose provided, but also that a low ZIKV dose of 3.0 x 10^1 $TCID_{50}$ can infect a mosquito.

Variability of viral titers in ZIKV-injected *Cx. pipiens*

To obtain better insight into the ZIKV replication dynamics in injected *Cx. pipiens* mosquitoes, viral body and saliva titers were measured by EPDAs. To validate ZIKV replication in the primary ZIKV vector *Ae. aegypti* (positive control), the bodies and salivas of ZIKV-injected *Ae. aegypti* were also titrated. ZIKV body titers in

Cx. pipiens injected with a dose of 1.0 x 10^4 $TCID_{50}$ were highly variable with maximum titers of 1.1 x 10^6 $TCID_{50}$/ml (*molestus*) and 6.3 x 10^5 $TCID_{50}$/ml (*pipiens*) (Fig. 5A, 5B). This showed that ZIKV is intrinsically capable of replication to high viral titers in *Cx. pipiens*. Median viral body titers of ZIKV-injected *Cx. pipiens* were 9.6 x 10^3 $TCID_{50}$/ml for *pipiens* and below the detection limit of 1.0 x 10^3 $TCID_{50}$/ml for *molestus*. For *Ae. aegypti*, a high median viral body titer of 6.32 x 10^6 $TCID_{50}$/ml was found (Fig. 5C).

Interestingly, four *Cx. pipiens molestus* mosquitoes with ZIKV-positive saliva showed viral body titers below the detection limit of 1.0 x 10^3 $TCID_{50}$/ml (Fig. 5A). Moreover, out of the three ZIKV-injected *Cx. pipiens pipiens* mosquitoes with ZIKV-positive saliva, two mosquitoes had relatively high viral body titers of 3.6 x 10^5 $TCID_{50}$/ml and 5.0 x 10^5 $TCID_{50}$/ml, whereas the third mosquito had a relatively low viral body titer of 8.0 x 10^3 $TCID_{50}$/ml (Fig. 5B). This indicated that viral dissemination into the saliva of *Cx. pipiens* does not always correlate with a high viral titer in the mosquito body.

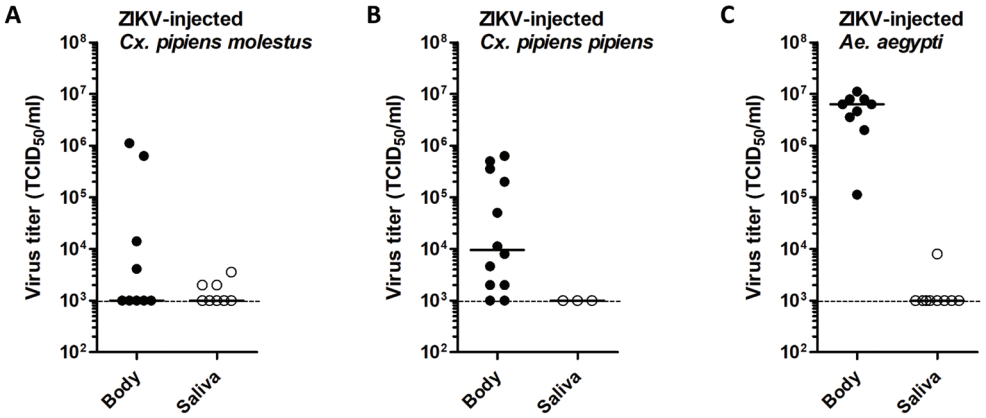

Figure 5. Virus titers in bodies and salivas of *Cx. pipiens molestus*, *Cx. pipiens pipiens*, and *Ae. aegypti* mosquitoes after intrathoracic injection with ZIKV. After injection, mosquitoes were incubated at 28°C for 14 days. Virus titers of the bodies and salivas were determined by EPDA for **(A)** ZIKV-injected *Cx. pipiens molestus*, **(B)** ZIKV-injected *Cx. pipiens pipiens* (injection dose: 1.0 x 10^4 $TCID_{50}$), **(C)** ZIKV-injected *Ae. aegypti*. Data points show individual mosquitoes infected with ZIKV. Lines show median virus titers. Dashed lines indicate the detection limit of the EPDA.

Discussion

In this study, we set out to determine the vector competence of Dutch *Cx. pipiens* (biotypes *molestus* and *pipiens*) for ZIKV and we found that *Cx. pipiens* was unable to experimentally transmit ZIKV after an infectious blood meal. However, to the best

of our knowledge, our study is the first study to demonstrate ZIKV dissemination to the saliva of *Cx. pipiens* mosquitoes after intrathoracic injection. Previous studies reported the presence of ZIKV in *Cx. pipiens* bodies (149, 150) and heads (149) after injection but no virus accumulation in the saliva (149, 150). This suggested that ZIKV is incapable of infecting the salivary glands and/or entering the saliva of *Cx. pipiens* (150). We showed, however, that ZIKV can accumulate in the mosquito saliva after an intrathoracic injection with a viral dose as low as 1.0 x 10^2 $TCID_{50}$. This viral dose for injection is similar or lower compared to other studies that did not report ZIKV presence in the saliva (149, 150). Based on our results, we conclude that ZIKV is intrinsically capable of dissemination to the saliva of *Cx. pipiens* upon forced infection.

Nonetheless, even after forced infection, ZIKV replication in *Cx. pipiens* appeared to be suboptimal, as 74% (*molestus*) and 78% (*pipiens*) of the *Cx. pipiens* injected with a viral dose of 1.0 x 10^4 $TCID_{50}$ of ZIKV showed virus-positive bodies compared to 100% of the ZIKV-injected *Ae. aegypti* and USUV-injected *Cx. pipiens*. These results suggest a general replication deficiency of ZIKV in *Culex* cells, which has also been observed by others (150). The underlying mechanisms responsible for the specific restriction of ZIKV in *Cx. pipiens* are currently unknown and need further investigation. Important factors that should be considered are physical barriers at the mosquito midgut and salivary glands, mosquito host factors required for virus replication, mosquito immune responses, and the mosquito midgut microbiome (60). Flaviviruses such as ZIKV, but also yellow fever virus and dengue virus, are primarily associated with *Aedes* vectors (156, 157). Other flaviviruses such as WNV and USUV are mainly associated with *Culex* vectors (156, 157). Genetic differences between the mosquito genera and/or between the respective flaviviruses likely constrain and maintain the observed vector specificity. However, arboviruses have previously shown to have the potential to quickly adapt to new vectors (158, 159), and therefore it is important to investigate the molecular basis underlying the vector specificity of ZIKV, and also whether virus evolutionary trajectories can be predicted that could potentially lead to new epidemic variants of ZIKV with altered vector specificity.

We provided evidence via injection experiments that the mosquito midgut acted as an important barrier against ZIKV dissemination in *Cx. pipiens*. Our finding with regard to the inability of *Cx. pipiens* to transmit ZIKV is in line with other recent studies suggesting that mosquitoes of the *Culex* genus are poor ZIKV vectors (119, 149-154, 160). Even at an incubation temperature as high as 28°C, *Cx. pipiens* did not accumulate ZIKV in the saliva after oral exposure (149, 150, 153). However, when considering the massive number of mosquitoes in the field and the fact that our laboratory study only measures vector competence and does not take into account all

factors contributing to the vectorial capacity of the *Cx. pipiens* mosquito species (60), we cannot completely rule out the possibility of ZIKV transmission by *Cx. pipiens* in the field. Nevertheless, the reports of others (119, 149-154) and our experiments with high numbers of tested *Cx. pipiens* mosquitoes and positive controls to validate the competence of the tested *Cx. pipiens* colonies and the used ZIKV isolate, consolidate the conclusion that *Cx. pipiens* is a highly inefficient vector for ZIKV.

Acknowledgements

The authors thank Marleen Abma-Henkens and Giel Göertz for assistance during mosquito experiments, Haidong Wang and Jelke Fros for advice about statistical analysis, Pieter Rouweler and other members of the insect rearing group from the Laboratory of Entomology from Wageningen University & Research for providing mosquitoes, Chantal Reusken for providing the Zika virus Suriname 2016 and Usutu virus the Netherlands 2016 isolates, and Barry Rockx and Marion Koopmans for their continued interest in the project. This research was funded by ZonMw under grant number 522003001 (project: ZikaRisk "Risk of Zika virus introductions for the Netherlands") and by the European Union's Horizon 2020 Research and Innovation Programme under grant number 734548 (project: ZIKAlliance).

Chapter 4 **Effect of blood source on vector competence of *Culex pipiens* biotypes for Usutu virus**

Sandra R. Abbo[1], Tessa M. Visser[2], Constantianus J.M. Koenraadt[2], Gorben P. Pijlman[1], Haidong Wang[1]

[1]Laboratory of Virology, Wageningen University & Research, Wageningen, the Netherlands
[2]Laboratory of Entomology, Wageningen University & Research, Wageningen, the Netherlands

Published in Parasites & Vectors (2021), 14, 194.

Abstract

Infectious blood meal experiments have been frequently performed with different virus-vector combinations to assess the transmission potential of arthropod-borne (arbo)viruses. A wide variety of host blood sources have been used to deliver arboviruses to their arthropod vectors in laboratory studies. The type of blood used during vector competence experiments does not always reflect the blood from the viraemic vertebrate hosts in the field, but little is known about the effect of blood source on the experimental outcome of vector competence studies. Here we investigated the effect of avian versus human blood on the infection and transmission rates of the zoonotic Usutu virus (USUV) in its primary mosquito vector *Culex pipiens*.

Cx. pipiens biotypes (*pipiens* and *molestus*) were orally infected with USUV through infectious blood meals containing either chicken or human whole blood. The USUV infection and transmission rates were determined by checking mosquito bodies and saliva for USUV presence after 14 days of incubation at 28°C. In addition, viral titers were determined for USUV-positive mosquito bodies and saliva.

Human and chicken blood lead to similar USUV transmission rates for *Cx. pipiens* biotype *pipiens* (18% and 15%, respectively), while human blood moderately but not significantly increased the transmission rate (30%) compared to chicken blood (17%) for biotype *molestus*. USUV infection rates with human blood were consistently higher in both *Cx. pipiens* biotypes compared to chicken blood. In virus-positive mosquitoes, USUV body and saliva titers did not differ between mosquitoes taking either human or chicken blood. Importantly, biotype *molestus* had much lower USUV saliva titers compared to biotype *pipiens*, regardless of which blood was offered.

In conclusion, infection of mosquitoes with human blood led to higher USUV infection rates as compared to chicken blood. However, the blood source had no effect on the vector competence for USUV. Interestingly, biotype *molestus* is less likely to transmit USUV compared to biotype *pipiens* due to very low virus titers in the saliva.

Graphical abstract

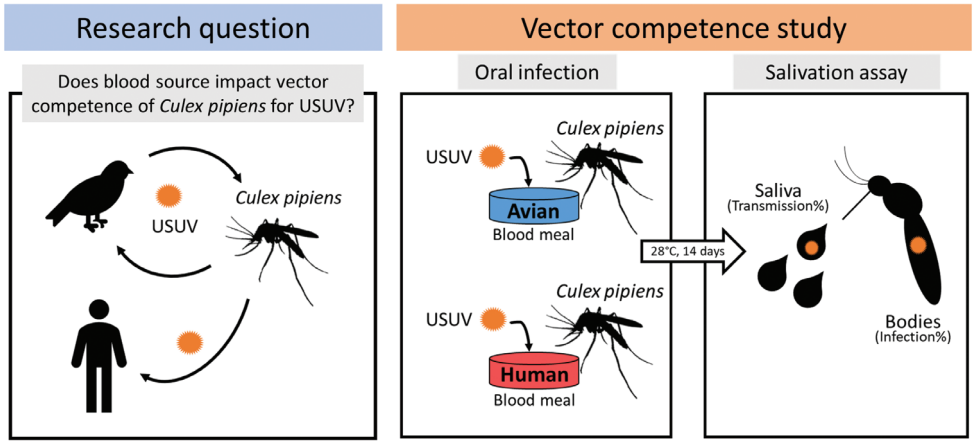

Introduction

Arthropod-borne (arbo)viruses can cause severe disease outbreaks in animals and humans. The spread of arboviruses is mainly determined by the presence of competent vectors, often mosquitoes. A female mosquito can acquire a virus during blood feeding on a viraemic vertebrate host. After the extrinsic incubation period, the infected mosquito can transmit the virus via the mosquito saliva by feeding on a next host (59, 62). The ability of a mosquito species to transmit a certain virus is defined as the vector competence (62, 89). Vector competence has been investigated for many virus-vector combinations (60, 63, 64), and helps to assess the risk of viral emergence and spread.

During vector competence studies, infectious blood meals are commonly offered via artificial feeding systems, where a mixture of virus and blood is contained in either a reservoir covered with a membrane (natural or Parafilm) or is supplied via droplets or a pledget of cotton wool (161). The type of blood used for artificial feeding differs per study but often resembles the blood from vertebrate hosts involved in the virus transmission cycles. However, the actual experimental setups can also be constrained by the availability of certain blood sources. Therefore, the blood used during vector competence experiments does not always resemble the blood from the viraemic hosts in the field. Little is known about the impact of blood source on vector competence (89).

The zoonotic Usutu virus (USUV; family *Flaviviridae*, genus *Flavivirus*) is currently circulating in Europe and is drawing increasing attention due to its substantial mortality in avian species and the potential to cause neurological disease in humans (11). Vector competence studies are therefore important to assess the

risk of USUV outbreaks in Europe and beyond. In the field, USUV is primarily transmitted between avian reservoir hosts and mosquitoes (30, 162-164). Humans and other mammals can be infected with USUV via mosquito bites, however they are considered dead-end hosts due to low levels of viraemia (27). Hence, the use of avian blood in the infectious blood meal experiments with USUV is therefore preferred (31). Nonetheless, infectious blood meals containing human blood (165), swine blood (166), sheep blood (167), horse blood (168), bovine blood (169) or rabbit blood (170) have been used to assess the vector competence of local mosquito species for USUV. The different outcomes of these studies are often attributed to virus strains or mosquito lines, while the use of different sources of blood during artificial feeding is often not discussed.

Here we investigated the effect of blood source on the transmission of USUV by the common house mosquito *Culex pipiens*, which is the primary vector for USUV in Europe (30). *Cx. pipiens* consists of two biotypes among which biotype *pipiens* prefers to feed on birds, whereas biotype *molestus* preferentially feeds on mammals including humans (147). We compared the USUV infection and transmission rates of both *Cx. pipiens* biotypes after ingestion of an infectious blood meal containing either chicken or human whole blood. The viral titers in the body and saliva of the USUV-positive mosquitoes were also compared.

Methods

Mosquitoes, cells and viruses

Previously established *Cx. pipiens* biotype *pipiens* and biotype *molestus* colonies from the Netherlands (148) were reared separately as described earlier (148). Mosquitoes were maintained at 23°C with a 16:8 light:dark cycle and a relative humidity of 60%.

African green monkey kidney Vero E6 cells were routinely cultured in Dulbecco's Modified Eagle Medium (DMEM; Gibco, Carlsbad, CA, USA) with 10% fetal bovine serum (FBS; Gibco), penicillin (100 U/ml; Sigma-Aldrich, Saint Louis, MO, USA) and streptomycin (100 µg/ml; Sigma-Aldrich) (P/S) at 37°C with 5% CO_2. Preceding virus infections, Vero cells were seeded in HEPES-buffered DMEM medium (Gibco) supplemented with 10% FBS and P/S. When Vero cells were incubated with mosquito body lysate or saliva, the HEPES-buffered DMEM medium was additionally supplemented with gentamycin (50 µg/ml; Gibco) and fungizone (2.5 µg/ml of amphotericin B and 2.1 µg/ml of sodium deoxycholate; Gibco). This medium will hereafter be referred to as DMEM HEPES complete.

Passage 5 and 6 virus stocks of USUV, the Netherlands 2016 (GenBank accession no. MH891847.1; EVAg Ref-SKU 011V-02153; obtained from Erasmus Medical Center, Rotterdam, the Netherlands), were grown on Vero cells. Viral

titers, expressed as 50% tissue culture infectious dose per millilitre ($TCID_{50}$/ml), were determined by end point dilution assays (EPDAs) on Vero cells using 60-well MicroWell plates (Nunc, Roskilde, Denmark).

Infectious blood meal

Before the infectious blood meal, 3-18 days old mosquitoes were starved for one day. Infectious blood meal experiments were conducted in the biosafety level 3 laboratory of Wageningen University & Research. Mosquitoes were orally exposed to chicken whole blood (Kemperkip, Uden, the Netherlands) or human whole blood (Sanquin Blood Supply Foundation, Nijmegen, the Netherlands) containing 10^7 $TCID_{50}$/ml of USUV. Mosquitoes were fed in a dark room for 1 hour using a Hemotek PS5 feeder (Discovery Workshops, Lancashire, United Kingdom). Infectious chicken blood was provided during four (*molestus*) and three (*pipiens*) independent experiments, whereas both biotypes were exposed to infectious human blood in three independent experiments. After the blood meal, mosquitoes were immobilised using 100% CO_2 and the fully engorged females were selected. A small number of females was stored at -80°C in SafeSeal micro tubes (Sarstedt, Nümbrecht, Germany) containing 0.5 mm zirconium oxide beads (Next Advance, Averill Park, NY, USA) to measure the viral titer in the mosquito body immediately after engorgement. All remaining females were incubated at 28°C for 14 days. A 6% glucose solution was provided as food source.

Salivation assay

Fourteen days post infection, mosquito saliva was collected by forced salivation as described earlier (128). Mosquitoes were first immobilised using 100% CO_2, and their legs and wings were removed. To collect mosquito saliva, the mosquito proboscis was inserted in a 200 µl pipet tip holding 5 µl of a 1:1 mixture of FBS and 50% sugar in autoclaved tap water. After 45 minutes, the samples containing mosquito saliva were mixed with 55 µl DMEM HEPES complete and stored at -80°C. The mosquito bodies were collected in SafeSeal micro tubes (Sarstedt) containing 0.5 mm zirconium oxide beads (Next Advance) and also stored at -80°C.

Infectivity assay

Mosquito body samples were taken from -80°C and directly homogenized in a Bullet Blender Storm (Next Advance) at maximum speed for 2 min. Next, homogenates were spun down in an Eppendorf 5424 centrifuge at 14,500 rpm for 1 min. 100 µl of DMEM HEPES complete was then added to each sample. The homogenates in medium were blended again at maximum speed for 2 min, and centrifuged at 14,500 rpm for 2 min. From each body or saliva sample, 30 µl was added to one well of a 96-well plate containing Vero cells in DMEM HEPES complete. After

2 hours at 37°C, the medium of the cells was removed and replenished with fresh DMEM HEPES complete. After 6 days incubation at 37°C, the cells were inspected for cytopathic effect (CPE), and each well was scored virus-positive or negative. For a subset of the results, these scores were also confirmed by reverse transcriptase PCR on total RNA isolated from Vero cells using primers against the region coding for USUV non-structural protein 5 as previously described (171). The infection and transmission rates were then calculated by expressing the number of virus-positive mosquito bodies or salivas as a percentage of the total number of mosquitoes analysed. Viral titers of mosquito bodies and saliva were measured using EPDAs on Vero cells. After 6 days at 37°C, wells were considered virus-positive or negative based on CPE.

Statistical analysis

Fisher's exact test was used to compare the infection and transmission rates between human and chicken infectious blood meals. Shapiro-Wilk test was used to check the normality of log transformed viral titer data sets. Then Mann-Whitney *U* test was used to compare the mean viral titers between two log transformed data sets. Statistical tests were performed in GraphPad Prism 5.

Results

The effect of blood source on USUV infection and transmission rates in *Cx. pipiens*

The effect of blood source on USUV infection and transmission was investigated for both biotypes. A selection of females was used to determine the viral titers in the mosquito bodies immediately after oral ingestion. For both *Cx. pipiens* biotypes, the mean viral titers in the mosquito bodies right after the oral feeding were similar between the two types of infectious blood meal [($p = 0.351$; Fig. 1A) and ($p = 0.267$; Fig.1B)]. All other fully engorged females were maintained at 28°C for 14 days. Out of the biotype *pipiens* mosquitoes fed with infectious chicken blood, 50% showed virus-positive bodies after 14 days, whereas human blood resulted in a higher body infection rate of 66% ($p = 0.003$; Fig. 2A). The percentage of mosquitoes with USUV-positive saliva was similar among the biotype *pipiens* mosquitoes exposed to either chicken or human infectious blood (15% and 18%, respectively; $p = 0.467$; Fig. 2A). For biotype *molestus*, the avian infectious blood infected 47% of the engorged mosquitoes, whereas the human infectious blood infected a significantly higher percentage of the mosquitoes (66%; $p = 0.026$; Fig. 2B). The USUV transmission rate was somewhat higher for biotype *molestus* provided with human blood (30%) compared to chicken blood (17%), but the significance was marginal ($p = 0.054$; Fig. 2B). Altogether, these results indicate that blood source did not significantly impact the vector competence of *Cx. pipiens* biotypes for USUV.

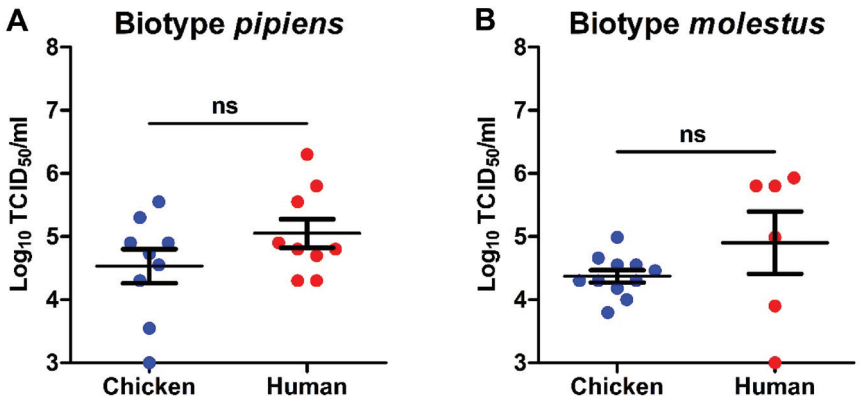

Figure 1. USUV uptake in *Cx. pipiens* mosquitoes immediately after engorgement of an infectious blood meal. The blood meal consisted of either chicken or human blood. Virus titers were determined by EPDAs for **(A)** biotype *pipiens* and **(B)** biotype *molestus*. Data points represent individual mosquitoes orally exposed to USUV. Lines among the dots indicate the mean viral titers. Error bars show the standard error of the mean. A non-significant difference is indicated by ns between two data sets (p>0.05; Mann-Whitney *U* test).

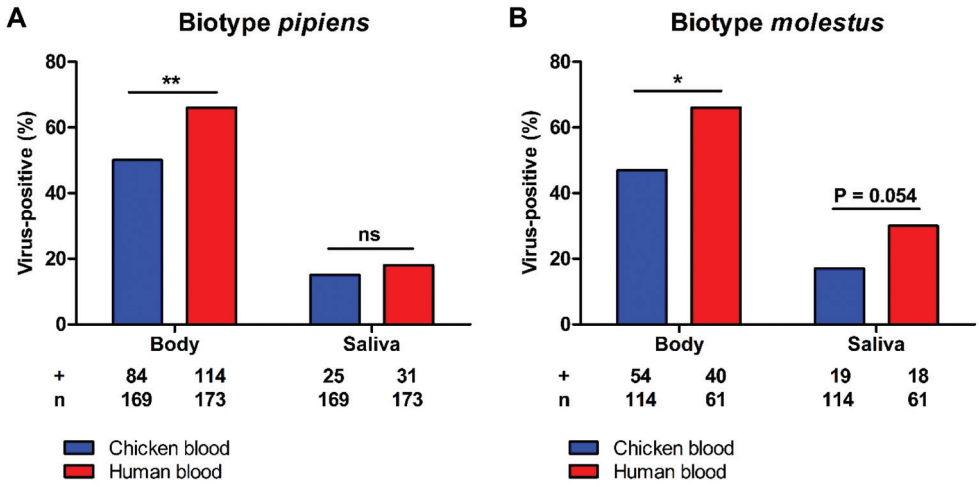

Figure 2. Infection and transmission of USUV after oral exposure of *Cx. pipiens* to infectious chicken or human blood. (A) *Cx. pipiens pipiens* and **(B)** *Cx. pipiens molestus* were incubated at 28°C, and analysed for infectious virus at 14 days post blood meal. The number of virus-positive mosquito bodies or saliva samples (indicated by +) is expressed as a percentage of the total number of mosquitoes tested (indicated by n). Asterisks (*, **) indicate a significant p value of <0.05 and <0.01, respectively, while ns represents a non-significant difference (Fisher's exact test).

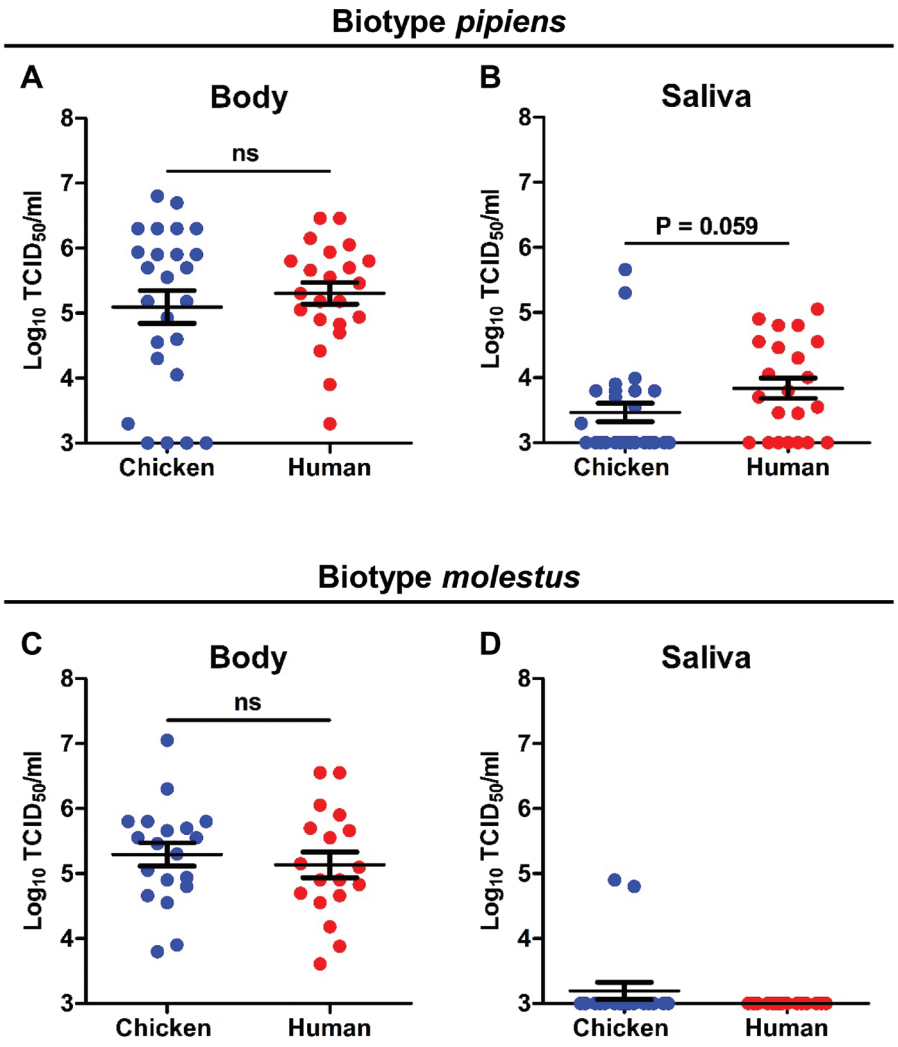

Figure 3. USUV titers in bodies and saliva of *Cx. pipiens* after oral exposure to infectious chicken or human blood. (A & B) *Cx. pipiens pipiens* and **(C & D)** *Cx. pipiens molestus* were incubated at 28°C, and virus titers were determined 14 days post infection. Data points represent individual mosquitoes exposed to USUV. Lines among the dots indicate the mean viral titers. Error bars show the standard error of the mean. A non-significant difference is indicated by ns ($p>0.05$; Mann-Whitney *U* test).

The effect of blood source on USUV titers in bodies and saliva of *Cx. pipiens*

We next looked at the USUV titers in *Cx. pipiens* bodies and saliva at 14 days after the oral ingestion. Although human blood resulted in a higher USUV infection rate for *Cx. pipiens* biotype *pipiens*, the mean viral body titers were not significantly different between mosquitoes that took up either a chicken or a human infectious blood meal ($10^{5.1}$ and $10^{5.3}$ $TCID_{50}$/ml, respectively; p = 0.898; Fig. 3A). The mean USUV saliva titers of *Cx. pipiens* biotype *pipiens* were slightly higher when mosquitoes were offered a human blood meal ($10^{3.8}$ $TCID_{50}$/ml) compared to a chicken blood meal ($10^{3.5}$ $TCID_{50}$/ml), although the difference is only marginally significant (p = 0.059; Fig. 3B). For *Cx. pipiens* biotype *molestus*, we found that the mean viral body titers showed similar values of $10^{5.3}$ and $10^{5.1}$ for chicken and human blood, respectively (p = 0.574; Fig. 3C). Surprisingly, viral saliva titers for biotype *molestus* were all below the detection limit of our EPDA (10^{3} $TCID_{50}$/ml) except two "outliers" (Fig. 3D). Therefore no differences can be observed between human and chicken blood. Collectively, these results show that blood source did not significantly affect the viral titers in *Cx. pipiens* biotypes after oral exposure to USUV.

Discussion

Infectious blood meal experiments are frequently performed on mosquitoes and other vector species to investigate their vector competence for arboviruses. Here we provided *Cx. pipiens*, the primary vector for USUV, with infectious blood meals containing either chicken or human whole blood, and investigated the effect of blood source on the infection and transmission of USUV. We found that both types of blood lead to comparable vector competence of the two *Cx. pipiens* biotypes for USUV. Other sources of mammalian blood, e.g. sheep (167) and rabbit (170), have been used to investigate the vector competence of *Culex* spp. for the prototype strain of USUV (SAAR-1776) under laboratory conditions. In line with our observations, these studies also confirmed the vector competence of *Culex* spp. for USUV. Interestingly, another study, in which equine blood was used, reported limited transmission of USUV (SAAR-1776) in two *Cx. pipiens* lines (168). It remains unclear whether the equine blood plays a role in contributing to the low viral transmission. Parallel oral infections using equine blood and another type of blood in the infectious blood meal experiments might be helpful to rule out any effect of blood source on the measured vector competence.

In our study, the source of blood used for oral feeding did not affect the virus titer in bodies of USUV-infected mosquitoes. A similar result was observed for *Culex tarsalis* mosquitoes infected with western equine encephalomyelitis virus (WEEV; family *Togaviridae*, genus *Alphavirus*), where mean titers of WEEV in mosquito bodies did not differ significantly when mosquitoes were provided with either chicken

or rabbit blood (172). Moreover, WEEV infection rates did not vary significantly among mosquitoes fed with chicken or rabbit blood (172). In our study, however, we found that human blood consistently generated a higher USUV infection rate among the tested *Cx. pipiens* biotypes compared to chicken blood. Further studies about the impact of different blood sources on the measured infection and transmission rates for other virus-vector combinations could help to further clarify the effect of blood source on the outcome of artificial feeding experiments, and will hopefully allow for a better assessment of the competence of vector species for arboviruses.

It is not entirely understood how host blood could impact arbovirus infection in the arthropod vector, but certain host-derived factors have a role to play (161). For example, species-specific serum proteases, of which the presence depends on the blood source, can cleave the outer capsid protein VP2 of African horse sickness virus, thereby resulting in enhanced infectivity in *Culicoides* midges (173). In addition, a recent study has shown that different types of ingested blood result in diverse bacterial compositions in the midgut of vector mosquito *Aedes aegypti* (174). The gut bacterial microbiome of mosquitoes has proven to be a potent modulator of arbovirus infection (175-177), and it is therefore possible that the host blood can influence arbovirus infection through modulation of the mosquito bacterial microbiome. Future studies on how host blood reshapes the microbiome in the mosquito midgut and potentially alters the outcome of arbovirus infection are therefore needed.

Finally, we found that the viral saliva titers of biotype *molestus* at 14 days post infection were much lower compared to the viral saliva titers of biotype *pipiens*, regardless of which blood was offered. These low viral saliva titers of biotype *molestus* may indicate a lower transmission potential for USUV compared to biotype *pipiens*. Since the mean viral titer in biotype *molestus* bodies was around 10^5 $TCID_{50}$/ml, which is also comparable to that of biotype *pipiens*, the low viral saliva titers in biotype *molestus* are unlikely due to insufficient viral replication in the mosquito bodies. In addition to that, both *Cx. pipiens* biotypes were maintained under the same conditions, thus the difference in USUV titers in the saliva between the two *Cx. pipiens* biotypes is very likely attributed to genetic factors determining the characteristics of mosquito midguts or salivary glands. This finding could suggest that biotype *molestus*, which preferentially feeds on mammals including humans, is a less efficient vector for USUV compared to biotype *pipiens*.

Acknowledgements

The authors thank Pieter Rouweler and other members of the insect rearing group from the Laboratory of Entomology from Wageningen University & Research for maintaining the mosquito colonies, Marleen Abma-Henkens for assistance during the mosquito experiments, Corinne Geertsema for cell culture maintenance, Chantal

Reusken for providing the Usutu virus the Netherlands 2016 isolate, and Monique van Oers for her continued interest in the project.

SRA was supported by the ZonMw project ZikaRisk ("Risk of Zika virus introductions for the Netherlands"), project number 522003001. HW was supported by the OneHealth postdoc grant UZOOTU ("USUTU virus: Zoonotic potential and fitness trade-offs between hosts and vectors") from the graduate school PE&RC.

Chapter 5 **The virome of the invasive Asian bush mosquito *Aedes japonicus* comprises highly prevalent novel viruses**

Sandra R. Abbo[1,*], João P. P. de Almeida[2,*], Roenick P. Olmo[3], Carlijn Balvers[1,4], Jet S. Griep[1,4], Charlotte Linthout[4], Constantianus J. M. Koenraadt[4], Jelke J. Fros[1], Eric R. G. R. Aguiar[2,5], Eric Marois[3], Gorben P. Pijlman[1], João T. Marques[2,3]

[1]Laboratory of Virology, Wageningen University & Research, Wageningen, the Netherlands
[2]Department of Biochemistry and Immunology, Instituto de Ciências Biológicas, Universidade Federal de Minas Gerais, Belo Horizonte, Brazil
[3]Université de Strasbourg, CNRS UPR9022, INSERM U1257, Strasbourg, France
[4]Laboratory of Entomology, Wageningen University & Research, Wageningen, the Netherlands
[5]Department of Biological Science, Center of Biotechnology and Genetics, State University of Santa Cruz, Ilhéus, Brazil

*These authors contributed equally to this work.

Abstract

The Asian bush mosquito *Aedes japonicus* is a vector species that is rapidly invading North America and Europe. Due to its potential to transmit multiple pathogenic arthropod-borne (arbo)viruses including Zika virus, West Nile virus and chikungunya virus, it is important to understand the biology of this mosquito in more detail. In addition to transmitting arboviruses, mosquitoes can also carry insect-specific viruses that receive increasing attention due to their potential effects on host physiology and arbovirus transmission. In this study, we provide an unprecedented and highly curated characterization of the virome of *Ae. japonicus* populations in the Netherlands and France by small RNA deep sequencing and *de novo* assembly. We applied a small RNA-based metagenomic approach that allowed a sequence-independent analysis based on virus-derived small RNAs produced by the host. This strategy revealed the presence of *Ae. japonicus* narnavirus 1 (AejapNV1) as well as three newly discovered virus species that we named *Ae. japonicus* totivirus 1 (AejapTV1), *Ae. japonicus* anphevirus 1 (AejapAV1) and *Ae. japonicus* bunyavirus 1 (AejapBV1). We also discovered viral sequences that were presumably derived from two additional novel viruses: *Ae. japonicus* bunyavirus 2 (AejapBV2) and *Ae. japonicus* rhabdovirus 1 (AejapRV1). All six viruses showed strong RNA interference responses, including the production of 21 nucleotide sized small interfering RNAs, thus indicating active replication in the host. Notably, the two bunyaviruses AejapBV1 and AejapBV2 belong to different viral families, *Phenuiviridae* and *Phasmaviridae*, but we have not been able to find an RNA-dependent RNA polymerase (RdRp) sequence for AejapBV2. Interestingly, for the ambigrammatic narnavirus AejapNV1, our small RNA-based metagenomic approach allowed us to assemble and characterize not only the ~3 kb long primary genome segment (S1) coding for the RdRp, but also a putative ~1 kb long, ambigrammatic secondary genome segment (S2) with unknown function, which might indicate that this narnavirus is bisegmented. AejapNV1 S1 and S2, AejapTV1, AejapAV1 and AejapBV1 were all successfully detected by reverse-transcriptase PCR in wild-caught *Ae. japonicus* mosquitoes. AejapNV1 and AejapTV1 were found at very high prevalence (87-100%) in adult females, adult males and larvae, suggesting that these viruses constitute an indispensable part of the biology of *Ae. japonicus* mosquito populations.

Introduction

Mosquitoes of the *Aedes* genus are responsible for mosquito-borne viral disease outbreaks worldwide. Especially the tropical yellow fever mosquito *Aedes aegypti* and the invasive Asian tiger mosquito *Aedes albopictus* pose a large threat to human health by transmitting medically important arthropod-borne (arbo)viruses including

Zika virus (ZIKV), chikungunya virus (CHIKV), dengue virus (DENV) and yellow fever virus (178, 179). For many years now, research has mainly focused on these two urban mosquito species, but also other *Aedes* species are becoming increasingly widespread (180-182) and their role in arbovirus transmission requires further attention.

An important member of the *Aedes* genus is the Asian bush mosquito *Aedes japonicus*, which originates in Northeast Asia and has proven to be a highly invasive mosquito species (92). During the past two decades, this mosquito quickly spread to North America and Europe, where it established large, permanent populations despite intensive control efforts (92, 94). *Ae. japonicus* is capable of transmitting multiple arboviruses including West Nile virus (112, 183), Japanese encephalitis virus (184), ZIKV (97, 165), Usutu virus (USUV) (165) and CHIKV (185), and it is therefore important to understand the biology of this exotic mosquito species in more detail.

In addition to transmitting arboviruses, mosquitoes can also carry insect-specific viruses (ISVs). Whereas arboviruses are maintained in transmission cycles between arthropods and vertebrate animals or humans, ISVs do not replicate in vertebrates, and only infect insects. ISVs can persistently infect mosquito populations, and have recently received increasing attention due to their potential effects on host physiology and arbovirus transmission (66-68, 186, 187). Exploring the diversity of ISVs may also help to better understand the evolution of arboviruses and to develop new strategies for arbovirus control (188).

Extensive virome analyses that have been performed for *Ae. aegypti* and *Ae. albopictus* (70, 187, 189, 190) indicated a large diversity of ISVs in both mosquito species. For *Ae. japonicus*, however, an in-depth virome analysis is still missing, although a first glimpse has revealed the presence of a novel narnavirus in this mosquito. This narnavirus was discovered in *Ae. japonicus* mosquitoes from the Netherlands and was named *Ae. japonicus* narnavirus 1 (AejapNV1) (165). Interestingly, AejapNV1 was also found in *Ae. japonicus* mosquitoes from Japan shortly thereafter (191), indicating that this virus might be widespread and closely associated with *Ae. japonicus*. Narnaviruses are positive-sense, single-stranded RNA viruses belonging to the genus *Narnavirus* in the family *Narnaviridae* (117). Classical narnaviruses infect yeasts and oomycetes, yet the presence of narnaviruses in mosquitoes and other arthropods has only recently been described (69, 192). Traditionally, narnaviruses are thought to be non-segmented viruses with a forward open reading frame (ORF) encoding just an RNA-dependent RNA polymerase (RdRp) and no other viral proteins, hence the name narna(= naked RNA)virus (117). However, AejapNV1 belongs to a novel group of ambigrammatic narnaviruses, which contain not only an ORF coding for the RdRp on the positive strand but also a

very long ORF with unknown function on the (reverse-complement) negative strand (192, 193). This reverse ORF (rORF) is remarkable, as positive-sense RNA viruses typically encode proteins on the positive strand only (192).

Metagenomic approaches have played an essential role in uncovering the virome of vector mosquitoes and the discovery of many novel ISVs (68). Despite the success of these approaches, certain aspects of virome analysis remain challenging to fulfil using large-scale nucleic acid sequencing, such as: the detection and classification of highly divergent viral sequences that do not align to any known reference sequence (i.e., the viral 'dark matter'), the association of sequences from different genomic segments of the same virus, and the differentiation of exogenous viruses from endogenous viral elements (EVEs).

Since all viruses produce RNA molecules at some point in their replication cycle, RNA sequencing is a convenient method to explore viromes. While sequencing of long RNAs detects direct products of viral replication and transcription, sequencing of small RNAs detects viral RNA products derived from host antiviral pathways. Viral small RNAs are produced in mosquitoes when viral double-stranded RNA (dsRNA) replication intermediates are recognized and cleaved by Dicer-2, a key protein of the antiviral RNA interference (RNAi) machinery, which results in the production of 21 nucleotide (nt) small interfering RNAs (siRNAs) (194). In addition to viral siRNAs, viral PIWI-interacting RNAs (piRNAs) of ~24-29 nt in length are also produced for some viruses (194). As a result, the portion of sequenced small RNAs is naturally enriched for viral sequences (195), consequently reducing the need for sample manipulation steps such as filter-based viral enrichment and ribosomal RNA depletion, while allowing for the assembly of high-quality viral contigs. Analysis of small RNAs can also provide evidence that viral sequences are derived from actively replicating viruses when siRNA patterns are identified, and allows for a sequence-independent characterization of the assembled sequences using small RNA abundancy and size profiles to associate different viral segments to the same virus and to uncover highly divergent viral sequences without known relatives in databases (195).

In the current study, we applied a small RNA-based metagenomic approach to analyze the virome of wild-caught *Ae. japonicus* mosquitoes from populations in the Netherlands and France. By *de novo* assembly and sequence-independent analysis of the small RNA reads from *Ae. japonicus*, we identified AejapNV1 and three novel virus species in mosquitoes from the Netherlands and France. Interestingly, for AejapNV1, not only the primary genome segment (S1) encoding the RdRp was found, but we also discovered an ambigrammatic secondary genome segment (S2) with unknown function. S2 did not align to any known sequence in the databases but could be associated to the same virus using our small RNA-based metagenomic

approach. We also found (partial) sequences derived from two putative, additional novel virus species. We analyzed the genome organisation and small RNA profiles of all six discovered viruses. Moreover, reverse transcriptase PCR (RT-PCR) was used to study the prevalence of the viruses in *Ae. japonicus* adults, larvae and eggs.

Methods

Small RNA library preparation and high-throughput sequencing

Ae. japonicus adult female mosquitoes from Strasbourg, France, were collected using human landing catches (HLCs) (165) and further identified using morphological characteristics. Two pools were made prior to RNA extraction, one containing two (FR_01) individuals and another containing four (FR_02) as shown in Fig. 1A. Total RNA was isolated using TRIzol (Invitrogen) following the manufacturer's protocol. Briefly, mosquitoes were transferred to 1.5 ml screw-capped tubes containing ceramic beads (1.4 mm in diameter, Omini) and ice-cold TRIzol (Invitrogen). Mosquitoes were grinded using a Precellys Evolution Homogenizer at 6,500 rpm in 3 cycles of 20 seconds each. Then, 10 µg of glycogen (Ambion) was added to the aqueous layer of each sample to facilitate pellet visualization upon RNA precipitation. RNAs were resuspended in RNAse-free water (Ambion) and stored at -80˚C until further notice. Total RNA was used as input for library preparation utilizing the kit NEBnext Multiplex Small RNA Library Prep Set for Illumina following the recommended protocol, except for one minor modification: the 5' adapter was replaced by an analogue that contains 6 extra nucleotides at the 3' extremity to improve barcoding precision, which is sequenced along with the cloned small RNA. Libraries were sequenced at the GenomEast sequencing platform at the Institut de Génétique et de Biologie Moléculaire et Cellulaire in Strasbourg, France, using Illumina HiSeq 4000 equipment. The *Ae. japonicus* small RNA libraries from Lelystad, the Netherlands, reanalyzed in this study were previously deposited in the NCBI sequence read archive (SRA) under BioProject PRJNA545039 (165). Libraries NL_01 and NL_02 were built from pools of four and six adult females, respectively (Fig. 1A).

Small RNA-based metagenomics for virus identification

Raw reads from small RNA libraries were submitted to adapter trimming using Cutadapt v1.12 (196), and Illumina libraries from France had the 6 inserted nucleotides trimmed with the adapters. Sequences with an average Phred quality below 20, ambiguous nucleotides, and/or a length shorter than 15 nt were discarded. The remaining sequences were mapped to genome sequences of *Ae. aegypti* (AaeL5) (197), *Ae. albopictus* (198), and bacterial reference genomes using Bowtie v1.3 (199). Unmapped reads from the previous step were assembled in contigs combining metaSPAdes (200) and Velvet v1.0.13 (201). More details about k-mers and read sizes

combinations for assemblies using small RNAs in the current work can be found in (195). Contigs larger than 200 nt were characterized based on sequence similarity against the NCBI *nt* database using BLAST+ (202) and against *nr* using DIAMOND (mode *--very-sensitive*) (203), considering significant hits with *e-values* lower than $1e^{-6}$ for nucleotide comparison or $1e^{-3}$ for amino acid comparison. For small RNA size profile and coverage analysis, reads unmapped to mosquito and bacterial genomes were aligned to viral and unknown contigs using Bowtie v1.3, allowing one mismatch. Size profiles of small RNAs matching reference sequences and 5' nt frequency were calculated using in-house Perl v5.16.3, BioPerl library v1.6.924 and R v4.0.5 scripts. Plots were generated in R using ggplot2 v3.3.5 package. For manual curation of putative viral contigs, top five BLAST and DIAMOND hits were analyzed to rule out the similarity to other organisms; ORF organization and small RNA profiles (size distribution and coverage) were analyzed to differentiate exogenous from endogenous viruses and check assemblies consistency. Contigs containing truncated ORFs and small RNA profiles without symmetric small RNA peaks at 21 nt were considered putative EVEs as described in (194). For more details on manual curation steps, see (187). Redundancy of curated viral contigs was removed using CD-HIT (204) requiring 90% coverage of the smaller sequence (*-aS*) with 90% of global identity (*-c*). Representative unique contigs from the previous step were used for co-occurrence analysis based on small RNA abundancy in each of the small RNA libraries using Reads Per Kilobase of transcript per Million reads (RPKM) values for reads ranging from 20 to 22 nt aligned to the viral and unknown contigs. Hierarchical contig clusters using RPKM values were constructed in R using Euclidean distance and average method. Z-scores were calculated based on the frequency of each small RNA size from 15 to 35 nt mapped to representative viral and unknown contigs considering each strand polarity separately using the library where the contig was originally assembled. Strand polarity for contig comparisons was adjusted based on the reads abundance per strand and coding ORFs direction of each contig. Heatmaps for RPKM and Z-score values were plotted using the package ComplexHeatmap in R (205). As an attempt of viral sequence extension as proposed by Sardi et al., 2020 (206), contigs grouped in the same cluster with sequence similarity hits to the same virus were submitted to a new assembly round using SPAdes (207) with the parameter *--trusted-contigs* using all the libraries in which that viral sequences were found. Small RNA coverage and ORF structures of the extended assemblies were manually inspected to avoid spurious extensions.

Phylogenetic analyses

We selected the contig containing the largest RdRp sequence for the identified viruses. For bunyaviruses, we also selected the contigs containing the largest

sequences of nucleocapsid and glycoprotein. The presence of conserved protein domains for RdRp, nucleocapsid, and glycoprotein was confirmed with NCBI Conserved Domain Search (https://www.ncbi.nlm.nih.gov/Structure/cdd/wrpsb.cgi). The contigs were searched for potential homologous viral sequences in the NCBI *nr* database using Blastx. Coding sequences were translated to amino acids, and multiple sequence alignments were performed using MAFFT (208). The best-fit protein evolution model was selected using MEGA-X (209) under the Akaike Information Criterion. Phylogenetic inference was executed with MEGA-X using Maximum Likelihood method. For all phylogenetic trees, clade robustness was assessed using the bootstrap method (1000 pseudoreplicates). The trees were viewed using iTOL version 6.5 (210).

Analyses of CpG dinucleotide frequency and GC content

Mononucleotide frequencies, dinucleotide frequencies and the observed/expected ratios of viral and unknown sequences were determined using the function Composition Scan within SSE version 1.4 (211).

Sequence alignment and RNA structure modelling

Narnavirus RNA sequences were aligned using MUSCLE version 3.8.1551 (212). Narnavirus RNA secondary structures were predicted using the RNAstructure web server version 6.3 with temperature set to 28°C (213). Pseudoknots in totivirus RNA were predicted with DotKnot version 1.3.2 (214). RNA folding was visualised using VARNA (215).

Mosquito collection and rearing for RT-PCR

To obtain mosquito samples for RT-PCR analyses, *Ae. japonicus* mosquitoes were collected in Lelystad, the Netherlands using oviposition traps, water reservoirs in local rain barrels and HLCs as described (165) during the summer of 2020. Adult females obtained from HLCs were stored at -80°C until further analysis, whereas eggs and larvae were kept in the laboratory at 23°C and 60% relative humidity. Adult males were grown from collected eggs and larvae as described (165), and subsequently stored at -80°C. Pools of 25 eggs or individual fourth instar larvae were also stored at -80°C.

The common house mosquito *Culex pipiens* (biotype *pipiens*) was used as negative control for the RT-PCR analyses. *Cx. pipiens pipiens* mosquitoes collected in Wageningen, the Netherlands during the summer of 2020, were used to establish a laboratory colony. Mosquitoes were fed with chicken whole blood (Kemperkip, Uden, the Netherlands) through Parafilm using a Hemotek PS5 feeder (Discovery Workshops, Lancashire, United Kingdom), and reared at 23°C and 60% relative humidity. Individual adult female mosquitoes were stored at -80°C for further analysis.

Mosquito RNA isolation for RT-PCR

Frozen mosquitoes were first homogenized using a Bullet Blender Storm (Next Advance, Averill Park, NY, USA) in combination with 0.5 mm zirconium oxide beads (Next Advance; for adult mosquitoes and larvae) or 0.9-2.0 mm stainless steel beads (Next Advance; for eggs) at maximum speed for 2 min. Afterwards, the homogenates were centrifuged at maximum speed in an Eppendorf 5424 centrifuge for 1 min. The pellets were resuspended in 450 µl lysis buffer from the innuPREP DNA/RNA Mini Kit (Analytik Jena, Jena, Germany) and subsequently incubated for 20 min to lyse. Next, RNA was isolated using the innuPREP DNA/RNA Mini Kit (Analytik Jena) according to manufacturer's instructions. RNA yields were measured using a NanoDrop ND-1000 spectrophotometer.

RT-PCR analysis

Viruses were detected by RT-PCR using a 2720 Thermal Cycler (Applied Biosystems, Foster City, CA, USA) and SuperScript III One-Step RT-PCR System with Platinum *Taq* DNA polymerase (Invitrogen) according to manufacturer's protocol. In the case of a dsRNA virus, total RNA was subjected to a 5 min incubation step at 95 °C prior to the RT-PCR reaction to denature the viral dsRNA. 50 ng of mosquito total RNA was used as input for RT-PCR, and each virus was amplified using specific primers targeting the viral RdRp sequence (Table 1). For AejapNV1, primers were not only designed for the primary segment (RdRp), but also for the secondary segment (Table 1). To test the RNA quality of the samples, RT-PCRs against mosquito ribosomal protein S7 RNA were also included (Table 1).

Results

Sequence similarity-based classification of contigs

To assess the collection of viruses found in *Ae. japonicus*, two new small RNA libraries of *Ae. japonicus* from France (FR_01 and FR_02) were sequenced and two published small RNA libraries of *Ae. japonicus* from the Netherlands (NL_01 and NL_02) (165) were reanalyzed. In total, 16 adult females were pooled, resulting in four samples (Fig. 1A). The libraries were processed and analyzed following a small RNA-based metagenomic strategy optimized to detect viral sequences (Fig. 1A) (187, 195). In total, 3,269 contiguous sequences (contigs) larger than 200 nt were assembled from the four individual libraries. Solely based on sequence similarity searches against NCBI non-redundant nucleotide and protein databases (*nt* and *nr*), contigs were classified into 229 viral, 1,563 non-viral, and 1,477 unknown sequences (Fig. 1A). The proportion of each class per library is shown in Figure 1B.

Table 1. Primer sets used in this study.

Target	Primer name	Primer sequence (5'→3')	Product (bp)
Ae. japonicus narnavirus 1 primary segment	AejapNV1 S1 FW	TCGAGGTGACGACCTGGTTG	1060
	AejapNV1 S1 RV	CTTGGCCTTGACGGTCAGCT	
Ae. japonicus narnavirus 1 secondary segment	AejapNV1 S2 FW	CCTTCCGTGGAGAATACTGG	774
	AejapNV1 S2 RV	TTTGGACGGTGATACCACGG	
Ae. japonicus totivirus 1	AejapTV1 FW	CCAATAGTGAACGCCTGGTC	998
	AejapTV1 RV	GGTGCTTCCAGATGAACACC	
Ae. japonicus anphevirus 1	AejapAV1 FW	ACGCCATGCTTGCTCTAATC	1043
	AejapAV1 RV	AGCAAGGTAGGAGTCGAAGG	
Ae. japonicus bunyavirus 1	AejapBV1 FW	ACCTTCCAGAGAGCATGGAG	1095
	AejapBV1 RV	TAGCATGGGTAGATTGCAGC	
Ribosomal protein S7	RPS7 FW	ATGGTTTTCGGATCAAAGGT	175
	RPS7 RV	CGATAGCCTTCTTGCTGTTG	

Curation of viral contigs based on small RNA profile and ORF analysis

In order to discriminate sequences derived from viruses and EVEs, a curator pipeline established by Olmo et al., 2021 was followed (187), which takes advantage of the small RNA profile and ORF analysis of each contig previously classified as viral by the sequence similarity approach. Applying this filter, 93 *bona fide* viral sequences were obtained out of the 229 viral contigs. CD-HIT was used to remove viral contig redundancy, resulting in 56 unique representative viral contigs. To evaluate only the natural circulating virome, 3 USUV and 14 ZIKV contigs from artificial infections assembled in libraries NL_01 and NL_02 were removed, obtaining a total of 39 unique representative sequences. Figure 1C shows an overview of the manual curation of viral contigs and filters to differentiate exogenous from endogenous viruses to establish the virome of *Ae. japonicus*.

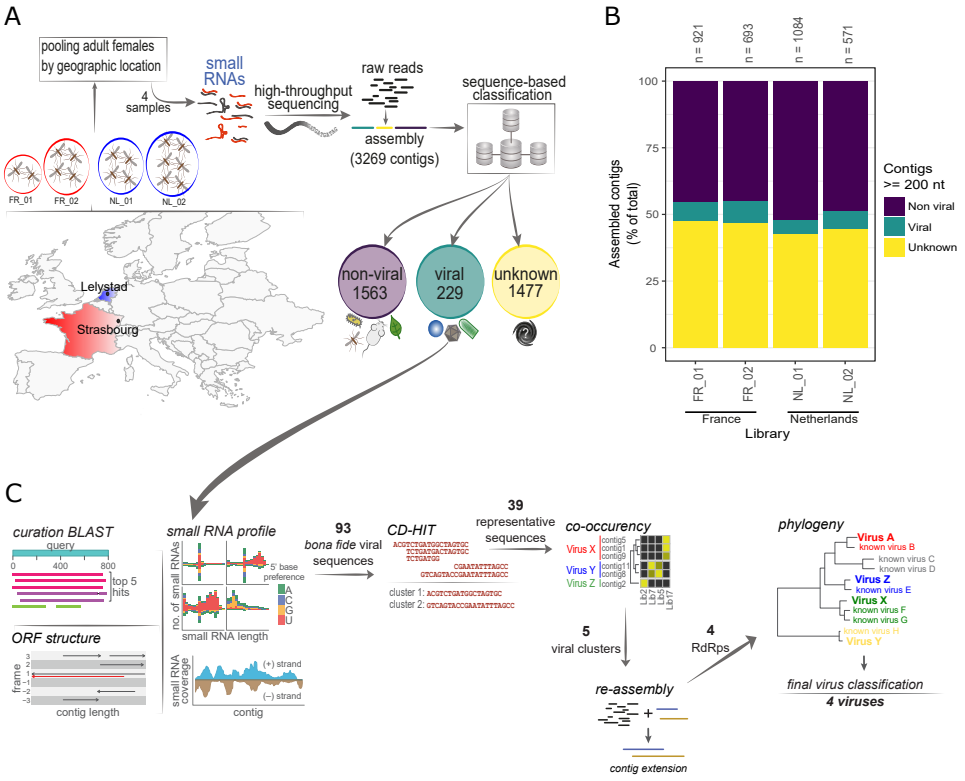

Figure 1. Analysis of the *Ae. japonicus* virome using a small RNA-based metagenomic approach. (A) Map of Europe indicating mosquito collection sites: Strasbourg, France (red) and Lelystad, the Netherlands (blue). Pools with the number of sampled mosquitoes from Strasbourg are indicated inside the red circles (FR_01 two mosquitoes and FR_02 four mosquitoes) and from Lelystad inside the blue circles (NL_01 four mosquitoes and NL_02 six mosquitoes). Captured mosquitoes were morphologically identified by species. Samples were used to prepare small RNA libraries for high-throughput sequencing. Sequencing results were analyzed using our metagenomic pipeline. Assembled contigs were classified into non-viral, viral, and unknown sequences based on sequence similarity against reference databases. **(B)** Individual results from our sequence similarity analysis for each of the four small RNA libraries in this study. The total number of contigs bigger than or equal to 200 nt (n) and the proportion of non-viral, viral and unknown contigs are shown. **(C)** Overview of the manual curation strategy to differentiate sequences of *bona fide* exogenous viruses from sequences potentially derived from EVEs. Curation consisted of BLAST search for similar viral sequences, inspection of ORF structure including continuity and overall extension throughout the contig, and the evaluation of the small RNA profile including symmetrical accumulation of RNAs with 21 nt length that mapped to each contig strand with no 5' base preference (siRNA signature) or accumulation of 24-29 nt RNAs with 5' U preference (piRNA signature) and overall contig coverage by small RNAs. Contigs presenting continuous ORFs and siRNA profile were clustered based on sequence similarity for redundancy removal using CD-HIT, and on co-occurrence in each library to identify groups of contigs that belong

to the same virus. Re-assembly was performed within these groups and resulting contigs were analyzed for the presence of functional protein domains. Potential polymerases were identified and used to classify viruses based on sequence similarity and phylogeny.

Small RNA-based co-occurrence and viral contig clustering

In order to try to associate different segments of the same virus, and determine the number of unique viruses, we evaluated co-occurrence of the viral sequences in the four libraries. In this regard, we determined the normalized number of small RNA reads mapped to each of the 39 representative viral contigs. In addition, the 22 unknown contigs larger than 500 nt that did not align to any known reference sequence in the databases but passed the same filters based on small RNA and ORF inspection were also included in the analysis. Contigs that consistently co-occurred, shared similar small RNA size profiles, and grouped in the same hierarchical cluster based on small RNA counts, were considered probable fragments from the same virus (Fig. 2).

This analysis identified five distinct clusters of co-occurring contigs in which most of the contigs showed significant similarity to the same reference virus. Contigs inferred to be from the same virus were colored equally (Fig. 2). In red, there is a consistent cluster containing contigs with high sequence similarity to AejapNV1 and one unknown contig (NL_02_Contig12989_12988). In blue, there are contigs with high sequence similarity to different segments of a bunyavirus (named *Ae. japonicus* bunyavirus 1 (AejapBV1)). These contigs form a consistent cluster, except for one contig with high similarity to a bunyavirus glycoprotein (FR_01_Contig9275_9274) that is out of this cluster. In green, there is a large consistent cluster of sequences with high similarity to an anphevirus (named *Ae. japonicus* anphevirus 1 (AejapAV1)), and two unknown contigs. There is a contig with high sequence similarity to an anphevirus (NL_01_Contig6957_6956) that falls out of the main green cluster and groups with other unknown contigs. There are two contigs with significant sequence similarity to a different bunyavirus (named *Ae. japonicus* bunyavirus 2 (AejapBV2); in purple) and one to a totivirus (named *Ae. japonicus* totivirus 1 (AejapTV1); in yellow) forming one cluster. In brown, there are two contigs with high sequence similarity to a rhabdovirus (named *Ae. japonicus* rhabdovirus 1 (AejapRV1) forming a clear cluster. All the non-colored contigs are unknown contigs that could not clearly be associated to a specific virus based on our clustering analysis.

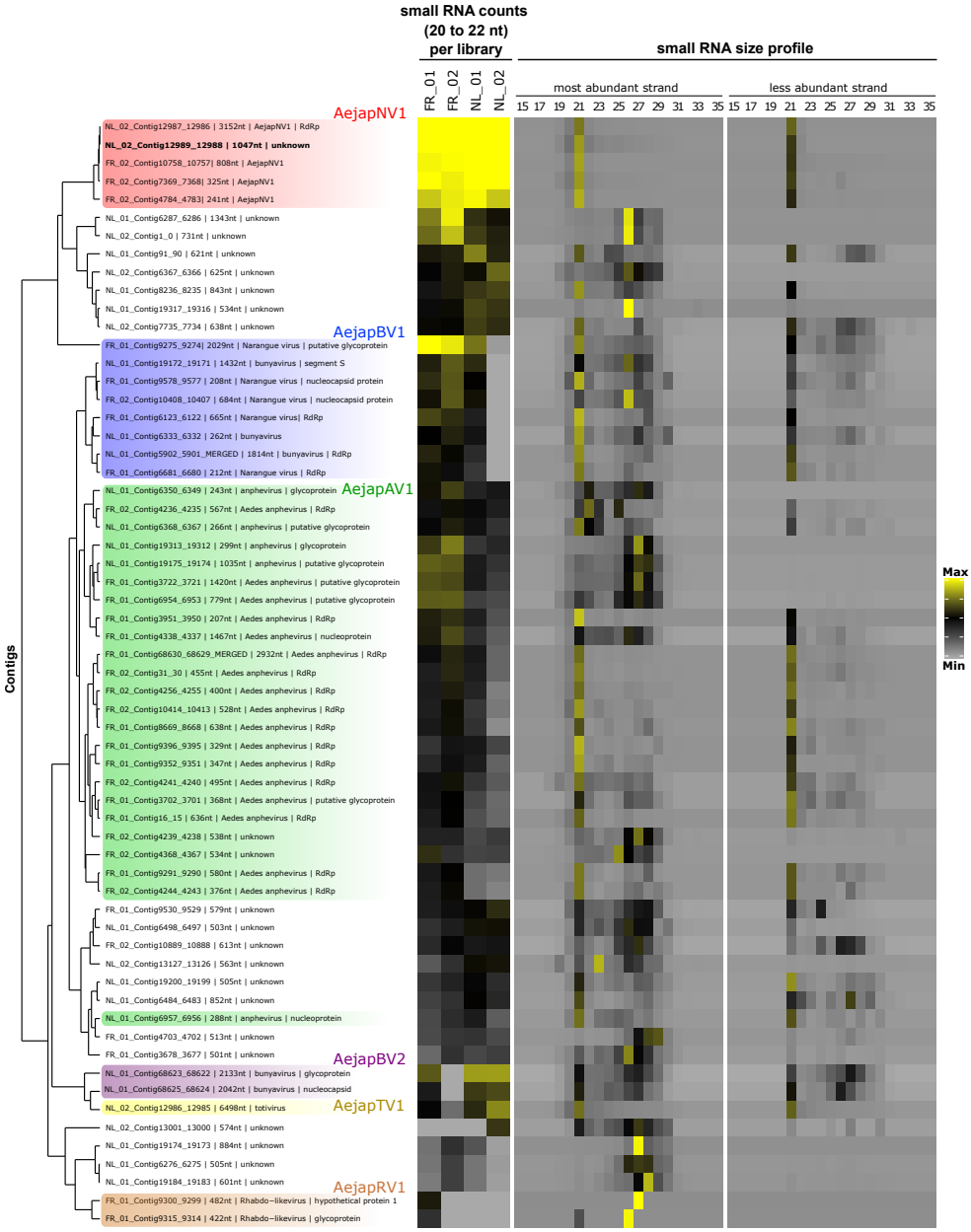

Figure 2. Co-occurrence of viral and unknown contigs. Hierarchical clustering of viral and unknown contigs assembled from small RNAs derived from *Ae. japonicus*. Clustering was based on Euclidean distance of RPKM values of small RNA counts with size from 20 to 22 nt in each library applying Average method. Contig clusters were defined using the dendrogram. Contigs inferred to be from the same virus were colored equally. Heatmap on the left represents the small RNA abundance for each curated contig in *Ae. japonicus* libraries. We plotted the Log2 of the

RPKM values of small RNA counts with sizes from 20 to 22 nt (maximum value: 10; minimum value: 0). Heatmap on the right represents Z-score values for small RNAs from each size from 15 to 35 nt divided by strand polarity in the library in which the contig was originally assembled (maximum value: 7; minimum value: -1).

Virus identification

To identify unique viruses based on the structure of the clusters (Fig. 2), we focused on sequences encoding viral polymerases. It was possible to identify contigs encoding viral polymerase sequences for four of our clusters of viral contigs. The largest contig within each cluster that showed significant sequence similarity to a viral polymerase was compared to the closest sequence in GenBank, which suggested that they represented at least four different viruses (Table 2). One virus, AejapNV1 (genus *Narnavirus*, family *Narnaviridae*), is known and had been previously identified as a possible ISV (165). According to phylogenetic analysis (Fig. 3), this virus clustered with other mosquito-associated narnaviruses containing long rORFs from the *Alphanarnavirus* clade (192).

The contigs containing viral polymerase sequences for AejapTV1, AejapAV1 and AejapBV1 (segment L) do not have significant sequence similarity at the nucleotide level to other viruses in GenBank and presented relatively low sequence similarity at the amino acid level to other viral sequences, indicating they represent new viral species (Table 2). Based on comparisons to the closest GenBank reference sequence, the entire segment L of AejapBV1 could not be assembled nor the entire genome of AejapAV1. In Supplementary Figure 1, the genomic structures of the reference sequences and the portions covered by our *de novo* assembled contigs are shown. Phylogenetic analyses confirmed that AejapTV1, AejapAV1 and AejapBV1 are likely new viruses (Fig. 3) belonging to the *Totiviridae*, *Xinmoviridae,* and *Phenuiviridae* families, respectively (Table 2). All three new viruses were most closely related to known ISVs (Fig. 3; Table 2), but their final classification requires biological characterization. All four identified viruses, one known and three new, have RNA genomes, either single-stranded (of positive or negative polarity) or double-stranded (Table 2).

We could also infer two other probable distinct virus species, AejapBV2 and AejapRV1, but for both, we were not able to find contigs coding for a viral polymerase protein (Table 2, Suppl. Fig. 1B and D). Despite the fact that the two contigs of AejapBV2 clustered with the contig of AejapTV1 based on their similar level of small RNA counts in the four libraries (Fig. 2), there is no further evidence to associate these sequences to the same virus. Instead, our overall analysis including small RNA size profiles (Fig. 2) and sequence comparisons indicate that they are distinct and belong to completely different viruses.

The entire genomic segments M and S of AejapBV1 and AejapBV2 could be successfully assembled, except for a small 5' portion of the AejapBV1 segment S in which, despite the concordant number of amino acids in the ORF, a start codon corresponding to the same region in the closest GenBank reference could not be identified (Suppl. Fig. 1A). The phylogenetic analysis of amino acid sequences shows that AejapBV2 contigs coding for the glycoprotein and nucleocapsid are distant from AejapBV1 equivalent sequences (Fig. 4). Based on the sequence similarity and phylogenetic analysis of nucleocapsid and glycoprotein of AejapBV2, this virus belongs to the family *Phasmaviridae* (Fig. 4; Table 2).

Apart from ZIKV and USUV, which were introduced by artificial infection, additional known arboviruses were not detected in our metagenomic analysis.

Table 2. Viruses discovered by *de novo* assembly of small RNA reads from *Ae. japonicus* mosquitoes collected in the Netherlands and France. For each virus (segment), the length in nucleotides of the largest assembled contig is shown (query size). These contigs were used for a BLAST search. The GenBank accession of the closest subject is indicated, as well as the query coverage, identity, and E-value. Asterisks indicate putative novel virus species, for which we were unable to detect RdRp sequences.

Virus	Segment	Virus family	Genome	Query size (nt)	Query coverage (%)	Identity (%)	E-value	Type	Subject accession
AejapNV1	1	*Narnaviridae*	+ssRNA	3152	100	100	0.0	nt	MK984721.2
	2			1047	N/A	N/A	N/A	N/A	N/A
AejapTV1	N/A	*Totiviridae*	dsRNA	6498	47	60	0.0	aa	AJT39583.1
AejapAV1	N/A	*Xinmoviridae*	-ssRNA	2932	99	58	0.0	aa	AWW13479.1
AejapBV1	L	*Phenuiviridae*	-ssRNA	1814	96	35	5.0e-9	aa	QHA33858.1
	M			2029	85	42	1.0e-142		QHA33860.1
	S			1432	55	44	8.0e-62		QHA33859.1
*AejapBV2	M	*Phasmaviridae*	-ssRNA	2133	88	44	0	aa	YP_009305132.1
	S			2042	52	54	5.0e-126		YP_009305134.1
*AejapRV1	N/A	Unknown	-ssRNA	482	57	38	2.0e-8	aa	QIS62330.1

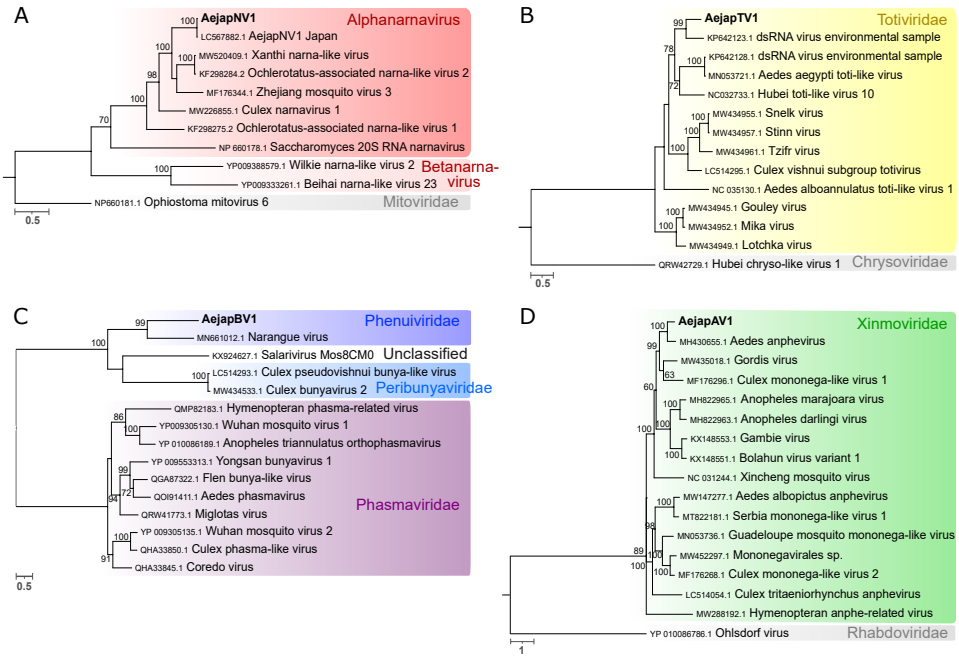

Figure 3. Phylogeny of viruses identified in *Ae. japonicus* mosquitoes. Phylogenetic trees were generated using the multiple sequence alignments of RdRp amino acid sequences. The trees were inferred by using the Maximum Likelihood method. The tree with the highest log likelihood is shown for each virus. Number of conserved sites and the substitution models used for each tree: **(A)** AejapNV1, 1446 sites, LG+G+F; **(B)** AejapTV1, 1269 sites, LG+G; **(C)** AejapBV1, 693 sites, LG+G+F; **(D)** AejapAV1, 1188 sites, LG+G+I+F. Node bootstraps were calculated with 1000 replicates and are shown close to each clade and values < 60 were omitted. Trees were midpoint-rooted, and RdRp sequences from distinct viral families were included in the alignments as outgroups. The trees are drawn to scale, branch lengths represent expected numbers of substitutions per amino acid site. Accession numbers for the nucleotide sequences from which the corresponding protein sequences were derived or the direct protein sequences are shown with the virus names. Viruses identified in this study are in bold.

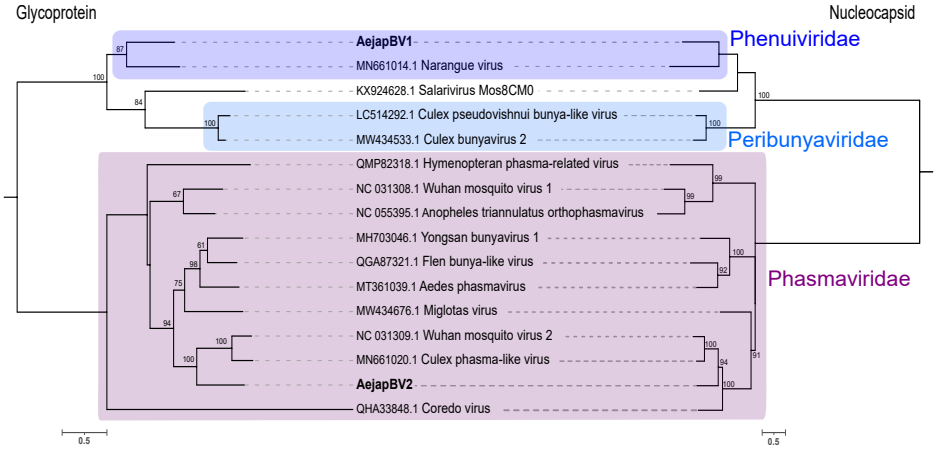

Figure 4. Phylogeny of glycoprotein and nucleocapsid of AejapBV1 and AejapBV2. Phylogenetic trees were generated using the glycoprotein and nucleocapsid amino acid sequences. The trees were inferred by using the Maximum Likelihood method. The trees with the highest log likelihood are shown. Number of conserved sites and the substitution models used for each tree: glycoprotein, 796 sites, WAG+G+F, and nucleocapsid, 573 sites, LG+G. Node bootstraps were calculated with 1000 replicates and are shown close to each clade and values < 60 were omitted. Trees were midpoint-rooted, and sequences from distinct viral families were included in the alignments. The trees are drawn to scale, branch lengths represent expected numbers of substitutions per amino acid site. Accession numbers for the nucleotide sequences from which the corresponding protein sequences were derived or the direct protein sequences are shown with the virus names. Viruses identified in this study are in bold.

Genome composition analysis

To further characterize the identified viruses (Table 2), the CpG dinucleotide usage and the GC content of their genomes were analyzed, as both these features are known to markedly differ between the genomes of distinct virus families (216-218) and can therefore help to classify viruses. The largest representative sequence of each virus or viral segment identified was analyzed (Table 2). Moreover, the 22 unknown contigs larger than 500 nt in length were also included in an attempt to find possible associations between the viral and unknown sequences. The L, M and S segments of AejapBV1 (blue) and the M and S segments of AejapBV2 (purple) all showed CpG underrepresentation and a relatively low GC content (Fig. 5). Thus, although these two bunyaviruses were found in distant, separate clusters based on small RNA counts (Fig. 2), features of their genome composition were similar. In contrast, AejapTV1 and AejapBV2 clustered together based on small RNA counts (Fig. 2), but these viruses greatly differed in their CpG usage and GC content (Fig. 5), thus suggesting that, despite their similar levels of produced small

RNAs, they are indeed different viruses. It was also found that the positive-stranded AejapNV1 (red) had a relatively high GC content, whereas for the negative-stranded AejapBV1, AejapBV2, AejapAV1 (green) and AejapRV1 (brown), the GC content was relatively low (Fig. 5). This is in accordance with a previous study in which positive-sense RNA viruses were shown to have significantly higher GC contents as compared to negative-sense RNA viruses (218). Interestingly, one of the unknown contigs (NL_02_Contig12989_12988; indicated by the arrow) showed a relatively high GC content and an unbiased CpG frequency, similar to AejapNV1 (Fig. 5). This contig also clustered together with AejapNV1 based on small RNA counts (Fig. 2; in bold), and the genome composition results hence further increase the likeliness that this unknown contig belongs to AejapNV1.

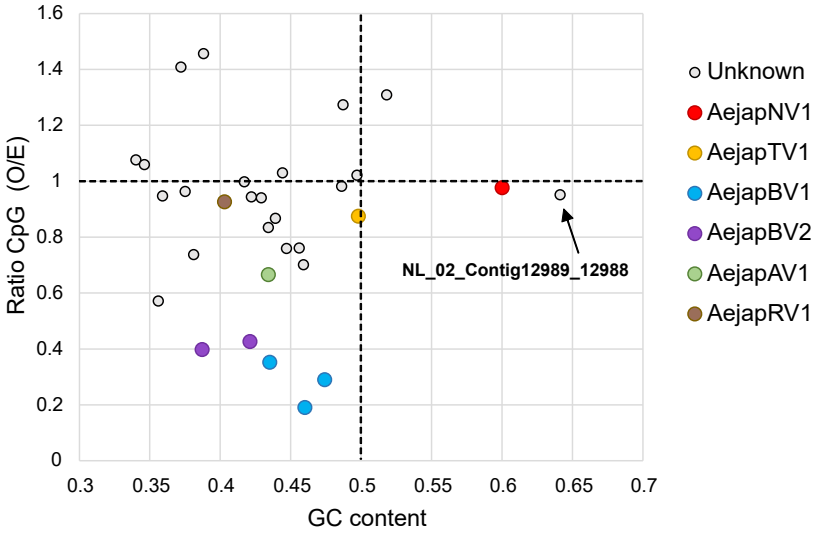

Figure 5. CpG dinucleotide usage and GC content of viral and unknown sequences discovered in *Ae. japonicus*. Data points indicate the ratio of GC content (X-axis) and CpG dinucleotide frequency (Y-axis) of individual viral or unknown sequences. The GC content of 0.5 (vertical dotted line) is the expected frequency if the genome would consist of 50% GC and 50% AT. The observed/expected (O/E) CpG ratio of 1.0 (horizontal dotted line) is the expected frequency of CpG occurrence when all mononucleotides in a given RNA sequence would be randomly distributed.

Small RNA profiles and genome organisation of AejapNV1

Within the cluster of assembled AejapNV1 sequences (Fig. 2; in red), we found the ~3 kb long, ambigrammatic AejapNV1 genome sequence encoding the RdRp (NL_02_Contig12987_12986) and an unknown sequence (NL_02_Contig12989_12988) of ~1 kb in length that did not align to any known sequence from the databases

but showed similar CpG usage and GC content as the AejapNV1 RdRp sequence (Fig. 5). The small RNA size distribution profile, small RNA coverage profiles, and ambigrammatic coding strategy of the unknown contig were also very similar to the AejapNV1 genome sequence coding for the RdRp (Fig. 6A, 6B). The unknown contig was therefore suspected to be part of AejapNV1 and named AejapNV1 segment 2 (S2), whilst the AejapNV1 sequence encoding the RdRp is now referred to as segment 1 (S1) (Table 2). For S1, a strong bias of mapped 24-29 nt small RNAs towards the positive RdRp strand was observed (Fig. 6A). Similarly, S2 also showed preference of mapped 24-29 nt small RNAs towards one specific strand (Fig. 6A). Analysis of the small RNA coverage profiles of AejapNV1 S1 and S2 for each small RNA length separately indicated a bias of small RNAs (18-35 nt in length) towards the same specific strand for each small RNA length, except for 21 nt small RNAs, which were found in similar quantities on both strands (Suppl. Fig. 2). This asymmetric pattern for small RNAs sized 18-20 nt and 22-35 nt is likely caused by non-specific degradation of the most abundant viral RNA strand (219), which is often the positive strand. For AejapNV1 S1, the small RNA bias was indeed towards the positive RdRp strand (Suppl. Fig. 2). It is therefore reasonable to assume that the positive strand of AejapNV1 S2 is the strand to which most small RNAs mapped.

To further investigate whether the putative S2 of AejapNV1 was indeed related to S1 and could thus be of narnaviral origin, the 5' and 3' termini of both segments were analyzed for the presence of conserved narnaviral sequences. The *Alphanarnavirus* clade contains the prototypical narnaviruses such as *Saccharomyces cerevisiae* 20S RNA narnavirus (Scer20SNV) and the mosquito-associated narnaviruses containing an rORF. These viruses contain short, complementary runs of G and C nucleotides at their 5' and 3' termini, respectively, and have a conserved RNA stem-loop (SL) structure at their 3' end (192, 220). In addition, it has very recently been described that the mosquito-associated, ambigrammatic *Culex* narnavirus 1 (CxNV1) (102) also consists of two segments (an RdRp segment, hereafter named S1, and a Robin segment, hereafter named S2), which both show these typical, conserved features at the 5' and 3' genomic termini (221). Using a multiple sequence alignment, the terminal sequences of AejapNV1 S1 and S2 were compared with genomes from four ambigrammatic narnaviruses found in mosquitoes (CxNV1 S1, GenBank MW226855.1; CxNV1 S2 Genbank MW226856.1; Xanthi narna-like virus (XaNLV), GenBank MW520409.1; *Ochlerotatus*-associated narna-like virus 2 (ONLV2), GenBank KF298284.2; *Ochlerotatus*-associated narna-like virus 1 (ONLV1), GenBank KF298275.1) and the yeast-infecting Scer20SNV (GenBank NC_004051.1). For all viruses and segments analyzed, short runs of G and C nucleotides were present at the 5' and 3' termini (Fig. 6C, indicated by asterisks). Based on RNA structure modelling, a conserved SL structure was predicted to occur

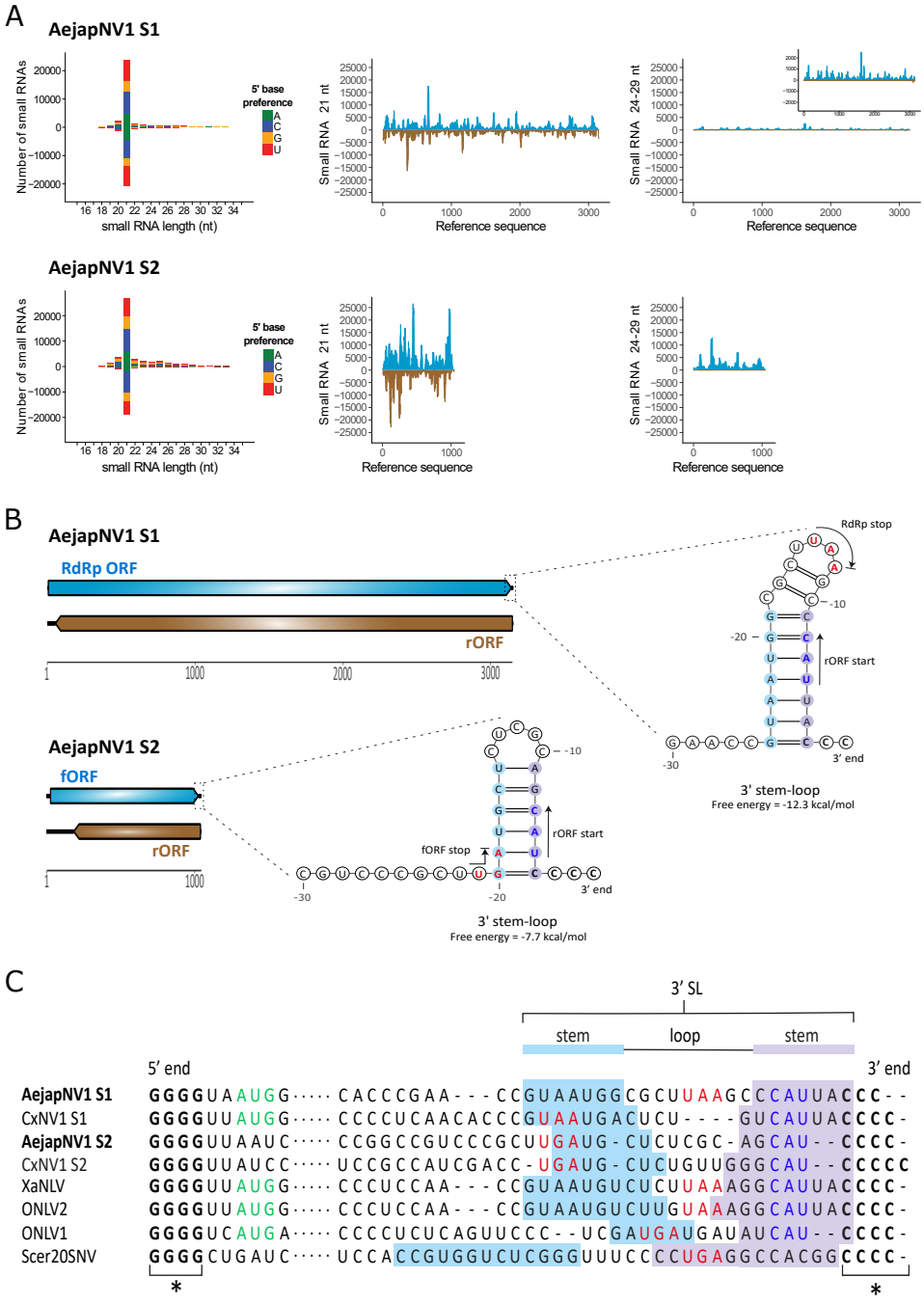

Figure 6. Small RNA profiles and genome organisation of AejapNV1. (A) Left: size distribution and 5' base preference of small RNAs derived from AejapNV1 S1 and S2. Middle and right: coverage of 21 and 24-29 nt sized small RNAs across S1 and S2. Viral reads mapping

to the positive strand are shown in blue, whereas viral reads mapping to the negative strand are shown in brown. **(B)** Genome organisation of AejapNV1. The ambigrammatic coding strategy of S1 and S2 is shown. RdRp ORF and forward ORF (fORF) on the positive strand are shown in blue, whereas reverse ORFs (rORFs) on the negative strand are shown in brown. Untranslated regions are indicated by black lines. Predicted stem-loop structures at the 3' terminus of the positive-sense RNA strand are also shown for both segments. The locations of start and stop codons are indicated by arrows and colored blue and red, respectively. **(C)** Multiple sequence alignment of the 5' and 3' termini of the positive strand for indicated narnaviruses. Asterisks (*) indicate conserved, complementary runs of G or C nucleotides at the 5' or 3' end, respectively. Dots represent the remainder of the viral genome. Start codons of RdRp ORF are in green, stop codons of RdRp ORF / fORF are in red, start codons of rORF are in blue. The start codons of the fORFs of AejapNV1 S2 and CxNV1 S2, as well as the start codon of the RdRp ORF of Scer20SNV, are located more than 10 nt downstream of the 5' end and therefore not shown in the alignment. The nucleotides involved in 3' stem-loop (3' SL) formation are indicated.

at the 3' terminus of AejapNV1 S1 and S2 (Fig. 6B, 6C). Similar conserved SL structures at the 3' terminus, differing in size and with covarying base pairs in the stem region (Fig. 6C), have previously been observed for CxNV1 S1 and S2 (221), ONLV1, ONLV2 (192) and Scer20SNV (220), and could also be found for XaNLV (Suppl. Fig. 3). The presence of these conserved narnaviral characteristics in the genomic termini of both S1 and S2 of AejapNV1 not only indicated that our small RNA sequencing method was able to recover (near) complete genomic sequences, but also further confirmed the presumed association between AejapNV1 S1 and the newly discovered S2.

Small RNA profiles and genome organisation of AejapTV1

Mapping of small RNAs on the AejapTV1 contig (Fig. 2; in yellow) resulted in a 21 nt siRNA peak (Fig. 7A), which suggests active RNA replication in mosquitoes. Small RNAs mapped across the entire assembled sequence (Fig. 7A), which contained a capsid ORF followed by an RdRp ORF (Fig. 7B). The two ORFs were encoded in different frames (Fig. 7B). Ribosomal frameshifting is one of the strategies employed by members of the family *Totiviridae* to express the RdRp (222, 223), and it was therefore investigated whether this strategy could potentially be employed by AejapTV1. Based on RNA structure modelling, a putative -1 ribosomal frameshift area was discovered at the end of the capsid ORF (Fig. 7B). The slippery site (GGAAAAC), present just before the stop codon of the capsid ORF, corresponded to the heptameric consensus motif typical for -1 ribosomal frameshifts and represents the area where the ribosome shifts back into another reading frame (224). Right after the slippery site, a spacer region of 5 nucleotides in length was found (Fig. 7B). This region was followed by a highly structured area consisting of a three-stemmed pseudoknot (Fig. 7B), which is expected to be responsible for pausing and relocating the ribosome.

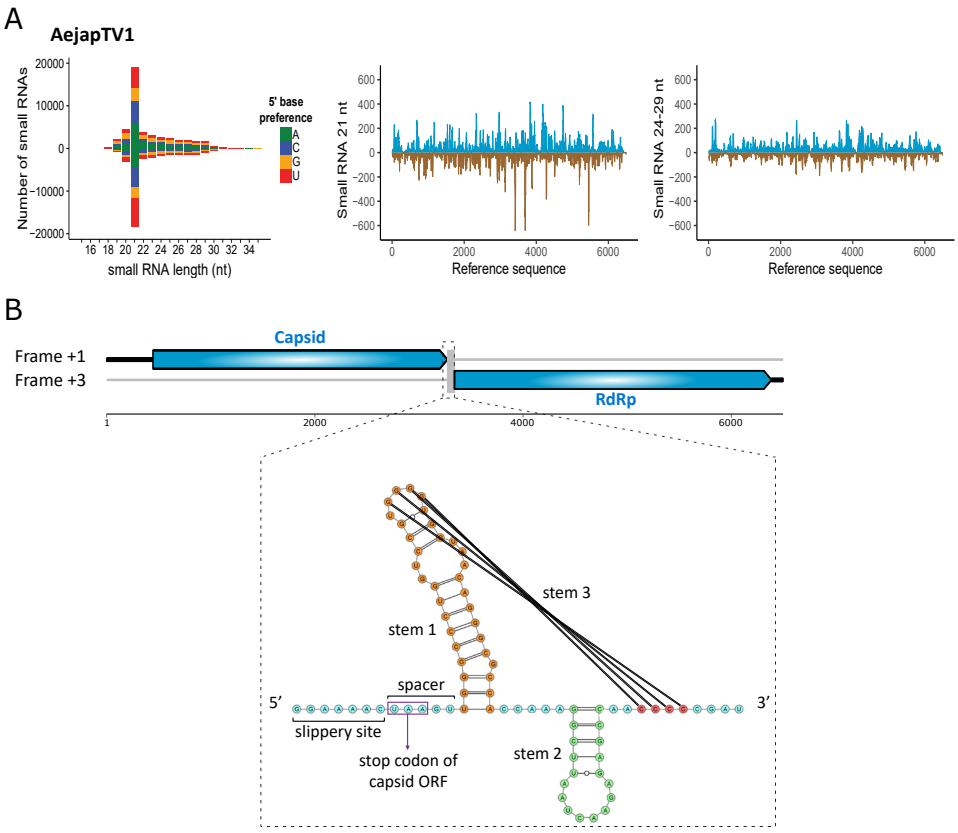

Figure 7. Small RNA profiles and genome organisation of AejapTV1. (A) Left: size distribution and 5' base preference of small RNAs derived from AejapTV1. Middle and right: coverage of 21 and 24-29 nt sized small RNAs across the genome of AejapTV1. Viral reads mapping to the positive strand are shown in blue, whereas viral reads mapping to the negative strand are shown in brown. **(B)** Genome organisation of AejapTV1. Untranslated regions are indicated by black lines. Capsid and RdRp ORFs on the positive strand are shown in blue. These ORFs are encoded in different frames, and a putative -1 ribosomal frameshift area was observed in between the two ORFs. This area consisted of a slippery heptamer, a spacer region, and a predicted three-stemmed pseudoknot with a free energy of -33.97 kcal/mol.

Small RNA profiles of AejapBV1, AejapBV2, AejapAV1 and AejapRV1

For AejapBV1 and AejapBV2, a 21 nt siRNA peak was observed for all three (Fig. 8A) or two (Fig. 8B) segments, respectively, and siRNAs aligned across entire segments. Also, piRNAs of ~24-29 nt in length were detected for both viruses (Fig. 8A, 8B). Antisense piRNAs showed preference for U nucleotides at their 5' position (Fig. 8A, 8B), which is in accordance with the common piRNA signature associated with ping-pong amplification (225).

Similar to AejapBV1 and AejapBV2, AejapAV1 also showed a 21 nt siRNA peak, as well as ~24-29 nt sized piRNAs with U nucleotide preference at the 5' end (Fig. 9A). AejapRV1 also produced siRNAs of 21 nt, as well as piRNA sized small RNAs (Fig. 9B).

Screening of field-collected *Ae. japonicus* mosquitoes for the presence of novel viruses

To evaluate whether the *de novo* assembled viruses were present in field-collected *Ae. japonicus*, RT-PCR assays were designed using primers targeting the RdRp coding region of AejapNV1, AejapTV1, AejapAV1 or AejapBV1. Moreover, RT-PCRs with primers targeting S2 of AejapNV1 were also performed to confirm the presence of this putative segment. All four viruses were successfully detected in (pools of) field-collected adult *Ae. japonicus* females, whilst they could not be detected in adult *Cx. pipiens* females that were tested in parallel (Fig. 10A). For AejapNV1, the presence of both S1 and S2 in *Ae. japonicus* was confirmed (Fig. 10A).

Next, *Ae. japonicus* adult females, adult males, larvae and egg pools were screened for the presence of AejapNV1 S1 and S2. Both segments were present at very high prevalence (close to 100%) in all tested mosquito life stages (Fig. 10B). Screening of *Ae. japonicus* mosquitoes for AejapTV1 resulted in 100% virus-positive adult females, 87% virus-positive adult males and 88% virus-positive larvae (Fig. 10C). The high prevalence of AejapNV1 and AejapTV1 in *Ae. japonicus* across all tested mosquito life stages may suggest vertical transmission of these viruses.

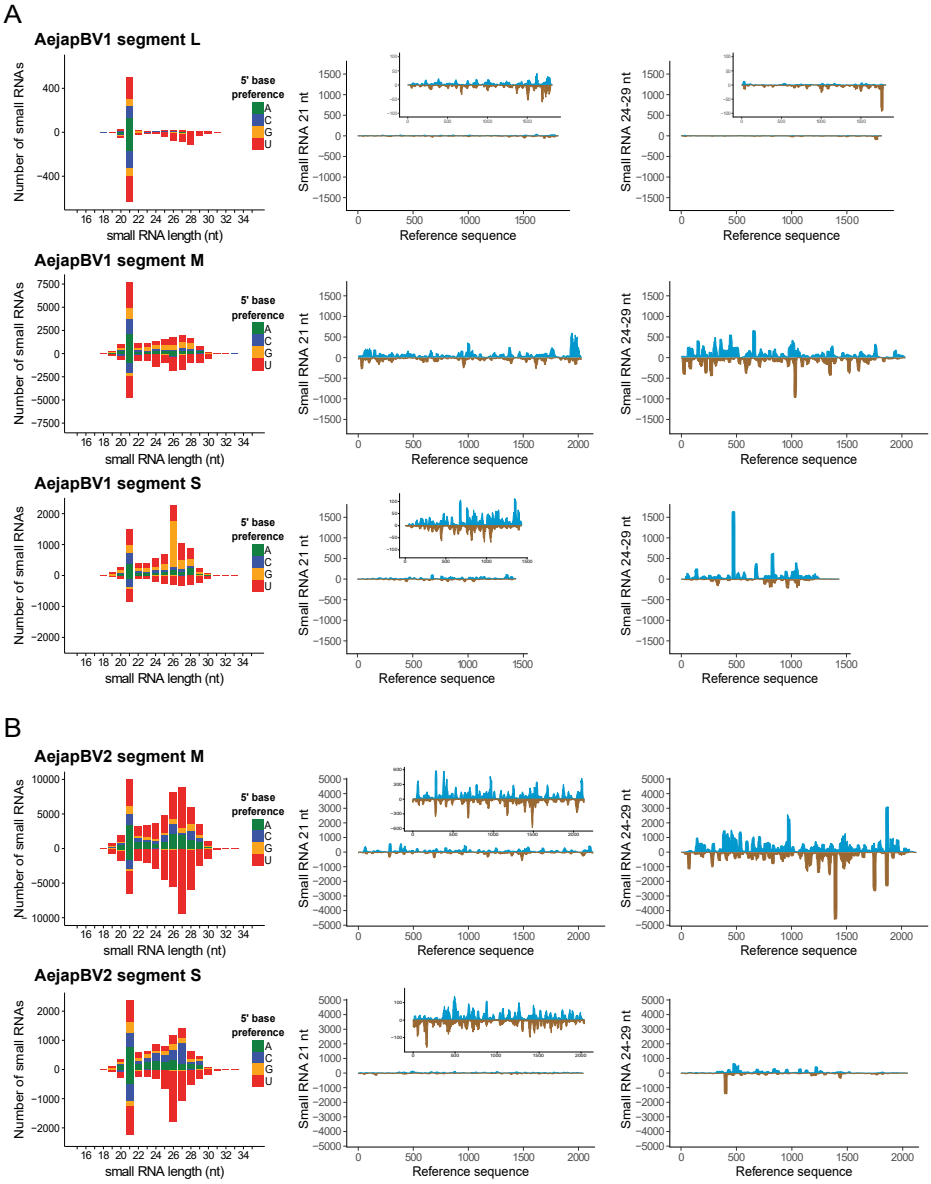

Figure 8. Small RNA profiles of AejapBV1 and AejapBV2. Size distribution and 5' base preference of small RNAs derived from **(A)** AejapBV1 segments L, M and S and **(B)** AejapBV2 segments M and S are shown on the left, whereas coverage of 21 and 24-29 nt sized small RNAs across the same segments of the respective viruses is shown in the middle and on the right. For the coverage profiles, viral reads mapping to the positive strand are indicated in blue, whereas viral reads mapping to the negative strand are indicated in brown.

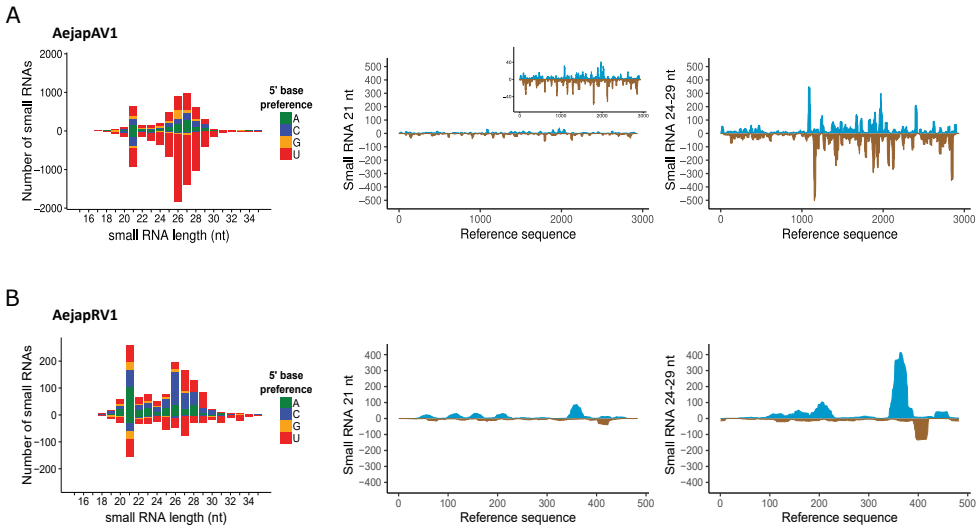

Figure 9. Small RNA profiles of AejapAV1 and AejapRV1. Size distribution and 5' base preference of small RNAs derived from **(A)** AejapAV1 and **(B)** AejapRV1 are shown on the left. In the middle and on the right, the coverage of 21 and 24-29 nt sized small RNAs across the assembled contigs of the same respective viruses is shown. For the coverage profiles, viral reads mapping to the positive strand are indicated in blue, whereas viral reads mapping to the negative strand are indicated in brown.

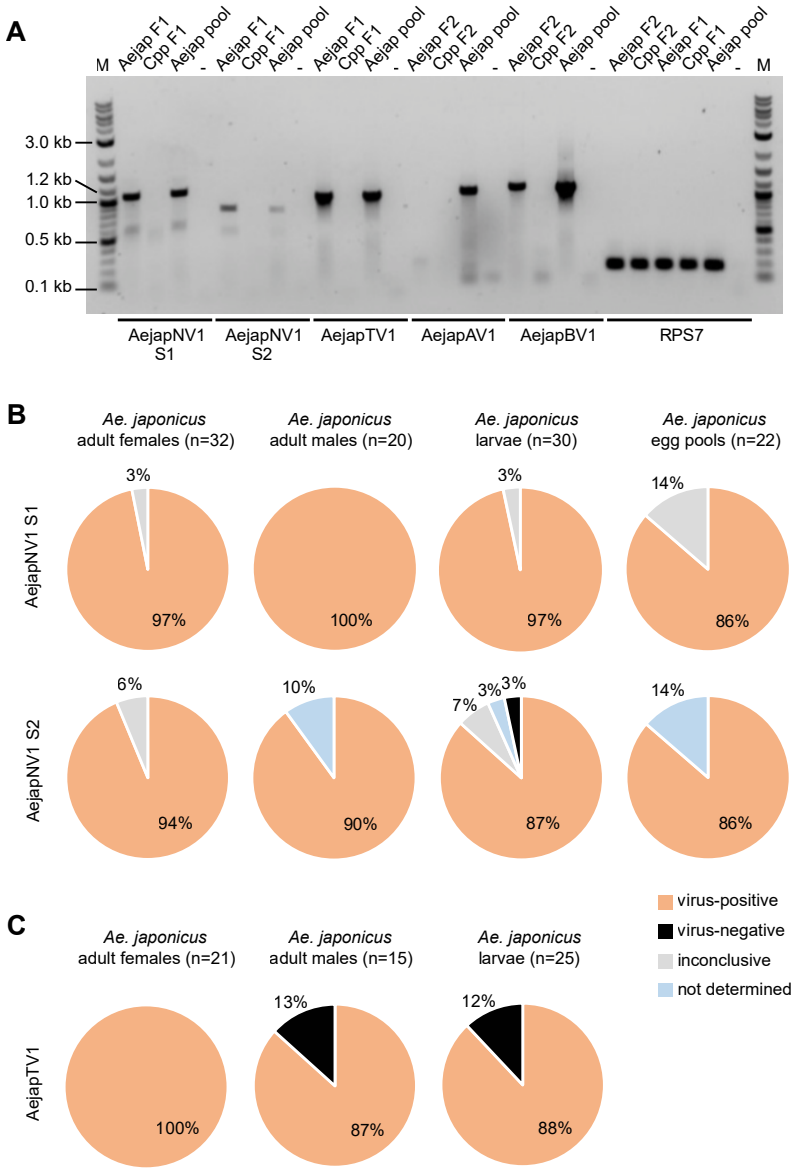

Figure 10. Detection of AejapNV1 S1 and S2, AejapTV1, AejapAV1 and AejapBV1 in field-collected *Ae. japonicus* from the Netherlands by RT-PCR. (A) Individual adult female *Ae. japonicus* (Aejap F1, F2), individual adult female *Cx. pipiens pipiens* (Cpp F1, F2), a pool of four *Ae. japonicus* adult females (indicated by 'Aejap pool') and a water sample (no RNA; negative control, indicated by '-') were tested for presence of the viruses. All samples were also tested for mosquito ribosomal protein S7 (RPS7) to check the quality of the RNA. Expected amplicon sizes were: 1060 bp (AejapNV1 S1), 774 bp (AejapNV1 S2), 998 bp (AejapTV1), 1043 bp (AejapAV1), 1095 bp (AejapBV1) and 175 bp (RPS7). Aejap F1 tested positive for

AejapNV1 S1 and S2, and also for AejapTV1. Aejap F2 tested negative for AejapAV1, but positive for AejapBV1. The pool of *Ae. japonicus* females was positive for all tested viruses. *Cx. pipiens* females tested negative for all viruses. The lanes indicated with 'M' contain the DNA marker. **(B)** Prevalence of AejapNV1 S1 and S2 in *Ae. japonicus* adult females, adult males, larvae and pools of 25 eggs. Individual samples were screened by RT-PCR. The number of samples tested is indicated by 'n'. Results were marked as inconclusive when samples tested virus-negative the first time, and this could not be confirmed a second time due to lack of RNA, whereas parallel samples in the same assay which tested virus-negative the first time, tested virus-positive the second time. **(C)** Prevalence of AejapTV1 in *Ae. japonicus* adult females, adult males and larvae. Individual samples were screened by RT-PCR. The number of samples tested is indicated by 'n'.

Discussion

In this study, we analysed the virome of *Ae. japonicus* and found four virus species and two putative virus species associated with this invasive vector mosquito. All six viruses showed potent siRNA responses, thus indicating active viral replication in their host (226).

Although only four libraries were sequenced, our small RNA-based metagenomic approach, initially proposed by Aguiar et al., 2015 (195), allowed us to address the three main challenges of eukaryotic viral metagenomics: i) the differentiation of exogenous viruses from EVEs, ii) the association of different segments of the same virus, and iii) the identification and classification of highly divergent viral sequences that do not align to any known reference sequence. Our initial search for siRNA profiles among the assembled contigs resulted in a confident dataset of *bona fide* exogenous viral sequences, allowing us to uncover the real circulating virome of *Ae. japonicus*. The clustering approach based on small RNA counts allowed us to estimate the number of unique viruses in our samples by associating contigs from distinct viral segments to the same virus (Fig. 2). After careful curation of the sequences and clustering analysis, we observed that this clustering approach is not perfect. In cases like the narrow clustering of contigs from AejapBV2 (purple) and AejapTV1 (yellow), it is clear that the contigs do not belong to the same virus. But such inconsistency can be immediately noticed when other sequence features and the small RNA size profiles (Fig. 2) are taken into account, thus not invalidating the overall benefits of this approach.

Of the *Ae. japonicus*-associated viruses, AejapNV1 induced the strongest RNAi response in *Ae. japonicus*. *De novo* assembly of small RNAs did not only yield the ~3 kb long primary genome segment S1 for AejapNV1, but interestingly also revealed the presence of the ~1 kb long secondary genome segment S2 (also ambigrammatic, but containing ORFs with no hits in the databases), which we could associate to the same virus using our small RNA-based approach. For each library, high numbers of small RNAs mapped to both S1 and S2. The small RNA

abundancies and size distribution profiles were very similar for both segments, and grouped separately from the other viruses (Fig. 2). This therefore suggested that the two genome segments S1 and S2 belong to the same virus, which was further confirmed by the similar CpG and GC content, the conserved genomic termini and unusual ambigrammatic nature of both segments. Bisegmented narnaviruses have also been discovered in Plasmodium (227), in a trypanosomatid (228, 229), and, very recently, in mosquitoes (230, 231). For the mosquito-associated, bisegmented, ambigrammatic CxNV1, the presence of the primary RdRp segment was found to be required for replication of the secondary ('Robin') segment in *Culex* mosquito cells, whereas the primary segment could persist in cell culture without the presence of the secondary segment (221). In our study, the primary and secondary genome segment of AejapNV1 co-occurred very frequently in field-collected *Ae. japonicus* mosquitoes, which is in accordance with previous findings for CxNV1 in wild-caught mosquitoes (230), thus suggesting that the secondary segment is of key importance for virus survival in the field. The function of the secondary genome segment is currently unknown, and future studies are needed to elucidate its role and evolutionary origin.

The discovery of AejapNV1 S2 is a successful application of our small RNA-based approach to recover viral sequences from the 'metagenomic dark matter' (232). Our small RNA contig clustering approach (Fig. 2) was critical to correlate the unknown contig to AejapNV1 and proceed to look for more evidence at sequence level that these sequences indeed belong to the same virus (Fig. 6).

However, the origin of a substantial portion of the dark matter remains enigmatic. Despite the presence of an siRNA profile, we could not clearly associate the majority of unknown contigs to any defined viral species in this study. Further studies will be necessary to determine if these unknown sequences with siRNA profile have a viral origin. *Ae. japonicus* does not have a reference genome sequence available, which prevents full efficacy of our initial read filters previous to contig assembly, which could lead to the assembly of contigs derived from unknown repetitive elements and/or overlapping mRNA fragments that may produce endogenous siRNAs (233).

De novo assembly of small RNAs also revealed the presence of AejapTV1 in *Ae. japonicus*. Between the capsid and RdRp ORFs, a putative -1 ribosomal frameshift area was identified. Similarly, a -1 ribosomal frameshift has also been predicted at the end of the capsid ORF for the mosquito-associated totiviruses *Armigeres subalbatus* totivirus and Omono River virus (234-236), thus suggesting that -1 ribosomal frameshifting is a common feature of these mosquito-associated totiviruses.

Besides AejapBV1, we could also detect another possible bunyavirus, AejapBV2, in *Ae. japonicus* collected in the Netherlands and France. Surprisingly,

we could not identify an RdRp for AejapBV2. Our small RNA sequencing and *de novo* assembly approach might not be sensitive enough to detect an RdRp sequence on a putative L segment for AejapBV2. However, high numbers of small RNAs were produced against the M and S segments of AejapBV2, and it is therefore unexpected that we were not able to assemble any contig for the putative L segment. Given the ability of bunyaviruses to reassort their segmented genomes, an alternative hypothesis could be that AejapBV2 uses the L segment of AejapBV1 for replication. Segment reassortments between bunyaviruses have frequently been observed and it has even been suggested that most if not all bunyaviruses currently present have arisen by reassortments (237, 238). However, AejapBV1 and AejapBV2 belong to two different bunyavirus families, *Phenuiviridae* and *Phasmaviridae*, respectively, which might render complementation or genetic exchange of genome segments less likely. In addition, this hypothesis would impose that AejapBV2 replication is dependent on the presence of the L segment of AejapBV1, but we could not detect AejapBV1 in our *Ae. japonicus* NL_02 small RNA library whereas AejapBV2 was present (Fig. 2). Therefore, evidence is lacking that AejapBV2 depends on the presence of the AejapBV1 L segment. Further, there is a striking difference in the amount of piRNAs produced by the segments M and S of AejapBV1 and 2 (Fig. 8). The vast amount of piRNAs produced by AejapBV2 compared to AejapBV1 may suggest that these viruses replicate in different tissues (195), thus also indicating that the assembled contigs belong to distinct bunyaviruses. Future studies will be needed to elucidate the replication strategy of AejapBV2 in *Ae. japonicus*.

Screening of wild-caught *Ae. japonicus* from the Netherlands for AejapNV1 indicated a very high prevalence (~100%) of the virus in all tested mosquito life stages (adult females, adult males, larvae and egg pools). These results may suggest vertical transmission of the virus, similar to narnaviruses discovered in fungi (239) and nematodes (240), for which vertical transmission has been shown. The very high percentage of mosquitoes that tested positive for AejapNV1 in our study is also in accordance with a recent study in Japan, where all of the tested *Ae. japonicus* mosquitoes harboured AejapNV1 (191). In addition, we also found high percentages of AejapTV1-positive *Ae. japonicus* mosquitoes in our study. Together, these findings raise the question of whether these highly abundant viruses could have an effect on arbovirus transmission by *Ae. japonicus*. The presence of these likely ISVs might add yet another complex variable to the risk assessment of arbovirus outbreaks by *Ae. japonicus*, and future studies are needed to dissect the role of the virome in arbovirus transmission.

In our study, AejapNV1, AejapTV1, AejapAV1, AejapBV1 and AejapBV2 were all detected in *Ae. japonicus* mosquitoes in the Netherlands and France. This indicates a high stability of the virome across mosquito populations, which has also

been observed for other mosquito species (70, 190), and may suggest that these viruses have coevolved with their mosquito host. Although the newly discovered virus species belong to different virus families and are thus highly diverse, they form a stable viral community in *Ae. japonicus* despite active antiviral RNAi responses, hence suggesting that these viruses should be considered important constituents of the biology of *Ae. japonicus* mosquito populations.

Acknowledgements

We thank Marleen Abma-Henkens for her assistance with *Ae. japonicus* collection in the field, Pieter Rouweler and other members of the insect rearing group from the Laboratory of Entomology from Wageningen University & Research for maintaining the *Cx. pipiens* colony, Giel Göertz for his contributions during the start of the project, Monique van Oers for her continued interest in the project, and Eric Snijder, Andrew Firth, Nina Lukhovitskaya and Katherine Brown for fruitful scientific discussions. We also thank all members of Marques Laboratory from Brazil and France, specially Isaque J. S. de Faria, who contributed with suggestions and discussions.

This study was supported by the European Union's Horizon 2020 Research and Innovation Programme (project: ZIKAlliance) under grant number 734548. SRA was also supported by the ZonMw project ZikaRisk ("Risk of Zika virus introductions for the Netherlands"), project number 522003001. The work of the Interdisciplinary Thematic Institute IMCBio, as part of the ITI 2021-2028 program of the University of Strasbourg, CNRS and Inserm, was supported by IdEx Unistra (ANR-10-IDEX-0002), by SFRI-STRAT'US project (ANR 20-SFRI-0012), and EUR IMCBio (IMCBio ANR-17-EURE-0023) under the framework of the French Investments for the Future Program as well as from the previous Labex NetRNA (ANR-10-LABX-0036). This work has also been supported by grants from Conselho Nacional de Desenvolvimento Científico e Tecnológico (CNPq) to JTM (grant CNPq/AWS 032/2019, process 440027/2020-9); Fundação de Amparo a Pesquisa do Estado de Minas Gerais (FAPEMIG); Institute for Advanced Studies of the University of Strasbourg (USIAS fellowship 2019) to JTM; Google Latin American Research Award (LARA 2019-2020) to JTM and JPPA. This work was also supported by Investissement d'Avenir Programs (ANR-10-LABX-0036 and ANR-11-EQPX-0022) to JTM. JTM is a CNPq Research Fellow. JPPA was also supported with a PHD fellowship from Coordenação de Aperfeiçoamento de Pessoal de Nível Superior - Brasil (CAPES). This study was financed in part by the Coordenação de Aperfeiçoamento de Pessoal de Nível Superior - Brasil (CAPES) - Finance Code 001 to JTM.

Supplementary information

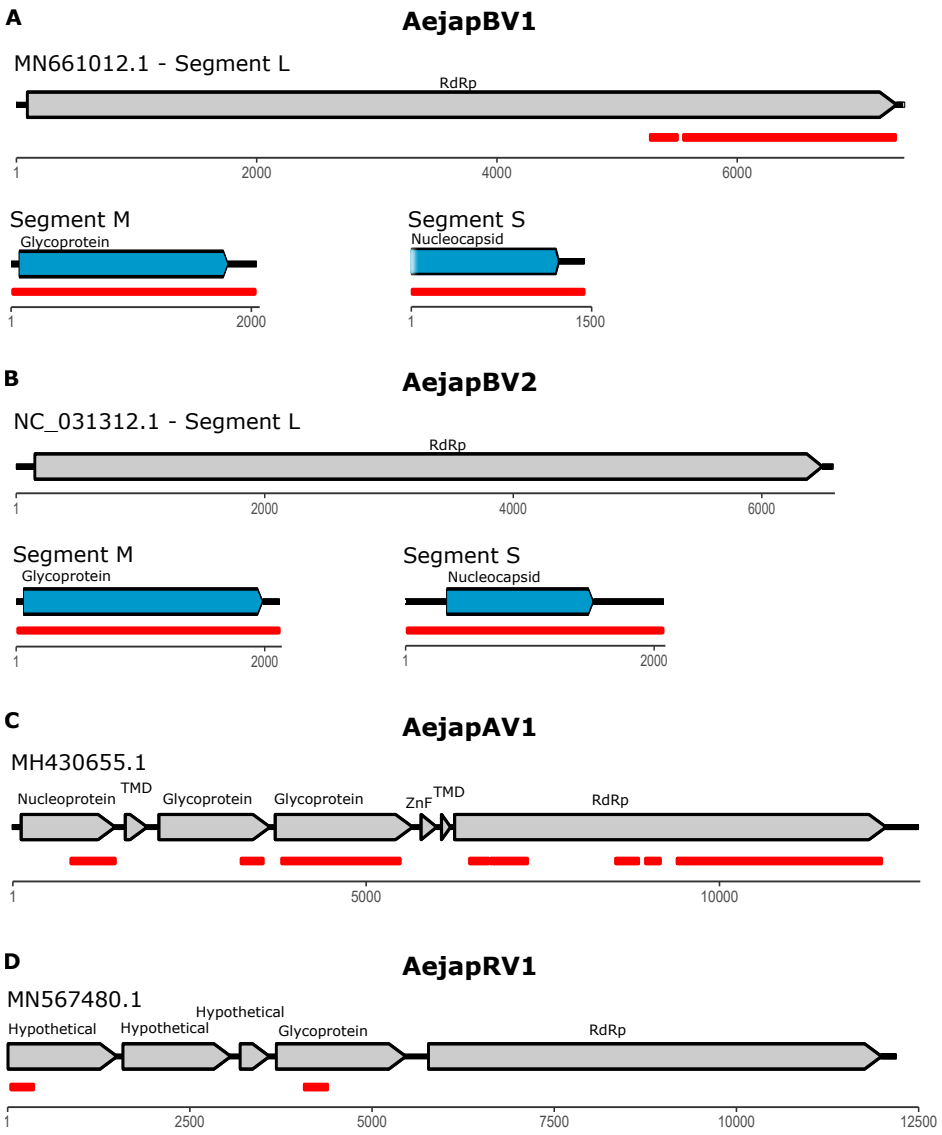

Supplementary Figure 1. Genomic organization of partially assembled viruses. Grey arrows represent ORFs from the closest GenBank reference viral sequence. Red lines indicate viral reference genome regions covered by our assembled contigs. Blue arrows represent ORFs from completely assembled viral segments in this work. Black lines indicate untranslated regions. **(A)** AejapBV1, **(B)** AejapBV2, **(C)** AejapAV1, **(D)** AejapRV1.

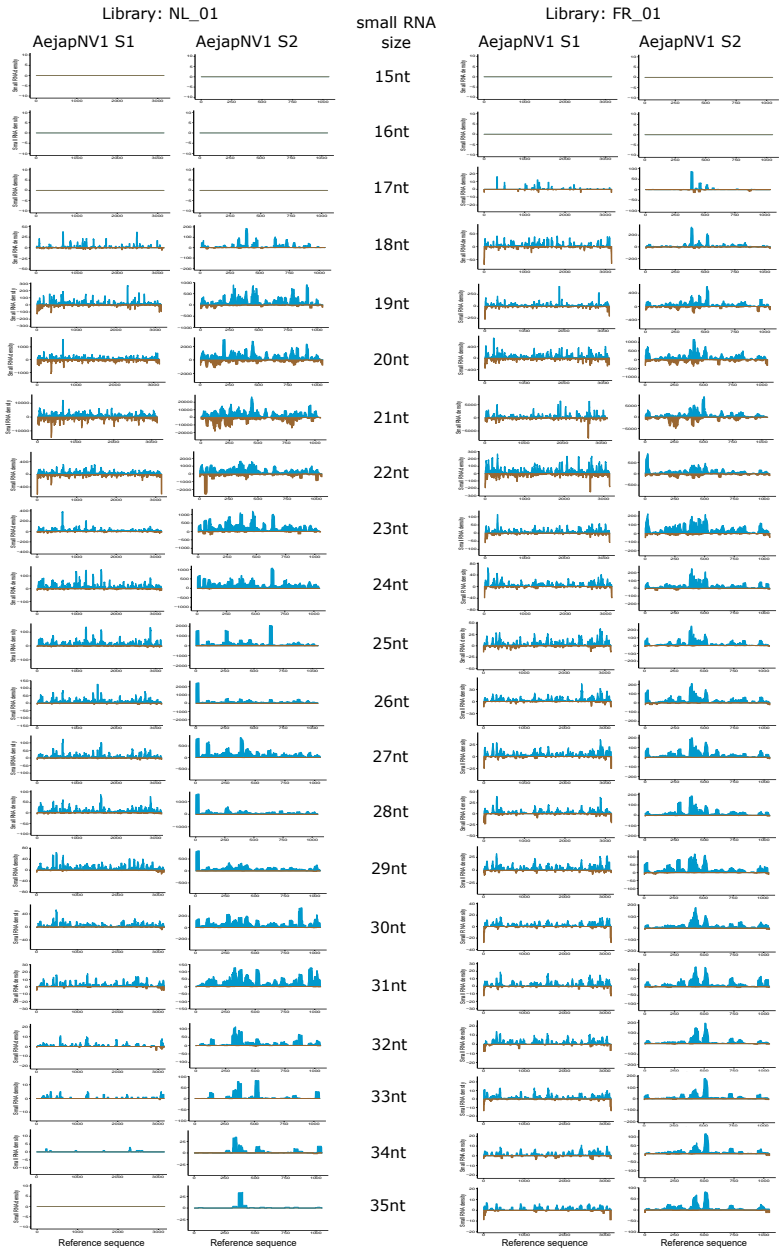

Supplementary Figure 2. Strand-specific small RNA coverage of AejapNV1 S1 and S2. Reads from sizes 15 to 35 nt from each library were aligned separately to segments S1 and S2. The blue area indicates small RNA read coverage of forward strand and the brown area of negative strand. The S1 sequence orientation was determined based on the RdRp coding ORF direction. A small RNA coverage bias towards the positive RdRp strand of S1 was seen, and a similar coverage bias was seen for S2, thus indicating the putative positive strand. Figure continues on next page.

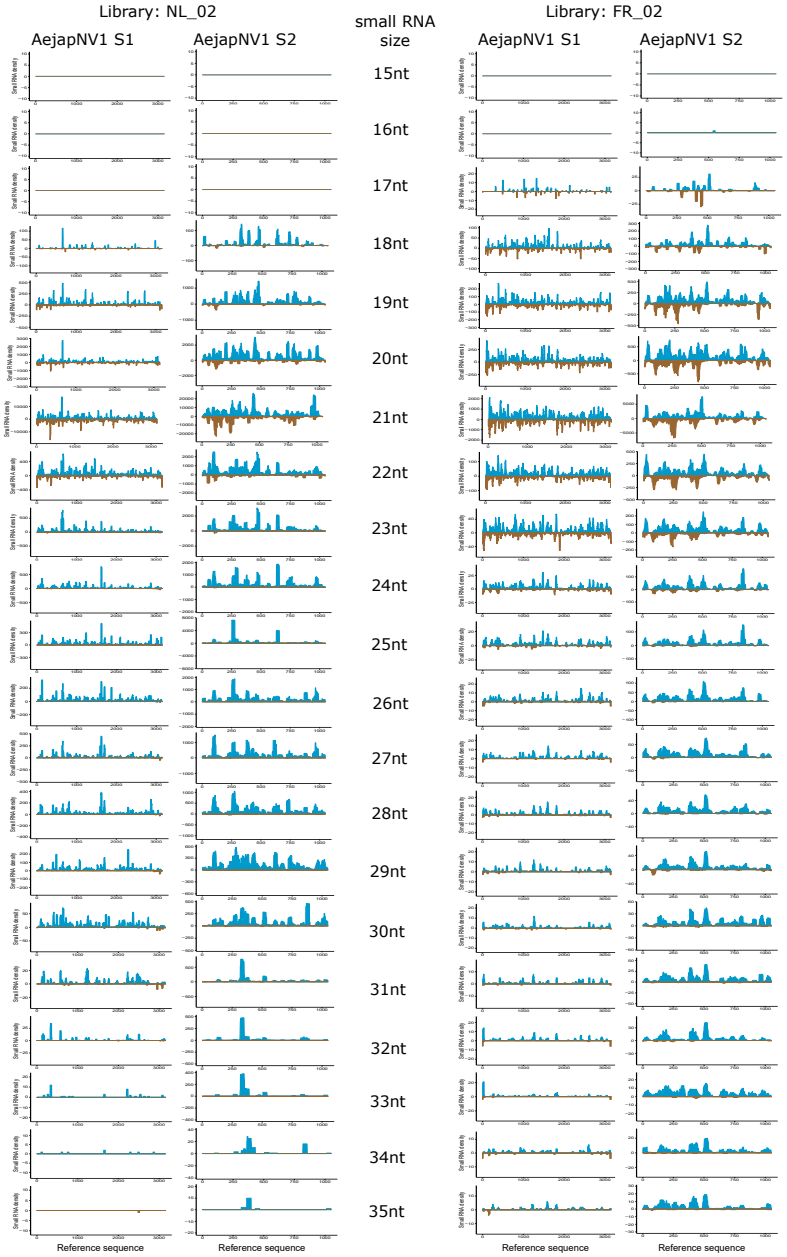

Supplementary Figure 2. Continued.

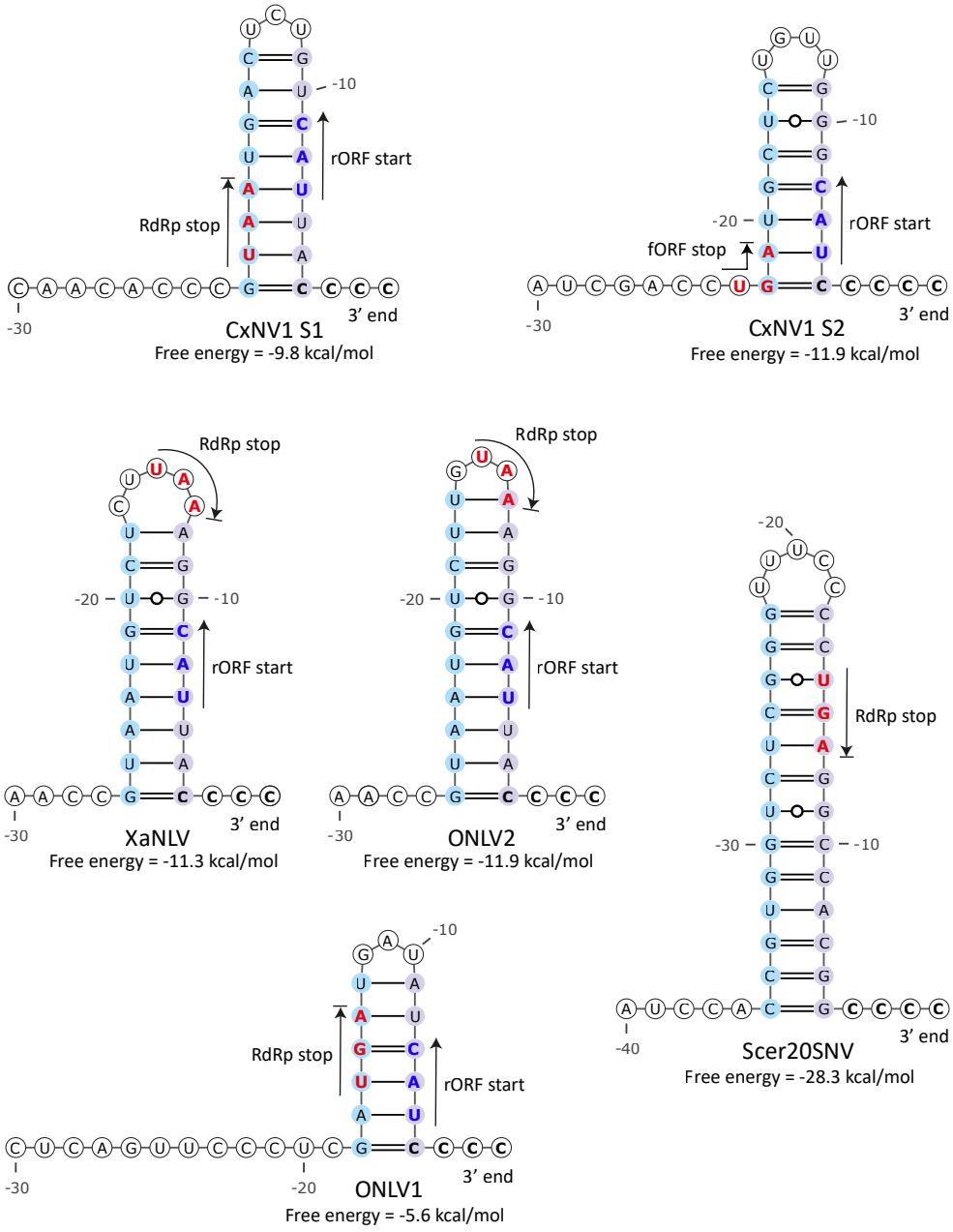

Supplementary Figure 3. Predicted 3' stem-loop structures of CxNV1 S1, CxNV1 S2, XaNLV, ONLV2, ONLV1 and Scer20SNV. The predicted RNA structures at the 3' terminus of the positive-sense RNA strand are shown. Locations of start and stop codons are indicated by arrows and colored blue and red, respectively.

Chapter 6 **Zika virus-like particle vaccines produced in insect cells**

Sandra R. Abbo[1], Natalie A. Prow[2], Kexin Yan[2], Corinne Geertsema[1], Tessy A. H. Hick[1,3], Jort J. Altenburg[3], Gwen Nowee[1], Chris van Toor[1], Jan W. van Lent[1], Bing Tang[2], Eri Nakayama[4], Stefan W. Metz[5], Jody Hobson-Peters[6], Roy A. Hall[6], Ricardo Correia[7], António Roldão[7], Dirk E. Martens[3], Monique M. van Oers[1], Andreas Suhrbier[2], Gorben P. Pijlman[1]

[1]Laboratory of Virology, Wageningen University & Research, Wageningen, the Netherlands
[2]Inflammation Biology Group, QIMR Berghofer Medical Research Institute, Brisbane, Australia
[3]Bioprocess Engineering, Wageningen University & Research, Wageningen, the Netherlands
[4]Department of Virology I, National Institute of Infectious Diseases, Tokyo, Japan
[5]Department of Microbiology and Immunology, University of North Carolina at Chapel Hill, Chapel Hill, USA
[6]School of Chemistry and Molecular Biosciences, University of Queensland, St. Lucia, Australia
[7]IBET, Instituto de Biologia Experimental e Tecnológica, Oeiras, Portugal

Abstract

Zika virus (ZIKV) caused outbreaks of unprecedented scale in South America and the Caribbean in 2015-2016, and continues to threaten public health in tropical regions. The virus can induce severe disease in humans, including congenital microcephaly and Guillain-Barré syndrome. No antivirals or vaccines are commercially available to treat or prevent ZIKV disease. Here we report the development of two prototype ZIKV vaccines: virus-like particles (VLPs) and subviral particles (SVPs). These non-replicative, enveloped ZIKV VLPs and SVPs were produced using the scalable baculovirus-insect cell expression system. High-level secretion of VLPs and SVPs into the culture fluid of *Spodoptera frugiperda* insect cells was achieved, and particles with diameters ranging from 20 to 60 nm were observed after purification. Upon vaccination of female IFNAR$^{-/-}$ mice with a single dose of 1 μg non-adjuvanted VLPs or SVPs, high levels of ZIKV-specific antibodies were detected whereas the levels of ZIKV-neutralising antibodies were limited. Similar results were obtained in a second study with male IFNAR$^{-/-}$ mice three times vaccinated with 1 μg adjuvanted VLPs or SVPs. In both studies, vaccination with VLPs or SVPs could not protect mice against ZIKV infection after viral challenge, although the viraemic period became shorter. Epitope analysis using monoclonal antibody ELISA revealed that the VLPs and SVPs do not display quaternary structure epitopes normally found on envelope (E) protein homodimers present on the surface of the ZIKV virion. These epitopes trigger strongly neutralising and protective antibody responses following natural ZIKV infection. We hypothesised that the insect cell culture medium of pH 6.2-6.4 induced a conformational change of the ZIKV E proteins from a dimeric, prefusion state into a postfusion state. To improve the efficacy of the ZIKV SVP vaccine, a variant with covalently linked E proteins to lock the dimeric state was generated. Furthermore, the vaccines were produced at pH 7.0 using adapted insect cells.

Introduction

Zika virus (ZIKV) is a mosquito-borne pathogen that caused an explosive outbreak of human disease in the Americas in 2015 and 2016 (241). Although ZIKV infections in humans were historically only associated with mild disease symptoms, the virus unexpectedly induced severe clinical symptoms during the epidemic in Central and South America. ZIKV can be vertically transmitted from mother to fetus during pregnancy, leading to congenital microcephaly and fetal demise (242). In adults, ZIKV infection can lead to Guillain-Barré syndrome (242). As very limited knowledge was available about the virus and its associated diseases, the World Health Organisation declared ZIKV a Public Health Emergency of International Concern in 2016 (22). Although the number of reported ZIKV infections is currently much lower, the virus

is still considered a public health threat due to its continued presence in tropical regions across the globe as well as its potential to spread into temperate areas (23).

ZIKV belongs to the genus *Flavivirus* in the family *Flaviviridae* and contains a positive-sense, single-stranded RNA genome of 11 kilobase pairs (kb) in length. The genome contains a single open reading frame (ORF) encoding both the structural and non-structural proteins (46). ZIKV possesses three different structural proteins: capsid (C) protein, precursor membrane (prM) protein and envelope (E) protein that together build a spherical virus particle of ~50 nm in diameter (50). Immature ZIKV particles bud into the endoplasmic reticulum (ER) lumen and travel through the Golgi apparatus to the cell surface. During this process, conformational changes in the E glycoprotein and cleavage of prM in the precursor peptide (pr) and M protein occur (54). Dissociation of pr upon entry in the extracellular environment results in mature, smooth particles displaying 90 E homodimers on their surface (243). Entry of ZIKV into host cells is mediated by the E protein and occurs via receptor-mediated endocytosis. After acidification of the endosome, the E dimers on the virion rearrange into E trimers to expose the fusion loop, after which fusion of the viral membrane with the host endosomal membrane takes place (50, 51). The highly structured E homodimer is a main target of neutralising antibodies during ZIKV infection in humans (244-246), and therefore also an important component of many experimental ZIKV vaccines (247-249).

Currently, no licenced vaccines or antiviral treatments are available to prevent or treat ZIKV infection in humans. Vaccines against ZIKV need to be effective, scalable and of low cost. Ideally, a ZIKV vaccine is non-replicative to safely protect the mother and the unborn child. Live-attenuated, inactivated, DNA, mRNA and viral vectored ZIKV vaccines have all entered human clinical trials (250), although safety risks and/or high production costs might become important drawbacks. It is therefore essential to continue the development of ZIKV candidate vaccines, based on different designs and production systems, to ultimately deliver a protective, safe and cost-effective vaccine that can prevent future ZIKV outbreaks. Here, we have developed two prototype vaccines against ZIKV using the baculovirus-insect cell expression system: a virus-like particle (VLP) vaccine and a subviral particle (SVP) vaccine. VLPs are produced by expressing the ZIKV structural proteins C, prM and E, which self-assemble into particles that are structurally identical to wild-type virus but do not contain a viral genome. SVPs also lack a viral genome but are produced by expression and self-assembly of only prM and E proteins. VLPs and SVPs are non-replicative and therefore considered attractive vaccine candidates for use in pregnant women. Both vaccines were tested for their immunogenicity and protective efficacy in mouse models of ZIKV disease.

Methods

Cell culture

Spodoptera frugiperda Sf21 (Gibco, Carlsbad, CA, USA), Sf9 (Gibco) and Sf9-ET (251) cells were grown at 27°C. Monolayers of Sf21 cells were cultured in Grace's medium (Gibco) supplemented with 10% fetal bovine serum (FBS; Gibco). Monolayers of Sf9-ET cells were grown in Sf900II medium (Gibco) containing 5% FBS and 100 µg/ml geneticin (Gibco). Monolayers and suspension cultures of Sf9 cells were maintained in Sf900II serum-free medium supplemented with 50 µg/ml gentamycin (Gibco). The African green monkey kidney Vero cell line was grown in RPMI 1640 medium supplemented with 10% FBS at 37°C and 5% CO_2.

Generation of recombinant baculoviruses

ZIKV structural cassettes CprME, prME and EΔTM (secreted E; lacking a transmembrane domain) were amplified from ZIKV Suriname 2016 cDNA (GenBank: KU937936.1; obtained from Erasmus Medical Center, Rotterdam, the Netherlands) by PCR using Phusion High-Fidelity DNA polymerase (New England Biolabs, Ipswich, MA, USA) and a 2720 Thermal Cycler (Applied Biosystems, Foster City, CA, USA). Primers (Table 1) contained attB recombination sites to enable Gateway cloning (Invitrogen, Carlsbad, CA, USA). The ZIKV structural cassettes were recombined into a pDONR207 plasmid (Invitrogen) and subsequently into a pDEST8 plasmid (Invitrogen) downstream of the baculovirus polyhedrin promoter. The pDEST8 plasmid containing the prME cassette was used to create an alternative pDEST8 plasmid containing a prME cassette with an alanine to cysteine substitution (A264C) as previously described for the production of stable, covalently linked dengue virus (DENV) and ZIKV E homodimers (247, 252-255). The A264C substitution was introduced by quick change PCR using primers described in Table 1. Next, the four cassettes (CprME, prME, prME-A264C, EΔTM) were transposed into the improved *Autographa californica* multiple capsid nucleopolyhedrovirus (AcMNPV) backbone BACe56 (256). Sf21 cells were transfected with purified recombinant bacmid DNA using ExpreS^2 TR (ExpreS^{2}ion Biotechnologies, Hørsholm, Denmark). Recombinant baculovirus titers were determined in Sf9-ET cells and expressed as 50% tissue culture infectious dose per millilitre ($TCID_{50}$/ml).

Table 1. Primer combinations used in this study. The attB site of each primer is shown in bold. The mutations used to create the A264C substitution are underlined.

Target	Primer name	Primer sequence (5'→3')	Product (kb)
ZIKV CprME	attB1-ZIKV-C-F	**GGGGACAAGTTTGTACAAAAAAGCAGGCT-TA**ACCATGAAAAACCCAAAAAAGAAATC	2.4
	attB2-ZIKV-Estem/anchor-R	**GGGGACCACTTTGTACAAGAAAGCTGGG-TA**TTAAGCAGAGACGGCTGTGGATA	
ZIKV prME	attB1-ZIKV-pr-F	**GGGGACAAGTTTGTACAAAAAAGCAGGCT-TA**ACCATGGGCGCAGATACTAGTGTCGG	2.0
	attB2-ZIKV-Estem/anchor-R	**GGGGACCACTTTGTACAAGAAAGCTGGG-TA**TTAAGCAGAGACGGCTGTGGATA	
ZIKV EΔTM	attB1-ZIKV-E-F	**GGGGACAAGTTTGTACAAAAAAGCAGGCT-TA**ACCATGTCAACGAGCCAAAAAGTCAT	1.3
	attB2-6xHis-tag-ZIKV-E-R	**GGGGACCACTTTGTACAAGAAAGCTGGG-TA**TTAGTGATGGTGATGGTGATGTTTTCCAATG-GTGCTGCCAC	
pDEST8/ZIKV-prME-A264C	ZIKV-E-A264C-F	TCAAGAAGGA<u>TGC</u>GTTCACACGGCCCTTGCTGG	8.5
	ZIKV-E-A264C-R	CCGTGTGAAC<u>GCA</u>TCCTTCTTGACTCCCTAGAA	

Production of ZIKV vaccines

For small-scale vaccine production, 8 x 10^6 Sf21 or Sf9 insect cells were seeded as monolayer in 75 cm^2 flasks. Cells were infected with recombinant baculovirus containing the ZIKV CprME structural cassette (BACe56/ZIKV-CprME), the ZIKV prME structural cassette (BACe56/ZIKV-prME) or the ZIKV prME-A264C structural cassette (BACe56/ZIKV-prME-A264C) for ZIKV VLP, ZIKV SVP or ZIKV SVP-A264C production, respectively. Soluble ZIKV E subunit was produced by infecting cells with recombinant baculovirus harbouring the structural cassette ZIKV EΔTM (BACe56/ZIKV-EΔTM). Uninfected cells as well as cells infected with recombinant baculovirus expressing a green fluorescent protein (BAC/GFP) (257) were used as negative controls. Cells were infected at a multiplicity of infection (MOI) of 10 $TCID_{50}$ units per cell (CprME, prME, EΔTM, GFP) or 0.4 $TCID_{50}$ units per cell (prME-A264C). After infection, cells were incubated at 27°C for 4 hours. Afterwards, the cell culture medium was replaced by fresh medium, and cells were incubated at 27°C for 3-4 days. For larger scale vaccine production, Sf9 suspension cultures containing 2.0-2.5 x 10^6 cells/ml were infected with BACe56/ZIKV-CprME or BACe56/ZIKV-prME or BACe56/ZIKV-prME-A264C at an MOI of 0.01-5 $TCID_{50}$ units per cell. Cells were incubated at 27°C for 3 days. Cells and

medium were harvested and separated by centrifugation at 1700 rpm for 5 min using a Heraeus Megafuge 40R centrifuge (Thermo Scientific, Waltham, MA, USA). The cell pellet was resuspended in PBS, and the supernatant containing the ZIKV VLPs/SVPs was filtered through a 0.45 μm filter.

Purification of ZIKV vaccines

First, 7% (w/v) polyethylene glycol (PEG)-6000 and 0.5 M NaCl were added to the filtered medium to precipitate the VLPs/SVPs. After 2 hours at room temperature (RT) and following centrifugation at 4700 rpm for 15 minutes using a Heraeus Megafuge 40R centrifuge (Thermo Scientific), the pellet was dissolved in GTNE buffer (200 mM glycine, 50 mM Tris/HCl, 100 mM NaCl, 1 mM EDTA, pH 7.3). Next, the VLPs/SVPs in GTNE were loaded onto a 30-80% (w/v) continuous sucrose gradient (prepared in GTNE) and subjected to centrifugation at 45,000 rpm for 2 hours using an SW55 rotor (Beckman, Brea, CA, USA). Twenty-five fractions were collected from the top of the gradient and analysed for the presence of ZIKV E protein using western blot. ZIKV E protein containing fractions were pooled and centrifuged again at 45,000 rpm for 2 hours. The pellet was then dissolved in GTNE buffer, and the pure VLPs/SVPs were stored at -80°C. Samples were subsequently analysed by western blot to detect and quantify ZIKV E protein, and by transmission electron microscopy to check the integrity of the particles.

ZIKV protein analysis

ZIKV proteins from cell fractions, medium fractions and purified VLP/SVP fractions were detected using sodium dodecyl sulphate polyacrylamide gel electrophoresis (SDS-PAGE) followed by western blot. Loading buffer containing SDS was added to the samples, after which the samples were incubated at 95°C for 10 minutes. After centrifugation at 14,000 rpm for 1 minute using an Eppendorf 5424 centrifuge, samples were run on a Mini-PROTEAN TGX gel (Bio-Rad, Veenendaal, the Netherlands). Next, a trans-blot semi-dry transfer cell (Bio-Rad) was used to transfer the proteins to an Immobilon-P membrane (Merck Millipore, Darmstadt, Germany). The membrane was blocked at 4°C overnight using 1% skimmed milk powder dissolved in PBS containing 0.05% Tween (PBS-T). Afterwards, the membrane was incubated at RT for 1 hour with pan-flavivirus α-E monoclonal antibody (mAb) 4G2 (99) diluted 1:1000 in 1% skimmed milk. After washing the membrane three times with PBS-T, alkaline phosphatase conjugated goat anti-mouse IgG secondary antibody (Sigma-Aldrich, Darmstadt, Germany) diluted 1:2500 in PBS-T was added. After 1 hour, the membrane was washed three times with PBS-T and subsequently incubated with alkaline phosphatase buffer as described (257) for 10 minutes. Lastly, the membrane was developed using NBT/BCIP (Roche Diagnostics, Almere, the Netherlands).

Quantification of ZIKV vaccines

The purified ZIKV vaccines were quantified using a dilution series of pure DENV serotype 4 E protein (The Native Antigen Company, Oxford, UK). Samples with pure ZIKV VLP/SVP and samples containing serial twofold dilutions of 3 µg DENV E were prepared and analysed by SDS-PAGE and western blot using the pan-flavivirus 4G2 mAb as described above. The intensity of protein bands was compared to estimate the concentration of ZIKV VLPs/SVPs in the purified fractions.

Transmission electron microscopy

Purified ZIKV VLPs/SVPs in GTNE buffer were loaded onto 200 mesh carbon coated copper grids (Electron Microscopy Sciences, Hatfield, PA, USA). After 2 min at RT, the excess of liquid was removed and 2% ammonium molybdate (pH 7) was added to the grids. After 30 s at RT, the excess of liquid was again removed. After air drying, the grids were analysed using a JEOL JEM-1011 transmission electron microscope. VLP/SVP diameters were determined using ImageJ (National Institutes of Health, Bethesda, MD, USA) in combination with in-house macros.

Vaccination and virus challenge

Female interferon-α/β receptor knockout ($IFNAR^{-/-}$) mice (C57BL/6J background; 13 weeks old) were immunised with a single dose of 1 µg ZIKV VLPs or SVPs per mouse. As negative control, a group of female $IFNAR^{-/-}$ mice was vaccinated with 1 µg CHIKV VLPs, which were produced and purified as described (257, 258). Male $IFNAR^{-/-}$ mice (12 weeks old) were immunised with three doses of 1 µg ZIKV VLPs or SVPs mixed in a 1:1 volume ratio with AddaVax adjuvant (InvivoGen, San Diego, CA, USA) (259). As negative controls, groups of male $IFNAR^{-/-}$ mice were vaccinated with CHIKV VLPs in combination with AddaVax adjuvant or immunised with PBS only. The vaccines were administered via the intramuscular route (40 µl into both quadriceps muscles). As positive control, male $IFNAR^{-/-}$ mice were infected in the base of the tail with 10^4 $TCID_{50}$ of ZIKV Natal (GenBank KU527068.1) to induce potent neutralising antibodies for protection against subsequent virus challenge. Female $IFNAR^{-/-}$ mice were challenged by subcutaneous infection of 10^3 $TCID_{50}$ ZIKV MR766 (GenBank LC002520.1) or 10^4 $TCID_{50}$ ZIKV Natal in the base of the tail. Male $IFNAR^{-/-}$ mice were challenged by subcutaneous infection of 10^3 $TCID_{50}$ ZIKV PRVABC59 (GenBank MH158237.1). All mouse work was conducted in accordance with the "Australian code for the care and use of animals for scientific purposes" as defined by the National Health and Medical Research Council of Australia. Mouse work was approved by the QIMR Berghofer Medical Research Institute animal ethics committee.

Antibody ELISA, neutralisation assays and virus titration

IgG responses were measured by standard ELISA using whole ZIKV MR766 as antigen as described (260, 261). The neutralising ability of mouse sera was also determined as described (260). Briefly, serum was heat-inactivated at 56°C for 30 min. Diluted serum was incubated with 100 $TCID_{50}$ of ZIKV Natal or PRVABC59 for 2 hours, and Vero cells (10^5 cells/ml) were added afterwards. Cells were fixed at 7 days post infection, and stained with crystal violet, after which the reciprocal 50% neutralisation titers were determined. Serum viraemia was measured by $TCID_{50}$ assays as previously reported (262).

Epitope display analysis

ZIKV VLP/SVP epitopes were characterised by ELISA using a panel of well-defined mouse or human derived mAbs targeting the flavivirus E protein (Table 2) (246, 247, 263, 264). ZIKV H/PF/2013 (GenBank KJ776791.2) wild-type virus and recombinant E subunit (247) were included for comparison. All analyses were carried out in duplicate. ZIKV VLPs, ZIKV SVPs, wild-type ZIKV and ZIKV E subunit were captured using 4G2 mAb (99) (for human detection antibodies) or 1M7 mAb (265) (for mouse detection antibodies). Flavivirus cross-reactive or ZIKV-specific detection antibodies (Table 2), derived from human or mouse, were used to detect epitopes. The DENV serotype 2 specific mAb 3H5 (266) was used as a negative control. Antibody binding was determined using alkaline phosphatase conjugated anti-human or anti-mouse IgG secondary antibodies (Sigma) in combination with alkaline phosphatase substrate (Sigma). Absorbance was measured at 405 nm.

Growth assays of insect cells at different pH

Sf9 suspension cultures (2 x 10^6 cells/ml at day 0) were grown in culture medium of uncontrolled pH or culture medium set to pH 6.6, 6.8 or 7.0. Culture medium was set to the desired pH using 0.5 M NaOH at day 0, and checked each day thereafter to ensure a constant pH. Cell concentration and cell viability were determined daily using a Countess II Automated Cell Counter (Invitrogen) according to supplied protocol.

Results

Production and purification of ZIKV VLPs and SVPs from insect cells

To produce ZIKV VLPs or SVPs in insect cells, recombinant baculoviruses expressing the structural cassette ZIKV CprME or prME (Fig. 1A), respectively, were constructed. A secreted ZIKV E subunit was produced for comparison by expressing the ZIKV E coding region without the C-terminal transmembrane domain (Fig. 1A, EΔTM). The prM and E sequences contained their native signal peptides for translocation to the ER. Recombinant baculoviruses BACe56/ZIKV-CprME,

BACe56/ZIKV-prME and BACe56/ZIKV-EΔTM were used to infect Sf21 cells at an MOI of 10 $TCID_{50}$ units per cell. Uninfected cells and cells infected with a recombinant baculovirus expressing green fluorescent protein (BAC/GFP) (257) were included as negative controls. After 4 days, signs of baculovirus infection were observed for infections with BACe56/ZIKV-CprME, BACe56/ZIKV-prME, BACe56/ZIKV-EΔTM and BAC/GFP (Fig. 1B). The infected cells showed an increased cell diameter, enlarged nuclei, detachment, growth arrest and lysis. Uninfected cells did not show these effects (Fig. 1B). Apart from the baculovirus infection signs, BACe56/ZIKV-prME infected cells also showed formation of big syncytia (Fig. 1B). The observed syncytia were most likely caused by fusogenic activity of the ZIKV E protein, which is also responsible for fusion of the viral envelope with the endosomal membrane during virus entry (270).

Table 2. Monoclonal antibodies (mAbs) used for epitope display analysis. A panel of well-defined mouse (M) or human (H) derived mAbs was used to characterise ZIKV VLP/SVP epitopes. E dimer epitope (EDE) dependent, flavivirus cross-reactive (F-CR), weakly, moderately or strongly (*W*/*M*/*S*) neutralising, E-domain I, II, III (DI, DII, DIII), fusion loop (FL), lateral ridge (LR), quaternary (Q),* not completely mapped.

mAb	M/H	Binding	Neutralisation *(W/M/S)*	E protein binding region	Binding DENV serotypes or ZIKV					Reference
					DV1	*DV2*	*DV3*	*DV4*	ZIKV	
4G2	M	F-CR	*W*	DII FL	++	++	+++	+++	+++	(99)
1M7	H	F-CR	*M*	DII FL	+++	++	+++	+++	+++	(265)
A11 (EDE2)	H	F-CR	DV:*S* ZIKV:*W*	DI/DII/DIII Q	+++	+++	+++	+++	+	(267)
B7 (EDE2)	H	F-CR	DV:*S* ZIKV:*W*	DI/DII/DIII Q	+++	+++	+++	+++	+	(267)
C8 (EDE1)	H	F-CR	DV:*S* ZIKV:*S*	DI/DII/DIII Q	+++	+++	+++	+++	++	(267)
C10 (EDE1)	H	F-CR	DV:*S* ZIKV:*S*	DI/DII/DIII Q	+++	+++	+++	+++	++	(267)
ZKA-64	H	ZIKV	ZIKV:*S*	DIII	-	-	-	-	+++	(268)
Z3L1	H	ZIKV	ZIKV:*S*	DI/DII	-	-	-	-	+++	(269)
Z23	H	ZIKV	ZIKV:*S*	DIII	-	-	-	-	+++	(269)
A9E	H	ZIKV	ZIKV:*S*	DI Q*	-	-	-	-	+++	(246)
G9E	H	ZIKV	ZIKV:*S*	DII Q*	-	-	-	-	+++	(246)
Z20	H	ZIKV	ZIKV:*S*	DII Q	-	-	-	-	+++	(269)
ZIKV-117	H	ZIKV	ZIKV:*S*	DII Q	-	-	-	-	+++	(244)
3H5	M	DV2	DV2:*S*	DIII LR	-	+++	-	-	-	(266)

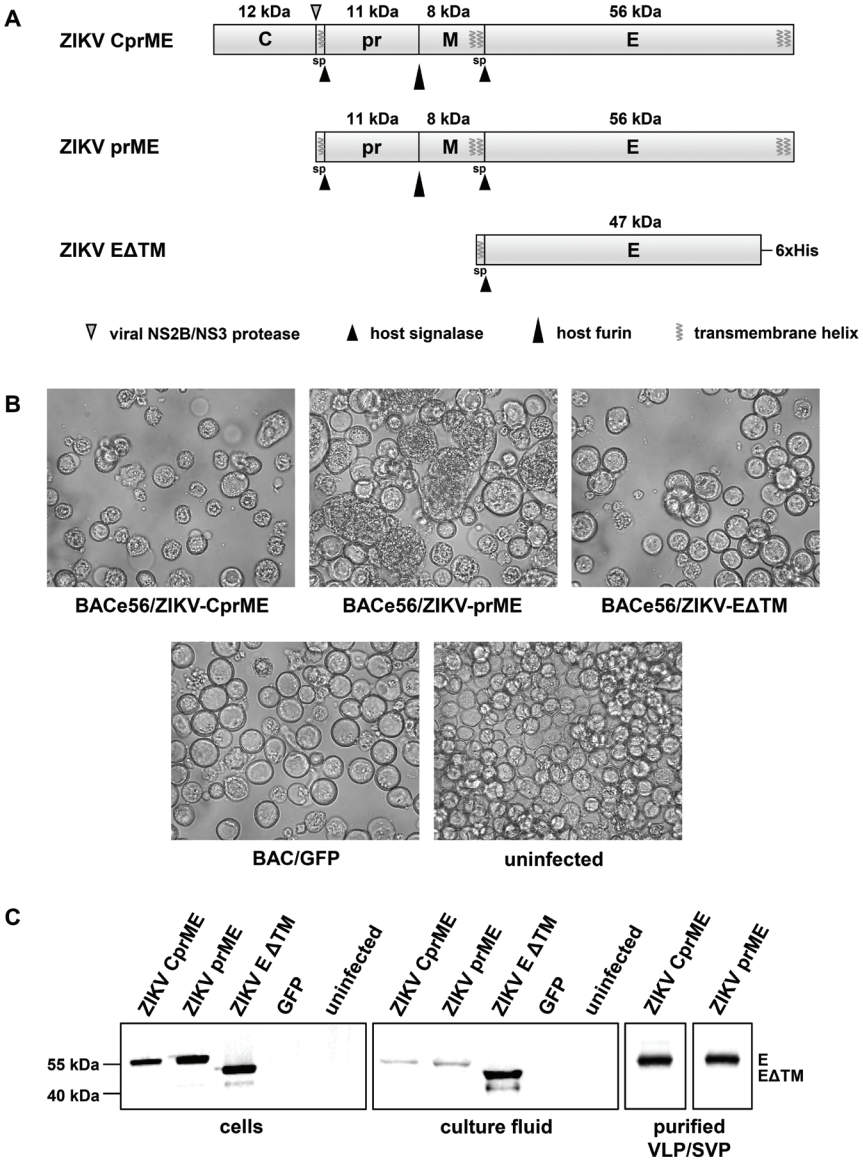

Figure 1. Production of ZIKV VLP and SVP using insect cells. (A) Schematic representation of the structural cassettes used for the production of ZIKV VLP (CprME), ZIKV SVP (prME) and secreted ZIKV E subunit (EΔTM) in insect cells. The molecular mass of each viral protein is shown in kDa. Cleavage sites of viral protease, host signalase and host furin are indicated, as well as predicted signal peptide (sp) sequences and transmembrane helices. ZIKV EΔTM contains a C-terminal histidine tag (6xHis). **(B)** Sf21 insect cells infected with indicated baculoviruses at 4 days post infection, or uninfected cells. **(C)** ZIKV E protein expression in Sf21 insect cells infected with recombinant baculoviruses containing the indicated cassettes at 4 days post

infection, in culture fluid derived thereof, and in VLP/SVP fractions obtained after sucrose gradient purification. Protein expression was measured by western blot using pan-flavivirus α-E 4G2 mAb.

Next, the baculovirus-infected cells and the culture fluid were analysed for the presence of ZIKV E protein by western blot using the pan-flavivirus mAb 4G2. Expression of ZIKV CprME and ZIKV prME structural cassettes resulted in the detection of a protein at ~55 kDa in both cell and medium fractions (Fig. 1C). This size corresponds to the predicted molecular mass of processed E protein (56 kDa). Expression of ZIKV-EΔTM showed a protein at ~50 kDa (Fig. 1C), which corresponds to the predicted molecular mass of processed EΔTM (47 kDa). As ZIKV E subunits are not considered effective vaccine candidates due to the lack of E homodimers with associated quaternary structure epitopes essential for the induction of strongly neutralising immune responses (247), we proceeded with purification of the VLPs and SVPs for vaccination studies. VLPs/SVPs were isolated from the culture fluid using PEG precipitation followed by 30-80% continuous sucrose gradient purification. The VLP/SVP purification was confirmed by western blot analysis (Fig. 1C).

Characterisation of ZIKV VLPs and SVPs

The purified VLPs/SVPs were analysed by transmission electron microscopy. Spherical particles with a diameter of ~20-60 nm were observed in the VLP (CprME) sample (Fig. 2A). Particles separated into two groups based on diameter. The larger VLPs had a diameter of 52-55 nm (Fig. 2B), which corresponds with the reported size of complete, infectious ZIKV virions (271).The smaller particles had a diameter of 24-27 nm (Fig. 2B), which corresponds to the size of ZIKV SVPs. Non-infectious SVPs of about ~20-30 nm in diameter have previously been observed during natural flavivirus infection (272) as well as during expression of recombinant flavivirus prME cassettes (273, 274), and contain M and E proteins but lack RNA and capsid. The purified SVP (prME) sample also contained spherical particles of ~20-60 nm in diameter (Fig. 2C), but particles with a diameter of 24-27 nm, indicative of ZIKV SVP production, were more abundant (Fig. 2D).

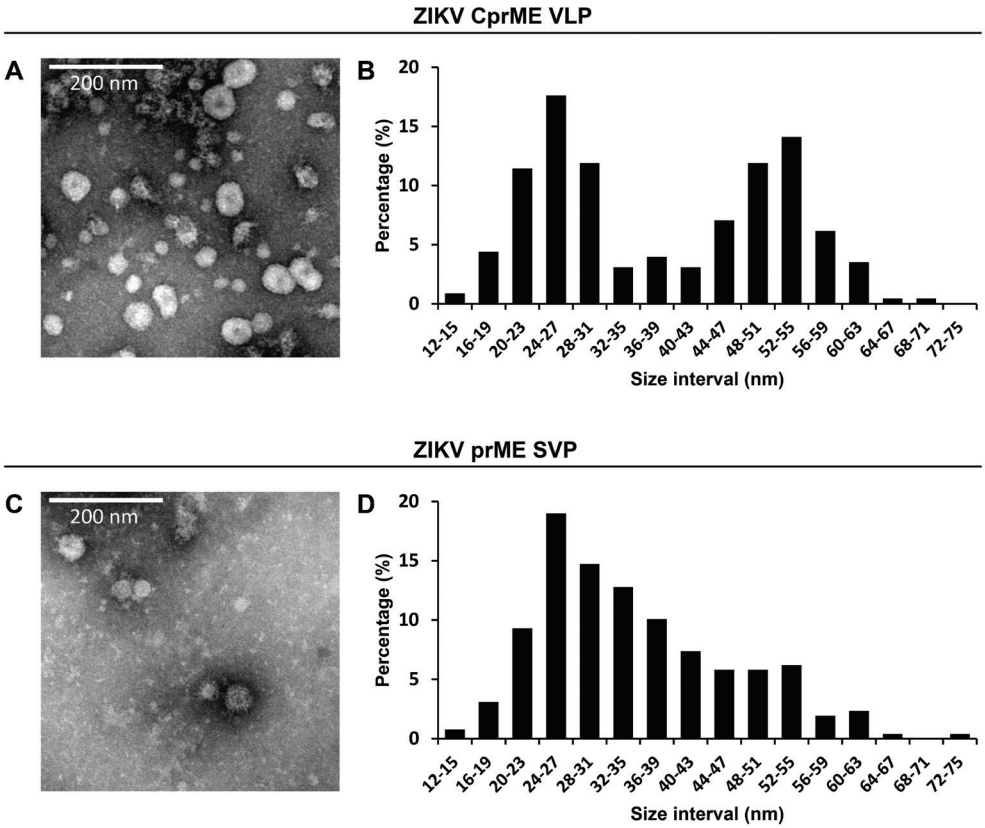

Figure 2. Electron microscopy analysis of ZIKV VLPs and SVPs. (A) Transmission electron microscopy photo of purified ZIKV VLPs (CprME). **(B)** Size distribution of particles in CprME fraction based on diameter measurements of 227 particles. **(C)** Transmission electron microscopy photo of purified ZIKV SVPs (prME). **(D)** Size distribution of particles in prME fraction based on diameter measurements of 258 particles.

Vaccine efficacy in IFNAR$^{-/-}$ mice

Next, the ZIKV VLP (CprME) and SVP (prME) vaccine candidates were produced at larger scale using suspension Sf9 insect cells to generate sufficient material for mouse trials. To evaluate the efficacy of the purified ZIKV VLP and SVP vaccine candidates, female IFNAR$^{-/-}$ mice were immunised with one dose of 1 μg of the purified VLPs (10 mice) or SVPs (5 mice), and antibody responses and protective ability against ZIKV infection were determined (Fig. 3A). As a negative control, another group of 5 mice was vaccinated with purified CHIKV VLPs (257). Four weeks post vaccination, high levels of ZIKV-specific antibodies were measured for mice vaccinated with ZIKV VLPs or SVPs, whereas no ZIKV-specific antibodies were detected after immunisation with CHIKV VLPs (Fig. 3B). After ZIKV VLP

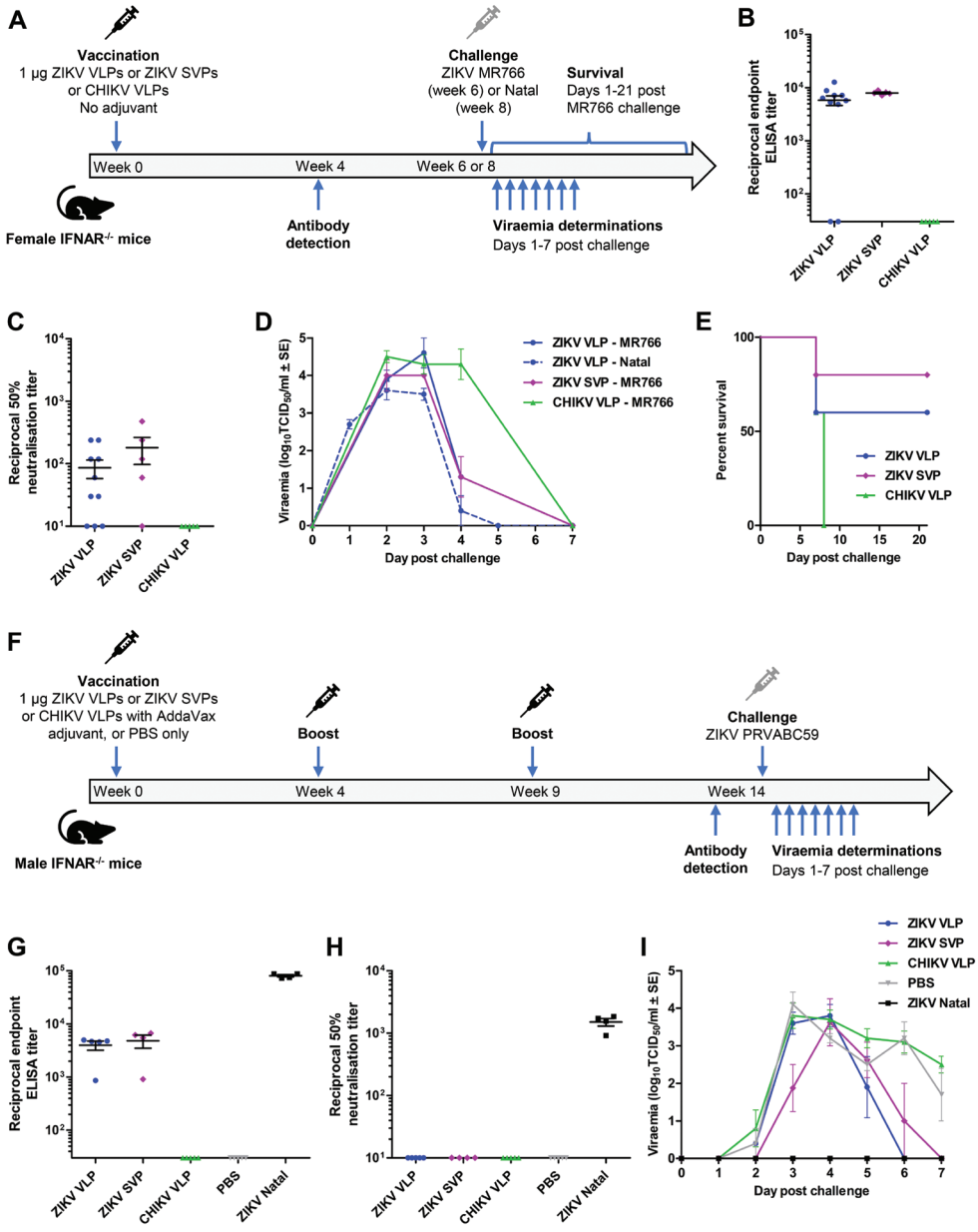

Figure 3. Vaccination of IFNAR$^{-/-}$ mice with ZIKV VLPs or SVPs, and challenge with wild-type ZIKV. (A) Timeline of vaccination of IFNAR$^{-/-}$ females with a single, non-adjuvanted dose of 1 µg ZIKV VLPs or ZIKV SVPs or CHIKV VLPs (negative control), antibody measurement after bleed, and viraemia and survival determinations after challenge with wild-type ZIKV. **(B)** ZIKV MR766 endpoint IgG ELISA titers in serum from IFNAR$^{-/-}$ females after immunisation with one dose of 1 µg ZIKV VLPs, ZIKV SVPs or CHIKV VLPs. Lines among the dots represent

the mean ELISA titers and error bars indicate the standard error of the mean. Limit of detection is 1 in 30 serum dilution. **(C)** ZIKV Natal 50% neutralisation titers in serum from IFNAR$^{-/-}$ females vaccinated as in (B). Lines among the dots show the mean neutralisation titers and error bars indicate the standard error of the mean. Limit of detection is 1 in 10 serum dilution. **(D)** ZIKV MR766 or Natal viraemia post challenge in IFNAR$^{-/-}$ females immunised as in (B) with n = 5 per group and with means from 5 mice plotted. **(E)** Survival of mice immunised as in (B) after MR766 challenge. Animals were euthanized when ethically defined end points had been reached. **(F)** Timeline of vaccination of IFNAR$^{-/-}$ males with three 1 µg doses of AddaVax adjuvanted ZIKV VLPs or ZIKV SVPs or CHIKV VLPs (negative control) or PBS only (negative control), antibody measurement after bleed, and viraemia determinations at days 1-7 post ZIKV challenge. **(G)** ZIKV MR766 endpoint IgG ELISA titers in serum from IFNAR$^{-/-}$ males after immunisation with three AddaVax adjuvanted doses of 1 µg ZIKV VLPs, ZIKV SVPs or CHIKV VLPs, or PBS only, or after infection with ZIKV Natal (positive control). Lines among the dots show the mean ELISA titers and error bars indicate the standard error of the mean. Limit of detection is 1 in 30 serum dilution. **(H)** ZIKV PRVABC59 50% neutralisation titers in serum from IFNAR$^{-/-}$ males vaccinated or infected as in (F). Lines among the dots show the mean neutralisation titers and error bars indicate the standard error of the mean. Limit of detection is 1 in 10 serum dilution. **(I)** ZIKV PRVABC59 viraemia post challenge in IFNAR$^{-/-}$ males immunised or infected as in (F) with n = 4-5 per group and with means from 4-5 mice plotted.

vaccination, 7 out of 10 mice developed neutralising antibodies against ZIKV (Fig. 3C). Following ZIKV SVP vaccination, 4 out of 5 mice showed neutralising antibody responses (Fig. 3C). CHIKV VLPs did not induce neutralisation titers against ZIKV. Next, mice were challenged with wild-type ZIKV. Of the mice immunised with ZIKV VLPs, 5 mice were challenged with the lethal African ZIKV MR766 isolate (275) to measure survival after infection, whereas the other 5 mice were infected with the non-lethal ZIKV Natal isolate to evaluate the protective ability against a more recent, Brazilian ZIKV isolate. All other mice were challenged with ZIKV MR766. Challenge took place at week 6 (MR766) or week 8 (Natal) post vaccination. All ZIKV VLP/SVP vaccinated mice developed high levels of viraemia post challenge (Fig. 3D), indicating that the ZIKV vaccines did not protect against ZIKV infection. Also, no correlation was found between the viraemia level of individual ZIKV VLP/SVP immunised mice and their reciprocal 50% neutralisation titer as measured at 4 weeks post vaccination (Suppl. Fig. 1). Interestingly however, at day 4 post MR766 challenge significantly lower viraemia was observed in mice vaccinated with ZIKV VLP as compared to CHIKV VLP ($p < 0.01$, t-test) as well as with ZIKV SVP versus CHIKV VLP ($p < 0.01$, t-test). Moreover, 3 (ZIKV VLP) or 4 (ZIKV SVP) out of 5 mice survived MR766 challenge, whereas all mice immunised with CHIKV VLP died at 7 or 8 days post challenge (Fig. 3E). The ZIKV VLP or SVP vaccinated mice that died after challenge all had shown neutralisation titers below the detection limit at week 4 post vaccination. Together, these results suggest a limited degree of protection of the ZIKV vaccines.

We next evaluated whether three doses of ZIKV VLPs or SVPs would be sufficient to protect mice from ZIKV infection (Fig. 3F). We used the well-described IFNAR$^{-/-}$ male mouse model (260, 261) in combination with non-lethal ZIKV PRVABC59 to evaluate the immunogenicity and protective ability of the ZIKV vaccines. As negative controls, groups of mice were vaccinated with either CHIKV VLPs or PBS only. As positive control, a group of mice was infected with ZIKV Natal (non-lethal) to induce sufficient neutralising antibodies to protect against subsequent virus challenge. Since AddaVax adjuvant has shown to strengthen neutralising immune responses induced by ZIKV VLPs derived from human cells (259), this adjuvant was added to all VLP/SVP vaccine formulations. After three doses of ZIKV VLPs or SVPs, similar levels of ZIKV-specific antibodies were induced as after one dose in IFNAR$^{-/-}$ female mice (Fig. 3G). Surprisingly, none of the male mice vaccinated with ZIKV VLPs or SVPs produced neutralising antibody titers above the detection limit, whereas mice infected with ZIKV Natal developed high levels of neutralising antibodies (Fig. 3H). Following challenge with ZIKV PRVABC59, all mice vaccinated with VLPs/SVPs or PBS developed high levels of viraemia, whereas mice previously infected with ZIKV Natal did not develop viraemia (Fig. 3I). Three doses of ZIKV VLPs or SVPs hence also did not protect against ZIKV infection. Nevertheless, ZIKV titers from mice immunised with ZIKV VLP were significantly lower at 6 and 7 days post challenge compared to mice vaccinated with CHIKV VLP ($p < 0.001$, t-test). Viraemia levels of ZIKV SVP vaccinated mice were also lower as compared to CHIKV VLP immunised mice, with a significant difference at day 7 ($p < 0.001$, t-test). These results thus indicate a limited efficacy of both ZIKV vaccines.

Epitope display analysis

Although vaccination of mice with ZIKV VLPs or SVPs lead to the production of ZIKV-specific antibodies, neutralising antibody titers were often low or absent, and the vaccines were unable to protect mice against ZIKV infection. In an attempt to unravel the possible cause underlying the ineffectiveness of the vaccines, the binding of a panel of well-described flavivirus cross-reactive or ZIKV-specific mAbs (Table 2) to E protein epitopes presumably present on the surface of the VLPs/SVPs (produced using Sf21 cell monolayers) was measured by ELISA, and compared to the binding of the mAbs to epitopes on wild-type ZIKV and recombinant E subunit.

ZIKV VLPs and SVPs were recognized by flavivirus cross-reactive mAbs 4G2 and 1M7 (Fig. 4A), which recognize low complexity fusion loop epitopes in domain II of the E protein and are weakly or moderately neutralising, respectively. In contrast, very low levels of the flavivirus cross-reactive E dimer epitope (EDE) dependent mAbs (A11, B7, C8, C10) bound to ZIKV VLPs or SVPs (Fig. 4A).

The low levels of bound EDE mAbs were comparable to the low levels bound to ZIKV E subunit, whilst much higher levels of these mAbs bound to wild-type ZIKV (Fig. 4A). Of the ZIKV-specific mAbs that recognize quaternary structure epitopes on the E protein, ZIKV-117 and G9E recognized VLPs and SVPs, whereas A9E only recognized wild-type virus and SVPs (Fig. 4B). Z20 readily bound wild-type ZIKV but did not react with ZIKV VLPs or SVPs (Fig. 4B). Of the ZIKV-specific mAbs binding lower complexity protein conformations (ZKA-64, Z3L1, Z23), ZKA64 recognized wild-type virus and VLPs/SVPs, Z3L1 recognized wild-type virus but not VLPs/SVPs, and Z23 did not recognize wild-type virus but did recognize VLPs/SVPs (Fig. 4B). Together, these results indicate that the structural conformation of displayed E proteins markedly differed between VLPs/SVPs and wild-type ZIKV, which is likely responsible for the lack of neutralising capacity against wild-type virus seen *in vivo* after VLP/SVP vaccination.

We hypothesised that VLP/SVP production in culture fluid of pH 6.2-6.4, which is the pH range commonly applied in the baculovirus-insect cell expression system but also the pH range at which flavivirus E protein mediated fusion occurs (276-278), induces an irreversible conformational transition of the ZIKV E proteins from a dimeric, prefusion state into a trimeric state to expose the fusion loop. This is expected to result in an inability of the VLPs/SVPs to induce high neutralising antibody titers against wild-type ZIKV. We next improved our vaccine design by developing a vaccine variant with covalently linked E proteins to lock the dimeric conformation that is needed for the induction of potent neutralising antibody responses.

Production of stabilised ZIKV SVPs from insect cells

Recent studies on DENV and ZIKV have shown that displaying stable E homodimers in vaccine formulations can be challenging to achieve, but that covalent linkage of the E proteins within a dimer can improve vaccine efficacy (247, 249, 252-255). Following this strategy, we introduced an alanine to cysteine mutation (A264C) in the E domain II region of our ZIKV prME structural cassette by quick change PCR on the pDEST8 plasmid containing ZIKV prME. We chose to only continue with the ZIKV prME construct because mAbs 1M7 and A9E bound to VLPs (CprME) at low levels but did effectively recognize SVPs (prME) and wild-type ZIKV (Fig. 4A, 4B), thus indicating that the E protein epitopes of SVPs (prME) might be closer resembling those of wild-type virus. The ZIKV prME-A264C structural cassette (Fig. 5A) was used to generate the recombinant baculovirus BACe56/ZIKV-prME-A264C. Cells expressing ZIKV prME-A264C formed large syncytia (Fig. 5B) comparable to cells expressing ZIKV prME (Fig. 1B), which suggests that the ZIKV E protein is still fusogenic.

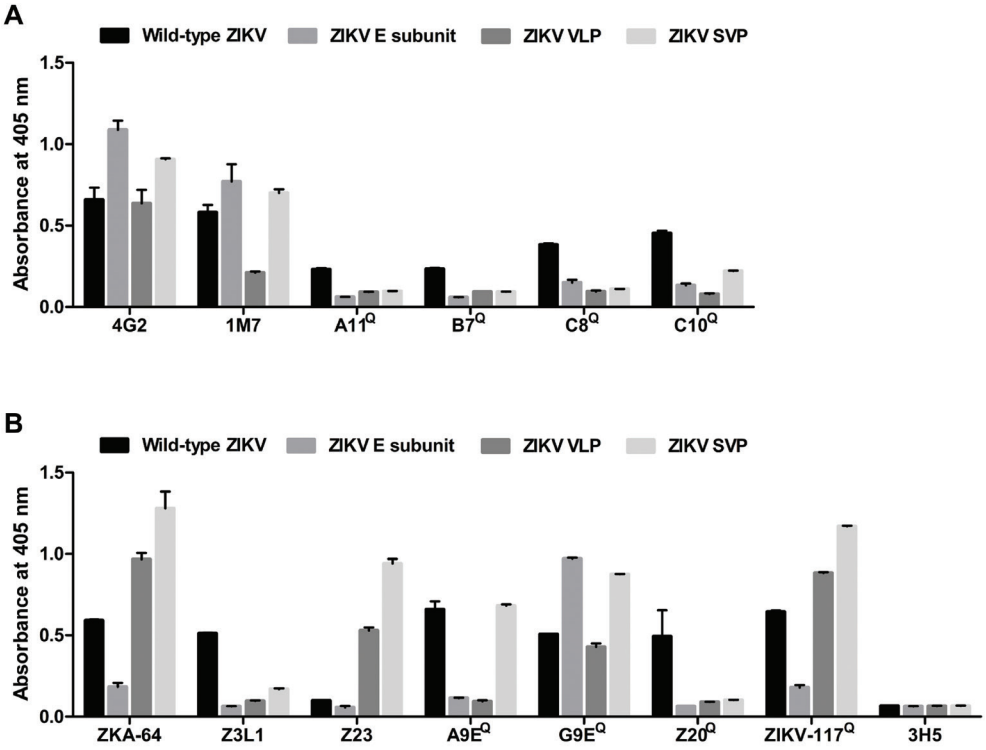

Figure 4. Epitope display analysis of ZIKV VLPs and SVPs. Binding of **(A)** flavivirus cross-reactive α-E mAbs 4G2, 1M7, A11, B7, C8 and C10, and **(B)** ZIKV-specific α-E mAbs ZKA-64, Z3L1, Z23, A9E, G9E, Z20 and ZIKV-117 to wild-type ZIKV, ZIKV E subunit, ZIKV VLP and ZIKV SVP. The mAbs that bind quaternary structure epitopes are marked with 'Q'. The DENV2-specific α-E mAb 3H5 was included as a negative control. The mean of two technical replicates is shown, with error bars indicating the standard deviation.

Infected insect cells were subsequently analysed by western blot using 4G2 mAb to detect ZIKV E protein. The analysis was carried out under non-reducing conditions to keep covalently linked E proteins intact. Cells expressing ZIKV prME-A264C showed E monomer at ~55 kDa, similar to cells expressing ZIKV prME (Fig. 5C). ZIKV prME-A264C expression also led to an additional protein band of higher molecular mass (Fig. 5C), likely representing the dimer with covalently linked E proteins.

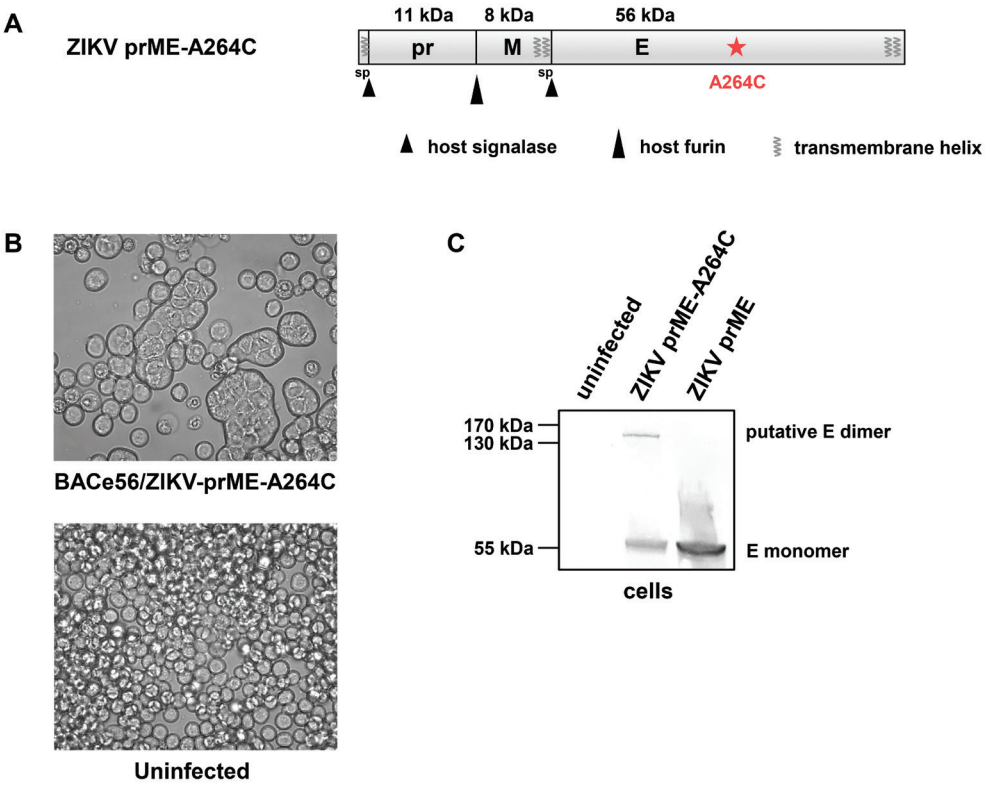

Figure 5. Production of ZIKV SVP with stabilised E protein dimers. (A) Schematic overview of the ZIKV prME structural cassette with alanine to cysteine (A264C) mutation for covalent linkage of E proteins to produce ZIKV SVPs with stabilised E homodimers. The molecular mass of each viral protein is shown in kDa. Cleavage sites of host signalase and host furin are indicated, as well as predicted signal peptide (sp) sequences and transmembrane helices. **(B)** Sf9 insect cells infected with indicated baculovirus at 3 days post infection, or uninfected cells. **(C)** ZIKV E protein expression in Sf9 insect cells infected with recombinant baculoviruses expressing the indicated cassettes measured by western blot using pan-flavivirus α-E 4G2 mAb.

Growth of insect cells in culture fluid of different pH

To prevent transition of E proteins to the postfusion state, we aimed to produce the vaccines at pH 7.0, which is above the threshold for flavivirus E protein mediated membrane fusion (276, 277). To investigate whether suspension Sf9 insect cells would be capable of vaccine production at higher pH, uninfected cells were grown for 3 days at uncontrolled pH, pH 6.6, pH 6.8 or pH 7.0, and cell concentration and cell viability were measured each day. The cells cultured in medium without pH control (for which the pH gradually dropped from 6.2 to 6.0 during the experiment) as well as the cells cultured in medium of pH 6.6 grew to cell densities of 10^7 cells/

ml (Fig. 6A) and showed high viability (Fig. 6B). However, cells grown at pH 6.8 and pH 7.0 did not grow (Fig. 6A) and showed low viability (Fig. 6B). This indicates that Sf9 insect cells are unable to grow and produce vaccines at neutral pH after an immediate pH switch, thus suggesting the need for long-term evolutionary adaptation using a progressive increase to pH 7.0.

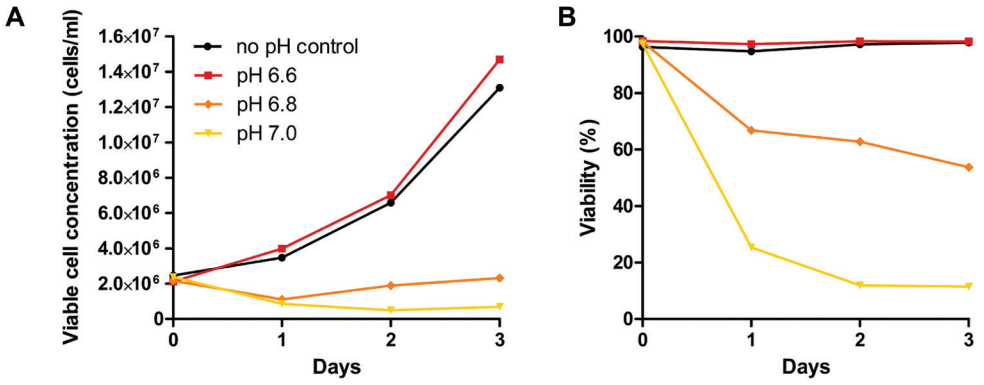

Figure 6. Growth of suspension Sf9 insect cells in culture media of different pH. Sf9 cells (cell density at day 0: 2 x 10^6 cells/ml) were grown in medium of uncontrolled pH, pH 6.6, pH 6.8 or pH 7.0 for 3 days, and **(A)** viable cell concentration and **(B)** cell viability were measured daily.

Production of ZIKV SVP and SVP-A264C using adapted insect cells

Next, ZIKV SVP and SVP-A264C vaccines were produced at pH 7.0 using Sf9 insect cells adapted to neutral pH via stepwise adaptive laboratory evolution as described (279). As control experiments, both vaccine variants were also produced using non-adapted Sf9 cells (at pH 6). A protein band of ~55 kDa in the purified samples indicated ZIKV E monomer (Fig. 7A). The samples obtained after ZIKV SVP-A264C purification also contained a higher molecular mass product indicative of ZIKV E dimers (Fig. 7A), hence suggesting the presence of ZIKV SVPs with covalently stabilised E proteins. Spherical particles of ~20-60 nm in diameter were observed in the purified samples by electron microscopy (Fig. 7B), indicating that prME-A264C expression resulted in SVP production, and that particles could also be formed at pH 7.

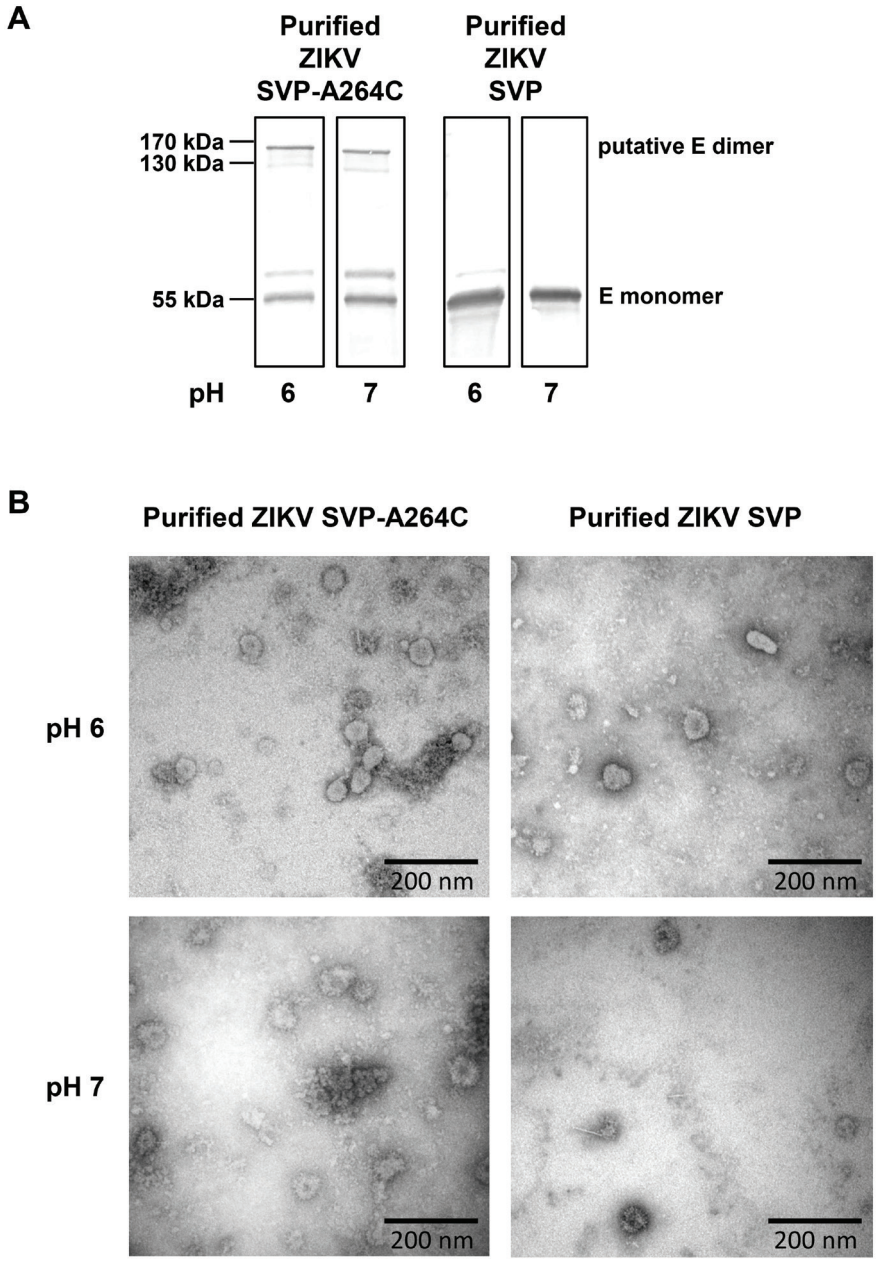

Figure 7. Characterisation of ZIKV SVP-A264C and SVP produced at pH 7 using adapted insect cells or at pH 6 using non-adapted insect cells. (A) ZIKV E protein expression in samples obtained after sucrose gradient purification, measured by western blot using pan-flavivirus α-E 4G2 mAb. **(B)** Transmission electron microscopy photos of purified samples.

Discussion

Despite low ZIKV transmission during the past few years, the threat of new ZIKV outbreaks remains looming on the horizon. Currently, no licenced vaccines or antivirals are available to protect humans against ZIKV infection. In this study, we produced two scalable ZIKV VLP-based vaccines using recombinant baculoviruses and insect cells, and tested the immunogenicity and protective ability of both vaccines in mouse models of ZIKV disease.

Expression of the ZIKV prME structural cassette in insect cells resulted in the formation of large syncytia. Similar cell-to-cell fusion has also been reported during infection of the flaviviruses DENV, St Louis encephalitis virus, Japanese encephalitis virus and yellow fever virus in mosquito cells, and was most prominent in culture fluids of pH < 7.0 (280-282), which is also the pH at which flavivirus E protein mediated fusion normally takes place (276-278). This suggests that the observed syncytia during ZIKV prME expression in insect cells are likely caused by the fusogenic activity of the ZIKV E protein, triggered by the low pH of the insect cell culture medium.

Expression of ZIKV CprME or prME in insect cells resulted in the production of VLPs or SVPs, respectively. Immunisation of IFNAR$^{-/-}$ mice with one or three doses of purified ZIKV VLPs or SVPs induced a limited neutralising antibody response against ZIKV and lack of protection against disease upon ZIKV challenge. A similar study also reported low levels of neutralising antibodies in response to immunisation with ZIKV SVPs from insect cells, and suggested that the SVPs might have a different conformation than wild-type virus (283). Based on these observations, we hypothesise that the limited capacity of the VLP and SVP vaccines to trigger neutralising antibodies and to protect against ZIKV infection is caused by incorrectly folded E proteins in the envelope of the VLP and SVP vaccines. The E proteins present in the vaccine formulation are likely arranged in an irreversible, postfusion, trimeric conformation induced by the low pH of the insect cell culture fluid, whilst potent neutralising antibodies during natural ZIKV infection are usually targeting the prefusion, dimeric E protein conformation, which was found to be largely absent in our VLP/SVP formulations according to epitope display analysis.

Following this hypothesis, it was still surprising that a single 1 µg dose of ZIKV VLPs or SVPs induced neutralising antibody levels above the detection limit (1 in 10 serum dilution) for 7 out of 10 mice and 4 out of 5 mice, respectively, whereas three 1 µg doses of ZIKV VLPs or SVPs did not induce neutralising antibody responses above the detection limit for any of the vaccinated mice. The vaccines administered in the single dose study were produced by infecting Sf9 suspension cells with recombinant baculoviruses using an MOI of 5 $TCID_{50}$ units per cell, whereas

the vaccines administered in the three-dose study were produced using an MOI of 0.01 $TCID_{50}$ units per cell. Sf9 cells infected at low MOI continue to grow for a relatively longer period as compared to Sf9 cells infected at high MOI, and might therefore more rapidly lower the pH of the culture fluid due to cellular metabolism. The presumed lower pH for Sf9 cells infected at lower MOI is expected to induce conformational changes towards the postfusion state for a larger proportion of the E proteins. Other factors differing between the two vaccination studies could also be (partly) responsible for the observed difference in neutralising antibody levels induced after one and three vaccine doses. These include mouse gender, the addition of adjuvant, and the wild-type ZIKV isolate used for the neutralisation assays.

Detailed epitope display analysis revealed that all four EDE-binding antibodies (A11, B7, C8, C10) did not effectively recognize the ZIKV VLPs and SVPs. These mAbs bind complex quaternary structure epitopes across the E dimer interface, and poorly recognize E proteins in the trimeric, postfusion state (284). These antibodies can neutralise ZIKV and DENV, and are thought to lock E dimers in the prefusion state (245, 267, 285). Especially the mAbs C8 and C10 are highly neutralising against ZIKV (245). The inability of these mAbs to bind the VLPs/SVPs thus suggests absence of E dimers, which are considered important components of many effective experimental ZIKV vaccines developed to date (247-249).

In an attempt to stabilise the E dimers, an A264C mutation (252) was introduced. However, syncytia were still observed upon expression of prME-A264C, indicating that E protein mediated fusion could still occur. Western blot analysis of cells expressing ZIKV prME-A264C showed, in addition to the putative E dimer protein band, also a protein band at ~55 kDa which corresponds to the E monomer. This indicates that part of the E proteins is not covalently linked as dimer and can thus still mediate membrane fusion. Whether or not the E proteins in the envelope of the SVPs are covalently linked and locked into the prefusion dimeric state should be investigated further by epitope display analysis, before the vaccine can be tested in $IFNAR^{-/-}$ mice. If needed, the amount of covalently bound E proteins could potentially be improved by introducing additional cysteine bridges in E protein domain II (L107C) and III (A319C) as previously described for a ZIKV E dimer based subunit vaccine (254).

Effective ZIKV prME (SVP) vaccines have been developed using mammalian cell production systems (249, 286, 287), although the further scale up of these vaccines might be hampered by high costs associated with DNA transfections. The pH range of mammalian cell culture fluid is usually 7.0-7.2 and thus is expected to prevent the conformational change of ZIKV E proteins towards the postfusion state, which likely explains the high efficacy of these vaccines in contrast to the vaccine candidates tested in the current study. A chimeric ZIKV prME vaccine with

an insect-specific flavivirus as backbone, which was produced in mosquito cells, however was recognized by the highly neutralising EDE mAb C8 and did protect against wild-type ZIKV in the same female and male IFNAR$^{-/-}$ mouse models as used in our study (248). Importantly, this vaccine was produced at pH 7 (unpublished data, Jody Hobson-Peters). The high effectiveness of this vaccine also implies that general differences between insect and mammalian production systems, e.g. their pathways of glycosylation (288), are less likely to be the cause of the failure of our Sf insect cell derived ZIKV VLP and SVP vaccines to confer protection in mice.

The proposed optimisation strategies for ZIKV SVP production in Sf insect cells will hopefully result in a safe and effective vaccine candidate for future use. Considering that ZIKV is predominantly circulating in low to middle income countries (241), the use of the baculovirus-insect cell expression system, known for its excellent scalability at low costs (289), could be advantageous to produce a cost-effective VLP-based vaccine.

Acknowledgements

We thank Marleen Abma-Henkens and Els Roode for cell culture maintenance, and Chantal Reusken for providing Zika virus Suriname 2016 cDNA.

SRA was supported by ZonMw (project: ZikaRisk “Risk of Zika virus introductions for the Netherlands”, grant number: 522003001) and by the graduate school PE&RC via a strategic fund award.

Supplementary information

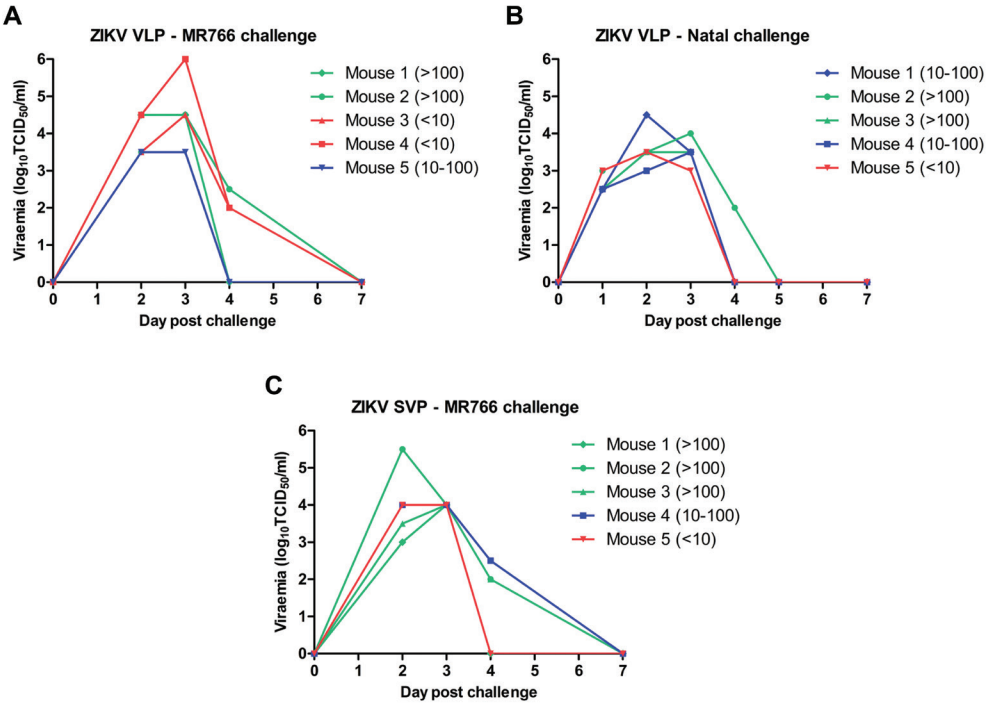

Supplementary Figure 1. ZIKV viraemia post challenge in individual mice vaccinated with a single dose of 1 µg ZIKV VLPs or SVPs. (A) ZIKV MR766 viraemia post challenge in individual IFNAR$^{-/-}$ females immunised with ZIKV VLPs. **(B)** ZIKV Natal viraemia post challenge in individual IFNAR$^{-/-}$ females immunised with ZIKV VLPs. **(C)** ZIKV MR766 viraemia post challenge in individual IFNAR$^{-/-}$ females immunised with ZIKV SVPs. The colour of the lines (green, blue, red) indicates the reciprocal 50% neutralisation titer measured in mouse serum (>100, 10-100, <10, respectively; also indicated behind the mouse number in the figure).

Chapter 7 **A scalable, non-adjuvanted virus-like particle vaccine from insect cells protects mice against Mayaro virus infection**

Sandra R. Abbo[1,*], Wilson Nguyen[2,*], Marleen H.C. Abma-Henkens[1], Denise van de Kamer[1], Niek H.A. Savelkoul[1], Corinne Geertsema[1], Thuy T.T. Le[2], Bing Tang[2], Kexin Yan[2], Monique M. van Oers[1], Andreas Suhrbier[2], Gorben P. Pijlman[1]

[1]Laboratory of Virology, Wageningen University & Research, Wageningen, the Netherlands
[2]Inflammation Biology Group, QIMR Berghofer Medical Research Institute, Brisbane, Australia

*These authors contributed equally to this work.

Manuscript submitted.

Abstract

Mayaro virus (MAYV) causes debilitating arthritic disease in humans and is emerging in tropical Central and South America. The virus is transmitted in an enzootic cycle between non-human primates and forest-dwelling mosquitoes. In recent years, MAYV has also caused an increasing number of human infections in non-forest areas. The recent discovery that the urban mosquito species *Aedes aegypti* and *Aedes albopictus*, which are the main vectors for Zika virus, dengue virus and chikungunya virus, are able to transmit MAYV is raising considerable concern. Currently, there are no licensed vaccines or antiviral drugs available to prevent or cure MAYV disease. In this study, we developed an enveloped virus-like particle (VLP) vaccine against MAYV using the scalable baculovirus-insect cell expression system. High-level secretion of MAYV VLPs in the culture fluid of Sf9 insect cells was achieved, and particles with a diameter of 64-70 nm were obtained after purification. In an optimised mouse model for MAYV disease, a prime-boost regime with two immunisations with 1 µg of non-adjuvanted MAYV VLPs induced potent neutralising antibody responses and completely protected the animals against viraemia, myositis, tendonitis and joint inflammation after challenge with wild-type MAYV. This MAYV VLP vaccine from insect cells thus proved to be an effective, scalable and safe vaccine candidate that can be further developed to prevent future MAYV outbreaks.

Introduction

The tropical regions of our planet harbour a large diversity of mosquito-borne viruses, some of which have shown to possess the potential to quickly spread across the human population and cause disease outbreaks of unprecedented scale. Chikungunya virus (CHIKV) was first identified in 1952 in Tanzania, has since then spread across the globe, and started a major outbreak in Latin America in 2013 (290). Zika virus (ZIKV), first detected in a sentinel rhesus monkey in a forest in Uganda in 1947, spread via Asia and Pacific islands to Latin America, where it caused a large outbreak in 2015 and 2016 (9). These mosquito-borne viruses continue to persist in urban areas, often through human-to-human transmission cycles via mosquitoes, and pose a substantial threat to human health worldwide.

Mayaro virus (MAYV), a tropical virus closely related to CHIKV, is currently emerging in Central and South America (14). MAYV infection in humans causes a fever for several days accompanied by headache, eye pain, myalgia, vomiting, diarrhoea, rash, and acute, often prolonged severe arthralgia (14, 32, 36). Rare severe manifestations of MAYV infection can include haemorrhagic presentations or encephalitis, potentially leading to mortality (33). In tropical rainforests, MAYV

is maintained in an enzootic transmission cycle between non-human primates and mosquitoes (14). Although non-human primates are thought to be the primary hosts for MAYV, also other vertebrates including sloths, rodents and birds have tested positive for the virus but their role in MAYV transmission is unclear (35, 291, 292). Forest-dwelling mosquitoes of the genus *Haemagogus* are considered the prime vectors for MAYV (35), which could explain the observation that human cases of MAYV disease are usually linked to residence in tropical forests. MAYV was first isolated from diseased forest workers in the Cat's Hill region of Mayaro County in Trinidad in 1954 (12, 13). Later, serological analyses revealed that antibodies against MAYV were frequently found in humans living in certain areas around the Amazon basin (293). Small MAYV outbreaks were occasionally reported (34, 294), as well as imported cases of MAYV infection in travellers returning from endemic areas to North America (36) and Europe (37, 38), but altogether MAYV infections remained limited to persons recently in contact with tropical forests.

However, in Haiti in 2015, an 8-year-old boy was diagnosed with a co-infection of MAYV and dengue virus (DENV) (39). This patient lived in a rural/semi-rural region of Haiti, which differed greatly from the humid, tropical forests where MAYV has previously been detected (39). This could therefore point towards a role of non-forest mosquito species in MAYV transmission. In addition, recent studies have shown that the urban mosquito species *Aedes aegypti* and *Aedes albopictus*, which are the main vectors for CHIKV, DENV and ZIKV, are capable of transmitting MAYV (41-44). The ability of these mosquitoes to vector MAYV raises concern of whether the virus could enter an urban transmission cycle as seen for CHIKV, DENV and ZIKV. This, together with the expanding world population, ongoing globalisation and rapid urbanisation, will certainly increase the pandemic potential of MAYV (14).

MAYV belongs to the genus *Alphavirus* and the family *Togaviridae*. The ~11.5 kb, single-stranded, positive-sense RNA genome encodes four non-structural proteins (nsP1-nsP4) in a single open reading frame (ORF), and immediately downstream is a second ORF coding for the structural proteins. The structural proteins include the capsid protein or C, and the two envelope glycoproteins E2 and E1 with their associated proteins E3 and 6K, respectively, and the transframe protein (resulting from a -1 ribosomal frameshift in 6K) (56, 295). The non-structural proteins are involved in replication of the RNA genome, whereas the structural proteins form a spherical virus particle of ~70 nm in diameter (56). C is on the inner side of the particle and forms a core of ~40 nm in diameter (56), whereas the glycoproteins face the outside and span the host-derived lipid membrane (57). The 240 E2-E1 heterodimers found on the surface of the virion form 80 trimeric spikes (57). The

structural proteins have important functions in assembly, receptor recognition and entry into cells (296) but are also the antigens of choice for vaccination.

Since MAYV might continue to spread further and could potentially induce large-scale epidemics, it is important to develop effective countermeasures. Currently, there are no licenced vaccines or antiviral drugs available to prevent or cure MAYV disease in humans (33). Several effective pre-clinal MAYV vaccines have been developed, including a live-attenuated vaccine (297, 298), a DNA vaccine (299), and two adenoviral-vectored vaccines (300, 301). Live-attenuated vaccines, however, might risk reversion to virulence (302), whereas immunity against the viral vector complicates sequential vaccinations for adenoviral-vectored vaccines (303). DNA vaccines are an attractive candidate due to their efficient production process and long shelf life, but often show poor immunogenicity in humans (304) .

Here we report the development of an enveloped MAYV virus-like particle (VLP) vaccine using a similar strategy as for the generation of a safe and effective enveloped CHIKV VLP vaccine (257). VLPs are structurally similar to the virus particle, but do not contain a viral genome. Self-assembly of the envelope and capsid proteins from the virus result in VLP formation (305). Since only the shell of the virus is present, and not its genetic material, immune responses will be induced, but no reversion to virulence can take place as the VLPs are not able to replicate (85). In this study, we used the scalable baculovirus-insect cell expression system to produce MAYV VLPs from insect cells. The purified VLPs were tested for efficacy in an optimised mouse model for MAYV disease.

Methods

Cell culture

The *Spodoptera frugiperda*-derived cell lines Sf21 (Gibco, Carlsbad, CA, USA), Sf9 (Gibco) and Sf9-ET (251) were grown at 27°C. Monolayers of Sf21 cells were grown in Grace's medium (Gibco) supplemented with 10% fetal bovine serum (FBS; Gibco). Monolayers of Sf9-ET cells were grown in Sf900II medium (Gibco) supplemented with 5% FBS and 100 µg/ml geneticin (Gibco). Monolayers and suspension cultures of Sf9 cells were grown in Sf900II serum-free medium supplemented with 50 µg/ml gentamycin (Gibco). The *Aedes albopictus*-derived cell line C6/36 was cultured in RPMI 1640 medium (Thermo Fisher Scientific, Scoresby, VIC, Australia) with 10% FBS (Sigma-Aldrich, Castle Hill, NSW, Australia) at 28°C and 5% CO_2. The African green monkey kidney Vero cell line was maintained in RPMI 1640 medium supplemented with 10% FBS at 37°C and 5% CO_2.

MAYV isolate

MAYV isolate BeH407 (GenBank: MK573238.1) was a generous gift from Prof. M.S. Diamond (Washington University School of Medicine, St Louis, MO, USA). MAYV BeH407 was propagated on C6/36 cells and titrated by $TCID_{50}$ assays using C6/36 and Vero cell lines as described (306, 307).

Generation of recombinant baculovirus

Total RNA was isolated from MAYV BeH407-infected cells using TRIzol reagent (Invitrogen, Carlsbad, CA, USA). cDNA was generated using SuperScript II Reverse Transcriptase (Invitrogen). The complete structural cassette of MAYV (C-E3-E2-6K-E1; 3729 bp; GenBank: MK573238.1) was then amplified and provided with BamHI and HindIII restriction sites by PCR using Phusion High-Fidelity DNA polymerase (New England Biolabs, Ipswich, MA, USA) and a 2720 Thermal Cycler (Applied Biosystems, Foster City, CA, USA). Next, the Bac-to-Bac baculovirus-insect cell expression system (Invitrogen) was used to insert the structural cassette of MAYV into the improved *Autographa californica* multiple capsid nucleopolyhedrovirus (AcMNPV) backbone BACe56 (256). The MAYV structural cassette was first ligated into pFastBac Dual (Invitrogen) behind the polyhedrin promoter and then transposed into BACe56. Transfection of Sf21 cells with purified recombinant bacmid DNA using ExpreS^2 TR (ExpreS^{2}ion Biotechnologies, Hørsholm, Denmark) resulted in the recovery of recombinant baculovirus. Virus titers in $TCID_{50}$/ml were measured using Sf9-ET cells.

MAYV VLP production and purification

For small-scale MAYV VLP production, 8 x 10^6 Sf9 cells were seeded as monolayer in a 75 cm^2 flask. Cells were infected with recombinant baculovirus containing the MAYV structural cassette (BACe56/MAYV) at a multiplicity of infection (MOI) of 2 $TCID_{50}$ units per cell. After infection, cells were incubated for 4 hours at 27°C. Afterwards, the medium was replaced by fresh Sf900II serum-free medium. For large-scale MAYV VLP production, ten Sf9 suspension cultures of 50 ml each containing 2.6 x 10^6 cells/ml were infected with BACe56/MAYV at an MOI of 0.2 $TCID_{50}$ units per cell. Cells were incubated at 27°C for 4 days. Afterwards, cells and medium were separated by centrifugation at 1700 rpm for 5 min. The cell pellet was dissolved in PBS. The supernatant containing the MAYV VLPs was first filtered through a filter with a pore size of 0.45 µm. Next, 7% (w/v) polyethylene glycol (PEG)-6000 and 0.5 M NaCl were added to the filtered medium to precipitate the VLPs. After 2 hours at room temperature (RT) and subsequent centrifugation at 4700 rpm for 15 minutes, the pellet was dissolved in GTNE buffer (200 mM glycine, 50 mM Tris/HCl, 100 mM NaCl, 1 mM EDTA, pH 7.3). VLPs were then purified on a discontinuous sucrose gradient (40%-70%, w/v) as described earlier (257, 258).

MAYV protein analysis

MAYV proteins from infected cell fractions and pure VLP fractions were detected using sodium dodecyl sulphate polyacrylamide gel electrophoresis (SDS-PAGE) and subsequent western blotting. First, loading buffer containing SDS and β-mercaptoethanol was added to the samples. Samples were then incubated for 10 minutes at 95°C. After centrifugation for 1 minute at 14,000 rpm, samples were run on a Mini-PROTEAN TGX gel (Bio-Rad, Veenendaal, the Netherlands). Afterwards, proteins were transferred to an Immobilon-P membrane (Merck Millipore, Darmstadt, Germany) using a trans-blot semi-dry transfer cell (Bio-Rad). The membrane was blocked at 4°C overnight using 1% skimmed milk powder in PBS containing 0.05% Tween (PBS-T). The next steps were performed at RT. The membrane was incubated with either antiserum from a MAYV-infected mouse diluted 1:250 in 1% skimmed milk, or anti-CHIKV capsid 5.5D11 monoclonal antibody (308) diluted 1:500 in 1% skimmed milk. After 1 hour, the membrane was washed three times with PBS-T. Subsequently, the membrane was incubated with alkaline phosphatase conjugated goat anti-mouse IgG secondary antibody (Sigma-Aldrich, Darmstadt, Germany) for 1 hour. Secondary antibody was diluted 1:2500 in PBS-T. After washing again three times with PBS-T, the membrane was incubated with alkaline phosphatase buffer as described (257) for 10 minutes. The membrane was then developed using NBT/BCIP (Roche Diagnostics, Almere, the Netherlands).

MAYV VLP quantification

The purified MAYV VLPs produced in Sf9 insect cells (named WUR MAYV VLPs) were quantified using a dilution series of pure MAYV VLPs from HEK293 human cells purchased at The Native Antigen Company (TNAC, Oxford, UK; design based on GenBank KM400591.1; named TNAC MAYV VLPs). Samples containing serial twofold dilutions of 0.50 µg TNAC MAYV VLPs were prepared. These samples and the purified fraction containing WUR MAYV VLPs were analysed using SDS-PAGE and western blot with antiserum from a MAYV-infected mouse as described above. Comparison of the band intensity for MAYV E2/E1 resulted in an estimated concentration of WUR MAYV VLPs in the purified fraction.

Transmission electron microscopy

Purified MAYV VLPs in GTNE buffer were loaded onto 200 mesh carbon coated copper grids (Electron Microscopy Sciences, Hatfield, PA, USA). After 2 min at RT, the excess of liquid was removed and 2% ammonium molybdate (pH 6.8) was added to the grids for 30 s at RT. Next, the excess of liquid was removed and the grids were air dried. Grids were analysed using a JEOL JEM-1400Plus transmission electron microscope. VLP diameters were measured using ImageJ (National Institutes of Health, Bethesda, MD, USA) in combination with in-house macros.

Mice, infection, virus titration and disease evaluation

All mouse work was conducted in accordance with the "Australian code for the care and use of animals for scientific purposes" as defined by the National Health and Medical Research Council of Australia. Mouse work was approved by the QIMR Berghofer Medical Research Institute animal ethics committee (P2235 A1606-618M). The conditions the mice were kept are as follows: light = 12:12 h dark/light cycle, 7:45 am sunrise and 7:45 pm sunset. 15 min light dark & dark light ramping time. Enclosures: M.I.C.E cage (Animal Care Systems, Centennial, CO, USA). Ventilation: 100% fresh air, 8 complete air exchanges/hr/room. Temperature: 22 + 1 ºC. In-house enrichment: paper cups, tissue paper, cardboard rolls. Bedding: PuraChips (Able Scientific, Perth, WA, Australia) (aspen fine). Food: double bagged Norco rat and mouse pellet (AIRR, Darra, QLD, Australia). Water: deionized water acidified with HCl (pH = 3.2).

To establish the model, female C57BL/6J mice (6-24 week old) were purchased from the Animal Resources Centre (Canning Vale, WA, Australia). Mice were infected with 10^4-10^6 $TCID_{50}$ of MAYV BeH407 subcutaneously into the top/side of each hind foot as described previously (306, 307, 309). Serum viraemia, foot swelling and histology were evaluated as described previously (306, 307, 309-311).

MAYV VLP vaccination and virus challenge

The WUR MAYV VLP, derived from Sf9 insect cells, and the TNAC MAYV VLP, derived from HEK293 human cells, were used to vaccinate mice (female C57BL/6J, 6-8 week old). The adjuvant as described (312) comprised QS-21 (50 µg/ml) (Creative Biolabs, Shirley, NY, USA), 3-O-desacyl-4'-monophosphoryl lipid A (MPLA) (50 µg/ml), cholesterol (250 µg/ml), dioleoyl phosphatidylcholine (1 mg/ml) (Sigma-Aldrich) constituted in PBS by sonication. The WUR MAYV VLP was mixed with adjuvant (1:1 v:v) for a total dose of 1 µg of VLP and 1 µg of adjuvant per mouse. The vaccines (with/without adjuvant) were mixed with RPMI 1640 medium and administered intramuscularly as described (307), with the dose split equally into both quadriceps muscles of restrained mice in 50 µl per muscle using an insulin syringe (Becton Dickinson, NJ, USA). Vaccinated mice were challenged with 10^5 $TCID_{50}$ of MAYV BeH407 into each hind foot, and viraemia, foot swelling and histology were evaluated as described above.

Antibody ELISA and neutralisation assays

IgG responses were determined by standard ELISA using whole MAYV BeH407 as antigen. The antigen was purified from infected C6/36 cell supernatants by 40% PEG-6000 precipitation (Sigma-Aldrich) and ultracentrifugation (Beckman Floor Standing Ultra, Beckman Coulter, CA, USA) at ~134,000 rcf at 4°C for 2 h through a 20% sucrose (Sigma-Aldrich) cushion. Endpoint ELISA titers were determined as

described (307, 313, 314). Briefly, serum samples, starting at a 1 in 30 dilution, were serially diluted 1 in 3 in duplicate and bound antibody detected using biotin-labelled rat anti-mouse-IgG (Thermo Fisher Scientific), streptavidin HRP (Biosource, Camarillo, CA, USA) and ABTS substrate (Sigma-Aldrich). Endpoint titers were interpolated when OD_{450} values reach the mean OD_{450} + 3 SE for naïve serum. Neutralisation assays were performed as described (307, 313). Briefly, mouse serum samples were heat-inactivated (56°C for 30 min) and incubated in duplicate with 150 $TCID_{50}$ of MAYV BeH407 at 37°C for 1 hour before Vero cells were added at a concentration of 10^5 cells/well. The initial serum dilution was 1 in 10, with serial dilutions of 1 in 2 in duplicate. After 5 days, cells were fixed and stained with formaldehyde and crystal violet and the 50% neutralising titers interpolated from optical density (OD_{590}) versus serum dilution plots as described (307, 314).

Histology

Histology and quantitation of staining were undertaken as described (306, 307, 309-311). In brief, feet were fixed in 10% formalin, decalcified with EDTA (Sigma-Aldrich), embedded in paraffin (Sigma-Aldrich) and sections stained with haematoxylin and eosin (H&E; Sigma-Aldrich). Slides were scanned using Aperio AT Turbo (Aperio, Vista, CA, USA) and analysed using Aperio ImageScope v10 software (Leica Biosystems Mt, Waverley, Australia) and the Positive Pixel Count v9 algorithm.

Statistics

Statistical analyses were performed using IBM SPSS Statistics for Windows v19.0 (IBM Corp., Armonk, NY, USA). The t-test was used when the difference in variances was <4, skewness was > minus 2 and kurtosis was <2. Otherwise, the non-parametric Kolmogorov-Smirnov test was used.

Results

Expression of MAYV structural proteins in insect cells using recombinant baculoviruses

To produce MAYV VLPs from insect cells, a recombinant baculovirus expressing the structural cassette of MAYV (C-E3-E2-6K-E1; Fig. 1A) was constructed. First, the sequence coding for the MAYV structural polyprotein was inserted downstream of the baculovirus polyhedrin promoter, and the construct was subsequently cloned into the improved baculovirus backbone BACe56 (256). This bacmid was used to transfect Sf21 insect cells to generate the recombinant baculovirus BACe56/MAYV. Sf9 insect cells were then infected with BACe56/MAYV at an MOI of 2 $TCID_{50}$ units per cell. At 4 days post infection, dense bodies were observed in the nuclei of infected insect cells (Fig. 1B, black arrow). These bodies suggest nuclear accumulation of

alphavirus capsid proteins, which has also been observed previously during CHIKV and salmonid alphavirus structural polyprotein expression in Sf insect cells (315). Next, MAYV protein expression in baculovirus-infected Sf9 cells was analysed by western blot using antiserum from a MAYV-infected mouse (Fig. 1C) and anti-CHIKV capsid monoclonal antibody 5.5D11 (Fig. 1D). Detection with mouse antiserum resulted in two protein bands around ~55 kDa (Fig. 1C), which likely correspond to the predicted molecular mass of unprocessed E3-E2 (54 kDa) and E2 and/or E1 (47 kDa each), and one protein band at ~35 kDa (Fig. 1C), which corresponds to the predicted molecular mass of capsid (34 kDa). Detection with anti-CHIKV capsid 5.5D11 antibody also showed MAYV capsid protein at ~35 kDa (Fig. 1D).

Characterisation of MAYV VLPs from insect cells

For large-scale MAYV VLP production, Sf9 cells were grown in suspension and infected with recombinant baculovirus at an MOI of 0.2 $TCID_{50}$ units per cell. At 4 days post infection, the culture medium was harvested. The VLPs were precipitated with PEG and purified on a 40%-70% discontinuous sucrose gradient. The isolated VLPs (named WUR VLPs) were then quantified by western blot analysis using a dilution series of commercial MAYV VLPs from HEK293 human cells (purchased at The Native Antigen Company; named TNAC VLPs) (Fig. 1E). Based on comparison of the protein band intensity of E2/E1 between insect cell-derived WUR VLPs and human cell-derived TNAC VLPs, the concentration of WUR VLPs was estimated in the purified fraction. Next, the pure WUR VLP fraction was analysed by transmission electron microscopy. Enveloped, spherical particles of ~70 nm in diameter were observed (Fig. 1F, black arrows), which is in accordance with the reported size of alphavirus virions (56). Some baculovirus particles could also be observed (Fig. 1F, white arrow). Next, the diameters of MAYV VLPs were measured, which showed that most VLPs were between 64 and 70 nm in diameter (Fig. 1G).

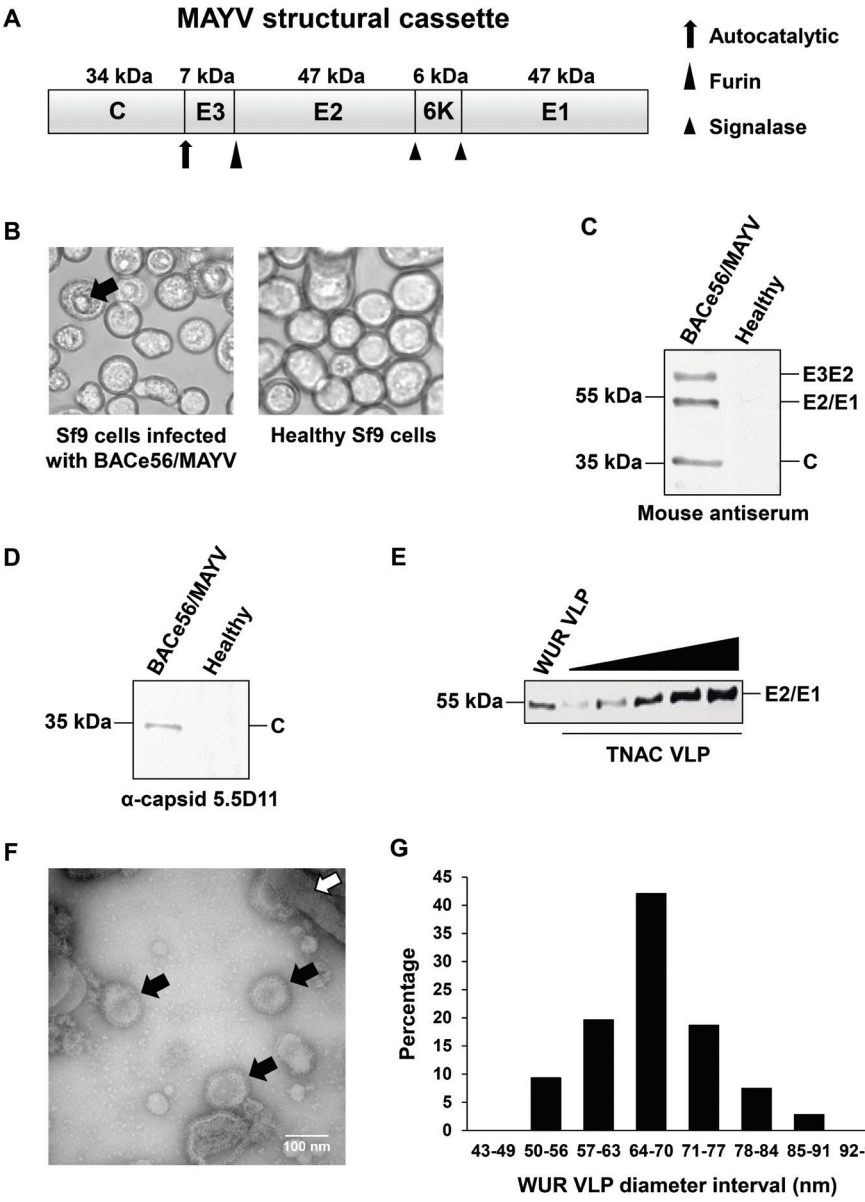

Figure 1. MAYV VLP production using insect cells and recombinant baculoviruses. (A) Schematic overview of the MAYV structural cassette expressed in insect cells. The molecular mass of each protein is shown in kDa. Autocatalytic, host furin and host signalase cleavage sites are indicated. **(B)** BACe56/MAYV-infected Sf9 insect cells and mock-infected, healthy Sf9 insect cells at 4 days post infection. Black arrow indicates dense nuclear body which presumably consists of accumulated MAYV core-like particles. MAYV structural protein expression in Sf9 cells was analysed at 4 days post infection by western blot using **(C)** antiserum derived from a MAYV-

infected mouse and **(D)** anti-CHIKV capsid antibody 5.5D11. **(E)** Detection of MAYV structural proteins in purified WUR VLP fraction from Sf9 insect cells and dilution series of TNAC MAYV VLPs from HEK293 human cells. **(F)** Transmission electron microscopy photo of purified WUR MAYV VLPs. Black arrows indicate MAYV VLPs; white arrow indicates baculovirus. **(G)** Size distribution of WUR MAYV VLPs based on diameter measurements of 107 VLPs.

MAYV BeH407 replication and pathogenesis in C57BL/6J adult mice

To test the immunogenicity and protective ability of MAYV VLP vaccines, a mouse model of MAYV disease was first developed. To characterise the MAYV BeH407 isolate and its ability to infect and cause disease in mice, adult 6-24 week old female C57BL/6J mice were infected subcutaneously in the hind feet with MAYV BeH407 at doses 10^4, 10^5 or 10^6 $TCID_{50}$. Viraemia for mice infected with 10^4 $TCID_{50}$ and 10^5 $TCID_{50}$ peaked on day 2 post infection compared to mice infected with 10^6 $TCID_{50}$, which peaked on day 1 post infection (Fig. 2A). Foot swelling is an indicator of arthritic disease in this mouse model, and peak foot swelling was observed on day 6 post infection for all doses (Fig. 2B), with a dose of 10^5 $TCID_{50}$ demonstrating the highest percentage increase of 22%. H&E staining of arthritic feet from MAYV-infected mice at day 6 post infection illustrated the characteristic mononuclear cellular infiltrates (32, 307, 316) evident in the muscle tissue (black ovals), tendon, synovial space and in the subcutaneous oedema (Fig. 2C). Quantitation using purple (nuclear) / red (cytoplasmic) staining ratios, a measure of leukocyte infiltration as these cells tend to have higher nuclear to cytoplasm ratios than resident cells, demonstrated significant differences between MAYV-infected mice compared to mock-infected mice (Fig. 2D). Thus, the human isolate MAYV BeH407 demonstrated inflammatory infiltrates in adult wild-type mice characteristic of alphaviral arthritides including myositis, tendonitis and arthritis.

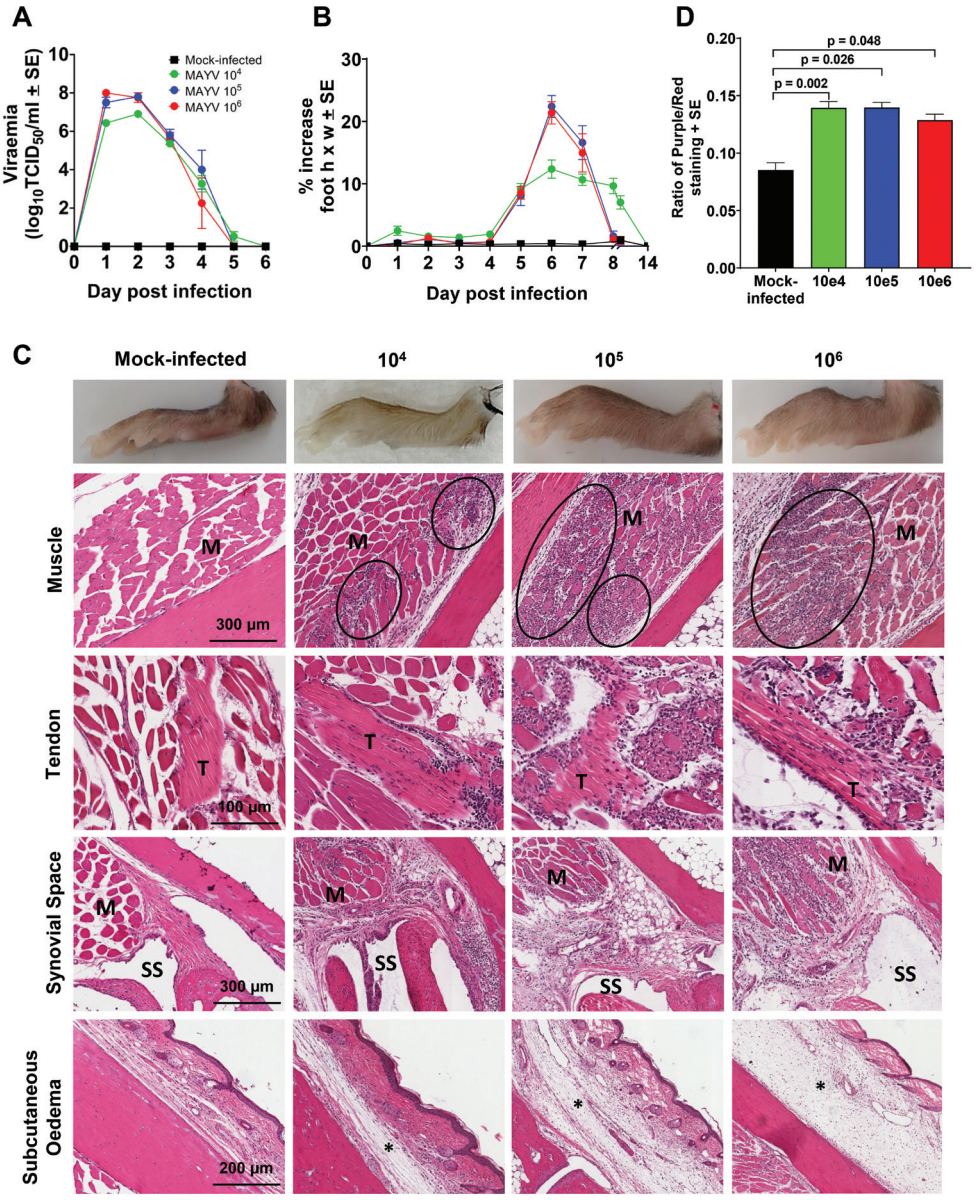

Figure 2. MAYV BeH407 in adult wild-type C57BL/6J mice. (A) Viraemia in adult female C57BL/6J mice (6-24 week old) infected with 10^4, 10^5 or 10^6 $TCID_{50}$ or mock-infected with PBS, with n = 4-6 mice per group. **(B)** Percentage increase in foot height x width (relative to day 0) for mice infected as in (A), with n = 8-12 feet from 4-6 mice per group per time point. **(C)** Photographs showing examples of feet on day 6 post infection, illustrating foot swelling in MAYV infected groups compared to the mock-infected control group. H&E staining of muscle (M), tendon (T), synovial space (SS), subcutaneous oedema (*) in foot sections from 6-24 week

old C57BL/6J wild-type female mice infected as in (A). Black ovals indicate some of the areas containing inflammatory infiltrates in the muscles. Inflammatory infiltrates near and in tendon areas are visible, as well as inflammatory infiltrates near joint tissues. **(D)** Ratio of nuclear (purple) to non-nuclear (red) staining of H&E stained foot sections (a measure of leucocyte infiltration). Data from 4-6 feet from 2-3 mice per group, with 3 sections scanned per foot and values averaged to produce one value for each foot. Statistics by Kolmogorov-Smirnov test.

Evaluation of VLP vaccines against MAYV infection and disease in C57BL/6J mice

To determine whether insect cell-derived MAYV VLPs could provide protection against MAYV infection and disease, groups of adult 6-8 week old female C57BL/6J mice were immunised with one or two doses of 1 μg WUR VLPs (with/without 1 μg of adjuvant QS-21), and antibody responses and protection against disease were determined (Fig. 3A). For comparison, another group of mice was vaccinated with 1 μg of human cell-derived TNAC VLPs (without adjuvant). As a negative control, mice were mock-vaccinated with RPMI 1640 medium only. After one vaccination of MAYV VLPs, MAYV-specific antibodies were observed by ELISA for both WUR VLPs and TNAC VLPs. TNAC VLPs induced significantly higher ELISA responses compared to WUR VLPs ($p = 0.026$; Fig. 3B) and also higher levels of neutralising antibodies ($p = 0.002$; Fig. 3C). One mouse vaccinated with WUR VLP without adjuvant and four mice vaccinated with WUR VLP with adjuvant showed neutralisation titers above the detection limit (Fig. 3C). No significant effect of the adjuvant on the immunogenicity of WUR VLPs was observed ($p = 0.93$ for ELISA titers, $p = 0.42$ for neutralisation titers; Fig. 3B, 3C).

Next, mice vaccinated with non-adjuvanted WUR VLP or TNAC VLP were boosted with 1 μg of the respective VLPs. The group WUR VLP with adjuvant did not receive a boost. Vaccination with two doses of 1 μg of WUR VLP and TNAC VLP generated high ELISA (Fig. 3B) and neutralising antibody responses (Fig. 3C) specific for MAYV. The mean ELISA titers against MAYV for WUR VLP and TNAC VLP after 2 shots were 41671 ± standard error of the mean (SE) 8518 and 117901 ± SE 23197, respectively (Fig. 3B), with a significant difference ($p = 0.026$) between the two groups. The mean neutralisation titers against MAYV for WUR VLPs and TNAC VLPs were 77 ± SE 15 and 385 ± SE 139, respectively (Fig. 3C), with a significant difference ($p = 0.026$) between the two groups. Vaccination with one dose of 1 μg of WUR VLP with 1 μg of QS-21 adjuvant also generated ELISA (Fig. 3B) and neutralising responses (Fig. 3C) specific for MAYV after 8 weeks. The mean ELISA and neutralisation titer against MAYV for the WUR VLP with adjuvant group at week 8 were 5668 ± SE 2012 (Fig. 3B) and 14 ± SE 4 (Fig. 3C), respectively. Significant differences were observed for both ELISA ($p = 0.002$) and neutralisation titers ($p = 0.026$) between the group with one dose of adjuvanted WUR VLPs and the group with two doses of non-adjuvanted WUR VLPs.

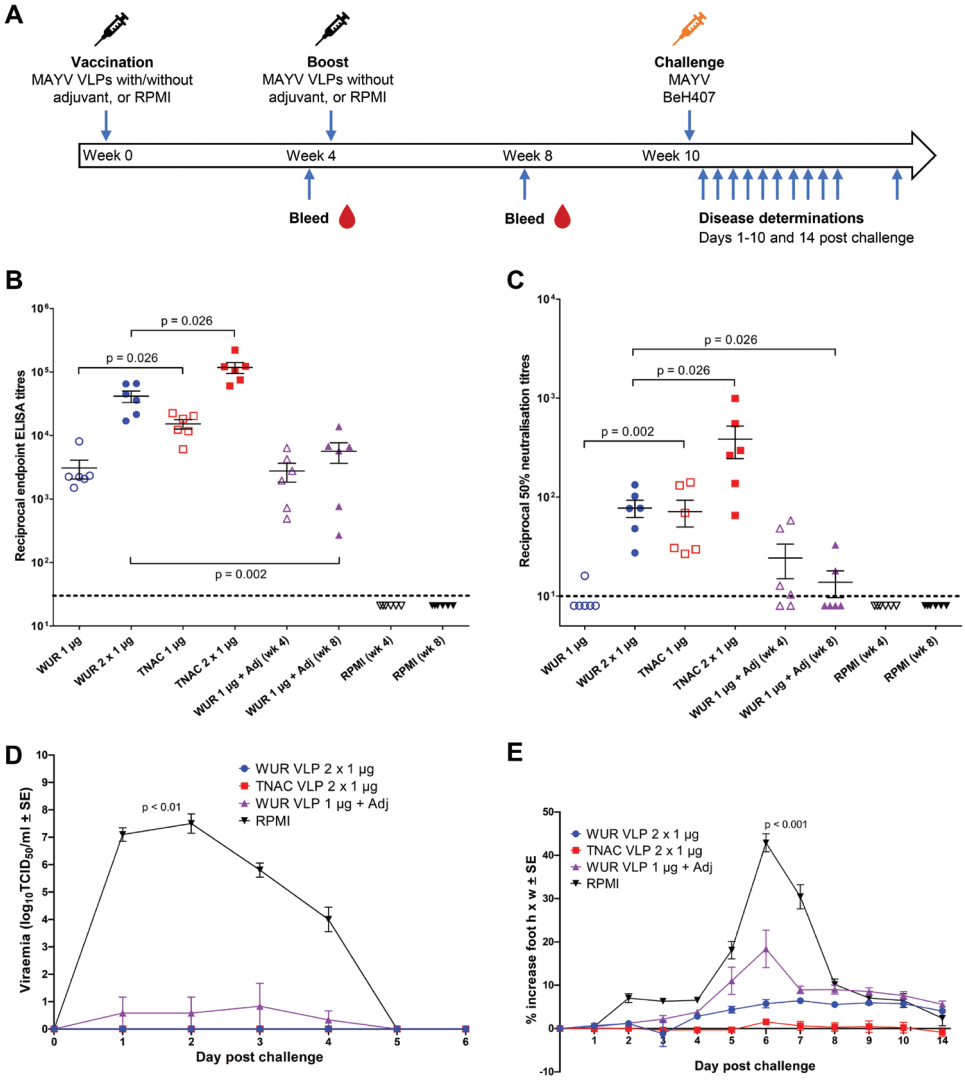

Figure 3. MAYV VLP vaccination and challenge with MAYV BeH407 in adult C57BL/6J mice. (A) Timeline of vaccination with two 1 µg doses of non-adjuvanted MAYV VLPs or with a single 1 µg dose of adjuvanted MAYV VLPs or with two doses of RPMI 1640 medium (negative control), antibody measurements after bleeds, and disease determinations of viraemia and foot swelling following MAYV BeH407 challenge. **(B)** MAYV BeH407 endpoint IgG ELISA titers after 1 or 2 vaccinations of female 6-8 week old C57BL/6J mice with non-adjuvanted MAYV VLPs or RPMI control, or 1 vaccination with MAYV VLPs with adjuvant. Lines among the dots indicate the mean ELISA titers and error bars show the standard error of the mean. Dashed line represents the limit of detection (1 in 30 serum dilution). Statistics by Kolmogorov-Smirnov test. **(C)** MAYV BeH407 50% neutralisation titers after 1 or 2 vaccinations with non-adjuvanted MAYV VLPs or RPMI control, or 1 vaccination with MAYV VLPs with adjuvant. Lines among

the dots indicate the mean neutralisation titers and error bars show the standard error of the mean. Dashed line represents the limit of detection (1 in 10 serum dilution). Statistics by Kolmogorov-Smirnov test. **(D)** MAYV BeH407 viraemia post challenge in mice vaccinated twice with non-adjuvanted MAYV VLPs or RPMI, or vaccinated once with MAYV VLPs with adjuvant (n = 5-6 per group). The limit of detection for each mouse was 10^2 $TCID_{50}$/ml, with means from 5/6 mice plotted. Statistics by Kolmogorov-Smirnov test. **(E)** Percentage increase in foot height x width (relative to day 0) for C57BL/6J mice vaccinated as in (D) with n = 6-12 feet from 3-6 mice per group per time point. Statistics by t-test.

Mice were challenged with MAYV BeH407 six weeks after the boost vaccination. A dose of 10^5 $TCID_{50}$ was used, as this dose caused the largest increase in foot swelling (Fig. 2B). Two doses of 1 μg of WUR VLP or TNAC VLP were sufficient to provide complete protection against viraemia (both statistically significant reductions in viraemia compared to mock-vaccinated mice on days 1 to 4 with $p < 0.01$; Fig. 3D), whilst one dose of 1 μg of WUR VLP with adjuvant also demonstrated a reduction in viraemia compared to the mock-vaccinated, infected group but no complete protection was observed (Fig. 3D). Additionally, two doses of 1 μg of WUR VLP and TNAC VLP were sufficient to provide protection against MAYV-induced foot swelling (both $p < 0.001$ compared to mock-vaccinated; Fig. 3E), whilst one dose of 1 μg of WUR VLP with adjuvant demonstrated only partial protection against foot swelling. Thus, two doses of 1 μg non-adjuvanted MAYV VLPs were sufficient to generate ELISA and neutralisation antibodies for subsequent complete protection against viraemia and foot swelling.

Histopathology of vaccinated C57BL/6J mice after MAYV challenge

H&E staining of feet from mice at 6 days post challenge illustrated the characteristic mononuclear cellular infiltrates (32, 307, 316) evident in muscle tissues (black ovals), in tendons, in surrounding joint regions and subcutaneous oedema regions in the mock-vaccinated RPMI control group and in the one shot WUR VLP with adjuvant group (Fig. 4A). Haemorrhage was observed in the mock-vaccinated RPMI control group only (Fig. 4A, black arrows). Mice vaccinated with two shots of VLPs (either WUR or TNAC) showed healthy tissues without cellular immune infiltrates. Quantitation using purple (nuclear) / red (cytoplasmic) staining ratios (Fig. 4B) demonstrated no statistically significant differences between mice which received two doses of the WUR VLP compared to two doses of the TNAC VLP. Significant differences were observed though between mice which received two doses of the WUR VLP ($p = 0.0095$) or two doses of the TNAC VLP ($p = 0.0095$) compared to the RPMI-vaccinated, infected mice. Therefore, two doses of the WUR VLP or TNAC VLP demonstrated protection against myositis, tendonitis, arthritis and haemorrhage.

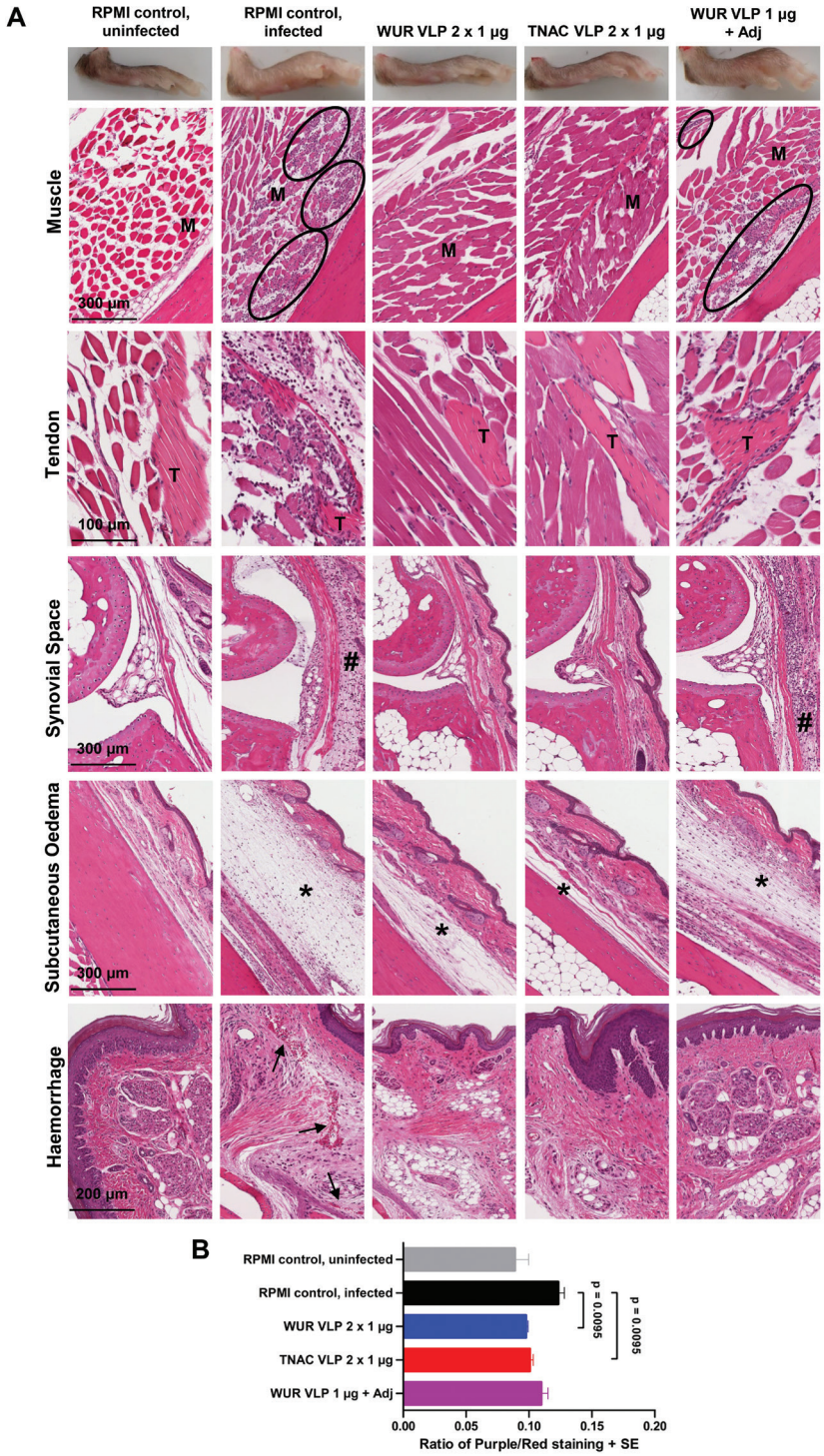
A
RPMI control, uninfected
RPMI control, infected
WUR VLP 2 x 1 µg
TNAC VLP 2 x 1 µg
WUR VLP 1 µg + Adj
Muscle
Tendon
Synovial Space
Subcutaneous Oedema
Haemorrhage
M
T
#
*
300 µm
100 µm
200 µm
B
RPMI control, uninfected
RPMI control, infected
WUR VLP 2 x 1 µg
TNAC VLP 2 x 1 µg
WUR VLP 1 µg + Adj
p = 0.0095
p = 0.0095
0.00
0.05
0.10
0.15
0.20
Ratio of Purple/Red staining + SE

Figure 4. Histopathology of MAYV VLP-vaccinated adult C57BL/6J mice after challenge with MAYV BeH407. (A) Photographs of mice feet at 6 days post challenge, illustrating swelling on day 6 in the RPMI-vaccinated, infected and the WUR VLP with adjuvant groups. H&E staining of tissues in foot sections from RPMI-vaccinated (uninfected or MAYV-infected) or VLP-vaccinated (MAYV-infected) adult C57BL/6J mice. Black ovals indicate some of the areas containing inflammatory infiltrates in the muscles (M). Inflammatory infiltrates near tendons (T) as well as inflammatory infiltrates near joint tissues (#) are seen. Subcutaneous oedema is shown (*). Haemorrhage is indicated by black arrows. **(B)** Ratio of nuclear (purple) to non-nuclear (red) staining of H&E stained foot sections (n = 2-3 mice, 4-6 feet per group, 3 sections per foot and values averaged to produce one value for each foot). Statistics by Kolmogorov-Smirnov test.

Discussion

MAYV has the potential to cause large epidemics worldwide, but no vaccine or antiviral treatment is available for human use (33). In this study, we developed a scalable MAYV VLP vaccine using recombinant baculoviruses and insect cells, which fully protected mice against viraemia and arthritic disease after challenge with wild-type MAYV.

After MAYV VLP production in insect cells and subsequent purification using a discontinuous sucrose gradient, VLPs with the expected diameter of ~70 nm were found in high quantities. However, baculovirus contaminants could also be observed in the VLP preparation. For use in humans, vaccines need to be highly purified and should not contain residual baculoviruses. For enveloped alphavirus VLPs, however, it is a challenge to completely remove the baculovirus particles from the final vaccine preparation, as physical properties, structure and size of the VLPs and the baculovirus virions are highly similar (85, 317). Thus, future research should focus on optimisation of the purification process or development of a large-scale baculovirus-based production system free of contaminating progeny baculovirus particles (85, 318).

In our mouse model, MAYV BeH407 induced arthritic foot swelling with 12% increase in foot height x width for a viral dose of 10^4 $TCID_{50}$. Foot swelling after CHIKV infection with a dose of 10^4 $TCID_{50}$ in the same mouse model was higher with an increase of 60% (260). This therefore indicates that the extent of the arthritic disease symptoms caused by these two alphaviruses differs in our mouse model. In contrast, others have shown comparable levels of foot swelling in wild-type C57BL/6J mice for CHIKV and MAYV using other virus isolates (319). This implies that distinct isolates of the same virus behave differently in this mouse model, which is in line with the large difference in foot swelling reported for CHIKV isolates from Thailand and Reunion Island (306).

In our study, two shots of 1 μg MAYV VLPs from insect cells were needed to induce high neutralising antibody levels and to protect mice against MAYV disease.

One shot of MAYV VLPs from insect cells (with/without adjuvant) did not result in high neutralising antibody responses. No positive effect of the adjuvant QS-21 was observed after one shot. This is in accordance with earlier work where the addition of Quil A adjuvant also did not improve neutralisation titers after immunisation with CHIKV VLPs (257), although different types and doses of adjuvants may improve the immunogenicity of alphavirus VLPs (320, 321). Interestingly, high neutralising antibody titers were observed for the non-adjuvanted MAYV VLP from human cells in our study, already after the first shot. It is unclear why MAYV VLPs from insect cells were found to be less immunogenic compared to MAYV VLPs from human cells, but a possible explanation could be that the insect cell-derived MAYV vaccine preparation contained residual cellular and baculoviral membranes, which might theoretically also present MAYV spikes. These MAYV proteins would be quantified as part of the vaccine preparation, but possibly do not present their epitopes in the same orientation and/or repetitive pattern as proteins on the VLPs and could thus be less immunogenic. In addition, potential differences in protein glycosylation patterns (322-324) and/or production pH (317) between insect cell-derived and human cell-derived MAYV VLPs may also play a role.

Despite that a booster immunisation with WUR VLPs was needed to induce neutralising antibody levels similar to a single shot with TNAC VLPs, the VLPs from insect cells can still be considered an attractive MAYV vaccine candidate due to the ease of scale up. The baculovirus expression system is commercially applied and routinely uses insect cell bioreactors of >1,000 litre working volume (325). In contrast, TNAC VLPs are produced by transient expression after transfection of nucleic acids into human HEK293 cells, which is efficient in small scale laboratory settings, but more cumbersome and costly during scale up. The baculovirus-insect cell expression system has already proven to be a suitable platform for the production of licenced human vaccines including an influenza virus subunit vaccine (326) and a human papillomavirus VLP vaccine (327). In addition, one of the leading vaccine candidates against covid-19 is produced using the baculovirus-insect cell expression system and has entered phase 3 clinical trials six months after the worldwide pandemic of SARS-CoV-2 was declared (328), which demonstrates the speed, scalability and efficiency of the platform.

A CHIKV vaccine is thought to be commercially feasible, and clinical trials have been conducted to test the safety, tolerability and efficacy of several CHIKV vaccine candidates in humans (86, 329-331). A live-attenuated CHIKV vaccine, based on a CHIKV infectious clone with a major deletion in the gene coding for nsP3, is the first CHIKV vaccine that has entered phase 3 clinical trials (332). Due to phylogenetic close proximity and antibody cross-reactivity between CHIKV and MAYV (333, 334), CHIKV vaccines are expected to provide (at least partial) cross-

protection against MAYV, and thus a CHIKV vaccine could potentially be used to prevent MAYV infection as well. However, after vaccination of mice with either a vaccinia vector based ZIKV/CHIKV vaccine or an adenovirus vector based CHIKV vaccine, cross-protection against MAYV was found to be absent in immunocompetent mice (307) or only partial in IFNAR knock-out mice (300), respectively, whereas complete protection was achieved against CHIKV in the same mouse models (260, 335). Moreover, in an immunocompetent mouse model, a live-attenuated CHIKV vaccine and an insect-specific alphavirus based CHIKV vaccine also did not cross-protect against MAYV disease (334). This therefore suggests that the development of a MAYV-specific vaccine is still required. And although a MAYV vaccine might currently not be commercially viable due to the small market size (307), this could rapidly change if MAYV would continue to emerge and follow the same route from tropical rainforest into urban area as CHIKV and ZIKV have previously taken (33, 336).

Acknowledgements

We thank Jan van Lent, Marcel Giesbers and Jelmer Vroom for their assistance with electron microscopy, Els Roode for cell culture maintenance, Victor van Gelder for his contribution to the design of the MAYV structural cassette construct, the QIMR Berghofer animal house for their assistance, Clay Winterford and Sang-Hee Park for their assistance with histology, Roy Hall and Jody Hobson-Peters for providing the antibody 5.5D11, and Michael Diamond for providing the MAYV BeH407 isolate.

AS is a member of the Global Virus Network (https://gvn.org/gvn-centers-of-excellence/asia-australia/australia/). SRA was supported by ZonMw (project: ZikaRisk “Risk of Zika virus introductions for the Netherlands”, grant number: 522003001) and by the graduate school PE&RC via a strategic fund award. WN was awarded a Research Training Program (Tuition fee offset and Living allowance stipend) PhD Scholarship from the Faculty of Medicine, University of Queensland, Australia, and a QIMR Berghofer Top Up Scholarship from the Higher Degrees Committee at QIMR Berghofer. The work was also supported by a project grant from the National Health and Medical Research Council (NHMRC) of Australia (APP1078468) and intramural seed funding from the Australian Infectious Disease Research Centre. AS is supported by an Investigator grant from the NHMRC (APP1173880).

Chapter 8 **General discussion**

Sandra R. Abbo[1]

[1]Laboratory of Virology, Wageningen University & Research, Wageningen, the Netherlands

In our globalised and urbanised world, obscure arthropod-borne (arbo)viruses can suddenly emerge and cause explosive outbreaks of human disease. The mosquito-borne Zika virus (ZIKV), Usutu virus (USUV) and Mayaro virus (MAYV) can cause disease in humans, and have been on the rise in recent years. This thesis addressed outstanding questions related to the vector competence of invasive and indigenous mosquito species present in the Netherlands for ZIKV and USUV to be able to better estimate the risk of viral outbreaks. In addition, the mosquito virome was studied to help understand the factors influencing vector competence. Lastly, virus-like particle (VLP) vaccines were developed that will hopefully contribute to confine and prevent future outbreaks of ZIKV and MAYV. In this chapter, the results from this thesis are discussed in a broader perspective, and recommendations for future research are given. Also, the mechanism underlying the vector specificity of ZIKV is further explored.

Risk of ZIKV outbreaks for the Netherlands

ZIKV caused a large outbreak of human illness in the Americas in 2015 and 2016 (9). Currently, ZIKV transmission occurs at much lower levels, but the virus is still present in tropical regions around the world (337, 338) and therefore remains a looming threat. Especially the introduction of the virus into new areas with naive populations could result in novel, major outbreaks of human disease. Knowledge of the mosquito vectors present in certain regions and their competence for ZIKV transmission is essential to assess the risk of new disease outbreaks.

In Europe, the largest risk of mosquito-borne ZIKV transmission is probably associated with the presence of the Asian tiger mosquito *Aedes albopictus*, a known vector not only for ZIKV but also for chikungunya virus (CHIKV) and dengue virus (DENV) (339). This invasive mosquito species is well adapted to temperate climates (340). Populations of *Ae. albopictus* are rapidly expanding, and can now be found in more than fifteen European countries (341). Importantly, in 2019, mosquito-borne ZIKV transmission was reported in the South of France, and *Ae. albopictus* was identified as the most probable vector (23). Multiple introductions of *Ae. albopictus* in the Netherlands have been reported (342, 343), and mosquito control programs are ongoing to prevent permanent establishment of this species (344).

Despite extensive control efforts, the invasive Asian bush mosquito *Aedes japonicus* has established a large and expanding population in Flevoland, the Netherlands (88, 94, 345). In Chapter 2, it was found that *Ae. japonicus* mosquitoes collected in Lelystad (Flevoland) can experimentally transmit ZIKV. After 14 days at 28°C, 3% of the tested mosquitoes accumulated ZIKV in their saliva, which is in accordance with a similar study using *Ae. japonicus* from Germany, where 10% of the artificially infected mosquitoes transmitted ZIKV at 27°C (97). These low

percentages might indicate that *Ae. japonicus* is not a highly competent vector for ZIKV. In addition, no complaints about mosquito biting nuisance in Lelystad have been received by the Netherlands Food and Consumer Product Safety Authority (NVWA) since the initial discovery of *Ae. japonicus* in the area (345), and no arboviral outbreaks associated with this mosquito species have been reported in Europe, despite the presence of widespread *Ae. japonicus* populations in multiple European countries (346). There are therefore no strong indications that the presence of *Ae. japonicus* in the Netherlands represents a high risk to public health.

Nevertheless, this exotic mosquito does still pose some risk to public health in the Netherlands, considering that in some cases poorly competent mosquito vectors can still sustain viral epidemics. This was observed during a yellow fever virus outbreak mediated by poorly competent *Aedes aegypti* mosquitoes in Nigeria in 1987 (347), where virus transmission could likely be maintained due to high densities of human-biting mosquitoes. Moreover, some studies suggest that *Ae. aegypti* mosquitoes from the field may not necessarily be highly competent vectors for ZIKV either, and that transmission of the virus in nature may be strongly influenced by vector density (136, 348). Since the population of *Ae. japonicus* in Flevoland is continuously expanding, and *Ae. japonicus* readily feeds on humans (based on human landing catches, Chapter 2), ZIKV transmission may be possible. It is thus important to better understand the factors contributing to the vectorial capacity of *Ae. japonicus* in Flevoland. For the *Ae. japonicus* population in Lelystad, the frequency of feeding events on humans throughout the day and the season is currently being investigated more conclusively to provide additional insights for risk assessment.

The current risk of ZIKV importation into the Netherlands via viraemic travellers is considered low, because limited ZIKV transmission has been reported worldwide during the past few years. Nonetheless, arboviruses are known for their unpredictability and can suddenly re-emerge, as exemplified by CHIKV and DENV, which both re-emerged after temporary periods of low transmission (349, 350) and caused their first outbreaks in Europe in Italy in 2007 (CHIKV) (351, 352) and in Madeira in 2012 (DENV) (353). Moreover, the unusual hot summers in the Netherlands in recent years (354) could increase the risk of ZIKV outbreaks, since ZIKV transmission by *Ae. japonicus* increases with temperature (97). In addition, arboviruses are known for their ability to switch vectors, as illustrated by the rapid emergence of CHIKV and Venezuelan equine encephalitis virus after adaptation to alternative vectors through only a single amino acid substitution (158, 355). The fact that ZIKV transmission by *Ae. japonicus* is possible also provides opportunity for the virus to adapt to this mosquito species, which could potentially lead to a new variant of ZIKV that can be more effectively transmitted by *Ae. japonicus*. To better

understand the possible risks associated with viral adaptation, ZIKV obtained from the saliva of experimentally infected *Ae. japonicus* could be sequenced to reveal putative dominant mutations that have arisen in the virus population. Whether or not these mutations contribute to increased virus transmissibility by *Ae. japonicus* could then be studied in detail.

In view of the current widespread, expanding population of *Ae. japonicus* in Flevoland, eradication efforts will likely not succeed. In this regard, the mosquito control program was terminated in 2018 due to increasing costs, which were considered disproportionate to the estimated minor public health risk associated with *Ae. japonicus* (356). Since eradication of *Ae. japonicus* proved unsuccessful, it might be worth considering to implement an arbovirus surveillance program among blood donors and *Ae. japonicus* mosquitoes in Flevoland, as this could function as an early warning system and alert Dutch clinicians in case of e.g. ZIKV transmission. When West Nile virus (WNV) was first discovered in the Netherlands during surveillance in birds and mosquitoes in 2020 (357), Dutch microbiological laboratories and specialists were alerted (358), and this resulted in detection of the virus in hospitalised patients shortly thereafter (359), thus showing the added value of surveillance. Given that *Ae. japonicus* can transmit a panel of different pathogenic arboviruses including CHIKV, DENV (185), Japanese encephalitis virus (184) and ZIKV, and that international travellers may be arriving at Lelystad Airport in the near future (360), arbovirus surveillance in the area could prove valuable.

The experimental ZIKV transmission rates of 3-10% for *Ae. japonicus* populations found in the Netherlands (Chapter 2) and Germany (97) were determined using field-collected mosquitoes. In this thesis, the naturally occurring virus species in field-collected *Ae. japonicus* mosquitoes were also analysed (Chapter 5). The virome of *Ae. japonicus* populations from the Netherlands and France consisted of highly diverse and abundant novel virus species. Recent studies on other mosquito species suggest that the virome of mosquitoes kept in the laboratory differs from mosquito populations in the field (70, 190), and that differences in the mosquito virome but also in bacterial and fungal communities present in mosquitoes can alter the outcomes of vector competence studies (66, 361-364). These findings emphasise the importance of the use of field-collected mosquitoes in vector competence experiments. Nonetheless, natural variation in the composition of bacterial, fungal and viral communities among mosquito populations or even among individual *Ae. japonicus* mosquitoes may also impact vector competence, and the potential effects of these microbiological communities on arbovirus transmission remain to be studied.

To further assess the risk of ZIKV transmission by mosquitoes in the Netherlands, also other *Aedes* species, both indigenous and invasive, should be

investigated in greater depth. *Aedes vexans*, the inland floodwater mosquito, is indigenous to the Netherlands. This mosquito can show aggressive human biting behaviour and reaches very high densities locally (365, 366). Multiple populations of *Ae. vexans* from the USA have shown to be capable of experimentally transmitting ZIKV (137, 365), thus underlining the need to also study this mosquito in the Netherlands. Two invasive *Aedes* species found in Europe are the Korean bush mosquito *Aedes koreicus* and the American rock pool mosquito *Aedes atropalpus*. *Ae. koreicus* has established populations in Italy, Switzerland, Slovenia, Hungary, Germany, and also in Belgium, where it is present very close to the border of the Netherlands (367). In September 2021, this mosquito was discovered for the first time in the Netherlands, after which monitoring and eradication programs in the collection area have been intensified (368). Importantly, *Ae. koreicus* mosquitoes from Germany have recently shown capable of experimentally transmitting ZIKV (369), and further studies on the vectorial capacity of this species for ZIKV are therefore needed. For *Ae. atropalpus*, no permanent populations have been detected in Europe, however in the Netherlands, multiple introductions have occurred (343, 370, 371). The vector status of *Ae. atropalpus* for ZIKV is currently unknown and requires investigation.

USUV in the Netherlands: current situation and risks

USUV was first discovered in the Netherlands in 2016 (90) and has since then been continuously detected in the country. Genomic monitoring in dead black birds suggests that some circulation of USUV between the Netherlands, Belgium and Germany takes place but that the virus also overwinters in the Netherlands (164).

The common house mosquito *Culex pipiens* is considered the primary vector for USUV in the Netherlands, and is classified into two biotypes: *pipiens* and *molestus* (147). Biotype *pipiens* showed much higher USUV titers in the saliva as compared to biotype *molestus* (Chapter 4). Since biotype *pipiens* preferentially feeds on birds whereas biotype *molestus* is more attracted to mammals including humans (147), the lower USUV saliva titers of biotype *molestus* may decrease the overall risk of USUV transmission to humans. It would be informative to study whether there is a difference in USUV transmissibility to mammals between biotype *molestus* and *pipiens*. Mouse models of USUV disease have been developed (372, 373), so this could be tested by allowing USUV-infected mosquitoes to feed on naive mice. Hybrids between *pipiens* and *molestus* (374) could be tested in this set-up as well, as they are expected to also be involved in bridging USUV between birds and humans. Importantly, the opportunistic feeder *Ae. japonicus* can also experimentally transmit USUV (Chapter 2) and a disseminated USUV infection has been reported in *Ae. japonicus* mosquitoes from the field (113). This indicates that *Ae. japonicus*

could also serve as a bridge vector, thereby increasing the risk of USUV transmission to humans.

USUV is closely related to WNV, which was for the first time detected in the Netherlands in mosquitoes, birds and hospitalised patients in 2020 (357, 359). Both USUV and WNV belong to the genus *Flavivirus* and are transmitted between avian reservoir hosts by *Cx. pipiens* mosquitoes. Although disease following USUV infection in humans is rare, WNV infection is more often associated with severe, neuroinvasive illness (359, 375). WNV and USUV co-circulate in many European countries, and co-infections have been reported in birds (376), mosquitoes (377) and humans (29). Since flaviviruses are known for their ability to influence the outcomes of subsequent infections with related flaviviruses (378), the early arrival and wide dispersal of USUV in the Netherlands may potentially impact WNV circulation. Interestingly, pre-infection of *Cx. pipiens* mosquitoes with USUV significantly reduced subsequent WNV transmission (379), which could have implications for the WNV transmission cycle. Moreover, USUV infection in Dutch blood donors is common (28), but it is unknown to what extent immune responses induced by a previous infection with USUV affect subsequent WNV infection in humans. A first study in mice has shown that previous exposure to USUV reduces susceptibility to WNV (380). Vice versa, pre-infection with WNV may also influence subsequent USUV infection as immunisation with a WNV subviral particle (SVP) vaccine induced low levels of cross-reactive antibodies to USUV (381). Future studies are needed to characterise to what extent co-circulation affects the epidemiology of USUV and WNV in the Netherlands and beyond.

The molecular determinants underlying the restriction of ZIKV in *Cx. pipiens*

Cx. pipiens is the main vector for USUV and WNV (30, 31, 128, 145), but was found unable to experimentally transmit ZIKV after an infectious blood meal (Chapter 3). The molecular determinants underlying mosquito vector competence for arboviruses are largely unknown, and it is unclear why *Cx. pipiens* is unable to transmit ZIKV. The midgut of *Cx. pipiens* was identified as an important barrier against ZIKV dissemination, since bypassing the midgut barrier by intrathoracic injection of ZIKV resulted in virus accumulation in mosquito saliva (Chapter 3). Nevertheless, even after forced infection by virus injection, ZIKV replication seemed suboptimal as only 74-78% of the injected *Cx. pipiens* mosquitoes became infected, whereas 100% of the injected *Ae. aegypti* mosquitoes showed ZIKV infection (Chapter 3). Similar as found by others (150), we observed a replication deficiency of ZIKV in cultured *Culex* cells (Fig. 1A, 1B), and concluded that *Cx. pipiens* is a highly inefficient vector

for ZIKV. The risk of ZIKV transmission by *Cx. pipiens* is therefore considered very low.

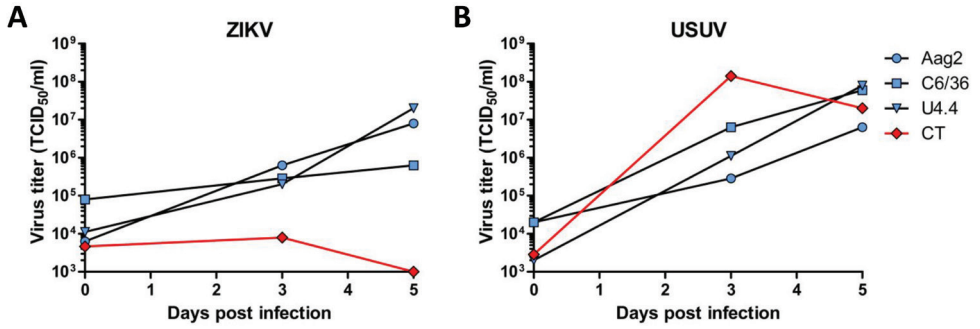

Figure 1. Replication of ZIKV and USUV in *Aedes* and *Culex* mosquito cells. Replication of **(A)** ZIKV and **(B)** USUV in *Ae. aegypti* (Aag2), *Ae. albopictus* (C6/36, U4.4) and *Cx. tarsalis* (CT) mosquito cells infected using a multiplicity of infection (MOI) of 1 $TCID_{50}$ unit per cell. Culture medium was harvested at the indicated time points, and virus titers in $TCID_{50}$/ml were measured by end point dilution assays using Vero cells.

Nonetheless, fuelled by high mutation rates and positive selection pressure on large mutant swarms within an individual host, RNA viruses can rapidly develop into new epidemic variants (382, 383). For arboviruses it has previously been shown that the acquisition of only one or a few adaptive amino acid changes can break host-specific barriers (158, 355, 384, 385). For WNV, for example, the amino acid substitution T249P in the NS3 helicase of a low-virulence variant resulted in a variant highly virulent to American crows (385). The acquired high virulence is thought to underly the sudden, massive die-off of birds during the rapid epidemic sweep of WNV through North America after introduction of the virus in 1999 (385). Another example comes from CHIKV. This arbovirus is typically transmitted from human to human by *Ae. aegypti*, but a single mutation in the viral envelope protein E1 (A226V) resulted in increased infectivity of the virus in *Ae. albopictus* (158). This mutation is thought to be responsible for the CHIKV epidemic on Reunion island, and expanded the potential distribution of CHIKV to all areas where *Ae. albopictus* is present, including Europe (158, 386, 387). Similar as for CHIKV, mutation(s) in the ZIKV genome could potentially also give rise to altered vector specificity. It is therefore important to i) better understand the molecular basis underlying the restriction of ZIKV in *Cx. pipiens* and to ii) investigate whether virus evolutionary trajectories that could lead to new epidemic variants of ZIKV with altered vector specificity can be predicted. Such studies could contribute to better risk assessments, more targeted surveillance, and improved outbreak preparedness and response (159). Moreover, studying virus-host interactions in non-competent mosquito species can

also enhance our fundamental understanding of the factors determining vector competence, as exemplified by previous work on the alphaviruses western equine encephalomyelitis virus (388, 389) and o'nyong nyong virus (ONNV) (390).

Passaging of an arbovirus in a mosquito host can provide insights into the potential for adaptation of the virus to the specific mosquito species (391). Since intrathoracic injection, but not artificial blood feeding of ZIKV, resulted in virus transmission by *Cx. pipiens*, we passaged ZIKV in *Cx. pipiens* mosquitoes (biotype *pipiens*) by intrathoracic injection to investigate the potential adaptation of ZIKV to *Cx. pipiens* mosquitoes. The virus was passaged three times (Fig. 2A). For the first passage, mosquitoes were injected with a ZIKV stock (dose of 10^4 $TCID_{50}$) derived from Vero cells. For the second and third passage, mosquitoes were injected with ZIKV obtained from the mosquito body that showed the highest virus titer after the previous passage (doses of 10^2 or 30 $TCID_{50}$, respectively). After injection, mosquitoes were left at 28°C for 14 days (Fig. 2A). Afterwards, virus presence in the body and saliva of each mosquito was determined (Fig. 2B), as well as viral titers in the mosquito bodies (Fig. 2C). In parallel with passage 2 and 3 experiments, groups of mosquitoes were injected with the same dose of the non-passaged ZIKV stock for comparison. Two passages of ZIKV resulted in more virus-positive bodies and saliva samples as compared to injection with non-passaged ZIKV stock (Fig. 2B), and after two passages, more mosquitoes with a positive body also showed accumulation of virus in the saliva (percent mosquitoes with virus-positive saliva out of mosquitoes that have a virus-positive body (S/B); Fig. 2B), although the differences were not significant ($p > 0.05$, Fisher's exact test). Interestingly, after passage 2, ZIKV showed significantly higher titers in the body of *Cx. pipiens* as compared to non-passaged ZIKV ($p < 0.05$, Mann-Whitney *U* test; indicated by asterisk in Fig. 2C). This may suggest that ZIKV shows adaptation to *Cx. pipiens*. Nevertheless, after each passage, the maximum virus body titer that could be used for passaging became lower. As a consequence, the infection and transmission rates had lowered substantially after passage 3 (Fig. 2B), and possible adaptation of the passaged virus as compared to the non-passaged virus could therefore not be observed after this passage. These results indicate that ZIKV does not readily adapt to *Cx. pipiens* mosquitoes. In addition to these results, only 2 out of 188 tested *Cx. pipiens* mosquitoes showed a ZIKV-positive body after an infectious blood meal containing a high virus titer (Chapter 3), and none of the mosquitoes accumulated ZIKV in the saliva. This indicates limited opportunity for the virus to adapt to *Cx. pipiens*, although, considering the total number of (genetically diverse) mosquitoes in the field, virus adaptation can certainly not be ruled out.

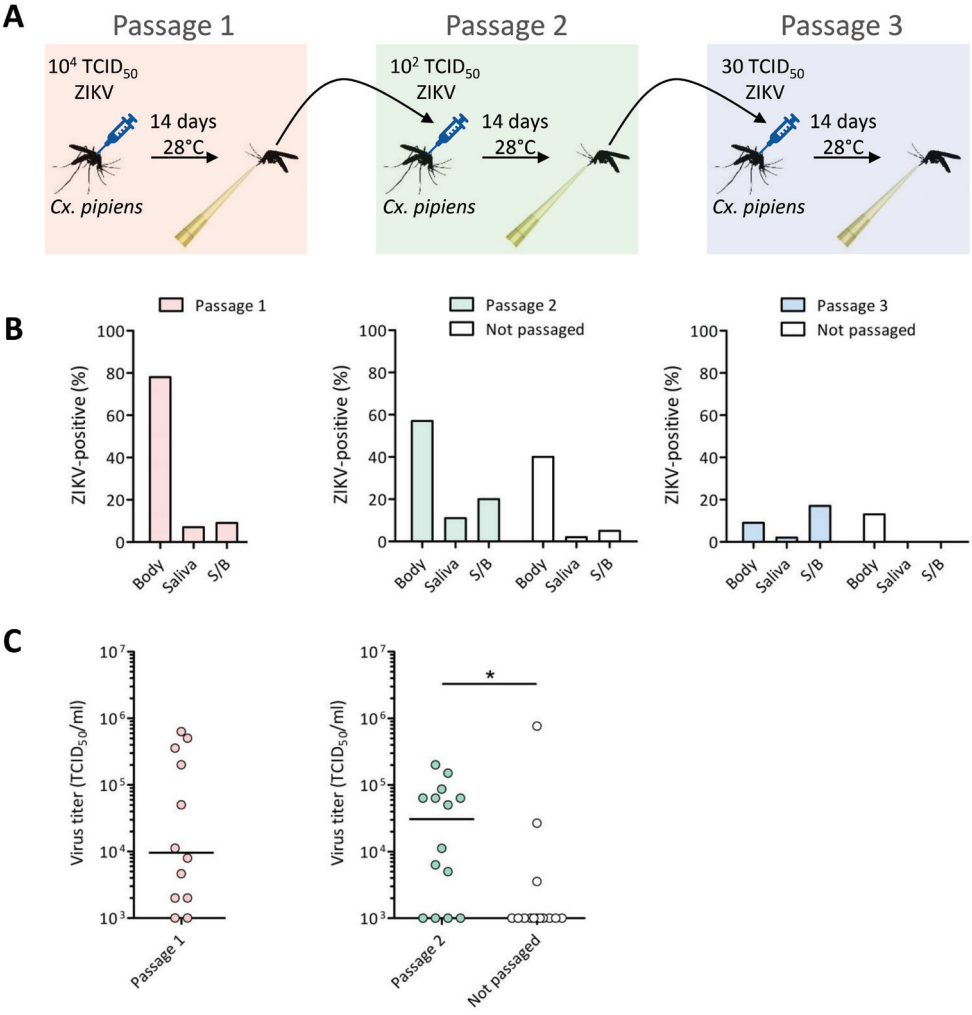

Figure 2. Passaging of ZIKV in *Cx. pipiens* mosquitoes by intrathoracic injection. (A) *Cx. pipiens* (biotype *pipiens*) mosquitoes were injected with 10^4 (passage 1), 10^2 (passage 2) or 30 (passage 3) $TCID_{50}$ of ZIKV. After incubation at 28°C for 14 days, the body and saliva from each mosquito were analysed for the presence of infectious virus by inoculation on Vero cells as described in Chapter 3. ZIKV obtained from the infected mosquito body with the highest viral titer was directly used to infect new mosquitoes by injection. **(B)** Percentages of ZIKV-positive body or saliva samples out of the total number of mosquitoes tested were determined after each passage. The percentages of mosquitoes with ZIKV-positive saliva out of the total number of infected mosquitoes are also shown (indicated by 'S/B'). During passage 2 and 3, parallel groups of mosquitoes were injected with non-passaged ZIKV from the initial stock (used to infect mosquitoes for passage 1) at similar $TCID_{50}$ as injections with passaged virus (10^2 or 30 $TCID_{50}$) for comparison. For these groups, infection and transmission percentages were also determined, as indicated by the white bars. For all experiments, the number of mosquitoes per group is 30-65.

(C) ZIKV titers in mosquito bodies after viral passage were measured by end point dilution assays using Vero cells. Data points represent individual mosquito bodies infected with ZIKV. Lines among the dots indicate the median viral titer. The asterisk (*) indicates a significant difference ($p < 0.05$, Mann-Whitney *U* test).

The passaged ZIKV from injected *Cx. pipiens* mosquitoes could be sequenced to study the mutations that have arisen during passaging. These mutations could potentially contribute to adaptation to *Culex* mosquitoes, although adaptation to replication in mosquitoes in general should also be considered, given the absence of host alternation during the experiment. Importantly, previous strong purifying selection during virus evolution in natural hosts and/or during viral passages in tissues or cells have likely shaped the composition of viral swarms present in the current virus stock used for passaging in mosquitoes. Also, a limited number of viral passages in the laboratory does by far not resemble the evolutionary time scale at which adaptive mutations usually accumulate, since these mutations usually depend on antecedent mutations that shape the evolutionary landscape (392-394). Therefore, novel methods that rely on the construction of artificial mutant swarms, such as virus barcoding (395) and deep mutational scanning (396), could be helpful to reveal a more complete overview of possible adaptive mutations in the ZIKV genome after replication in *Cx. pipiens*. The effect of individual mutations or specific groups of mutations on virus transmission by *Cx. pipiens* mosquitoes can then be studied using reverse genetics. Next, the effect of the discovered mutations on the complex transmission cycle of ZIKV should be studied in detail, since arbovirus evolution is normally also constrained by host alternation (397).

Factors that could contribute to the restriction of ZIKV in *Cx. pipiens* are physical barriers at the mosquito midgut and salivary glands, mosquito host factors required for virus replication, mosquito immune responses and/or the mosquito midgut microbiome (60). Approaching the research question about the molecular basis of ZIKV restriction in *Culex* from the site of the mosquito could be done by the construction of genetic mutants of mosquitoes and mosquito cell lines (398) or by transient gene silencing via delivery of *in vitro* synthesized double-stranded RNA (dsRNA) into mosquitoes or mosquito cell lines (399). A draft genome assembly of *Cx. pipiens* subspecies *pallens*, which has recently become available (400), can provide valuable assistance. For example, knock down or knock out of immune genes could provide insights into the factors restricting ZIKV replication, although these strategies might be challenging due to the large genome size of mosquitoes and the many possible candidate genes that could be targeted. ZIKV itself, however, is well characterized and has a small genome length. Developing chimeric viruses between ZIKV and a flavivirus that replicates well in *Culex* cells, and assessing the replication of these chimeric viruses in *Culex* cells and in *Cx. pipiens* mosquitoes

could therefore be a promising strategy to pinpoint the molecular basis underlying ZIKV restriction in *Culex*. Once the viral genetic elements that restrict ZIKV replication have been identified, this also enables a more targeted search for the host factors that determine ZIKV restriction in *Cx. pipiens* mosquitoes.

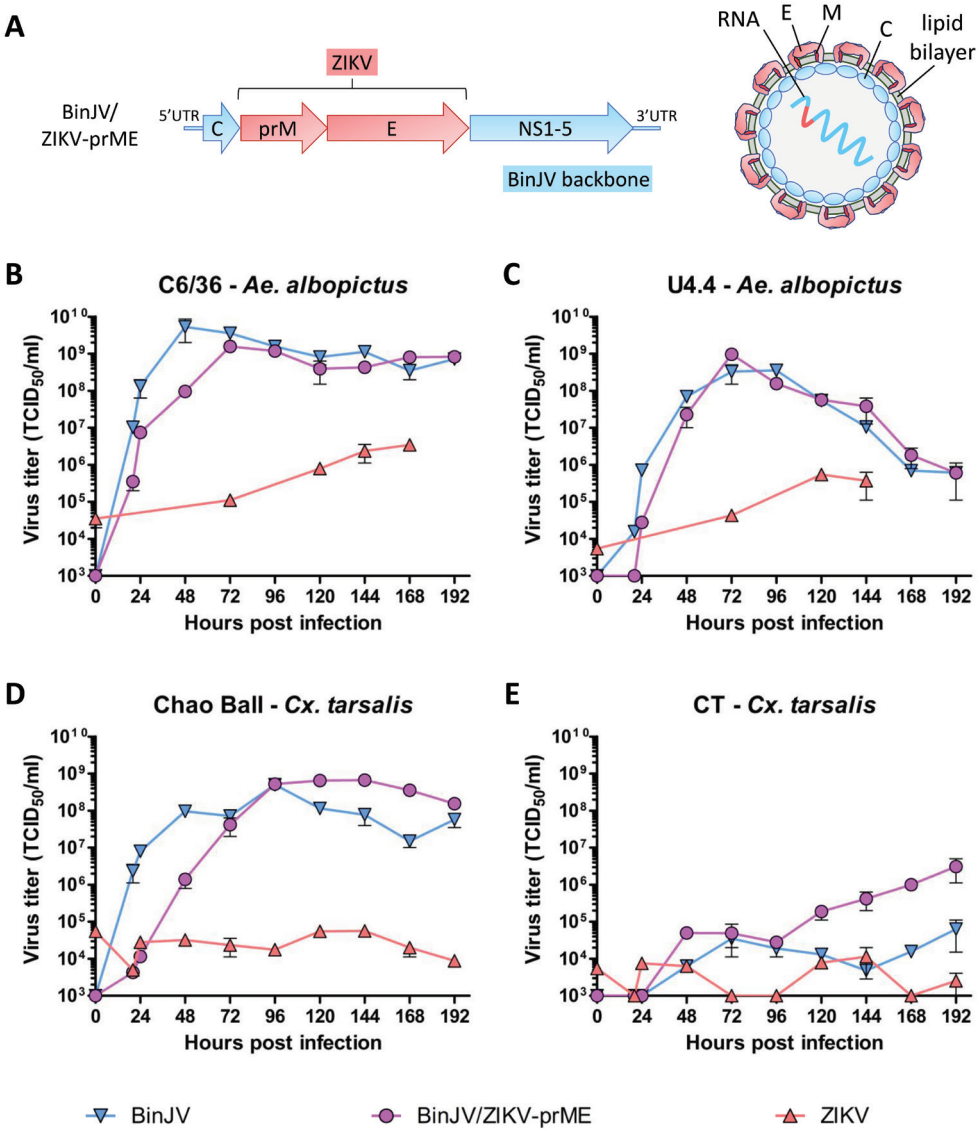

Figure 3. Replication of BinJV, BinJV/ZIKV-prME chimera and ZIKV in *Aedes* and *Culex* mosquito cells. (A) Schematic overview of the genome organisation and virion structure of the chimeric virus BinJV/ZIKV-prME. **(B)** C6/36 and **(C)** U4.4 *Ae. albopictus* mosquito cells and **(D)** Chao Ball and **(E)** CT *Cx. tarsalis* mosquito cells were infected with BinJV, BinJV/ZIKV-prME

and ZIKV at an MOI of 1 $TCID_{50}$ unit per cell, and culture medium was harvested at the indicated hours post infection. Virus titers were determined using end point dilution assays on Vero cells (ZIKV) or C6/36 cells (BinJV, BinJV/ZIKV-prME). The experiment was carried out in duplicate, and mean values were plotted, with error bars showing the standard error of the mean.

A chimeric virus between ZIKV and the insect-specific flavivirus (ISF) Binjari virus (BinJV) has previously been developed using the circular polymerase extension reaction (CPER) method (248). This chimera (Fig. 3A) encodes the precursor membrane (prM) and envelope (E) structural proteins of ZIKV, whereas the remainder of the genome is derived from BinJV (i.e. the capsid, the non-structural proteins and the untranslated regions (UTRs)). We assessed the growth of wild-type BinJV, chimeric BinJV/ZIKV-prME and wild-type ZIKV in *Aedes* and *Culex* mosquito cells. All three viruses showed replication in C6/36 and U4.4 *Ae. albopictus* cells (Fig. 3B, 3C). BinJV/ZIKV-prME replicated efficiently in Chao Ball and CT *Cx. tarsalis* cells at comparable levels as wild-type BinJV, whereas ZIKV replication was severely impaired in both *Culex* cell lines (Fig. 3D, 3E). These results show that the prM and E proteins of ZIKV do not restrict ZIKV replication in *Culex* cells, thus indicating that ZIKV limitation in *Culex* occurs post-entry. This is in accordance with a recent study, which suggested that restriction of ZIKV in *Culex* occurs downstream of cell entry based on ZIKV internalization dynamics in *Culex* cells (401). Interestingly, our results suggest low levels of ZIKV replication in Chao Ball and CT cells (Fig. 3D, 3E), thus indicating that *Culex* cells are not completely refractory to ZIKV. This finding is in line with the detection of ZIKV replication in *Cx. pipiens* post intrathoracic inoculation (Chapter 3).

Since the restriction was found to take place post-entry, we hypothesised that elevation of CpG dinucleotides in the viral genome, which has previously been shown to enhance ZIKV replication in *Aedes* mosquito cells and ZIKV transmission by *Ae. aegypti* mosquitoes through yet unknown mechanisms (261), could potentially contribute to overcome the restriction of ZIKV in *Culex*. We compared replication of wild-type ZIKV with replication of a CpG-high ZIKV mutant (with 190 additional CpG dinucleotides, introduced by synonymous changes (261)) in *Aedes* and *Culex* cells. As a positive control, the growth of WNV was also measured. As expected, the CpG-high mutant replicated to higher titers in *Ae. aegypti* Aag2 cells compared to wild-type ZIKV (Fig. 4A). However, both the CpG-high mutant and wild-type ZIKV did not replicate in *Cx. tarsalis* Chao Ball cells, whereas WNV grew to high titers on this cell line (Fig. 4B). This therefore suggests that the evolutionary pressure on CpG dinucleotides in viral genomes is likely not responsible for the specific restriction of ZIKV in *Culex*.

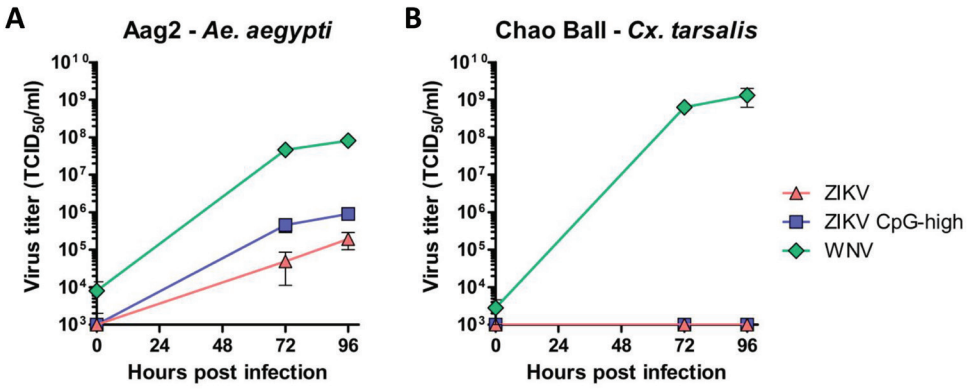

Figure 4. Replication of ZIKV, ZIKV CpG-high mutant and WNV in *Aedes* and *Culex* mosquito cells. Mosquito cells **(A)** Aag2 (*Ae. aegypti*) and **(B)** Chao Ball (*Cx. tarsalis*) were infected with wild-type ZIKV, a synonymous ZIKV mutant with 190 additional CpG dinucleotides (CpG-high) or WNV. Infections were performed using an MOI of 0.5 $TCID_{50}$ unit per cell for wild-type ZIKV and WNV. To account for potential differences in infectivity between wild-type and mutant (CpG-high) ZIKV, CpG-high ZIKV inoculum was based on RNA copy numbers that were equivalent to the RNA copy numbers of the wild-type ZIKV inoculum (at MOI 0.5). Medium was collected at the indicated hours post infection. Viral titers were determined using end point dilution assays on Vero cells. The experiment was carried out in duplicate, and mean values were plotted, with error bars showing the standard error of the mean.

To further investigate the molecular determinants underlying ZIKV restriction, additional chimeras could be developed using the CPER method, after which their ability to replicate in *Culex* cells can be determined. For the alphavirus ONNV, the determinant of vector specificity for *Anopheles gambiae* mosquitoes resides in non-structural protein 3 (390), indicating that non-structural proteins of arboviruses can also be crucial to overcome vector specific barriers. Thus, exchanging (parts of) the non-structural cassettes of a *Culex*-associated flavivirus and ZIKV could be a strategy to provide insights into the involvement of non-structural proteins in vector specificity. However, molecular interactions between different regions of the genome, between proteins and/or between proteins and the genome (e.g. between ZIKV NS2A protein and the 3' UTR (402)) could possibly be disrupted during exchange of genome sections, which might result in impaired virus replication. Hence, careful characterization of replication of each chimera in *Aedes* cells is also needed. Since the 3' UTR of flaviviruses and the subgenomic flavivirus RNAs derived thereof are proven determinants of mosquito vector competence (116, 403, 404), exchange of 3' UTR regions between a *Culex*-associated flavivirus and ZIKV might also lift the restriction. Finally, the chimeras should not only be tested in *Culex* cell lines but also in *Cx. pipiens* mosquitoes. Infectious blood meal experiments with *Cx. pipiens* would be informative to specifically investigate the

ability of the chimeras to overcome the mosquito midgut barrier. For ZIKV chimera design, it is therefore advisable to use a flavivirus that can be efficiently transmitted by *Cx. pipiens* after oral exposure, e.g. USUV.

ZIKV vaccine development: challenges and prospects

The baculovirus-insect cell expression system has delivered protective VLP vaccines against the arboviruses CHIKV (257) and MAYV (Chapter 7). Nevertheless, the ZIKV VLP and SVP vaccines produced with this expression platform required optimisation to improve their efficacy in mouse models (Chapter 6). It was hypothesised that the E proteins displayed on the surface of the ZIKV VLPs/SVPs have arranged into an undesired trimeric, postfusion conformation due to the low pH of ~6.2 in the baculovirus-insect cell expression system, whereas the dimeric, prefusion state is the conformation that usually induces high levels of neutralising antibodies during natural ZIKV infection (244-246). In Chapter 6, the ZIKV SVP vaccine candidate was improved by production at pH 7.0 using adapted insect cells, and by introducing a cysteine bridge between the E proteins of a dimer to lock the dimeric state. These improved candidate vaccines can now be tested using the epitope display analysis described in Chapter 6. Ideally, most if not all ZIKV E proteins in the envelope of the VLP/SVP should form dimers to maximise the capacity of the vaccines to trigger highly neutralising antibodies such as the E dimer epitope binding monoclonal antibody (mAb) C8. The level of epitope occupancy by mAb C8 on VLPs/SVPs could be determined by cryo-electron microscopy as described by others (248).

If needed, additional strategies could be considered to further improve the ZIKV vaccine candidates. First, the production of ZIKV VLPs/SVPs using insect cells adapted to an even slightly higher pH (e.g. pH 7.5 instead of pH 7.0) might be beneficial. Although studies on other flaviviruses have identified pH values ranging from 6.6 to 6.9 as the threshold for E protein mediated fusion (276, 277), it has recently been suggested for ZIKV that even at pH 7.4 a certain, limited degree of fusion can still occur (278). Second, exploring whether increased prM processing by furin (e.g. using a stable furin-overexpressing cell line (405)) improves vaccine efficacy, is also a possibility. Flaviviruses are known for their ability to form partly immature virions during natural infection due to incomplete cleavage of prM. The prM content of virions varies depending on the cell type, but appears larger for virions from mosquito cells than from mammalian cells (406, 407). The presence of uncleaved prM can affect antibody responses in multiple ways, including the promotion of antibody-dependent enhancement (ADE) and the induction of specific immune responses targeting differential epitopes on partly immature virions, which are not found on completely mature virions (407). Studying and, if necessary, altering the prM content of the ZIKV VLPs/SVPs might therefore contribute to improved

vaccine efficacy. Third, the highly dynamic structure of the ZIKV virion may need attention. This phenomenon, referred to as 'viral breathing', results in continuous alterations in the availability of epitopes for antibodies (408), and the kinetics of breathing are thought to be virus strain dependent (409, 410). Since viral breathing can affect antibody responses, increasing the understanding of this process might benefit ZIKV VLP/SVP vaccine development.

Given the high complexity and dynamic nature of flavivirus virions and thus also of VLPs/SVPs derived thereof, it is recommended to carefully characterise the antigenic structure of ZIKV VLPs/SVPs after production of each vaccine batch, for example by a standardized ELISA screen using C8 or C10 mAbs. In addition, it has recently been suggested for ZIKV that assaying the capacity of vaccine-induced antibodies to neutralize mature (reporter) viruses could provide better correlates of protection as compared to using conventional neutralisation assays in which the capacity of antibodies to neutralise an uncontrolled mixture of immature and mature (reporter) virus particles is determined (411). In Chapter 6, some of the sera from individual mice vaccinated with one dose of ZIKV VLPs/SVPs showed reasonably high neutralising antibody titers (still active after >100-fold dilution) as determined by conventional neutralisation assays, however high levels of ZIKV viraemia were observed post challenge. Surprisingly, similar levels of neutralisation titers protected mice from viraemia during another study using the same interferon-α/β receptor knockout ($IFNAR^{-/-}$) female mouse model (260). Since not only the quantity but also the quality of induced antibodies might be of importance (411), determining the ability of antibodies present in the mouse sera after ZIKV VLP/SVP immunisation to specifically neutralise mature ZIKV may provide better insights into the true capacity of these vaccines to protect against ZIKV infection *in vivo*. This is especially interesting since a recent study on DENV directly isolated from humans showed that mature forms of the virus predominate, which was in stark contrast with DENV derived from laboratory cell cultures for which the majority of the particles were structurally immature (412). Future studies are needed to compare the maturation pattern of ZIKV virions obtained from cell lines, humans and also mosquitoes.

Despite the before-mentioned challenges associated with ZIKV vaccine development, a significant number of vaccines against ZIKV has proven effective in animal studies and some of these vaccines subsequently moved into human clinical trials (413). Importantly, however, it should be considered that ZIKV circulates in the same areas as the closely related DENV, and that these viruses share high amino acid identity within their E protein (268, 414). Decades of flavivirus research have shown that immune interactions induced by closely related viruses can result in immunopathogenesis and life-threatening clinical manifestations in humans. Sequential DENV infections with different serotypes, for instance, can lead to ADE,

with vascular leakage, shock and even death as possible consequences (82, 415, 416). Moreover, the implementation of the first licenced DENV vaccine, Dengvaxia, was abrogated due to an increased risk for individuals seronegative at first vaccination of developing severe disease during subsequent natural DENV infection (79). In addition, in a Nicaraguan pediatric cohort study, individuals who experienced a single prior ZIKV infection or a prior DENV infection followed by a ZIKV infection were found to be at higher risk of acquiring severe disease during subsequent DENV infection as compared to flavivirus-naive individuals (414). Of major concern is, therefore, whether ZIKV vaccination might enhance illness during a subsequent DENV infection. Especially a certain intermediate level of pre-existing ZIKV antibodies was found associated with increased risk of DENV disease (414), and it is thus of crucial importance that antibody responses following ZIKV vaccination will exceed this intermediate level.

The highest neutralizing antibody response reported by a ZIKV vaccine during clinical trials so far resulted from two immunisations with an aluminium hydroxide adjuvanted, inactivated ZIKV vaccine (417, 418). This vaccine was safe and well tolerated in both flavivirus-primed and flavivirus-naive individuals during the 57 days of follow-up measurements (417). The participants will be followed for two years (417), and this will be essential to identify potential long-term risks (including outcomes of later DENV infection) associated with ZIKV vaccination. In the case that health risks associated with subsequent DENV infection would arise, it may be an option to obtain more balanced immune responses by combining a ZIKV vaccine with a single or perhaps even two different tetravalent DENV vaccines (419, 420) via a sequential strategy (first DENV, then ZIKV (421, 422)) followed by boosts if necessary (418), although this will require in-depth studies on the efficacy and safety of the combined vaccines as well as coordinated immunisation programs. Alternatively, ZIKV vaccines that are specifically designed to abolish ADE of DENV infection through modifications to the conserved, ADE-promoting fusion loop epitope (254, 423) could be attractive candidates for further testing.

Notwithstanding the recent advances in vaccine development and the improved understanding of ADE, the delivery of effective and safe ZIKV and DENV vaccines for human use may remain challenging to achieve, given the complex interactions of these viruses with the immune system of their human host. Similar as for malaria (424, 425), the control of arboviruses such as ZIKV and DENV therefore requires an integrated approach encompassing the pathogens, the hosts, the environment, and the mosquito vectors.

Arbovirus control using insect-specific viruses

New strategies to control pathogenic arboviruses are continuously being developed,

and the use of insect-specific viruses (ISVs) as agents to combat the transmission of arboviruses such as ZIKV and DENV is a novel idea that may hold promise for the future. In recent years, numerous ISVs have been discovered, many of which belong to virus families that also harbour arboviruses of medical importance (426). The phylogenetic relatedness between these ISVs and arboviruses may suggest that ISVs could impact arbovirus transmission (426), possibly through direct competition or indirectly, by altering insect physiology and/or immunity (68). Although the interactions between arboviruses and ISVs *in vivo* are still largely unexplored, recent work has shown that the presence of the ISF cell fusing agent virus reduced the dissemination of ZIKV and DENV in *Ae. aegypti* mosquitoes (66), hence rendering this ISF a potential agent for biological arbovirus control.

Genetically engineered ISVs could potentially also be used to combat arbovirus transmission by mosquitoes. Chimeras between the ISF BinJV and ZIKV or DENV (BinJV/ZIKV-prME, BinJV/DENV-prME) successfully protected mice from infection and disease upon challenge with wild-type ZIKV or DENV, respectively (248, 427, 428), and these vaccine candidates are currently being developed further for human use. It would be interesting to test whether pre-infection ('vaccination') of mosquitoes with these chimeric viruses could also prevent subsequent wild-type ZIKV or DENV infection in mosquitoes, and if this is the case, via which mechanism.

ISVs that are highly abundant in mosquito populations and transmitted vertically would be attractive candidates for arbovirus control. Mosquito-associated narnaviruses have been discovered in multiple *Aedes* and *Culex* species, and were found at high prevalence in mosquito populations (Chapter 5). Moreover, the presence in mosquito eggs and larvae suggested vertical transmission (Chapter 5). Since narnaviruses induce exceptionally strong small interfering RNA (siRNA) responses (Chapter 5) (102), and it has recently been shown that triggering the siRNA pathway by insertion of ZIKV sequences into the *Ae. aegypti* genome can lead to ZIKV resistance in mosquitoes (429), it would be interesting to investigate whether inserting a ZIKV or DENV sequence into a narnavirus genome would also decrease the susceptibility of mosquitoes to subsequent ZIKV or DENV infection.

Alternatively, the development of genetically modified ISVs that target arboviruses by the production of antivirals, antibodies (430), dsRNA, or molecules that sequester insect host factors required for the arbovirus infection cycle (186, 431), could also contribute to prevent the transmission of arboviruses by mosquitoes. Thus, although the prevention and control of arboviral diseases will remain challenging, these novel ideas may open up more opportunities to combat pathogenic arboviruses than ever before.

Acknowledgements

I thank Kirsten Bronsvoort, Marjolein Dijkema and Corinne Geertsema for their contributions to the virus growth curves, Jody Hobson-Peters and Roy Hall for providing wild-type BinJV and the BinJV/ZIKV chimera, Jelke Fros for providing the ZIKV CpG-high mutant, Tessa Visser and Pieter Rouweler for rearing mosquitoes, and Marleen Abma-Henkens for cell culture maintenance.

References

1. WHO. 2020. Vector-borne diseases. https://www.who.int/news-room/fact-sheets/detail/vector-borne-diseases. Accessed 14 July 2021.
2. ECDC. n.d. Vector-borne diseases. https://www.ecdc.europa.eu/en/climate-change/climate-change-europe/vector-borne-diseases. Accessed 14 July 2021.
3. Mayer SV, Tesh RB, Vasilakis N. 2017. The emergence of arthropod-borne viral diseases: A global prospective on dengue, chikungunya and zika fevers. Acta Trop 166:155-163.
4. Weaver SC, Charlier C, Vasilakis N, Lecuit M. 2018. Zika, chikungunya, and other emerging vector-borne viral diseases. Annu Rev Med 69:395-408.
5. WHO. 2014. Fact sheet yellow fever. https://apps.who.int/iris/bitstream/handle/10665/204192/Fact_Sheet_WHD_2014_EN_1635.pdf. Accessed 14 July 2021.
6. Caminade C, McIntyre KM, Jones AE. 2019. Impact of recent and future climate change on vector-borne diseases. Ann N Y Acad Sci 1436:157-173.
7. Wilder-Smith A, Gubler DJ, Weaver SC, Monath TP, Heymann DL, Scott TW. 2017. Epidemic arboviral diseases: priorities for research and public health. Lancet Infect Dis 17:e101-e106.
8. Dick GW, Kitchen SF, Haddow AJ. 1952. Zika virus. I. Isolations and serological specificity. Trans R Soc Trop Med Hyg 46:509-520.
9. Musso D, Gubler DJ. 2016. Zika virus. Clin Microbiol Rev 29:487-524.
10. Weissenbock H, Kolodziejek J, Url A, Lussy H, Rebel-Bauder B, Nowotny N. 2002. Emergence of Usutu virus, an African mosquito-borne flavivirus of the Japanese encephalitis virus group, central Europe. Emerg Infect Dis 8:652-656.
11. Pecorari M, Longo G, Gennari W, Grottola A, Sabbatini A, Tagliazucchi S, Savini G, Monaco F, Simone M, Lelli R, Rumpianesi F. 2009. First human case of Usutu virus neuroinvasive infection, Italy, August-September 2009. Euro Surveill 14:19446.
12. Casals J, Whitman L. 1957. Mayaro virus: a new human disease agent. I. Relationship to other arbor viruses. Am J Trop Med Hyg 6:1004-1011.
13. Anderson CR, Downs WG, Wattley GH, Ahin NW, Reese AA. 1957. Mayaro virus: a new human disease agent. II. Isolation from blood of patients in Trinidad, B.W.I. Am J Trop Med Hyg 6:1012-1016.
14. Diagne CT, Bengue M, Choumet V, Hamel R, Pompon J, Misse D. 2020. Mayaro virus pathogenesis and transmission mechanisms. Pathogens 9:738.
15. MacNamara FN. 1954. Zika virus: a report on three cases of human infection during an epidemic of jaundice in Nigeria. Trans R Soc Trop Med Hyg 48:139-145.
16. Althouse BM, Vasilakis N, Sall AA, Diallo M, Weaver SC, Hanley KA. 2016. Potential for Zika virus to establish a sylvatic transmission cycle in the Americas. PLoS Negl Trop Dis 10:e0005055.
17. Zanluca C, Melo VC, Mosimann AL, Santos GI, Santos CN, Luz K. 2015. First report of autochthonous transmission of Zika virus in Brazil. Mem Inst Oswaldo Cruz 110:569-572.
18. Campos GS, Bandeira AC, Sardi SI. 2015. Zika virus outbreak, Bahia, Brazil. Emerg Infect Dis 21:1885-1886.
19. Lowe R, Barcellos C, Brasil P, Cruz OG, Honorio NA, Kuper H, Carvalho MS. 2018. The Zika virus epidemic in Brazil: from discovery to future implications. Int J Environ Res Public Health 15:96.

20. Gutierrez-Bugallo G, Piedra LA, Rodriguez M, Bisset JA, Lourenco-de-Oliveira R, Weaver SC, Vasilakis N, Vega-Rua A. 2019. Vector-borne transmission and evolution of Zika virus. Nat Ecol Evol 3:561-569.
21. Miner JJ, Diamond MS. 2017. Zika virus pathogenesis and tissue tropism. Cell Host Microbe 21:134-142.
22. Heymann DL, Hodgson A, Sall AA, Freedman DO, Staples JE, Althabe F, Baruah K, Mahmud G, Kandun N, Vasconcelos PF, Bino S, Menon KU. 2016. Zika virus and microcephaly: why is this situation a PHEIC? Lancet 387:719-721.
23. Giron S, Franke F, Decoppet A, Cadiou B, Travaglini T, Thirion L, Durand G, Jeannin C, L'Ambert G, Grard G, Noel H, Fournet N, Auzet-Caillaud M, Zandotti C, Aboukais S, Chaud P, Guedj S, Hamouda L, Naudot X, Ovize A, Lazarus C, de Valk H, Paty MC, Leparc-Goffart I. 2019. Vector-borne transmission of Zika virus in Europe, southern France, August 2019. Euro Surveill 24:1900655.
24. Nikolay B, Diallo M, Boye CS, Sall AA. 2011. Usutu virus in Africa. Vector Borne Zoonotic Dis 11:1417-1423.
25. Weissenbock H, Bakonyi T, Rossi G, Mani P, Nowotny N. 2013. Usutu virus, Italy, 1996. Emerg Infect Dis 19:274-277.
26. Cadar D, Luhken R, van der Jeugd H, Garigliany M, Ziegler U, Keller M, Lahoreau J, Lachmann L, Becker N, Kik M, Oude Munnink BB, Bosch S, Tannich E, Linden A, Schmidt V, Koopmans MP, Rijks J, Desmecht D, Groschup MH, Reusken C, Schmidt-Chanasit J. 2017. Widespread activity of multiple lineages of Usutu virus, western Europe, 2016. Euro Surveill 22:30452.
27. Pacenti M, Sinigaglia A, Martello T, De Rui ME, Franchin E, Pagni S, Peta E, Riccetti S, Milani A, Montarsi F, Capelli G, Doroldi CG, Bigolin F, Santelli L, Nardetto L, Zoccarato M, Barzon L. 2019. Clinical and virological findings in patients with Usutu virus infection, northern Italy, 2018. Euro Surveill 24:1900180.
28. Zaaijer HL, Slot E, Molier M, Reusken C, Koppelman M. 2019. Usutu virus infection in Dutch blood donors. Transfusion 59:2931-2937.
29. Aberle SW, Kolodziejek J, Jungbauer C, Stiasny K, Aberle JH, Zoufaly A, Hourfar MK, Weidner L, Nowotny N. 2018. Increase in human West Nile and Usutu virus infections, Austria, 2018. Euro Surveill 23:1800545.
30. Calzolari M, Gaibani P, Bellini R, Defilippo F, Pierro A, Albieri A, Maioli G, Luppi A, Rossini G, Balzani A, Tamba M, Galletti G, Gelati A, Carrieri M, Poglayen G, Cavrini F, Natalini S, Dottori M, Sambri V, Angelini P, Bonilauri P. 2012. Mosquito, bird and human surveillance of West Nile and Usutu viruses in Emilia-Romagna Region (Italy) in 2010. PLoS One 7:e38058.
31. Fros JJ, Miesen P, Vogels CB, Gaibani P, Sambri V, Martina BE, Koenraadt CJ, van Rij RP, Vlak JM, Takken W, Pijlman GP. 2015. Comparative Usutu and West Nile virus transmission potential by local *Culex pipiens* mosquitoes in north-western Europe. One Health 1:31-36.
32. Suhrbier A, Jaffar-Bandjee MC, Gasque P. 2012. Arthritogenic alphaviruses - an overview. Nat Rev Rheumatol 8:420-429.
33. Acosta-Ampudia Y, Monsalve DM, Rodriguez Y, Pacheco Y, Anaya JM, Ramirez-Santana C. 2018. Mayaro: an emerging viral threat? Emerg Microbes Infect 7:1-11.

34. LeDuc JW, Pinheiro FP, Travassos da Rosa AP. 1981. An outbreak of Mayaro virus disease in Belterra, Brazil. II. Epidemiology. Am J Trop Med Hyg 30:682-688.
35. Hoch AL, Peterson NE, LeDuc JW, Pinheiro FP. 1981. An outbreak of Mayaro virus disease in Belterra, Brazil. III. Entomological and ecological studies. Am J Trop Med Hyg 30:689-698.
36. Tesh RB, Watts DM, Russell KL, Damodaran C, Calampa C, Cabezas C, Ramirez G, Vasquez B, Hayes CG, Rossi CA, Powers AM, Hice CL, Chandler LJ, Cropp BC, Karabatsos N, Roehrig JT, Gubler DJ. 1999. Mayaro virus disease: an emerging mosquito-borne zoonosis in tropical South America. Clin Infect Dis 28:67-73.
37. Hassing RJ, Leparc-Goffart I, Blank SN, Thevarayan S, Tolou H, van Doornum G, van Genderen PJ. 2010. Imported Mayaro virus infection in the Netherlands. J Infect 61:343-345.
38. Llagonne-Barets M, Icard V, Leparc-Goffart I, Prat C, Perpoint T, Andre P, Ramiere C. 2016. A case of Mayaro virus infection imported from French Guiana. J Clin Virol 77:66-68.
39. Lednicky J, De Rochars VM, Elbadry M, Loeb J, Telisma T, Chavannes S, Anilis G, Cella E, Ciccozzi M, Okech B, Salemi M, Morris JG, Jr. 2016. Mayaro virus in child with acute febrile illness, Haiti, 2015. Emerg Infect Dis 22:2000-2002.
40. Hotez PJ, Murray KO. 2017. Dengue, West Nile virus, chikungunya, Zika - and now Mayaro? PLoS Negl Trop Dis 11:e0005462.
41. Long KC, Ziegler SA, Thangamani S, Hausser NL, Kochel TJ, Higgs S, Tesh RB. 2011. Experimental transmission of Mayaro virus by *Aedes aegypti*. Am J Trop Med Hyg 85:750-757.
42. Wiggins K, Eastmond B, Alto BW. 2018. Transmission potential of Mayaro virus in Florida *Aedes aegypti* and *Aedes albopictus* mosquitoes. Med Vet Entomol 32:436-442.
43. Pereira TN, Carvalho FD, De Mendonca SF, Rocha MN, Moreira LA. 2020. Vector competence of *Aedes aegypti*, *Aedes albopictus*, and *Culex quinquefasciatus* mosquitoes for Mayaro virus. PLoS Negl Trop Dis 14:e0007518.
44. Dieme C, Ciota AT, Kramer LD. 2020. Transmission potential of Mayaro virus by *Aedes albopictus*, and *Anopheles quadrimaculatus* from the USA. Parasit Vectors 13:613.
45. Figueiredo LTM. 2019. Human urban arboviruses can infect wild animals and jump to sylvatic maintenance cycles in South America. Front Cell Infect Microbiol 9:259.
46. Lindenbach BD, Rice CM. 2003. Molecular biology of flaviviruses. Adv Virus Res 59:23-61.
47. Brinton MA, Basu M. 2015. Functions of the 3' and 5' genome RNA regions of members of the genus *Flavivirus*. Virus Res 206:108-119.
48. Goertz GP, Abbo SR, Fros JJ, Pijlman GP. 2018. Functional RNA during Zika virus infection. Virus Res 254:41-53.
49. Nelemans T, Kikkert M. 2019. Viral innate immune evasion and the pathogenesis of emerging RNA virus infections. Viruses 11:961.
50. Hasan SS, Sevvana M, Kuhn RJ, Rossmann MG. 2018. Structural biology of Zika virus and other flaviviruses. Nat Struct Mol Biol 25:13-20.
51. Kielian M. 2006. Class II virus membrane fusion proteins. Virology 344:38-47.
52. Mukhopadhyay S, Kuhn RJ, Rossmann MG. 2005. A structural perspective of the flavivirus life cycle. Nat Rev Microbiol 3:13-22.

53. Harrison SC. 2008. Viral membrane fusion. Nat Struct Mol Biol 15:690-698.
54. Plevka P, Battisti AJ, Junjhon J, Winkler DC, Holdaway HA, Keelapang P, Sittisombut N, Kuhn RJ, Steven AC, Rossmann MG. 2011. Maturation of flaviviruses starts from one or more icosahedrally independent nucleation centres. EMBO Rep 12:602-606.
55. Smit JM, Moesker B, Rodenhuis-Zybert I, Wilschut J. 2011. Flavivirus cell entry and membrane fusion. Viruses 3:160-171.
56. Strauss JH, Strauss EG. 1994. The alphaviruses: gene expression, replication, and evolution. Microbiol Rev 58:491-562.
57. Jose J, Snyder JE, Kuhn RJ. 2009. A structural and functional perspective of alphavirus replication and assembly. Future Microbiol 4:837-856.
58. Kielian M, Chanel-Vos C, Liao M. 2010. Alphavirus entry and membrane fusion. Viruses 2:796-825.
59. Franz AW, Kantor AM, Passarelli AL, Clem RJ. 2015. Tissue barriers to arbovirus infection in mosquitoes. Viruses 7:3741-3767.
60. Vogels CB, Goertz GP, Pijlman GP, Koenraadt CJ. 2017. Vector competence of European mosquitoes for West Nile virus. Emerg Microbes Infect 6:e96.
61. Hardy JL, Houk EJ, Kramer LD, Reeves WC. 1983. Intrinsic factors affecting vector competence of mosquitoes for arboviruses. Annu Rev Entomol 28:229-262.
62. Ruckert C, Ebel GD. 2018. How do virus-mosquito interactions lead to viral emergence? Trends Parasitol 34:310-321.
63. Martinet JP, Ferte H, Failloux AB, Schaffner F, Depaquit J. 2019. Mosquitoes of north-western Europe as potential vectors of arboviruses: a review. Viruses 11:1059.
64. Epelboin Y, Talaga S, Epelboin L, Dusfour I. 2017. Zika virus: An updated review of competent or naturally infected mosquitoes. PLoS Negl Trop Dis 11:e0005933.
65. Kramer LD, Ciota AT. 2015. Dissecting vectorial capacity for mosquito-borne viruses. Curr Opin Virol 15:112-118.
66. Baidaliuk A, Miot EF, Lequime S, Moltini-Conclois I, Delaigue F, Dabo S, Dickson LB, Aubry F, Merkling SH, Cao-Lormeau VM, Lambrechts L. 2019. Cell-fusing agent virus reduces arbovirus dissemination in *Aedes aegypti* mosquitoes *in vivo*. J Virol 93:e0070519.
67. Romo H, Kenney JL, Blitvich BJ, Brault AC. 2018. Restriction of Zika virus infection and transmission in *Aedes aegypti* mediated by an insect-specific flavivirus. Emerg Microbes Infect 7:181.
68. de Almeida JP, Aguiar ER, Armache JN, Olmo RP, Marques JT. 2021. The virome of vector mosquitoes. Curr Opin Virol 49:7-12.
69. Shi M, Lin XD, Tian JH, Chen LJ, Chen X, Li CX, Qin XC, Li J, Cao JP, Eden JS, Buchmann J, Wang W, Xu J, Holmes EC, Zhang YZ. 2016. Redefining the invertebrate RNA virosphere. Nature 540:539-543.
70. Zakrzewski M, Rasic G, Darbro J, Krause L, Poo YS, Filipovic I, Parry R, Asgari S, Devine G, Suhrbier A. 2018. Mapping the virome in wild-caught *Aedes aegypti* from Cairns and Bangkok. Sci Rep 8:4690.
71. Wang L, Rosales Rosas AL, De Coninck L, Shi C, Bouckaert J, Matthijnssens J, Delang L. 2021. Establishment of *Culex modestus* in Belgium and a glance into the virome of Belgian mosquito species. mSphere 6:e01229-01220.

72. Collins ND, Barrett AD. 2017. Live attenuated yellow fever 17D vaccine: a legacy vaccine still controlling outbreaks in modern day. Curr Infect Dis Rep 19:14.
73. Beck A, Tesh RB, Wood TG, Widen SG, Ryman KD, Barrett AD. 2014. Comparison of the live attenuated yellow fever vaccine 17D-204 strain to its virulent parental strain Asibi by deep sequencing. J Infect Dis 209:334-344.
74. Heinsbroek E, Ruitenberg EJ. 2010. The global introduction of inactivated polio vaccine can circumvent the oral polio vaccine paradox. Vaccine 28:3778-3783.
75. O'Hagan DT, Rappuoli R. 2004. The safety of vaccines. Drug Discov Today 9:846-854.
76. CDC. n.d. Japanese encephalitis. https://www.cdc.gov/japaneseencephalitis/vaccine/index.html. Accessed 23 July 2021.
77. Ruzek D, Avsic Zupanc T, Borde J, Chrdle A, Eyer L, Karganova G, Kholodilov I, Knap N, Kozlovskaya L, Matveev A, Miller AD, Osolodkin DI, Overby AK, Tikunova N, Tkachev S, Zajkowska J. 2019. Tick-borne encephalitis in Europe and Russia: Review of pathogenesis, clinical features, therapy, and vaccines. Antiviral Res 164:23-51.
78. Katzelnick LC, Harris E, Participants in the Summit on Dengue Immune Correlates of P. 2017. Immune correlates of protection for dengue: State of the art and research agenda. Vaccine 35:4659-4669.
79. Wilder-Smith A. 2020. Dengue vaccine development: status and future. Bundesgesundheitsblatt Gesundheitsforschung Gesundheitsschutz 63:40-44.
80. Wilder-Smith A, Hombach J, Ferguson N, Selgelid M, O'Brien K, Vannice K, Barrett A, Ferdinand E, Flasche S, Guzman M, Novaes HM, Ng LC, Smith PG, Tharmaphornpilas P, Yoon IK, Cravioto A, Farrar J, Nolan TM. 2019. Deliberations of the strategic advisory group of experts on immunization on the use of CYD-TDV dengue vaccine. Lancet Infect Dis 19:e31-e38.
81. Sridhar S, Luedtke A, Langevin E, Zhu M, Bonaparte M, Machabert T, Savarino S, Zambrano B, Moureau A, Khromava A, Moodie Z, Westling T, Mascarenas C, Frago C, Cortes M, Chansinghakul D, Noriega F, Bouckenooghe A, Chen J, Ng SP, Gilbert PB, Gurunathan S, DiazGranados CA. 2018. Effect of dengue serostatus on dengue vaccine safety and efficacy. N Engl J Med 379:327-340.
82. Katzelnick LC, Gresh L, Halloran ME, Mercado JC, Kuan G, Gordon A, Balmaseda A, Harris E. 2017. Antibody-dependent enhancement of severe dengue disease in humans. Science 358:929-932.
83. Henein S, Adams C, Bonaparte M, Moser JM, Munteanu A, Baric R, de Silva AM. 2021. Dengue vaccine breakthrough infections reveal properties of neutralizing antibodies linked to protection. J Clin Invest 131:e147066.
84. Dyer O. 2019. Philippines measles outbreak is deadliest yet as vaccine scepticism spurs disease comeback. BMJ 364:l739.
85. Pijlman GP. 2015. Enveloped virus-like particles as vaccines against pathogenic arboviruses. Biotechnol J 10:659-670.
86. Chen GL, Coates EE, Plummer SH, Carter CA, Berkowitz N, Conan-Cibotti M, Cox JH, Beck A, O'Callahan M, Andrews C, Gordon IJ, Larkin B, Lampley R, Kaltovich F, Gall J, Carlton K, Mendy J, Haney D, May J, Bray A, Bailer RT, Dowd KA, Brockett B, Gordon D, Koup RA, Schwartz R, Mascola JR, Graham BS, Pierson TC, Donastorg Y, Rosario N, Pape JW, Hoen B, Cabie A, Diaz C, Ledgerwood JE, Team VRCS. 2020. Effect of a chikungunya virus-like particle vaccine on safety and tolerability outcomes: a randomized clinical trial. JAMA 323:1369-1377.

87. Musso D, Rodriguez-Morales AJ, Levi JE, Cao-Lormeau VM, Gubler DJ. 2018. Unexpected outbreaks of arbovirus infections: lessons learned from the Pacific and tropical America. Lancet Infect Dis 18:e355-e361.
88. Ibanez-Justicia A, Kampen H, Braks M, Schaffner F, Steeghs M, Werner D, Zielke D, den Hartog W, Brooks M, Dik M, van de Vossenberg B, Scholte EJ. 2014. First report of established population of *Aedes japonicus japonicus* (Theobald, 1901) (Diptera, Culicidae) in the Netherlands. J Eur Mosq Control Assoc 32:9-13.
89. Azar SR, Weaver SC. 2019. Vector competence: what has Zika virus taught us? Viruses 11:867.
90. Rijks JM, Kik ML, Slaterus R, Foppen RPB, Stroo A, IJzer J, Stahl J, Grone A, Koopmans MGP, van der Jeugd HP, Reusken CBEM. 2016. Widespread Usutu virus outbreak in birds in the Netherlands, 2016. Euro Surveill 21:30391.
91. Grottola A, Marcacci M, Tagliazucchi S, Gennari W, Di Gennaro A, Orsini M, Monaco F, Marchegiano P, Marini V, Meacci M, Rumpianesi F, Lorusso A, Pecorari M, Savini G. 2017. Usutu virus infections in humans: a retrospective analysis in the municipality of Modena, Italy. Clin Microbiol Infect 23:33-37.
92. Kampen H, Werner D. 2014. Out of the bush: the Asian bush mosquito *Aedes japonicus japonicus* (Theobald, 1901) (Diptera, Culicidae) becomes invasive. Parasit Vectors 7:59.
93. ECDC. 2019. *Aedes japonicus* - current known distribution: January 2019. https://ecdc.europa.eu/en/disease-vectors/surveillance-and-disease-data/mosquito-maps. Accessed 5 August 2019.
94. Ibanez-Justicia A, Teekema S, den Hartog W, Jacobs F, Dik M, Stroo A. 2018. The effectiveness of Asian bush mosquito (*Aedes japonicus japonicus*) control actions in colonised peri-urban areas in the Netherlands. J Med Entomol 55:673-680.
95. Sanchez-Vargas I, Scott JC, Poole-Smith BK, Franz AW, Barbosa-Solomieu V, Wilusz J, Olson KE, Blair CD. 2009. Dengue virus type 2 infections of *Aedes aegypti* are modulated by the mosquito's RNA interference pathway. PLoS Pathog 5:e1000299.
96. Scott JC, Brackney DE, Campbell CL, Bondu-Hawkins V, Hjelle B, Ebel GD, Olson KE, Blair CD. 2010. Comparison of dengue virus type 2-specific small RNAs from RNA interference-competent and -incompetent mosquito cells. PLoS Negl Trop Dis 4:e848.
97. Jansen S, Heitmann A, Luhken R, Jost H, Helms M, Vapalahti O, Schmidt-Chanasit J, Tannich E. 2018. Experimental transmission of Zika virus by *Aedes japonicus japonicus* from southwestern Germany. Emerg Microbes Infect 7:192.
98. Reed LJ, Muench H. 1938. A simple method of estimating fifty per cent endpoints. Am J Epidemiol 27:493-497.
99. Gentry MK, Henchal EA, McCown JM, Brandt WE, Dalrymple JM. 1982. Identification of distinct antigenic determinants on dengue-2 virus using monoclonal antibodies. Am J Trop Med Hyg 31:548-555.
100. O'Brien CA, Hobson-Peters J, Yam AW, Colmant AM, McLean BJ, Prow NA, Watterson D, Hall-Mendelin S, Warrilow D, Ng ML, Khromykh AA, Hall RA. 2015. Viral RNA intermediates as targets for detection and discovery of novel and emerging mosquito-borne viruses. PLoS Negl Trop Dis 9:e0003629.
101. Harrison JJ. 2019. Discovery and characterisation of novel insect-specific viruses and investigation of their host-restriction. PhD Thesis, The University of Queensland. https://espace.library.uq.edu.au/view/UQ:283f16e.

102. Goertz GP, Miesen P, Overheul GJ, van Rij RP, van Oers MM, Pijlman GP. 2019. Mosquito small RNA responses to West Nile and insect-specific virus infections in *Aedes* and *Culex* mosquito cells. Viruses 11:271.
103. Goecks J, Nekrutenko A, Taylor J, GalaxyTeam. 2010. Galaxy: a comprehensive approach for supporting accessible, reproducible, and transparent computational research in the life sciences. Genome Biol 11:R86.
104. Langmead B, Salzberg SL. 2012. Fast gapped-read alignment with Bowtie 2. Nat Methods 9:357-359.
105. Antoniewski C. 2014. Computing siRNA and piRNA overlap signatures. Methods Mol Biol 1173:135-146.
106. Goertz GP, Vogels CBF, Geertsema C, Koenraadt CJM, Pijlman GP. 2017. Mosquito co-infection with Zika and chikungunya virus allows simultaneous transmission without affecting vector competence of *Aedes aegypti*. PLoS Negl Trop Dis 11:e0005654.
107. Goenaga S, Kenney JL, Duggal NK, Delorey M, Ebel GD, Zhang B, Levis SC, Enria DA, Brault AC. 2015. Potential for co-infection of a mosquito-specific flavivirus, Nhumirim virus, to block West Nile virus transmission in mosquitoes. Viruses 7:5801-5812.
108. Hall-Mendelin S, McLean BJ, Bielefeldt-Ohmann H, Hobson-Peters J, Hall RA, van den Hurk AF. 2016. The insect-specific Palm Creek virus modulates West Nile virus infection in and transmission by Australian mosquitoes. Parasit Vectors 9:414.
109. Morazzani EM, Wiley MR, Murreddu MG, Adelman ZN, Myles KM. 2012. Production of virus-derived ping-pong-dependent piRNA-like small RNAs in the mosquito soma. PLoS Pathog 8:e1002470.
110. Vodovar N, Bronkhorst AW, van Cleef KW, Miesen P, Blanc H, van Rij RP, Saleh MC. 2012. Arbovirus-derived piRNAs exhibit a ping-pong signature in mosquito cells. PLoS One 7:e30861.
111. Huber K, Jansen S, Leggewie M, Badusche M, Schmidt-Chanasit J, Becker N, Tannich E, Becker SC. 2014. *Aedes japonicus japonicus* (Diptera: *Culicidae*) from Germany have vector competence for Japan encephalitis virus but are refractory to infection with West Nile virus. Parasitol Res 113:3195-3199.
112. Veronesi E, Paslaru A, Silaghi C, Tobler K, Glavinic U, Torgerson P, Mathis A. 2018. Experimental evaluation of infection, dissemination, and transmission rates for two West Nile virus strains in European *Aedes japonicus* under a fluctuating temperature regime. Parasitol Res 117:1925-1932.
113. Camp JV, Kolodziejek J, Nowotny N. 2019. Targeted surveillance reveals native and invasive mosquito species infected with Usutu virus. Parasit Vectors 12:46.
114. Saldana MA, Etebari K, Hart CE, Widen SG, Wood TG, Thangamani S, Asgari S, Hughes GL. 2017. Zika virus alters the microRNA expression profile and elicits an RNAi response in *Aedes aegypti* mosquitoes. PLoS Negl Trop Dis 11:e0005760.
115. Hussain M, Torres S, Schnettler E, Funk A, Grundhoff A, Pijlman GP, Khromykh AA, Asgari S. 2012. West Nile virus encodes a microRNA-like small RNA in the 3' untranslated region which up-regulates GATA4 mRNA and facilitates virus replication in mosquito cells. Nucleic Acids Res 40:2210-2223.
116. Goertz GP, Fros JJ, Miesen P, Vogels CBF, van der Bent ML, Geertsema C, Koenraadt CJM, van Rij RP, van Oers MM, Pijlman GP. 2016. Noncoding subgenomic flavivirus RNA is processed by the mosquito RNA interference machinery and determines West Nile virus transmission by *Culex pipiens* mosquitoes. J Virol 90:10145-10159.

117. Hillman BI, Cai G. 2013. The family *Narnaviridae*: simplest of RNA viruses. Adv Virus Res 86:149-176.
118. Shi M, Neville P, Nicholson J, Eden JS, Imrie A, Holmes EC. 2017. High-resolution metatranscriptomics reveals the ecological dynamics of mosquito-associated RNA viruses in Western Australia. J Virol 91:e0068017.
119. Heitmann A, Jansen S, Luhken R, Leggewie M, Badusche M, Pluskota B, Becker N, Vapalahti O, Schmidt-Chanasit J, Tannich E. 2017. Experimental transmission of Zika virus by mosquitoes from central Europe. Euro Surveill 22:30437.
120. ECDC. 2019. *Aedes albopictus* - current known distribution: January 2019. https://ecdc.europa.eu/en/disease-vectors/surveillance-and-disease-data/mosquito-maps. Accessed 5 August 2019.
121. ECDC. 2019. Rapid risk assessment: Zika virus disease in Var department, France. October 2019. https://www.ecdc.europa.eu/en/publications-data/rapid-risk-assessment-zika-virus-disease-var-department-france. Accessed 2 December 2019.
122. ECDC. 2019. Epidemiological update: second case of locally acquired Zika virus disease in Hyères, France. October 2019. https://www.ecdc.europa.eu/en/news-events/epidemiological-update-second-case-locally-acquired-zika-virus-disease-hyeres-france. Accessed 2 December 2019.
123. ECDC. 2019. Epidemiological update: third case of locally acquired Zika virus disease in Hyères, France. October 2019. https://www.ecdc.europa.eu/en/news-events/epidemiological-update-third-case-locally-acquired-zika-virus-disease-hyeres-france. Accessed 2 December 2019.
124. Roundy CM, Azar SR, Rossi SL, Huang JH, Leal G, Yun R, Fernandez-Salas I, Vitek CJ, Paploski IA, Kitron U, Ribeiro GS, Hanley KA, Weaver SC, Vasilakis N. 2017. Variation in *Aedes aegypti* mosquito competence for Zika virus transmission. Emerg Infect Dis 23:625-632.
125. Armstrong PM, Ehrlich H, Bransfield A, Warren JL, Pitzer VE, Brackney DE. 2018. Successive bloodmeals enhance virus dissemination within mosquitoes and increase transmission potential. Preprint. https://www.biorxiv.org/content/10.1101/246306v1.full. Accessed 5 August 2019.
126. Zouache K, Fontaine A, Vega-Rua A, Mousson L, Thiberge JM, Lourenco-De-Oliveira R, Caro V, Lambrechts L, Failloux AB. 2014. Three-way interactions between mosquito population, viral strain and temperature underlying chikungunya virus transmission potential. Proc Biol Sci 281:20141078.
127. Tesla B, Demakovsky LR, Mordecai EA, Ryan SJ, Bonds MH, Ngonghala CN, Brindley MA, Murdock CC. 2018. Temperature drives Zika virus transmission: evidence from empirical and mathematical models. Proc Biol Sci 285:20180795.
128. Fros JJ, Geertsema C, Vogels CB, Roosjen PP, Failloux AB, Vlak JM, Koenraadt CJ, Takken W, Pijlman GP. 2015. West Nile virus: high transmission rate in north-western European mosquitoes indicates its epidemic potential and warrants increased surveillance. PLoS Negl Trop Dis 9:e0003956.
129. Moore CA, Staples JE, Dobyns WB, Pessoa A, Ventura CV, Fonseca EB, Ribeiro EM, Ventura LO, Neto NN, Arena JF, Rasmussen SA. 2017. Characterizing the pattern of anomalies in congenital Zika syndrome for pediatric clinicians. JAMA Pediatr 171:288-295.

130. Kraemer MU, Sinka ME, Duda KA, Mylne AQ, Shearer FM, Barker CM, Moore CG, Carvalho RG, Coelho GE, Van Bortel W, Hendrickx G, Schaffner F, Elyazar IR, Teng HJ, Brady OJ, Messina JP, Pigott DM, Scott TW, Smith DL, Wint GR, Golding N, Hay SI. 2015. The global distribution of the arbovirus vectors *Aedes aegypti* and *Ae. albopictus*. Elife 4:e08347.
131. Haddow AJ, Williams MC, Woodall JP, Simpson DI, Goma LK. 1964. Twelve isolations of Zika virus from *Aedes* (*Stegomyia*) *africanus* (Theobald) taken in and above a Uganda forest. Bull World Health Organ 31:57-69.
132. Marchette NJ, Garcia R, Rudnick A. 1969. Isolation of Zika virus from *Aedes aegypti* mosquitoes in Malaysia. Am J Trop Med Hyg 18:411-415.
133. Ferreira-de-Brito A, Ribeiro IP, Miranda RM, Fernandes RS, Campos SS, Silva KA, Castro MG, Bonaldo MC, Brasil P, Lourenco-de-Oliveira R. 2016. First detection of natural infection of *Aedes aegypti* with Zika virus in Brazil and throughout South America. Mem Inst Oswaldo Cruz 111:655-658.
134. Guerbois M, Fernandez-Salas I, Azar SR, Danis-Lozano R, Alpuche-Aranda CM, Leal G, Garcia-Malo IR, Diaz-Gonzalez EE, Casas-Martinez M, Rossi SL, Del Rio-Galvan SL, Sanchez-Casas RM, Roundy CM, Wood TG, Widen SG, Vasilakis N, Weaver SC. 2016. Outbreak of Zika virus infection, Chiapas State, Mexico, 2015, and first confirmed transmission by *Aedes aegypti* mosquitoes in the Americas. J Infect Dis 214:1349-1356.
135. Ledermann JP, Guillaumot L, Yug L, Saweyog SC, Tided M, Machieng P, Pretrick M, Marfel M, Griggs A, Bel M, Duffy MR, Hancock WT, Ho-Chen T, Powers AM. 2014. *Aedes hensilli* as a potential vector of Chikungunya and Zika viruses. PLoS Negl Trop Dis 8:e3188.
136. Chouin-Carneiro T, Vega-Rua A, Vazeille M, Yebakima A, Girod R, Goindin D, Dupont-Rouzeyrol M, Lourenco-de-Oliveira R, Failloux AB. 2016. Differential susceptibilities of *Aedes aegypti* and *Aedes albopictus* from the Americas to Zika virus. PLoS Negl Trop Dis 10:e0004543.
137. Gendernalik A, Weger-Lucarelli J, Garcia Luna SM, Fauver JR, Ruckert C, Murrieta RA, Bergren N, Samaras D, Nguyen C, Kading RC, Ebel GD. 2017. American *Aedes vexans* mosquitoes are competent vectors of Zika virus. Am J Trop Med Hyg 96:1338-1340.
138. Diallo D, Sall AA, Diagne CT, Faye O, Faye O, Ba Y, Hanley KA, Buenemann M, Weaver SC, Diallo M. 2014. Zika virus emergence in mosquitoes in southeastern Senegal, 2011. PLoS One 9:e109442.
139. Elizondo-Quiroga D, Medina-Sanchez A, Sanchez-Gonzalez JM, Eckert KA, Villalobos-Sanchez E, Navarro-Zuniga AR, Sanchez-Tejeda G, Correa-Morales F, Gonzalez-Acosta C, Arias CF, Lopez S, Del Angel RM, Pando-Robles V, Elizondo-Quiroga AE. 2018. Zika virus in salivary glands of five different species of wild-caught mosquitoes from Mexico. Sci Rep 8:809.
140. Fu S, Song S, Liu H, Li Y, Li X, Gao X, Xu Z, Liu G, Wang D, Tian Z, Zhou J, He Y, Lei W, Wang H, Wang B, Lu X, Liang G. 2017. Zika virus isolated from mosquitoes: a field and laboratory investigation in China, 2016. Sci China Life Sci 60:1364-1371.

141. Guedes DR, Paiva MH, Donato MM, Barbosa PP, Krokovsky L, Rocha S, Saraiva K, Crespo MM, Rezende TM, Wallau GL, Barbosa RM, Oliveira CM, Melo-Santos MA, Pena L, Cordeiro MT, Franca RFO, Oliveira AL, Peixoto CA, Leal WS, Ayres CF. 2017. Zika virus replication in the mosquito *Culex quinquefasciatus* in Brazil. Emerg Microbes Infect 6:e69.
142. Guo XX, Li CX, Deng YQ, Xing D, Liu QM, Wu Q, Sun AJ, Dong YD, Cao WC, Qin CF, Zhao TY. 2016. *Culex pipiens quinquefasciatus*: a potential vector to transmit Zika virus. Emerg Microbes Infect 5:e102.
143. Smartt CT, Shin D, Kang S, Tabachnick WJ. 2018. *Culex quinquefasciatus* (Diptera: Culicidae) from Florida transmitted Zika virus. Front Microbiol 9:768.
144. Farajollahi A, Fonseca DM, Kramer LD, Marm Kilpatrick A. 2011. "Bird biting" mosquitoes and human disease: a review of the role of *Culex pipiens* complex mosquitoes in epidemiology. Infect Genet Evol 11:1577-1585.
145. Ciota AT, Kramer LD. 2013. Vector-virus interactions and transmission dynamics of West Nile virus. Viruses 5:3021-3047.
146. Alaniz AJ, Carvajal MA, Bacigalupo A, Cattan PE. 2018. Global spatial assessment of *Aedes aegypti* and *Culex quinquefasciatus*: a scenario of Zika virus exposure. Epidemiol Infect 147:1-11.
147. Byrne K, Nichols RA. 1999. *Culex pipiens* in London Underground tunnels: differentiation between surface and subterranean populations. Heredity 82:7-15.
148. Vogels CB, Fros JJ, Goertz GP, Pijlman GP, Koenraadt CJ. 2016. Vector competence of northern European *Culex pipiens* biotypes and hybrids for West Nile virus is differentially affected by temperature. Parasit Vectors 9:393.
149. Amraoui F, Atyame-Nten C, Vega-Rua A, Lourenco-de-Oliveira R, Vazeille M, Failloux AB. 2016. *Culex* mosquitoes are experimentally unable to transmit Zika virus. Euro Surveill 21:30333.
150. Kenney JL, Romo H, Duggal NK, Tzeng WP, Burkhalter KL, Brault AC, Savage HM. 2017. Transmission incompetence of *Culex quinquefasciatus* and *Culex pipiens pipiens* from North America for Zika virus. Am J Trop Med Hyg 96:1235-1240.
151. Boccolini D, Toma L, Di Luca M, Severini F, Romi R, Remoli ME, Sabbatucci M, Venturi G, Rezza G, Fortuna C. 2016. Experimental investigation of the susceptibility of Italian *Culex pipiens* mosquitoes to Zika virus infection. Euro Surveill 21:30328.
152. Aliota MT, Peinado SA, Osorio JE, Bartholomay LC. 2016. *Culex pipiens* and *Aedes triseriatus* Mosquito Susceptibility to Zika Virus. Emerg Infect Dis 22:1857-1859.
153. Weger-Lucarelli J, Ruckert C, Chotiwan N, Nguyen C, Garcia Luna SM, Fauver JR, Foy BD, Perera R, Black WC, Kading RC, Ebel GD. 2016. Vector competence of American mosquitoes for three strains of Zika virus. PLoS Negl Trop Dis 10:e0005101.
154. Huang YJ, Ayers VB, Lyons AC, Unlu I, Alto BW, Cohnstaedt LW, Higgs S, Vanlandingham DL. 2016. *Culex* species mosquitoes and Zika virus. Vector Borne Zoonotic Dis 16:673-676.
155. Armbruster P, Hutchinson RA. 2002. Pupal mass and wing length as indicators of fecundity in *Aedes albopictus* and *Aedes geniculatus* (Diptera: Culicidae). J Med Entomol 39:699-704.

156. Gaunt MW, Sall AA, de Lamballerie X, Falconar AK, Dzhivanian TI, Gould EA. 2001. Phylogenetic relationships of flaviviruses correlate with their epidemiology, disease association and biogeography. J Gen Virol 82:1867-1876.
157. Grard G, Moureau G, Charrel RN, Holmes EC, Gould EA, de Lamballerie X. 2010. Genomics and evolution of *Aedes*-borne flaviviruses. J Gen Virol 91:87-94.
158. Tsetsarkin KA, Vanlandingham DL, McGee CE, Higgs S. 2007. A single mutation in chikungunya virus affects vector specificity and epidemic potential. PLoS Pathog 3:e201.
159. Stapleford KA, Coffey LL, Lay S, Borderia AV, Duong V, Isakov O, Rozen-Gagnon K, Arias-Goeta C, Blanc H, Beaucourt S, Haliloglu T, Schmitt C, Bonne I, Ben-Tal N, Shomron N, Failloux AB, Buchy P, Vignuzzi M. 2014. Emergence and transmission of arbovirus evolutionary intermediates with epidemic potential. Cell Host Microbe 15:706-716.
160. Lourenco-de-Oliveira R, Marques JT, Sreenu VB, Atyame Nten C, Aguiar E, Varjak M, Kohl A, Failloux AB. 2018. *Culex quinquefasciatus* mosquitoes do not support replication of Zika virus. J Gen Virol 99:258-264.
161. Wilson AJ, Harrup LE. 2018. Reproducibility and relevance in insect-arbovirus infection studies. Curr Opin Insect Sci 28:105-112.
162. Chvala S, Bakonyi T, Bukovsky C, Meister T, Brugger K, Rubel F, Nowotny N, Weissenbock H. 2007. Monitoring of Usutu virus activity and spread by using dead bird surveillance in Austria, 2003-2005. Vet Microbiol 122:237-245.
163. Honig V, Palus M, Kaspar T, Zemanova M, Majerova K, Hofmannova L, Papezik P, Sikutova S, Rettich F, Hubalek Z, Rudolf I, Votypka J, Modry D, Ruzek D. 2019. Multiple lineages of Usutu Virus *(Flaviviridae*, *Flavivirus*) in blackbirds (*Turdus merula*) and mosquitoes (*Culex pipiens*, *Cx. modestus*) in the Czech Republic (2016-2019). Microorganisms 7:568.
164. Oude Munnink BB, Munger E, Nieuwenhuijse DF, Kohl R, van der Linden A, Schapendonk CME, van der Jeugd H, Kik M, Rijks JM, Reusken C, Koopmans M. 2020. Genomic monitoring to understand the emergence and spread of Usutu virus in the Netherlands, 2016-2018. Sci Rep 10:2798.
165. Abbo SR, Visser TM, Wang H, Goertz GP, Fros JJ, Abma-Henkens MHC, Geertsema C, Vogels CBF, Koopmans MPG, Reusken CBEM, Hall-Mendelin S, Hall RA, van Oers MM, Koenraadt CJM, Pijlman GP. 2020. The invasive Asian bush mosquito *Aedes japonicus* found in the Netherlands can experimentally transmit Zika virus and Usutu virus. PLoS Negl Trop Dis 14:e0008217.
166. Puggioli A, Bonilauri P, Calzolari M, Lelli D, Carrieri M, Urbanelli S, Pudar D, Bellini R. 2017. Does *Aedes albopictus* (Diptera: Culicidae) play any role in Usutu virus transmission in Northern Italy? Experimental oral infection and field evidences. Acta Trop 172:192-196.
167. Cook CL, Huang YS, Lyons AC, Alto BW, Unlu I, Higgs S, Vanlandingham DL. 2018. North American *Culex pipiens* and *Culex quinquefasciatus* are competent vectors for Usutu virus. PLoS Negl Trop Dis 12:e0006732.
168. Hernandez-Triana LM, de Marco MF, Mansfield KL, Thorne L, Lumley S, Marston D, Fooks AA, Johnson N. 2018. Assessment of vector competence of UK mosquitoes for Usutu virus of African origin. Parasit Vectors 11:381.

169. Holicki CM, Scheuch DE, Ziegler U, Lettow J, Kampen H, Werner D, Groschup MH. 2020. German *Culex pipiens* biotype *molestus* and *Culex torrentium* are vector-competent for Usutu virus. Parasit Vectors 13:625.
170. Nikolay B, Diallo M, Faye O, Boye CS, Sall AA. 2012. Vector competence of *Culex neavei* (Diptera: Culicidae) for Usutu virus. Am J Trop Med Hyg 86:993-996.
171. Abbo SR, Vogels CBF, Visser TM, Geertsema C, van Oers MM, Koenraadt CJM, Pijlman GP. 2020. Forced Zika Virus Infection of *Culex pipiens* Leads to Limited Virus Accumulation in Mosquito Saliva. Viruses 12:659.
172. Mahmood F, Chiles RE, Fang Y, Reisen WK. 2004. Methods for studying the vector competence of *Culex tarsalis* for western equine encephalomyelitis virus. J Am Mosq Control Assoc 20:277-282.
173. Marchi PR, Rawlings P, Burroughs JN, Wellby M, Mertens PP, Mellor PS, Wade-Evans AM. 1995. Proteolytic cleavage of VP2, an outer capsid protein of African horse sickness virus, by species-specific serum proteases enhances infectivity in *Culicoides*. J Gen Virol 76:2607-2611.
174. Muturi EJ, Dunlap C, Ramirez JL, Rooney AP, Kim CH. 2019. Host blood-meal source has a strong impact on gut microbiota of *Aedes aegypti*. FEMS Microbiol Ecol 95:fiy213.
175. Wu P, Sun P, Nie K, Zhu Y, Shi M, Xiao C, Liu H, Liu Q, Zhao T, Chen X, Zhou H, Wang P, Cheng G. 2019. A gut commensal bacterium promotes mosquito permissiveness to arboviruses. Cell Host Microbe 25:101-112.
176. Apte-Deshpande A, Paingankar M, Gokhale MD, Deobagkar DN. 2012. *Serratia odorifera* a midgut inhabitant of *Aedes aegypti* mosquito enhances its susceptibility to dengue-2 virus. PLoS One 7:e40401.
177. Ramirez JL, Short SM, Bahia AC, Saraiva RG, Dong Y, Kang S, Tripathi A, Mlambo G, Dimopoulos G. 2014. Chromobacterium Csp_P reduces malaria and dengue infection in vector mosquitoes and has entomopathogenic and in vitro anti-pathogen activities. PLoS Pathog 10:e1004398.
178. Souza-Neto JA, Powell JR, Bonizzoni M. 2019. *Aedes aegypti* vector competence studies: A review. Infect Genet Evol 67:191-209.
179. Kraemer MUG, Reiner RC, Jr., Brady OJ, Messina JP, Gilbert M, Pigott DM, Yi D, Johnson K, Earl L, Marczak LB, Shirude S, Davis Weaver N, Bisanzio D, Perkins TA, Lai S, Lu X, Jones P, Coelho GE, Carvalho RG, Van Bortel W, Marsboom C, Hendrickx G, Schaffner F, Moore CG, Nax HH, Bengtsson L, Wetter E, Tatem AJ, Brownstein JS, Smith DL, Lambrechts L, Cauchemez S, Linard C, Faria NR, Pybus OG, Scott TW, Liu Q, Yu H, Wint GRW, Hay SI, Golding N. 2019. Past and future spread of the arbovirus vectors *Aedes aegypti* and *Aedes albopictus*. Nat Microbiol 4:854-863.
180. Montarsi F, Martini S, Dal Pont M, Delai N, Ferro Milone N, Mazzucato M, Soppelsa F, Cazzola L, Cazzin S, Ravagnan S, Ciocchetta S, Russo F, Capelli G. 2013. Distribution and habitat characterization of the recently introduced invasive mosquito *Aedes koreicus* [*Hulecoeteomyia koreica*], a new potential vector and pest in north-eastern Italy. Parasit Vectors 6:292.
181. Janssen N, Graovac N, Vignjevic G, Bogojevic MS, Turic N, Klobucar A, Kavran M, Petric D, Cupina AI, Fischer S, Werner D, Kampen H, Merdic E. 2020. Rapid spread and population genetics of *Aedes japonicus japonicus* (Diptera: Culicidae) in southeastern Europe (Croatia, Bosnia and Herzegovina, Serbia). PLoS One 15:e0241235.

182. Pagac BB, Spring AR, Stawicki JR, Dinh TL, Lura T, Kavanaugh MD, Pecor DB, Justi SA, Linton YM. 2021. Incursion and establishment of the Old World arbovirus vector *Aedes* (*Fredwardsius*) *vittatus* (Bigot, 1861) in the Americas. Acta Trop 213:105739.
183. Turell MJ, O'Guinn ML, Dohm DJ, Jones JW. 2001. Vector competence of North American mosquitoes (Diptera: Culicidae) for West Nile virus. J Med Entomol 38:130-134.
184. Takashima I, Rosen L. 1989. Horizontal and vertical transmission of Japanese encephalitis virus by *Aedes japonicus* (Diptera: Culicidae). J Med Entomol 26:454-458.
185. Schaffner F, Vazeille M, Kaufmann C, Failloux AB, Mathis A. 2011. Vector competence of *Aedes japonicus* for chikungunya and dengue viruses. Eur Mosq Bull 29:141-142.
186. Agboli E, Leggewie M, Altinli M, Schnettler E. 2019. Mosquito-specific viruses - transmission and interaction. Viruses 11:873.
187. Olmo RP, Todjro YMH, Aguiar ERGR, de Almeida JPP, Armache JN, de Faria IJS, Ferreira FV, Silva ATS, de Souza KPR, Vilela APP, Tan CH, Diallo M, Gaye A, Paupy C, Obame-Nkoghe J, Visser TM, Koenraadt CJM, Wongsokarijo MA, Cruz ALC, Prieto MT, Parra MCP, Nogueira ML, Avelino-Silva V, Mota RN, Borges MAZ, Drumond BP, Kroon EG, Sedda L, Marois E, Imler J-L, Marques JT. 2021. Insect-specific viruses regulate vector competence in *Aedes aegypti* mosquitoes via expression of histone H4. Preprint. https://www.biorxiv.org/content/10.1101/2021.06.05.447047v1. Accessed 24 August 2021.
188. Bolling BG, Weaver SC, Tesh RB, Vasilakis N. 2015. Insect-specific virus discovery: significance for the arbovirus community. Viruses 7:4911-4928.
189. Shi C, Beller L, Deboutte W, Yinda KC, Delang L, Vega-Rua A, Failloux AB, Matthijnssens J. 2019. Stable distinct core eukaryotic viromes in different mosquito species from Guadeloupe, using single mosquito viral metagenomics. Microbiome 7:121.
190. Shi C, Zhao L, Atoni E, Zeng W, Hu X, Matthijnssens J, Yuan Z, Xia H. 2020. Stability of the virome in lab- and field-collected *Aedes albopictus* mosquitoes across different developmental stages and possible core viruses in the publicly available virome data of *Aedes* mosquitoes. mSystems 5: e0064020.
191. Faizah AN, Kobayashi D, Amoa-Bosompem M, Higa Y, Tsuda Y, Itokawa K, Miura K, Hirayama K, Sawabe K, Isawa H. 2020. Evaluating the competence of the primary vector, *Culex tritaeniorhynchus*, and the invasive mosquito species, *Aedes japonicus japonicus*, in transmitting three Japanese encephalitis virus genotypes. PLoS Negl Trop Dis 14:e0008986.
192. Dinan AM, Lukhovitskaya NI, Olendraite I, Firth AE. 2020. A case for a negative-strand coding sequence in a group of positive-sense RNA viruses. Virus Evol 6:veaa007.
193. DeRisi JL, Huber G, Kistler A, Retallack H, Wilkinson M, Yllanes D. 2019. An exploration of ambigrammatic sequences in narnaviruses. Sci Rep 9:17982.
194. Aguiar ER, Olmo RP, Marques JT. 2016. Virus-derived small RNAs: molecular footprints of host-pathogen interactions. Wiley Interdiscip Rev RNA 7:824-837.
195. Aguiar ER, Olmo RP, Paro S, Ferreira FV, de Faria IJ, Todjro YM, Lobo FP, Kroon EG, Meignin C, Gatherer D, Imler JL, Marques JT. 2015. Sequence-independent characterization of viruses based on the pattern of viral small RNAs produced by the host. Nucleic Acids Res 43:6191-6206.

196. Martin M. 2011. Cutadapt removes adapter sequences from high-throughput sequencing reads. EMBnet J 17:10-12.
197. Matthews BJ, Dudchenko O, Kingan SB, Koren S, Antoshechkin I, Crawford JE, Glassford WJ, Herre M, Redmond SN, Rose NH, Weedall GD, Wu Y, Batra SS, Brito-Sierra CA, Buckingham SD, Campbell CL, Chan S, Cox E, Evans BR, Fansiri T, Filipovic I, Fontaine A, Gloria-Soria A, Hall R, Joardar VS, Jones AK, Kay RGG, Kodali VK, Lee J, Lycett GJ, Mitchell SN, Muehling J, Murphy MR, Omer AD, Partridge FA, Peluso P, Aiden AP, Ramasamy V, Rasic G, Roy S, Saavedra-Rodriguez K, Sharan S, Sharma A, Smith ML, Turner J, Weakley AM, Zhao Z, Akbari OS, Black WCt, Cao H, et al. 2018. Improved reference genome of *Aedes aegypti* informs arbovirus vector control. Nature 563:501-507.
198. Chen XG, Jiang X, Gu J, Xu M, Wu Y, Deng Y, Zhang C, Bonizzoni M, Dermauw W, Vontas J, Armbruster P, Huang X, Yang Y, Zhang H, He W, Peng H, Liu Y, Wu K, Chen J, Lirakis M, Topalis P, Van Leeuwen T, Hall AB, Jiang X, Thorpe C, Mueller RL, Sun C, Waterhouse RM, Yan G, Tu ZJ, Fang X, James AA. 2015. Genome sequence of the Asian tiger mosquito, *Aedes albopictus*, reveals insights into its biology, genetics, and evolution. Proc Natl Acad Sci U S A 112:E5907-5915.
199. Langmead B, Trapnell C, Pop M, Salzberg SL. 2009. Ultrafast and memory-efficient alignment of short DNA sequences to the human genome. Genome Biol 10:R25.
200. Nurk S, Meleshko D, Korobeynikov A, Pevzner PA. 2017. metaSPAdes: a new versatile metagenomic assembler. Genome Res 27:824-834.
201. Zerbino DR, Birney E. 2008. Velvet: algorithms for *de novo* short read assembly using de Bruijn graphs. Genome Res 18:821-829.
202. Camacho C, Coulouris G, Avagyan V, Ma N, Papadopoulos J, Bealer K, Madden TL. 2009. BLAST+: architecture and applications. BMC Bioinformatics 10:421.
203. Buchfink B, Reuter K, Drost HG. 2021. Sensitive protein alignments at tree-of-life scale using DIAMOND. Nat Methods 18:366-368.
204. Fu L, Niu B, Zhu Z, Wu S, Li W. 2012. CD-HIT: accelerated for clustering the next-generation sequencing data. Bioinformatics 28:3150-3152.
205. Gu Z, Eils R, Schlesner M. 2016. Complex heatmaps reveal patterns and correlations in multidimensional genomic data. Bioinformatics 32:2847-2849.
206. Sardi SI, Carvalho RH, Pacheco LGC, Almeida JPPD, Belitardo EMMDA, Pinheiro CS, Campos GS, Aguiar ERGR. 2020. High-quality resolution of the outbreak-related Zika virus genome and discovery of new viruses using ion torrent-based metatranscriptomics. Viruses 12:782.
207. Bankevich A, Nurk S, Antipov D, Gurevich AA, Dvorkin M, Kulikov AS, Lesin VM, Nikolenko SI, Pham S, Prjibelski AD, Pyshkin AV, Sirotkin AV, Vyahhi N, Tesler G, Alekseyev MA, Pevzner PA. 2012. SPAdes: a new genome assembly algorithm and its applications to single-cell sequencing. J Comput Biol 19:455-477.
208. Katoh K, Misawa K, Kuma K, Miyata T. 2002. MAFFT: a novel method for rapid multiple sequence alignment based on fast Fourier transform. Nucleic Acids Res 30:3059-3066.
209. Kumar S, Stecher G, Li M, Knyaz C, Tamura K. 2018. MEGA X: Molecular evolutionary genetics analysis across computing platforms. Mol Biol Evol 35:1547-1549.
210. Letunic I, Bork P. 2021. Interactive Tree Of Life (iTOL) v5: an online tool for phylogenetic tree display and annotation. Nucleic Acids Res 49:W293-W296.

211. Simmonds P. 2012. SSE: a nucleotide and amino acid sequence analysis platform. BMC Res Notes 5:50.
212. Edgar RC. 2004. MUSCLE: multiple sequence alignment with high accuracy and high throughput. Nucleic Acids Res 32:1792-1797.
213. Reuter JS, Mathews DH. 2010. RNAstructure: software for RNA secondary structure prediction and analysis. BMC Bioinformatics 11:129.
214. Sperschneider J, Datta A. 2010. DotKnot: pseudoknot prediction using the probability dot plot under a refined energy model. Nucleic Acids Res 38:e103.
215. Darty K, Denise A, Ponty Y. 2009. VARNA: Interactive drawing and editing of the RNA secondary structure. Bioinformatics 25:1974-1975.
216. Di Giallonardo F, Schlub TE, Shi M, Holmes EC. 2017. Dinucleotide composition in animal RNA viruses is shaped more by virus family than by host species. J Virol 91:e0238116.
217. Cheng X, Virk N, Chen W, Ji S, Ji S, Sun Y, Wu X. 2013. CpG usage in RNA viruses: data and hypotheses. PLoS One 8:e74109.
218. Auewarakul P. 2005. Composition bias and genome polarity of RNA viruses. Virus Res 109:33-37.
219. Han YH, Luo YJ, Wu Q, Jovel J, Wang XH, Aliyari R, Han C, Li WX, Ding SW. 2011. RNA-based immunity terminates viral infection in adult *Drosophila* in the absence of viral suppression of RNA interference: characterization of viral small interfering RNA populations in wild-type and mutant flies. J Virol 85:13153-13163.
220. Fujimura T, Esteban R. 2007. Interactions of the RNA polymerase with the viral genome at the 5'- and 3'-ends contribute to 20S RNA narnavirus persistence in yeast. J Biol Chem 282:19011-19019.
221. Retallack H, Popova KD, Laurie MT, Sunshine S, DeRisi JL. 2021. Persistence of ambigrammatic narnaviruses requires translation of the reverse open reading frame. J Virol 95:e0010921.
222. Ghabrial SA, Nibert ML. 2009. *Victorivirus*, a new genus of fungal viruses in the family *Totiviridae*. Arch Virol 154:373-379.
223. Firth AE, Brierley I. 2012. Non-canonical translation in RNA viruses. J Gen Virol 93:1385-1409.
224. Bekaert M, Bidou L, Denise A, Duchateau-Nguyen G, Forest JP, Froidevaux C, Hatin I, Rousset JP, Termier M. 2003. Towards a computational model for -1 eukaryotic frameshifting sites. Bioinformatics 19:327-335.
225. Miesen P, Joosten J, van Rij RP. 2016. PIWIs go viral: arbovirus-derived piRNAs in vector mosquitoes. PLoS Pathog 12:e1006017.
226. Wu Q, Luo Y, Lu R, Lau N, Lai EC, Li WX, Ding SW. 2010. Virus discovery by deep sequencing and assembly of virus-derived small silencing RNAs. Proc Natl Acad Sci U S A 107:1606-1611.
227. Charon J, Grigg MJ, Eden JS, Piera KA, Rana H, William T, Rose K, Davenport MP, Anstey NM, Holmes EC. 2019. Novel RNA viruses associated with *Plasmodium vivax* in human malaria and *Leucocytozoon* parasites in avian disease. PLoS Pathog 15:e1008216.

228. Grybchuk D, Akopyants NS, Kostygov AY, Konovalovas A, Lye LF, Dobson DE, Zangger H, Fasel N, Butenko A, Frolov AO, Votypka J, d'Avila-Levy CM, Kulich P, Moravcova J, Plevka P, Rogozin IB, Serva S, Lukes J, Beverley SM, Yurchenko V. 2018. Viral discovery and diversity in trypanosomatid protozoa with a focus on relatives of the human parasite *Leishmania*. Proc Natl Acad Sci U S A 115:E506-E515.
229. Lye LF, Akopyants NS, Dobson DE, Beverley SM. 2016. A narnavirus-like element from the trypanosomatid protozoan parasite *Leptomonas seymouri*. Genome Announc 4:e0071316.
230. Batson J, Dudas G, Haas-Stapleton E, Kistler AL, Li LM, Logan P, Ratnasiri K, Retallack H. 2021. Single mosquito metatranscriptomics identifies vectors, emerging pathogens and reservoirs in one assay. Elife 10:e68353.
231. Dudas G, Huber G, Wilkinson M, Yllanes D. 2021. Polymorphism of genetic ambigrams. Virus Evol 7:veab038.
232. Krishnamurthy SR, Wang D. 2017. Origins and challenges of viral dark matter. Virus Res 239:136-142.
233. Ghildiyal M, Seitz H, Horwich MD, Li C, Du T, Lee S, Xu J, Kittler EL, Zapp ML, Weng Z, Zamore PD. 2008. Endogenous siRNAs derived from transposons and mRNAs in *Drosophila* somatic cells. Science 320:1077-1081.
234. Zhai Y, Attoui H, Mohd Jaafar F, Wang HQ, Cao YX, Fan SP, Sun YX, Liu LD, Mertens PP, Meng WS, Wang D, Liang G. 2010. Isolation and full-length sequence analysis of *Armigeres subalbatus* totivirus, the first totivirus isolate from mosquitoes representing a proposed novel genus (*Artivirus*) of the family *Totiviridae*. J Gen Virol 91:2836-2845.
235. Isawa H, Kuwata R, Hoshino K, Tsuda Y, Sakai K, Watanabe S, Nishimura M, Satho T, Kataoka M, Nagata N, Hasegawa H, Bando H, Yano K, Sasaki T, Kobayashi M, Mizutani T, Sawabe K. 2011. Identification and molecular characterization of a new nonsegmented double-stranded RNA virus isolated from *Culex* mosquitoes in Japan. Virus Res 155:147-155.
236. Zhang Y, Qiang X, Guo X, Peng H, Qin S, Cui Y, Fan H, Zhou H, Zhang J, Wang J, Tong Y. 2021. Identification and molecular characterization of a new Omono River virus isolated from *Culex Tritaeniorhynchus* in Yunnan, China. Virol Sin 36:152-154.
237. Briese T, Calisher CH, Higgs S. 2013. Viruses of the family *Bunyaviridae*: are all available isolates reassortants? Virology 446:207-216.
238. Kapuscinski ML, Bergren NA, Russell BJ, Lee JS, Borland EM, Hartman DA, King DC, Hughes HR, Burkhalter KL, Kading RC, Stenglein MD. 2021. Genomic characterization of 99 viruses from the bunyavirus families *Nairoviridae*, *Peribunyaviridae,* and *Phenuiviridae*, including 35 previously unsequenced viruses. PLoS Pathog 17:e1009315.
239. Espino-Vazquez AN, Bermudez-Barrientos JR, Cabrera-Rangel JF, Cordova-Lopez G, Cardoso-Martinez F, Martinez-Vazquez A, Camarena-Pozos DA, Mondo SJ, Pawlowska TE, Abreu-Goodger C, Partida-Martinez LP. 2020. Narnaviruses: novel players in fungal-bacterial symbioses. ISME J 14:1743-1754.
240. Richaud A, Frezal L, Tahan S, Jiang H, Blatter JA, Zhao G, Kaur T, Wang D, Felix MA. 2019. Vertical transmission in *Caenorhabditis* nematodes of RNA molecules encoding a viral RNA-dependent RNA polymerase. Proc Natl Acad Sci U S A 116:24738-24747.

241. Weaver SC, Costa F, Garcia-Blanco MA, Ko AI, Ribeiro GS, Saade G, Shi PY, Vasilakis N. 2016. Zika virus: History, emergence, biology, and prospects for control. Antiviral Res 130:69-80.
242. Pierson TC, Diamond MS. 2018. The emergence of Zika virus and its new clinical syndromes. Nature 560:573-581.
243. Sirohi D, Kuhn RJ. 2017. Zika virus structure, maturation, and receptors. J Infect Dis 216:S935-S944.
244. Sapparapu G, Fernandez E, Kose N, Bin C, Fox JM, Bombardi RG, Zhao H, Nelson CA, Bryan AL, Barnes T, Davidson E, Mysorekar IU, Fremont DH, Doranz BJ, Diamond MS, Crowe JE. 2016. Neutralizing human antibodies prevent Zika virus replication and fetal disease in mice. Nature 540:443-447.
245. Barba-Spaeth G, Dejnirattisai W, Rouvinski A, Vaney MC, Medits I, Sharma A, Simon-Loriere E, Sakuntabhai A, Cao-Lormeau VM, Haouz A, England P, Stiasny K, Mongkolsapaya J, Heinz FX, Screaton GR, Rey FA. 2016. Structural basis of potent Zika-dengue virus antibody cross-neutralization. Nature 536:48-53.
246. Collins MH, Tu HA, Gimblet-Ochieng C, Liou GA, Jadi RS, Metz SW, Thomas A, McElvany BD, Davidson E, Doranz BJ, Reyes Y, Bowman NM, Becker-Dreps S, Bucardo F, Lazear HM, Diehl SA, de Silva AM. 2019. Human antibody response to Zika targets type-specific quaternary structure epitopes. JCI Insight 4:e124588.
247. Metz SW, Thomas A, Brackbill A, Forsberg J, Miley MJ, Lopez CA, Lazear HM, Tian S, de Silva AM. 2019. Oligomeric state of the ZIKV E protein defines protective immune responses. Nat Commun 10:4606.
248. Hobson-Peters J, Harrison JJ, Watterson D, Hazlewood JE, Vet LJ, Newton ND, Warrilow D, Colmant AMG, Taylor C, Huang B, Piyasena TBH, Chow WK, Setoh YX, Tang B, Nakayama E, Yan K, Amarilla AA, Wheatley S, Moore PR, Finger M, Kurucz N, Modhiran N, Young PR, Khromykh AA, Bielefeldt-Ohmann H, Suhrbier A, Hall RA. 2019. A recombinant platform for flavivirus vaccines and diagnostics using chimeras of a new insect-specific virus. Sci Transl Med 11:aax7888.
249. De Lorenzo G, Tandavanitj R, Doig J, Setthapramote C, Poggianella M, Sanchez-Velazquez R, Scales HE, Edgar JM, Kohl A, Brewer J, Burrone OR, Patel AH. 2020. Zika virus-like particles bearing a covalent dimer of envelope protein protect mice from lethal challenge. J Virol 95:e0141520.
250. Castanha PMS, Marques ETA. 2020. A glimmer of hope: recent updates and future challenges in Zika vaccine development. Viruses 12:1371.
251. Hopkins R, Esposito D. 2009. A rapid method for titrating baculovirus stocks using the Sf-9 Easy Titer cell line. Biotechniques 47:785-788.
252. Rouvinski A, Dejnirattisai W, Guardado-Calvo P, Vaney MC, Sharma A, Duquerroy S, Supasa P, Wongwiwat W, Haouz A, Barba-Spaeth G, Mongkolsapaya J, Rey FA, Screaton GR. 2017. Covalently linked dengue virus envelope glycoprotein dimers reduce exposure of the immunodominant fusion loop epitope. Nat Commun 8:15411.
253. Slon Campos JL, Marchese S, Rana J, Mossenta M, Poggianella M, Bestagno M, Burrone OR. 2017. Temperature-dependent folding allows stable dimerization of secretory and virus-associated E proteins of Dengue and Zika viruses in mammalian cells. Sci Rep 7:966.

254. Slon Campos JL, Dejnirattisai W, Jagger BW, Lopez-Camacho C, Wongwiwat W, Durnell LA, Winkler ES, Chen RE, Reyes-Sandoval A, Rey FA, Diamond MS, Mongkolsapaya J, Screaton GR. 2019. A protective Zika virus E-dimer-based subunit vaccine engineered to abrogate antibody-dependent enhancement of dengue infection. Nat Immunol 20:1291-1298.
255. Thomas A, Thiono DJ, Kudlacek ST, Forsberg J, Premkumar L, Tian S, Kuhlman B, de Silva AM, Metz SW. 2020. Dimerization of dengue virus E subunits impacts antibody function and domain focus. J Virol 94:e0074520.
256. Pijlman GP, Grose C, Hick TAH, Breukink HE, van den Braak R, Abbo SR, Geertsema C, van Oers MM, Martens DE, Esposito D. 2020. Relocation of the attTn7 transgene insertion site in bacmid DNA enhances baculovirus genome stability and recombinant protein expression in insect cells. Viruses 12:1448.
257. Metz SW, Gardner J, Geertsema C, Le TT, Goh L, Vlak JM, Suhrbier A, Pijlman GP. 2013. Effective chikungunya virus-like particle vaccine produced in insect cells. PLoS Negl Trop Dis 7:e2124.
258. Metz SW, Pijlman GP. 2016. Production of chikungunya virus-like particles and subunit vaccines in insect cells. Methods Mol Biol 1426:297-309.
259. Boigard H, Alimova A, Martin GR, Katz A, Gottlieb P, Galarza JM. 2017. Zika virus-like particle (VLP) based vaccine. PLoS Negl Trop Dis 11:e0005608.
260. Prow NA, Liu L, Nakayama E, Cooper TH, Yan K, Eldi P, Hazlewood JE, Tang B, Le TT, Setoh YX, Khromykh AA, Hobson-Peters J, Diener KR, Howley PM, Hayball JD, Suhrbier A. 2018. A vaccinia-based single vector construct multi-pathogen vaccine protects against both Zika and chikungunya viruses. Nat Commun 9:1230.
261. Fros JJ, Visser I, Tang B, Yan K, Nakayama E, Visser TM, Koenraadt CJM, van Oers MM, Pijlman GP, Suhrbier A, Simmonds P. 2021. The dinucleotide composition of the Zika virus genome is shaped by conflicting evolutionary pressures in mammalian hosts and mosquito vectors. PLoS Biol 19:e3001201.
262. Setoh YX, Prow NA, Peng N, Hugo LE, Devine G, Hazlewood JE, Suhrbier A, Khromykh AA. 2017. *De novo* generation and characterization of new Zika virus isolate using sequence data from a microcephaly case. mSphere 2:e0019017.
263. Metz SW, Thomas A, White L, Stoops M, Corten M, Hannemann H, de Silva AM. 2018. Dengue virus-like particles mimic the antigenic properties of the infectious dengue virus envelope. Virol J 15:60.
264. Wang Q, Yan J, Gao GF. 2017. Monoclonal antibodies against Zika virus: therapeutics and their implications for vaccine design. J Virol 91:e0104917.
265. Smith SA, de Alwis AR, Kose N, Jadi RS, de Silva AM, Crowe JE, Jr. 2014. Isolation of dengue virus-specific memory B cells with live virus antigen from human subjects following natural infection reveals the presence of diverse novel functional groups of antibody clones. J Virol 88:12233-12241.
266. Pitcher TJ, Sarathy VV, Matsui K, Gromowski GD, Huang CY, Barrett ADT. 2015. Functional analysis of dengue virus (DENV) type 2 envelope protein domain 3 type-specific and DENV complex-reactive critical epitope residues. J Gen Virol 96:288-293.

267. Rouvinski A, Guardado-Calvo P, Barba-Spaeth G, Duquerroy S, Vaney MC, Kikuti CM, Navarro Sanchez ME, Dejnirattisai W, Wongwiwat W, Haouz A, Girard-Blanc C, Petres S, Shepard WE, Despres P, Arenzana-Seisdedos F, Dussart P, Mongkolsapaya J, Screaton GR, Rey FA. 2015. Recognition determinants of broadly neutralizing human antibodies against dengue viruses. Nature 520:109-113.

268. Stettler K, Beltramello M, Espinosa DA, Graham V, Cassotta A, Bianchi S, Vanzetta F, Minola A, Jaconi S, Mele F, Foglierini M, Pedotti M, Simonelli L, Dowall S, Atkinson B, Percivalle E, Simmons CP, Varani L, Blum J, Baldanti F, Cameroni E, Hewson R, Harris E, Lanzavecchia A, Sallusto F, Corti D. 2016. Specificity, cross-reactivity, and function of antibodies elicited by Zika virus infection. Science 353:823-826.

269. Wang Q, Yang H, Liu X, Dai L, Ma T, Qi J, Wong G, Peng R, Liu S, Li J, Li S, Song J, Liu J, He J, Yuan H, Xiong Y, Liao Y, Li J, Yang J, Tong Z, Griffin BD, Bi Y, Liang M, Xu X, Qin C, Cheng G, Zhang X, Wang P, Qiu X, Kobinger G, Shi Y, Yan J, Gao GF. 2016. Molecular determinants of human neutralizing antibodies isolated from a patient infected with Zika virus. Sci Transl Med 8:369ra179.

270. Kaufmann B, Rossmann MG. 2011. Molecular mechanisms involved in the early steps of flavivirus cell entry. Microbes Infect 13:1-9.

271. Sirohi D, Chen Z, Sun L, Klose T, Pierson TC, Rossmann MG, Kuhn RJ. 2016. The 3.8 A resolution cryo-EM structure of Zika virus. Science 352:467-470.

272. Smith TJ, Brandt WE, Swanson JL, McCown JM, Buescher EL. 1970. Physical and biological properties of dengue-2 virus and associated antigens. J Virol 5:524-532.

273. Mason PW, Pincus S, Fournier MJ, Mason TL, Shope RE, Paoletti E. 1991. Japanese encephalitis virus-vaccinia recombinants produce particulate forms of the structural membrane proteins and induce high levels of protection against lethal JEV infection. Virology 180:294-305.

274. Schalich J, Allison SL, Stiasny K, Mandl CW, Kunz C, Heinz FX. 1996. Recombinant subviral particles from tick-borne encephalitis virus are fusogenic and provide a model system for studying flavivirus envelope glycoprotein functions. J Virol 70:4549-4557.

275. Nakayama E, Kato F, Tajima S, Ogawa S, Yan K, Takahashi K, Sato Y, Suzuki T, Kawai Y, Inagaki T, Taniguchi S, Le TT, Tang B, Prow NA, Uda A, Maeki T, Lim CK, Khromykh AA, Suhrbier A, Saijo M. 2021. Neuroinvasiveness of the MR766 strain of Zika virus in IFNAR$^{-/-}$ mice maps to prM residues conserved amongst African genotype viruses. PLoS Pathog 17:e1009788.

276. Guirakhoo F, Heinz FX, Mandl CW, Holzmann H, Kunz C. 1991. Fusion activity of flaviviruses: comparison of mature and immature (prM-containing) tick-borne encephalitis virions. J Gen Virol 72 (Pt 6):1323-1329.

277. Moesker B, Rodenhuis-Zybert IA, Meijerhof T, Wilschut J, Smit JM. 2010. Characterization of the functional requirements of West Nile virus membrane fusion. J Gen Virol 91:389-393.

278. Rawle RJ, Webster ER, Jelen M, Kasson PM, Boxer SG. 2018. pH dependence of Zika membrane fusion kinetics reveals an off-pathway state. ACS Cent Sci 4:1503-1510.

279. Correia R, Fernandes B, Alves PM, Carrondo MJT, Roldao A. 2020. Improving influenza HA-VLPs production in insect High Five cells via adaptive laboratory evolution. Vaccines 8:589.

280. Summers PL, Cohen WH, Ruiz MM, Hase T, Eckels KH. 1989. Flaviviruses can mediate fusion from without in *Aedes albopictus* mosquito cell cultures. Virus Res 12:383-392.
281. Randolph VB, Stollar V. 1990. Low pH-induced cell fusion in flavivirus-infected *Aedes albopictus* cell cultures. J Gen Virol 71 (Pt 8):1845-1850.
282. Zaitseva E, Yang ST, Melikov K, Pourmal S, Chernomordik LV. 2010. Dengue virus ensures its fusion in late endosomes using compartment-specific lipids. PLoS Pathog 6:e1001131.
283. Dai S, Zhang T, Zhang Y, Wang H, Deng F. 2018. Zika virus baculovirus-expressed virus-like particles induce neutralizing antibodies in mice. Virol Sin 33:213-226.
284. Dejnirattisai W, Wongwiwat W, Supasa S, Zhang X, Dai X, Rouvinski A, Jumnainsong A, Edwards C, Quyen NTH, Duangchinda T, Grimes JM, Tsai WY, Lai CY, Wang WK, Malasit P, Farrar J, Simmons CP, Zhou ZH, Rey FA, Mongkolsapaya J, Screaton GR. 2015. A new class of highly potent, broadly neutralizing antibodies isolated from viremic patients infected with dengue virus. Nat Immunol 16:170-177.
285. Zhang S, Kostyuchenko VA, Ng TS, Lim XN, Ooi JSG, Lambert S, Tan TY, Widman DG, Shi J, Baric RS, Lok SM. 2016. Neutralization mechanism of a highly potent antibody against Zika virus. Nat Commun 7:13679.
286. Vang L, Morello CS, Mendy J, Thompson D, Manayani D, Guenther B, Julander J, Sanford D, Jain A, Patel A, Shabram P, Smith J, Alexander J. 2021. Zika virus-like particle vaccine protects AG129 mice and rhesus macaques against Zika virus. PLoS Negl Trop Dis 15:e0009195.
287. Espinosa D, Mendy J, Manayani D, Vang L, Wang C, Richard T, Guenther B, Aruri J, Avanzini J, Garduno F, Farness P, Gurwith M, Smith J, Harris E, Alexander J. 2018. Passive transfer of immune sera induced by a Zika virus-like particle vaccine protects AG129 mice against lethal Zika virus challenge. EBioMedicine 27:61-70.
288. Tomiya N, Narang S, Lee YC, Betenbaugh MJ. 2004. Comparing N-glycan processing in mammalian cell lines to native and engineered lepidopteran insect cell lines. Glycoconj J 21:343-360.
289. Felberbaum RS. 2015. The baculovirus expression vector system: A commercial manufacturing platform for viral vaccines and gene therapy vectors. Biotechnol J 10:702-714.
290. Weaver SC, Forrester NL. 2015. Chikungunya: Evolutionary history and recent epidemic spread. Antiviral Res 120:32-39.
291. de Thoisy B, Gardon J, Salas RA, Morvan J, Kazanji M. 2003. Mayaro virus in wild mammals, French Guiana. Emerg Infect Dis 9:1326-1329.
292. Calisher CH, Gutierrez E, Maness KS, Lord RD. 1974. Isolation of Mayaro virus from a migrating bird captured in Louisiana in 1967. Bull Pan Am Health Organ 8:243-248.
293. Black FL, Hierholzer WJ, Pinheiro F, Evans AS, Woodall JP, Opton EM, Emmons JE, West BS, Edsall G, Downs WG, Wallace GD. 1974. Evidence for persistence of infectious agents in isolated human populations. Am J Epidemiol 100:230-250.
294. Causey OR, Maroja OM. 1957. Mayaro virus: a new human disease agent. III. Investigation of an epidemic of acute febrile illness on the river Guama in Para, Brazil, and isolation of Mayaro virus as causative agent. Am J Trop Med Hyg 6:1017-1023.
295. Firth AE, Chung BY, Fleeton MN, Atkins JF. 2008. Discovery of frameshifting in Alphavirus 6K resolves a 20-year enigma. Virol J 5:108.

296. Li L, Jose J, Xiang Y, Kuhn RJ, Rossmann MG. 2010. Structural changes of envelope proteins during alphavirus fusion. Nature 468:705-708.
297. Weise WJ, Hermance ME, Forrester N, Adams AP, Langsjoen R, Gorchakov R, Wang E, Alcorn MD, Tsetsarkin K, Weaver SC. 2014. A novel live-attenuated vaccine candidate for Mayaro fever. PLoS Negl Trop Dis 8:e2969.
298. Mota MTO, Costa VV, Sugimoto MA, Guimaraes GF, Queiroz-Junior CM, Moreira TP, de Sousa CD, Santos FM, Queiroz VF, Passos I, Hubner J, Souza DG, Weaver SC, Teixeira MM, Nogueira ML. 2020. In-depth characterization of a novel live-attenuated Mayaro virus vaccine candidate using an immunocompetent mouse model of Mayaro disease. Sci Rep 10:5306.
299. Choi H, Kudchodkar SB, Reuschel EL, Asija K, Borole P, Ho M, Wojtak K, Reed C, Ramos S, Bopp NE, Aguilar PV, Weaver SC, Kim JJ, Humeau L, Tebas P, Weiner DB, Muthumani K. 2019. Protective immunity by an engineered DNA vaccine for Mayaro virus. PLoS Negl Trop Dis 13:e0007042.
300. Campos RK, Preciado-Llanes L, Azar SR, Kim YC, Brandon O, Lopez-Camacho C, Reyes-Sandoval A, Rossi SL. 2020. Adenoviral-vectored Mayaro and chikungunya virus vaccine candidates afford partial cross-protection from lethal challenge in A129 mouse model. Front Immunol 11:591885.
301. Powers JM, Haese NN, Denton M, Ando T, Kreklywich C, Bonin K, Streblow CE, Kreklywich N, Smith P, Broeckel R, DeFilippis V, Morrison TE, Heise MT, Streblow DN. 2021. Non-replicating adenovirus based Mayaro virus vaccine elicits protective immune responses and cross protects against other alphaviruses. PLoS Negl Trop Dis 15:e0009308.
302. Hanley KA. 2011. The double-edged sword: How evolution can make or break a live-attenuated virus vaccine. Evolution (N Y) 4:635-643.
303. Ahi YS, Bangari DS, Mittal SK. 2011. Adenoviral vector immunity: its implications and circumvention strategies. Curr Gene Ther 11:307-320.
304. Hobernik D, Bros M. 2018. DNA vaccines - how far from clinical use? Int J Mol Sci 19:3605.
305. Grgacic EV, Anderson DA. 2006. Virus-like particles: passport to immune recognition. Methods 40:60-65.
306. Gardner J, Anraku I, Le TT, Larcher T, Major L, Roques P, Schroder WA, Higgs S, Suhrbier A. 2010. Chikungunya virus arthritis in adult wild-type mice. J Virol 84:8021-8032.
307. Nguyen W, Nakayama E, Yan K, Tang B, Le TT, Liu L, Cooper TH, Hayball JD, Faddy HM, Warrilow D, Allcock RJN, Hobson-Peters J, Hall RA, Rawle DJ, Lutzky VP, Young P, Oliveira NM, Hartel G, Howley PM, Prow NA, Suhrbier A. 2020. Arthritogenic alphavirus vaccines: serogrouping versus cross-protection in mouse models. Vaccines 8:209.
308. Goh LYH, Hobson-Peters J, Prow NA, Gardner J, Bielefeldt-Ohmann H, Suhrbier A, Hall RA. 2015. Monoclonal antibodies specific for the capsid protein of chikungunya virus suitable for multiple applications. J Gen Virol 96:507-512.
309. Poo YS, Rudd PA, Gardner J, Wilson JA, Larcher T, Colle MA, Le TT, Nakaya HI, Warrilow D, Allcock R, Bielefeldt-Ohmann H, Schroder WA, Khromykh AA, Lopez JA, Suhrbier A. 2014. Multiple immune factors are involved in controlling acute and chronic chikungunya virus infection. PLoS Negl Trop Dis 8:e3354.

310. Rudd PA, Wilson J, Gardner J, Larcher T, Babarit C, Le TT, Anraku I, Kumagai Y, Loo YM, Gale M, Jr., Akira S, Khromykh AA, Suhrbier A. 2012. Interferon response factors 3 and 7 protect against chikungunya virus hemorrhagic fever and shock. J Virol 86:9888-9898.
311. Wilson JA, Prow NA, Schroder WA, Ellis JJ, Cumming HE, Gearing LJ, Poo YS, Taylor A, Hertzog PJ, Di Giallonardo F, Hueston L, Le Grand R, Tang B, Le TT, Gardner J, Mahalingam S, Roques P, Bird PI, Suhrbier A. 2017. RNA-Seq analysis of chikungunya virus infection and identification of granzyme A as a major promoter of arthritic inflammation. PLoS Pathog 13:e1006155.
312. Yan K, Vet LJ, Tang B, Hobson-Peters J, Rawle DJ, Le TT, Larcher T, Hall RA, Suhrbier A. 2020. A yellow fever virus 17D infection and disease mouse model used to evaluate a chimeric Binjari-yellow fever virus vaccine. Vaccines 8:368.
313. Wang D, Suhrbier A, Penn-Nicholson A, Woraratanadharm J, Gardner J, Luo M, Le TT, Anraku I, Sakalian M, Einfeld D, Dong JY. 2011. A complex adenovirus vaccine against chikungunya virus provides complete protection against viraemia and arthritis. Vaccine 29:2803-2809.
314. Rawle DJ, Nguyen W, Dumenil T, Parry R, Warrilow D, Tang B, Le TT, Slonchak A, Khromykh AA, Lutzky VP, Yan K, Suhrbier A. 2020. Sequencing of historical isolates, k-mer mining and high serological cross-reactivity with Ross River virus argue against the presence of Getah virus in Australia. Pathogens 9:848.
315. Hikke MC, Geertsema C, Wu V, Metz SW, van Lent JW, Vlak JM, Pijlman GP. 2016. Alphavirus capsid proteins self-assemble into core-like particles in insect cells: A promising platform for nanoparticle vaccine development. Biotechnol J 11:266-273.
316. Rulli NE, Guglielmotti A, Mangano G, Rolph MS, Apicella C, Zaid A, Suhrbier A, Mahalingam S. 2009. Amelioration of alphavirus-induced arthritis and myositis in a mouse model by treatment with bindarit, an inhibitor of monocyte chemotactic proteins. Arthritis Rheum 60:2513-2523.
317. Wagner JM, Pajerowski JD, Daniels CL, McHugh PM, Flynn JA, Balliet JW, Casimiro DR, Subramanian S. 2014. Enhanced production of chikungunya virus-like particles using a high-pH adapted S*podoptera frugiperda* insect cell line. PLoS One 9:e94401.
318. Marek M, van Oers MM, Devaraj FF, Vlak JM, Merten OW. 2011. Engineering of baculovirus vectors for the manufacture of virion-free biopharmaceuticals. Biotechnol Bioeng 108:1056-1067.
319. de Castro-Jorge LA, de Carvalho RVH, Klein TM, Hiroki CH, Lopes AH, Guimaraes RM, Fumagalli MJ, Floriano VG, Agostinho MR, Slhessarenko RD, Ramalho FS, Cunha TM, Cunha FQ, da Fonseca BAL, Zamboni DS. 2019. The NLRP3 inflammasome is involved with the pathogenesis of Mayaro virus. PLoS Pathog 15:e1007934.
320. Akahata W, Yang ZY, Andersen H, Sun S, Holdaway HA, Kong WP, Lewis MG, Higgs S, Rossmann MG, Rao S, Nabel GJ. 2010. A virus-like particle vaccine for epidemic Chikungunya virus protects nonhuman primates against infection. Nat Med 16:334-338.
321. Aichinger G, Ehrlich HJ, Aaskov JG, Fritsch S, Thomasser C, Draxler W, Wolzt M, Muller M, Pinl F, Van Damme P, Hens A, Levy J, Portsmouth D, Holzer G, Kistner O, Kreil TR, Barrett PN. 2011. Safety and immunogenicity of an inactivated whole virus Vero cell-derived Ross River virus vaccine: a randomized trial. Vaccine 29:9376-9384.

322. Gavrilov BK, Rogers K, Fernandez-Sainz IJ, Holinka LG, Borca MV, Risatti GR. 2011. Effects of glycosylation on antigenicity and immunogenicity of classical swine fever virus envelope proteins. Virology 420:135-145.
323. Fournillier A, Wychowski C, Boucreux D, Baumert TF, Meunier JC, Jacobs D, Muguet S, Depla E, Inchauspe G. 2001. Induction of hepatitis C virus E1 envelope protein-specific immune response can be enhanced by mutation of N-glycosylation sites. J Virol 75:12088-12097.
324. Lancaster C, Pristatsky P, Hoang VM, Casimiro DR, Schwartz RM, Rustandi R, Ha S. 2016. Characterization of N-glycosylation profiles from mammalian and insect cell derived chikungunya VLP. J Chromatogr B Analyt Technol Biomed Life Sci 1032:218-223.
325. Vicente T, Roldao A, Peixoto C, Carrondo MJ, Alves PM. 2011. Large-scale production and purification of VLP-based vaccines. J Invertebr Pathol 107 Suppl:S42-48.
326. Cox MM, Izikson R, Post P, Dunkle L. 2015. Safety, efficacy, and immunogenicity of Flublok in the prevention of seasonal influenza in adults. Ther Adv Vaccines 3:97-108.
327. Herrero R, Gonzalez P, Markowitz LE. 2015. Present status of human papillomavirus vaccine development and implementation. Lancet Oncol 16:e206-216.
328. Novavax. 2020. Novavax initiates phase 3 efficacy trial of COVID-19 vaccine in the United Kingdom. https://www.novavax.com/covid-19-coronavirus-vaccine-candidate-updates. Accessed 8 April 2021.
329. Ramsauer K, Schwameis M, Firbas C, Mullner M, Putnak RJ, Thomas SJ, Despres P, Tauber E, Jilma B, Tangy F. 2015. Immunogenicity, safety, and tolerability of a recombinant measles-virus-based chikungunya vaccine: a randomised, double-blind, placebo-controlled, active-comparator, first-in-man trial. Lancet Infect Dis 15:519-527.
330. Wressnigg N, Hochreiter R, Zoihsl O, Fritzer A, Bezay N, Klingler A, Lingnau K, Schneider M, Lundberg U, Meinke A, Larcher-Senn J, Corbic-Ramljak I, Eder-Lingelbach S, Dubischar K, Bender W. 2020. Single-shot live-attenuated chikungunya vaccine in healthy adults: a phase 1, randomised controlled trial. Lancet Infect Dis 20:1193-1203.
331. Suhrbier A. 2019. Rheumatic manifestations of chikungunya: emerging concepts and interventions. Nat Rev Rheumatol 15:597-611.
332. Valneva. 2020. Valneva initiates phase 3 clinical study for its chikungunya vaccine candidate VLA1553. https://valneva.com/press-release/valneva-initiates-phase-3-clinical-study-for-its-chikungunya-vaccine-candidate-vla1553/. Accessed 14 April 2021.
333. Martins KA, Gregory MK, Valdez SM, Sprague TR, Encinales L, Pacheco N, Cure C, Porras-Ramirez A, Rico-Mendoza A, Chang A, Pitt ML, Nasar F. 2019. Neutralizing antibodies from convalescent chikungunya virus patients can cross-neutralize Mayaro and Una viruses. Am J Trop Med Hyg 100:1541-1544.
334. Webb EM, Azar SR, Haller SL, Langsjoen RM, Cuthbert CE, Ramjag AT, Luo H, Plante K, Wang T, Simmons G, Carrington CVF, Weaver SC, Rossi SL, Auguste AJ. 2019. Effects of chikungunya virus immunity on Mayaro virus disease and epidemic potential. Sci Rep 9:20399.

335. Campos RK, Preciado-Llanes L, Azar SR, Lopez-Camacho C, Reyes-Sandoval A, Rossi SL. 2019. A single and un-adjuvanted dose of a chimpanzee adenovirus-vectored vaccine against chikungunya virus fully protects mice from lethal disease. Pathogens 8:231.
336. Aguilar-Luis MA, Del Valle-Mendoza J, Silva-Caso W, Gil-Ramirez T, Levy-Blitchtein S, Bazan-Mayra J, Zavaleta-Gavidia V, Cornejo-Pacherres D, Palomares-Reyes C, Del Valle LJ. 2020. An emerging public health threat: Mayaro virus increases its distribution in Peru. Int J Infect Dis 92:253-258.
337. ECDC. 2019. Rapid risk assessment: Zika virus transmission worldwide. https://www.ecdc.europa.eu/sites/default/files/documents/zika-risk-assessment-9-april-2019.pdf. Accessed 28 December 2021.
338. WHO. 2021. Zika virus disease – India. https://www.who.int/emergencies/disease-outbreak-news/item/zika-virus-disease-india. Accessed 28 December 2021.
339. Boyer S, Calvez E, Chouin-Carneiro T, Diallo D, Failloux AB. 2018. An overview of mosquito vectors of Zika virus. Microbes Infect 20:646-660.
340. Medlock JM, Hansford KM, Schaffner F, Versteirt V, Hendrickx G, Zeller H, Van Bortel W. 2012. A review of the invasive mosquitoes in Europe: ecology, public health risks, and control options. Vector Borne Zoonotic Dis 12:435-447.
341. ECDC. 2021. *Aedes albopictus* - current known distribution: October 2021. https://www.ecdc.europa.eu/en/publications-data/aedes-albopictus-current-known-distribution-october-2021. Accessed 21 December 2021.
342. Hofhuis A, Reimerink J, Reusken C, Scholte EJ, Boer A, Takken W, Koopmans M. 2009. The hidden passenger of lucky bamboo: do imported *Aedes albopictus* mosquitoes cause dengue virus transmission in the Netherlands? Vector Borne Zoonotic Dis 9:217-220.
343. Scholte EJ, Den Hartog W, Dik M, Schoelitsz B, Brooks M, Schaffner F, Foussadier R, Braks M, Beeuwkes J. 2010. Introduction and control of three invasive mosquito species in the Netherlands, July-October 2010. Euro Surveill 15:19710.
344. RIVM. 2021. Exotische steekmuggen: beleid bij invasieve exotische steekmuggen in Nederland. https://lci.rivm.nl/richtlijnen/exotische-steekmuggen. Accessed 21 December 2021.
345. Stroo A, Ibanez-Justicia A, Braks M. 2018. Towards a policy decision on *Aedes japonicus:* risk assessment of *Aedes japonicus* in the Netherlands. https://www.rivm.nl/publicaties/towards-a-policy-decision-on-aedes-japonicus-risk-assessment-of-aedes-japonicus-in. Accessed 21 December 2021.
346. Koban MB, Kampen H, Scheuch DE, Frueh L, Kuhlisch C, Janssen N, Steidle JLM, Schaub GA, Werner D. 2019. The Asian bush mosquito *Aedes japonicus japonicus* (Diptera: Culicidae) in Europe, 17 years after its first detection, with a focus on monitoring methods. Parasit Vectors 12:109.
347. Miller BR, Monath TP, Tabachnick WJ, Ezike VI. 1989. Epidemic yellow fever caused by an incompetent mosquito vector. Trop Med Parasitol 40:396-399.
348. Fernandes RS, David MR, De Abreu FVS, Ferreira-de-Brito A, Gardinali NR, Lima SMB, Andrade MCR, Kugelmeier T, Oliveira JM, Pinto MA, Lourenco-de-Oliveira R. 2020. Low *Aedes aegypti* vector competence for Zika virus from viremic rhesus macaques. Viruses 12:1345.

349. Chaudhary S, Jain J, Kumar R, Shrinet J, Weaver SC, Auguste AJ, Sunil S. 2021. Chikungunya virus molecular evolution in India since its re-emergence in 2005. Virus Evol 7:veab074.
350. Rodriguez-Barraquer I, Cordeiro MT, Braga C, de Souza WV, Marques ET, Cummings DA. 2011. From re-emergence to hyperendemicity: the natural history of the dengue epidemic in Brazil. PLoS Negl Trop Dis 5:e935.
351. Rezza G, Nicoletti L, Angelini R, Romi R, Finarelli AC, Panning M, Cordioli P, Fortuna C, Boros S, Magurano F, Silvi G, Angelini P, Dottori M, Ciufolini MG, Majori GC, Cassone A, group Cs. 2007. Infection with chikungunya virus in Italy: an outbreak in a temperate region. Lancet 370:1840-1846.
352. Amraoui F, Failloux AB. 2016. Chikungunya: an unexpected emergence in Europe. Curr Opin Virol 21:146-150.
353. Lourenco J, Recker M. 2014. The 2012 Madeira dengue outbreak: epidemiological determinants and future epidemic potential. PLoS Negl Trop Dis 8:e3083.
354. AMSinstitute. 2020. 100 years of Dutch summers: The clock is ticking on climate change. https://www.ams-institute.org/news/100-years-of-dutch-summers-the-clock-is-ticking-on-climate-change/. Accessed 23 December 2021.
355. Brault AC, Powers AM, Ortiz D, Estrada-Franco JG, Navarro-Lopez R, Weaver SC. 2004. Venezuelan equine encephalitis emergence: enhanced vector infection from a single amino acid substitution in the envelope glycoprotein. Proc Natl Acad Sci U S A 101:11344-11349.
356. Bruins B. 2018. Kamerbrief over stopzetten bestrijding *Aedes japonicus* in Flevoland. https://www.rijksoverheid.nl/documenten/kamerstukken/2018/07/10/kamerbrief-over-advies-stopzetten-bestrijding-aedes-japonicus-in-flevoland. Accessed 23 December 2021.
357. Sikkema RS, Schrama M, van den Berg T, Morren J, Munger E, Krol L, van der Beek JG, Blom R, Chestakova I, van der Linden A, Boter M, van Mastrigt T, Molenkamp R, Koenraadt CJ, van den Brand JM, Oude Munnink BB, Koopmans MP, van der Jeugd H. 2020. Detection of West Nile virus in a common whitethroat (*Curruca communis*) and *Culex* mosquitoes in the Netherlands, 2020. Euro Surveill 25:2001704.
358. ErasmusMC. 2020. OHPACT: First West Nile virus patient in the Netherlands. https://www.erasmusmc.nl/en/research/departments/viroscience/articles/first-west-nile-virus-patient-in-the-netherlands. Accessed 23 December 2021.
359. Vlaskamp DR, Thijsen SF, Reimerink J, Hilkens P, Bouvy WH, Bantjes SE, Vlaminckx BJ, Zaaijer H, van den Kerkhof HH, Raven SF, Reusken CB. 2020. First autochthonous human West Nile virus infections in the Netherlands, July to August 2020. Euro Surveill 25:2001904.
360. Rijksoverheid. 2021. Ontwikkeling Lelystad Airport. https://www.rijksoverheid.nl/onderwerpen/luchtvaart/ontwikkeling-lelystad-airport. Accessed 23 December 2021.
361. Xi Z, Ramirez JL, Dimopoulos G. 2008. The *Aedes aegypti* Toll pathway controls dengue virus infection. PLoS Pathog 4:e1000098.
362. Dong Y, Morton JC, Jr., Ramirez JL, Souza-Neto JA, Dimopoulos G. 2012. The entomopathogenic fungus *Beauveria bassiana* activate toll and JAK-STAT pathway-controlled effector genes and anti-dengue activity in *Aedes aegypti*. Insect Biochem Mol Biol 42:126-132.

363. Hegde S, Rasgon JL, Hughes GL. 2015. The microbiome modulates arbovirus transmission in mosquitoes. Curr Opin Virol 15:97-102.
364. Cirimotich CM, Ramirez JL, Dimopoulos G. 2011. Native microbiota shape insect vector competence for human pathogens. Cell Host Microbe 10:307-310.
365. O'Donnell KL, Bixby MA, Morin KJ, Bradley DS, Vaughan JA. 2017. Potential of a northern population of *Aedes vexans* (Diptera: Culicidae) to transmit Zika virus. J Med Entomol 54:1354-1359.
366. Ibanez-Justicia A, Stroo A, Dik M, Beeuwkes J, Scholte EJ. 2015. National mosquito (Diptera: Culicidae) survey in the Netherlands 2010-2013. J Med Entomol 52:185-198.
367. ECDC. 2021. *Aedes koreicus* - current known distribution: October 2021. https://www.ecdc.europa.eu/en/publications-data/aedes-koreicus-current-known-distribution-october-2021. Accessed 21 December 2021.
368. NVWA. 2021. Larven van Koreaanse bosmug gevonden bij Montfoort. https://www.nvwa.nl/nieuws-en-media/nieuws/2021/10/07/nvwa-larven-van-koreaanse-bosmug-gevonden-bij-montfoort. Accessed 21 December 2021.
369. Jansen S, Cadar D, Lühken R, Pfitzner WP, Jöst H, Oerther S, Helms M, Zibrat B, Kliemke K, Becker N, Vapalahti O, Rossini G, Heitmann A. 2021. Vector competence of the invasive mosquito species *Aedes koreicus* for arboviruses and interference with a novel insect specific virus. Viruses 13:2507.
370. Scholte EJ, Den Hartog W, Braks M, Reusken C, Dik M, Hessels A. 2009. First report of a North American invasive mosquito species *Ochlerotatus atropalpus* (Coquillett) in the Netherlands, 2009. Euro Surveill 14:19400.
371. ECDC. 2021. *Aedes atropalpus* - current known distribution: October 2021. https://www.ecdc.europa.eu/en/publications-data/aedes-atropalpus-current-known-distribution-october-2021. Accessed 21 December 2021.
372. Cle M, Barthelemy J, Desmetz C, Foulongne V, Lapeyre L, Bollore K, Tuaillon E, Erkilic N, Kalatzis V, Lecollinet S, Beck C, Pirot N, Glasson Y, Gosselet F, Alvarez Martinez MT, Van de Perre P, Salinas S, Simonin Y. 2020. Study of Usutu virus neuropathogenicity in mice and human cellular models. PLoS Negl Trop Dis 14:e0008223.
373. Kuchinsky SC, Hawks SA, Mossel EC, Coutermarsh-Ott S, Duggal NK. 2020. Differential pathogenesis of Usutu virus isolates in mice. PLoS Negl Trop Dis 14:e0008765.
374. Vogels CB, van de Peppel LJ, van Vliet AJ, Westenberg M, Ibanez-Justicia A, Stroo A, Buijs JA, Visser TM, Koenraadt CJ. 2015. Winter activity and aboveground hybridization between the two biotypes of the West Nile virus vector *Culex pipiens*. Vector Borne Zoonotic Dis 15:619-626.
375. Kramer LD, Li J, Shi PY. 2007. West Nile virus. Lancet Neurol 6:171-181.
376. Santos PD, Michel F, Wylezich C, Hoper D, Keller M, Holicki CM, Szentiks CA, Eiden M, Muluneh A, Neubauer-Juric A, Thalheim S, Globig A, Beer M, Groschup MH, Ziegler U. 2021. Co-infections: Simultaneous detections of West Nile virus and Usutu virus in birds from Germany. Transbound Emerg Dis 00:1– 17.
377. Cabanova V, Sikutova S, Strakova P, Sebesta O, Vichova B, Zubrikova D, Miterpakova M, Mendel J, Hurnikova Z, Hubalek Z, Rudolf I. 2019. Co-circulation of West Nile and Usutu flaviviruses in mosquitoes in Slovakia, 2018. Viruses 11:639.
378. Rathore APS, St John AL. 2020. Cross-reactive immunity among flaviviruses. Front Immunol 11:334.

379. Wang H, Abbo SR, Visser TM, Westenberg M, Geertsema C, Fros JJ, Koenraadt CJM, Pijlman GP. 2020. Competition between Usutu virus and West Nile virus during simultaneous and sequential infection of *Culex pipiens* mosquitoes. Emerg Microbes Infect 9:2642-2652.
380. Blazquez AB, Escribano-Romero E, Martin-Acebes MA, Petrovic T, Saiz JC. 2015. Limited susceptibility of mice to Usutu virus (USUV) infection and induction of flavivirus cross-protective immunity. Virology 482:67-71.
381. Merino-Ramos T, Blazquez AB, Escribano-Romero E, Canas-Arranz R, Sobrino F, Saiz JC, Martin-Acebes MA. 2014. Protection of a single dose West Nile virus recombinant subviral particle vaccine against lineage 1 or 2 strains and analysis of the cross-reactivity with Usutu virus. PLoS One 9:e108056.
382. Domingo E. 2010. Mechanisms of viral emergence. Vet Res 41:38.
383. Domingo E, Perales C. 2019. Viral quasispecies. PLoS Genet 15:e1008271.
384. Anishchenko M, Bowen RA, Paessler S, Austgen L, Greene IP, Weaver SC. 2006. Venezuelan encephalitis emergence mediated by a phylogenetically predicted viral mutation. Proc Natl Acad Sci U S A 103:4994-4999.
385. Brault AC, Huang CY, Langevin SA, Kinney RM, Bowen RA, Ramey WN, Panella NA, Holmes EC, Powers AM, Miller BR. 2007. A single positively selected West Nile viral mutation confers increased virogenesis in American crows. Nat Genet 39:1162-1166.
386. Schuffenecker I, Iteman I, Michault A, Murri S, Frangeul L, Vaney MC, Lavenir R, Pardigon N, Reynes JM, Pettinelli F, Biscornet L, Diancourt L, Michel S, Duquerroy S, Guigon G, Frenkiel MP, Brehin AC, Cubito N, Despres P, Kunst F, Rey FA, Zeller H, Brisse S. 2006. Genome microevolution of chikungunya viruses causing the Indian Ocean outbreak. PLoS Med 3:e263.
387. Vazeille M, Moutailler S, Coudrier D, Rousseaux C, Khun H, Huerre M, Thiria J, Dehecq JS, Fontenille D, Schuffenecker I, Despres P, Failloux AB. 2007. Two chikungunya isolates from the outbreak of La Reunion (Indian Ocean) exhibit different patterns of infection in the mosquito, *Aedes albopictus*. PLoS One 2:e1168.
388. Houk EJ, Kramer LD, Hardy JL, Presser SB. 1986. An interspecific mosquito model for the mesenteronal infection barrier to western equine encephalomyelitis virus (*Culex tarsalis* and *Culex pipiens*). Am J Trop Med Hyg 35:632-641.
389. Houk EJ, Arcus YM, Hardy JL, Kramer LD. 1990. Binding of western equine encephalomyelitis virus to brush border fragments isolated from mesenteronal epithelial cells of mosquitoes. Virus Res 17:105-117.
390. Saxton-Shaw KD, Ledermann JP, Borland EM, Stovall JL, Mossel EC, Singh AJ, Wilusz J, Powers AM. 2013. O'nyong nyong virus molecular determinants of unique vector specificity reside in non-structural protein 3. PLoS Negl Trop Dis 7:e1931.
391. Amraoui F, Pain A, Piorkowski G, Vazeille M, Couto-Lima D, de Lamballerie X, Lourenco-de-Oliveira R, Failloux AB. 2018. Experimental adaptation of the yellow fever virus to the mosquito *Aedes albopictus* and potential risk of urban epidemics in Brazil, South America. Sci Rep 8:14337.
392. Tsetsarkin KA, Chen R, Leal G, Forrester N, Higgs S, Huang J, Weaver SC. 2011. Chikungunya virus emergence is constrained in Asia by lineage-specific adaptive landscapes. Proc Natl Acad Sci U S A 108:7872-7877.

393. Syenina A, Vijaykrishna D, Gan ES, Tan HC, Choy MM, Siriphanitchakorn T, Cheng C, Vasudevan SG, Ooi EE. 2020. Positive epistasis between viral polymerase and the 3' untranslated region of its genome reveals the epidemiologic fitness of dengue virus. Proc Natl Acad Sci U S A 117:11038-11047.
394. Bellone R, Lequime S, Jupille H, Goertz GP, Aubry F, Mousson L, Piorkowski G, Yen PS, Gabiane G, Vazeille M, Sakuntabhai A, Pijlman GP, de Lamballerie X, Lambrechts L, Failloux AB. 2020. Experimental adaptation of dengue virus 1 to *Aedes albopictus* mosquitoes by *in vivo* selection. Sci Rep 10:18404.
395. Weger-Lucarelli J, Garcia SM, Ruckert C, Byas A, O'Connor SL, Aliota MT, Friedrich TC, O'Connor DH, Ebel GD. 2018. Using barcoded Zika virus to assess virus population structure *in vitro* and in *Aedes aegypti* mosquitoes. Virology 521:138-148.
396. Setoh YX, Amarilla AA, Peng NYG, Griffiths RE, Carrera J, Freney ME, Nakayama E, Ogawa S, Watterson D, Modhiran N, Nanyonga FE, Torres FJ, Slonchak A, Periasamy P, Prow NA, Tang B, Harrison J, Hobson-Peters J, Cuddihy T, Cooper-White J, Hall RA, Young PR, Mackenzie JM, Wolvetang E, Bloom JD, Suhrbier A, Khromykh AA. 2019. Determinants of Zika virus host tropism uncovered by deep mutational scanning. Nat Microbiol 4:876-887.
397. Coffey LL, Vasilakis N, Brault AC, Powers AM, Tripet F, Weaver SC. 2008. Arbovirus evolution *in vivo* is constrained by host alternation. Proc Natl Acad Sci U S A 105:6970-6975.
398. Rozen-Gagnon K, Yi S, Jacobson E, Novack S, Rice CM. 2021. A selectable, plasmid-based system to generate CRISPR/Cas9 gene edited and knock-in mosquito cell lines. Sci Rep 11:736.
399. McFarlane M, Laureti M, Levee T, Terry S, Kohl A, Pondeville E. 2021. Improved transient silencing of gene expression in the mosquito female *Aedes aegypti*. Insect Mol Biol 30:355-365.
400. Peng C, Qian Z, Xinyu Z, Qianqian L, Maoqing G, Zhong Z, Ruiling Z. 2021. A draft genome assembly of *Culex pipiens pallens* (Diptera: Culicidae) using PacBio sequencing. Genome Biol Evol 13: evab005.
401. MacLeod HJ, Dimopoulos G. 2020. Detailed analyses of Zika virus tropism in *Culex quinquefasciatus* reveal systemic refractoriness. mBio 11:e0176520.
402. Zhang X, Xie X, Xia H, Zou J, Huang L, Popov VL, Chen X, Shi PY. 2019. Zika virus NS2A-mediated virion assembly. mBio 10:e0237519.
403. Goertz GP, van Bree JWM, Hiralal A, Fernhout BM, Steffens C, Boeren S, Visser TM, Vogels CBF, Abbo SR, Fros JJ, Koenraadt CJM, van Oers MM, Pijlman GP. 2019. Subgenomic flavivirus RNA binds the mosquito DEAD/H-box helicase ME31B and determines Zika virus transmission by *Aedes aegypti*. Proc Natl Acad Sci U S A 116:19136-19144.
404. Slonchak A, Hugo LE, Freney ME, Hall-Mendelin S, Amarilla AA, Torres FJ, Setoh YX, Peng NYG, Sng JDJ, Hall RA, van den Hurk AF, Devine GJ, Khromykh AA. 2020. Zika virus noncoding RNA suppresses apoptosis and is required for virus transmission by mosquitoes. Nat Commun 11:2205.
405. Mukherjee S, Sirohi D, Dowd KA, Chen Z, Diamond MS, Kuhn RJ, Pierson TC. 2016. Enhancing dengue virus maturation using a stable furin over-expressing cell line. Virology 497:33-40.

406. Murray JM, Aaskov JG, Wright PJ. 1993. Processing of the dengue virus type 2 proteins prM and C-prM. J Gen Virol 74 (Pt 2):175-182.
407. Pierson TC, Diamond MS. 2012. Degrees of maturity: the complex structure and biology of flaviviruses. Curr Opin Virol 2:168-175.
408. Kuhn RJ, Dowd KA, Beth Post C, Pierson TC. 2015. Shake, rattle, and roll: Impact of the dynamics of flavivirus particles on their interactions with the host. Virology 479-480:508-517.
409. Dowd KA, DeMaso CR, Pierson TC. 2015. Genotypic differences in dengue virus neutralization are explained by a single amino acid mutation that modulates virus breathing. mBio 6:e01559-01515.
410. Rey FA, Stiasny K, Vaney MC, Dellarole M, Heinz FX. 2018. The bright and the dark side of human antibody responses to flaviviruses: lessons for vaccine design. EMBO Rep 19:206-224.
411. Maciejewski S, Ruckwardt TJ, Morabito KM, Foreman BM, Burgomaster KE, Gordon DN, Pelc RS, DeMaso CR, Ko SY, Fisher BE, Yang ES, Nair D, Foulds KE, Todd JP, Kong WP, Roy V, Aleshnick M, Speer SD, Bourne N, Barrett AD, Nason MC, Roederer M, Gaudinski MR, Chen GL, Dowd KA, Ledgerwood JE, Alter G, Mascola JR, Graham BS, Pierson TC. 2020. Distinct neutralizing antibody correlates of protection among related Zika virus vaccines identify a role for antibody quality. Sci Transl Med 12:eaaw9066.
412. Raut R, Corbett KS, Tennekoon RN, Premawansa S, Wijewickrama A, Premawansa G, Mieczkowski P, Ruckert C, Ebel GD, De Silva AD, de Silva AM. 2019. Dengue type 1 viruses circulating in humans are highly infectious and poorly neutralized by human antibodies. Proc Natl Acad Sci U S A 116:227-232.
413. Diamond MS, Ledgerwood JE, Pierson TC. 2019. Zika virus vaccine development: progress in the face of new challenges. Annu Rev Med 70:121-135.
414. Katzelnick LC, Narvaez C, Arguello S, Lopez Mercado B, Collado D, Ampie O, Elizondo D, Miranda T, Bustos Carillo F, Mercado JC, Latta K, Schiller A, Segovia-Chumbez B, Ojeda S, Sanchez N, Plazaola M, Coloma J, Halloran ME, Premkumar L, Gordon A, Narvaez F, de Silva AM, Kuan G, Balmaseda A, Harris E. 2020. Zika virus infection enhances future risk of severe dengue disease. Science 369:1123-1128.
415. Sangkawibha N, Rojanasuphot S, Ahandrik S, Viriyapongse S, Jatanasen S, Salitul V, Phanthumachinda B, Halstead SB. 1984. Risk factors in dengue shock syndrome: a prospective epidemiologic study in Rayong, Thailand. I. The 1980 outbreak. Am J Epidemiol 120:653-669.
416. Nisalak A, Clapham HE, Kalayanarooj S, Klungthong C, Thaisomboonsuk B, Fernandez S, Reiser J, Srikiatkhachorn A, Macareo LR, Lessler JT, Cummings DA, Yoon IK. 2016. Forty years of dengue surveillance at a tertiary pediatric hospital in Bangkok, Thailand, 1973-2012. Am J Trop Med Hyg 94:1342-1347.
417. Han HH, Diaz C, Acosta CJ, Liu M, Borkowski A. 2021. Safety and immunogenicity of a purified inactivated Zika virus vaccine candidate in healthy adults: an observer-blind, randomised, phase 1 trial. Lancet Infect Dis 21:1282-1292.
418. Castanha PMS, Marques ETA. 2021. Zika vaccines: can we solve one problem without creating another one? Lancet Infect Dis 21:1198-1200.
419. Macias A, Ruiz-Palacios G, Ramos-Castaneda J. 2020. Combine dengue vaccines to optimize effectiveness. Vaccine 38:4801-4804.

420. Wilder-Smith A. 2020. Dengue vaccine development by the year 2020: challenges and prospects. Curr Opin Virol 43:71-78.
421. Zambrano B, Noriega F, Dayan GH, Rivera DM, Arredondo JL, Reynales H, Luz K, Deseda C, Bonaparte MI, Langevin E, Wu Y, Cortes M, Savarino S, DiazGranados CA. 2021. Zika and dengue interactions in the context of a large dengue vaccine clinical trial in Latin America. Am J Trop Med Hyg 104:136-144.
422. Larocca RA, Abbink P, Ventura JD, Chandrashekar A, Mercado N, Li Z, Borducchi E, De La Barrera RA, Eckels KH, Modjarrad K, Busch MP, Michael NL, Barouch DH. 2021. Impact of prior dengue immunity on Zika vaccine protection in rhesus macaques and mice. PLoS Pathog 17:e1009673.
423. Dai L, Xu K, Li J, Huang Q, Song J, Han Y, Zheng T, Gao P, Lu X, Yang H, Liu K, Xia Q, Wang Q, Chai Y, Qi J, Yan J, Gao GF. 2021. Protective Zika vaccines engineered to eliminate enhancement of dengue infection via immunodominance switch. Nat Immunol 22:958-968.
424. Shiff C. 2002. Integrated approach to malaria control. Clin Microbiol Rev 15:278-293.
425. Koenraadt CJM, Takken W. 2018. Integrated approach to malaria control. Science 359:528-529.
426. Vasilakis N, Tesh RB. 2015. Insect-specific viruses and their potential impact on arbovirus transmission. Curr Opin Virol 15:69-74.
427. Choo JJY, Vet LJ, McMillan CLD, Harrison JJ, Scott CAP, Depelsenaire ACI, Fernando GJP, Watterson D, Hall RA, Young PR, Hobson-Peters J, Muller DA. 2021. A chimeric dengue virus vaccine candidate delivered by high density microarray patches protects against infection in mice. NPJ Vaccines 6:66.
428. Hazlewood JE, Rawle DJ, Tang B, Yan K, Vet LJ, Nakayama E, Hobson-Peters J, Hall RA, Suhrbier A. 2020. A Zika vaccine generated using the chimeric insect-specific Binjari virus platform protects against fetal brain infection in pregnant mice. Vaccines 8:496.
429. Williams AE, Sanchez-Vargas I, Reid WR, Lin J, Franz AWE, Olson KE. 2020. The antiviral small-interfering RNA pathway induces Zika virus resistance in transgenic *Aedes aegypti*. Viruses 12:1231.
430. Buchman A, Gamez S, Li M, Antoshechkin I, Li HH, Wang HW, Chen CH, Klein MJ, Duchemin JB, Crowe JE, Jr., Paradkar PN, Akbari OS. 2020. Broad dengue neutralization in mosquitoes expressing an engineered antibody. PLoS Pathog 16:e1008103.
431. Patterson EI, Villinger J, Muthoni JN, Dobel-Ober L, Hughes GL. 2020. Exploiting insect-specific viruses as a novel strategy to control vector-borne disease. Curr Opin Insect Sci 39:50-56.

Summary

Three pathogenic mosquito-borne viruses that have been on the rise in recent years are Zika virus (ZIKV), Usutu virus (USUV) and Mayaro virus (MAYV). ZIKV was first discovered in Uganda in 1947, emerged in the Pacific in 2007, and unexpectedly caused a large-scale epidemic of human illness in Central and South America in 2015 and 2016. The most alarming characteristic of ZIKV is its ability to cause severe congenital microcephaly. The zoonotic USUV, first identified in South Africa in 1959, has spread throughout Europe in recent years, causing massive bird die-off and rare but severe neuroinvasive disease in humans. The tropical MAYV, often referred to as 'the next Zika', is currently emerging in Central and South America, and infection in humans can result in long-lasting, debilitating arthralgia. The rapid emergence of these three previously hidden arthropod-borne (arbo)viruses urged for an in-depth analysis of the mosquito vectors capable of transmitting these viruses, as well as for the development of effective strategies to confine and prevent epidemics of these arboviral diseases.

Although the number of ZIKV cases has declined after the outbreak in the Americas, the virus is currently still present in tropical regions and therefore remains a threat to public health. Especially in areas with human populations naive to the virus, ZIKV may suddenly emerge, which could result in new, major outbreaks of disease. Since arboviruses replicate in both their vertebrate host and invertebrate vector, the risk of ZIKV outbreaks in a particular region is also determined by the presence of competent mosquito vectors. It is therefore important to obtain knowledge of the mosquito species present in certain areas and their competence for ZIKV transmission. In this thesis, it was investigated how effectively indigenous and invasive mosquito species present in the Netherlands transmit ZIKV in the laboratory. The invasive Asian bush mosquito *Aedes japonicus*, permanently established in Flevoland, the Netherlands, was found capable of experimentally transmitting ZIKV, hence suggesting that this mosquito species could be a vector for ZIKV. The indigenous common house mosquito *Culex pipiens*, however, was unable to transmit ZIKV after an infectious blood meal. Nevertheless, bypassing the mosquito midgut by intrathoracic injection of ZIKV resulted in limited virus accumulation in *Cx. pipiens* saliva. This indicates that the mosquito midgut normally restricts ZIKV dissemination in *Cx. pipiens* after oral exposure. Additionally, a general replication deficiency of ZIKV in *Culex* mosquito cells was identified, which occurred post-entry. These results indicate that *Cx. pipiens* should be considered a highly inefficient vector for ZIKV.

Cx. pipiens mosquitoes can, however, effectively transmit USUV. This virus is maintained in an enzootic transmission cycle between avian hosts and mosquito

vectors. Humans and other mammals can also become infected via mosquito bites but are thought to be dead-end hosts due to low levels of viraemia. Thus, when local mosquitoes are evaluated for their ability to transmit USUV under experimental conditions, the use of avian blood for the infectious blood meal would be preferable. Nonetheless, the origin of blood used to study vector competence generally varies between studies, while it is unknown to what extent the blood source affects the experimental outcomes. In this thesis, it was found that the use of chicken or human blood resulted in comparable vector competence of *Cx. pipiens* for USUV. Interestingly, this study also revealed that the USUV titers in the saliva of the two biotypes of *Cx. pipiens* (*pipiens* and *molestus*) markedly differed. Biotype *molestus* accumulated much lower titers of USUV in the saliva as compared to biotype *pipiens*, regardless of which blood type was offered. This may indicate that biotype *molestus* is a less efficient vector for USUV than biotype *pipiens*, which is especially interesting considering that biotype *pipiens* preferentially feeds on birds, whereas biotype *molestus* is more attracted to mammals including humans. Importantly, we also found that the opportunistic feeder *Ae. japonicus* is capable of experimentally transmitting USUV, thus making this mosquito species a potential bridge vector between birds and humans.

Besides arboviruses, mosquitoes can also carry insect-specific viruses (ISVs) that are unable to replicate and cause disease in vertebrates. Recently, ISVs have received increasing attention due to their ability to influence arbovirus transmission, and it is therefore important to characterize the collection of viruses (i.e., the virome) present in mosquito vectors. ISV replication in mosquito cells activates RNA interference (RNAi)-based immune responses, resulting in the production of viral-derived small RNAs (~18-30 nucleotides in size). Sequencing and *de novo* assembly of these small RNAs provides an overview of the ISVs present in mosquito populations. In this thesis, highly diverse and abundant novel virus species were discovered in *Ae. japonicus* populations in the Netherlands and France using a small RNA-based metagenomic approach. Strong RNAi responses, including the production of 21 nucleotide sized small interfering RNAs, were seen against these viruses, which is indicative of active virus replication in the host. The newly discovered *Ae. japonicus* narnavirus 1 (AejapNV1) showed the strongest RNAi response. Narnaviruses have been described as non-segmented, positive-sense RNA viruses with only a forward open reading frame (ORF) coding for the RNA-dependent RNA polymerase (RdRp). Interestingly, AejapNV1 showed an ambigrammatic coding strategy with a forward ORF encoding the RdRp on the positive strand and a reverse ORF with unknown function on the negative strand. This was remarkable, as positive-sense RNA viruses usually code for proteins only on the positive strand. In addition, *de novo* small RNA assembly revealed a second ambigrammatic AejapNV1 genome segment

with unknown function, which indicates that this virus is bisegmented. Screening of *Ae. japonicus* mosquitoes from the Netherlands for the presence of the newly discovered viruses revealed a very high prevalence of the tested viruses in adult females, adult males and larvae. Furthermore, comparing the small RNA libraries obtained from Dutch and French mosquitoes indicated that *Ae. japonicus* harbours a stable core virome across mosquito populations, hence suggesting that the virome has coevolved with the mosquito host.

The arboviruses ZIKV and MAYV can cause severe illness in humans and have the potential to invade new geographical areas, whilst no licenced antivirals or vaccines are available to treat or prevent disease. Here, virus-like particle (VLP) vaccines against both these viruses were developed using the scalable baculovirus-insect cell expression system. VLPs are structurally identical to wild-type virus, but do not harbour a viral genome. Such non-replicative particles display repetitive patterns of epitopes, known to effectively trigger potent immune responses. Indeed, vaccination of mice with MAYV VLPs induced high levels of neutralising antibodies, and completely protected the animals from viraemia and arthritic disease after challenge with wild-type MAYV, allowing this vaccine to be further developed and tested for human use. Immunisation of mice with two developed ZIKV vaccine candidates, VLPs and subviral particles (SVPs), however, only induced limited levels of ZIKV-neutralising antibodies and did not protect against wild-type ZIKV infection, although the viraemic period became shorter. Epitope analysis by monoclonal antibody ELISA showed that the ZIKV VLPs and SVPs do not display quaternary structure epitopes normally present on envelope (E) protein homodimers found on the ZIKV virion. These epitopes induce potent neutralising antibodies following natural ZIKV infection in humans. The low pH of the insect cell culture medium during production of the VLPs/SVPs potentially led to a conformational transition of the E proteins from a prefusion, dimeric state into a postfusion, trimeric state. To improve the efficacy of the ZIKV SVP vaccine, a variant with covalently linked E proteins to lock the dimeric conformation was developed. In addition, the vaccines were produced at neutral pH using adapted insect cells to prevent the conformational transition towards the trimeric state. The improved vaccine candidates now await further testing in mouse models of ZIKV disease.

In conclusion, the results of this thesis enhance our understanding of the mosquito vectors involved in ZIKV and USUV transmission. Also, the developed VLP vaccines against ZIKV and MAYV will hopefully help to control outbreaks of these arboviral diseases in the future.

Samenvatting

Het Zika virus (ZIKV), het Usutu virus (USUV) en het Mayaro virus (MAYV) zijn drie pathogene virussen die door muggen worden overgedragen en de laatste jaren in opkomst zijn. ZIKV werd voor het eerst ontdekt in Uganda in 1947, dook op in het Pacifisch gebied in 2007, en veroorzaakte in 2015 en 2016 een grootschalige epidemie van humane ziekte in Centraal- en Zuid-Amerika. De meest alarmerende eigenschap van ZIKV is het vermogen om ernstige aangeboren microcefalie te veroorzaken. Het zoönotische USUV, voor het eerst geïdentificeerd in Zuid-Afrika in 1959, heeft zich gedurende de afgelopen jaren verspreid over Europa, waar het virus massale sterfte onder vogels veroorzaakt, alsook zeldzame maar ernstige neurologische ziekteverschijnselen bij mensen. Het tropische MAYV, vaak 'de volgende Zika' genoemd, verspreidt zich op het moment in Centraal- en Zuid-Amerika, en infecties in mensen kunnen leiden tot langdurige, slopende artralgie. ZIKV, USUV en MAYV behoren tot de arbovirussen, een groep van virussen die door arthropoden (geleedpotigen) wordt overgedragen. De snelle opkomst van deze drie eerder verborgen arbovirussen vroeg om een diepgaande analyse van de muggenvectoren die in staat zijn om deze virussen over te dragen, en ook om de ontwikkeling van effectieve strategieën om epidemieën van deze arbovirale ziektes te beperken en te voorkomen.

Alhoewel het aantal ZIKV gevallen is afgenomen na de uitbraak in Centraal- en Zuid-Amerika, is het virus op dit moment nog steeds aanwezig in tropische gebieden. Het virus blijft daarom een bedreiging voor de volksgezondheid. Met name in gebieden met menselijke populaties die naïef zijn voor het virus, zou ZIKV plotseling kunnen opduiken. Dit zou kunnen resulteren in nieuwe, grote uitbraken van deze infectieziekte. Gegeven dat arbovirussen repliceren in hun gewervelde gastheer evenals in hun ongewervelde vector, wordt het risico van ZIKV uitbraken in een specifieke regio mede bepaald door de aanwezigheid van competente muggenvectoren. Het is daarom belangrijk om kennis op te doen van de muggensoorten die aanwezig zijn in een bepaald gebied en van hun bekwaamheid in het overdragen van ZIKV. In dit proefschrift wordt onderzocht hoe effectief inheemse en invasieve muggensoorten die aanwezig zijn in Nederland ZIKV kunnen overdragen in het laboratorium. De invasieve Aziatische bosmug *Aedes japonicus*, die zich permanent heeft gevestigd in Flevoland (Nederland), werd in staat bevonden om ZIKV experimenteel over te dragen. Dit suggereert dat deze muggensoort een vector voor ZIKV zou kunnen zijn. De inheemse noordelijke huissteekmug *Culex pipiens* was echter niet in staat om ZIKV over te dragen na een infectieuze bloedmaaltijd. Desalniettemin leidde het injecteren van ZIKV in de thorax, waarbij de middendarm van de mug omzeild wordt, tot een beperkte mate van virus ophoping in het *Cx. pipiens* speeksel. Dit geeft

aan dat de muggendarm gewoonlijk de verspreiding van ZIKV beperkt in *Cx. pipiens* na orale toediening. Aanvullend hierop werd er een algemene replicatie beperking van ZIKV in *Culex* muggencellen geïdentificeerd, welke na entree plaatsvond. Deze resultaten geven aan dat *Cx. pipiens* beschouwd kan worden als een zeer inefficiënte vector voor ZIKV.

Cx. pipiens muggen kunnen USUV echter goed overbrengen. Dit virus wordt overgedragen tussen vogels en muggen in een enzoötische transmissie cyclus. Mensen en andere zoogdieren kunnen ook geïnfecteerd worden via muggenbeten maar worden gezien als eindgastheren vanwege hun lage niveaus van viremie. Wanneer lokale muggen worden geëvalueerd met betrekking tot hun vermogen voor het overdragen van USUV onder experimentele condities, heeft het gebruik van vogelbloed voor de infectieuze bloedmaaltijd daarom de voorkeur. Toch varieert in het algemeen de oorsprong van het bloed dat gebruikt wordt om vectorcompetentie te bestuderen tussen studies, terwijl het onbekend is in hoeverre de oorsprong van het bloed de experimentele uitkomsten beïnvloedt. In dit proefschrift werd gevonden dat het gebruik van kippenbloed en mensenbloed leidde tot vergelijkbare vectorcompetentie van *Cx. pipiens* voor USUV. Interessant genoeg liet deze studie ook zien dat de USUV titers in het speeksel van de twee biotypen van *Cx. pipiens* (*pipiens* en *molestus*) duidelijk verschilden. Biotype *molestus* hoopte veel lagere titers van USUV op in het speeksel vergeleken met biotype *pipiens*, ongeacht welk bloedtype werd aangeboden. Dit zou erop kunnen wijzen dat biotype *molestus* een minder efficiënte vector voor USUV is dan biotype *pipiens*, wat vooral interessant is gegeven dat biotype *pipiens* bij voorkeur voedt op vogels, terwijl biotype *molestus* meer aangetrokken wordt tot zoogdieren inclusief mensen. We vonden ook dat de opportunistische voeder *Ae. japonicus* in staat is om USUV experimenteel over te dragen. Dit maakt deze muggensoort een potentiële overbruggingsvector tussen vogels en mensen.

Naast arbovirussen kunnen muggen ook insect-specifieke virussen meedragen, welke niet in staat zijn om te repliceren en ziekte te veroorzaken in gewervelden. Deze virussen staan in toenemende mate in de belangstelling vanwege hun vermogen om de overdracht van arbovirussen te beïnvloeden, en het is daarom belangrijk om de verzameling van virussen (i.e., het viroom) aanwezig in muggenvectoren te karakteriseren. Replicatie van insect-specifieke virussen in muggencellen activeert RNA interferentie (RNAi)-gebaseerde immuunresponsen, en dit resulteert in de productie van virus-afgeleide kleine RNAs (met lengtes van ~18-30 nucleotiden). Het sequencen en *de novo* assembleren van deze kleine RNAs geeft een overzicht van de insect-specifieke virussen die aanwezig zijn in muggenpopulaties. In dit proefschrift werden zeer diverse en talrijke nieuwe virussoorten ontdekt in *Ae. japonicus* populaties in Nederland en Frankrijk met

behulp van een kleine RNA-gebaseerde metagenomische benadering. Er werden sterke RNAi responsen gevonden tegen deze virussen, en de productie van kleine interfererende RNAs met een lengte van 21 nucleotiden wees op actieve replicatie van de virussen in hun gastheer. Het nieuw ontdekte virus *Ae. japonicus* narnavirus 1 (AejapNV1) liet de sterkste RNAi respons zien. Narnavirussen staan bekend als ongesegmenteerde, positief strengs RNA virussen met alleen een voorwaarts open leesraam (open reading frame, ORF) coderend voor een RNA-afhankelijke RNA polymerase (RNA-dependent RNA polymerase, RdRp). Interessant genoeg liet AejapNV1 een ambigrammatische coderingsstrategie zien met een voorwaartse ORF coderend voor een RdRp op de positieve streng en een omgekeerd ORF met onbekende functie op de negatieve streng. Dit was opmerkelijk, aangezien positief strengs RNA virussen gewoonlijk alleen voor eiwitten coderen op de positieve streng. Het *de novo* assembleren van de kleine RNAs onthulde bovendien een tweede ambigrammatisch AejapNV1 genoomsegment met onbekende functie, en dit wijst erop dat dit virus uit twee segmenten bestaat. Het screenen van *Ae. japonicus* muggen uit Nederland op de aanwezigheid van de nieuw ontdekte virussen liet zien dat de geteste virussen heel veel voorkomen in volwassen vrouwtjes, volwassen mannetjes en larven. Gebaseerd op vergelijkingen tussen kleine RNA bibliotheken van Nederlandse en Franse muggen werd er verder gevonden dat *Ae. japonicus* muggenpopulaties een stabiel kernviroom bevatten. Dit suggereert dat het viroom co-evolueert met de muggengastheer.

De arbovirussen ZIKV en MAYV kunnen ernstige ziekte veroorzaken bij mensen en hebben de potentie om nieuwe geografische regio's binnen te dringen, terwijl er geen goedgekeurde antivirale behandelingen of vaccins beschikbaar zijn om ziekte te behandelen of te voorkomen. Tegen beide virussen werden hier vaccins gemaakt op basis van virusachtige deeltjes (virus-like particles, VLPs). Deze vaccins werden geproduceerd met behulp van het opschaalbare baculovirus-insectencel expressie systeem. VLPs zijn structureel identiek aan wild-type virus, maar herbergen geen viraal genoom. Zulke niet-replicerende deeltjes bezitten aan de buitenzijde repetitieve patronen van epitopen die krachtige immuunresponsen in gang kunnen zetten. Inderdaad leidde vaccinatie van muizen met MAYV VLPs tot de productie van hoge niveaus van neutraliserende antilichamen, en werden de dieren compleet beschermd tegen viremie en artritis na infectie met wild-type MAYV. Dit MAYV vaccin kan daarom verder ontwikkeld en getest worden voor humaan gebruik. Immunisatie van muizen met twee ontwikkelde ZIKV kandidaat-vaccins, VLPs en subvirale deeltjes (subviral particles, SVPs), induceerde echter alleen beperkte niveaus van ZIKV neutraliserende antilichamen en beschermde niet tegen wild-type ZIKV infectie, alhoewel de viremische fase korter werd. Epitoop analyse met behulp van monoklonale antilichaam ELISA gaf aan dat de ZIKV VLPs en SVPs geen

quaternaire structuur epitopen bezitten die normaal gevonden worden op envelop (E) eiwit homodimeren aanwezig op het ZIKV virion. Deze epitopen wekken krachtige neutraliserende antilichamen op na een natuurlijke ZIKV infectie in mensen. De lage pH van het kweekmedium van de insectencellen tijdens productie van de VLPs/SVPs zou mogelijk kunnen leiden tot een conformationele verandering van de E eiwitten van een prefusie dimeer staat naar een postfusie trimeer staat. Om de werkzaamheid van het ZIKV SVP vaccin te verbeteren werd een variant met covalent gekoppelde E eiwitten ontwikkeld om de dimeer conformatie op slot te zetten. Daarnaast werden de vaccins geproduceerd bij neutrale pH met aangepaste insectencellen om de conformationele verandering richting de trimeer staat te voorkomen. De verbeterde kandidaat-vaccins zullen getest worden in muizenmodellen van ZIKV ziekte.

Concluderend versterken de resultaten van dit proefschrift ons begrip van de muggenvectoren die betrokken zijn bij ZIKV en USUV overdracht. Daarnaast zullen de ontwikkelde VLP vaccins tegen ZIKV en MAYV hopelijk bijdragen aan het indammen en voorkomen van uitbraken van deze arbovirale ziektes in de toekomst.

List of abbreviations

ABTS	2,2'-azino-bis(3-ethylbenzothiazoline-6-sulfonic acid)
AcMNPV	*Autographa californica* multiple capsid nucleopolyhedrovirus
ADE	antibody-dependent enhancement
Ae.	*Aedes*
AejapAV1	*Aedes japonicus* anphevirus 1
AejapBV1	*Aedes japonicus* bunyavirus 1
AejapBV2	*Aedes japonicus* bunyavirus 2
AejapNV1	*Aedes japonicus* narnavirus 1
AejapRV1	*Aedes japonicus* rhabdovirus 1
AejapTV1	*Aedes japonicus* totivirus 1
arbovirus	arthropod-borne virus
BinJV	Binjari virus
bp	base pair
C	capsid
CHIKV	chikungunya virus
CPE	cytopathic effect
CPER	circular polymerase extension reaction
Cx.	*Culex*
CxNV1	*Culex* narnavirus 1
DENV	dengue virus
DMEM	Dulbecco's Modified Eagle Medium
dsRNA	double-stranded RNA
E	envelope
EDE	E dimer epitope
EPDA	end point dilution assay
ER	endoplasmic reticulum
EVE	endogenous viral element
FBS	fetal bovine serum
fORF	forward open reading frame
GFP	green fluorescent protein
H&E	haematoxylin and eosin
HLC	human landing catch
$IFNAR^{-/-}$	interferon-α/β receptor knockout
ISF	insect-specific flavivirus
ISV	insect-specific virus
JEV	Japanese encephalitis virus
kb	kilobase pair

mAb	monoclonal antibody
MAYV	Mayaro virus
MOI	multiplicity of infection
MPLA	3-O-desacyl-4'-monophosphoryl lipid A
nsP	non-structural protein (for alphaviruses)
NS	non-structural protein (for flaviviruses)
nt	nucleotide
ONLV1	*Ochlerotatus*-associated narna-like virus 1
ONLV2	*Ochlerotatus*-associated narna-like virus 2
ONNV	o'nyong nyong virus
ORF	open reading frame
PBS-T	PBS containing 0.05% Tween
PEG	polyethylene glycol
piRNA	PIWI-interacting RNA
pr	precursor peptide
prM	precursor membrane
P/S	penicillin/streptomycin
RdRp	RNA-dependent RNA polymerase
RNAi	RNA interference
rORF	reverse open reading frame
RPKM	Reads Per Kilobase of transcript per Million reads
RPS7	ribosomal protein S7
RT	room temperature
RT-PCR	reverse transcriptase PCR
S1	primary genome segment
S2	secondary genome segment
Scer20SNV	*Saccharomyces cerevisiae* 20S RNA narnavirus
SDS-PAGE	sodium dodecyl sulphate polyacrylamide gel electrophoresis
SE	standard error of the mean
siRNA	small interfering RNA
SL	stem-loop
SRA	sequence read archive
SVP	subviral particle
TBEV	tick-borne encephalitis virus
$TCID_{50}$/ml	50% tissue culture infectious dose per millilitre
USUV	Usutu virus
UTR	untranslated region
VLP	virus-like particle
WEEV	western equine encephalomyelitis virus

WNV	West Nile virus
XaNLV	Xanthi narna-like virus
YFV	yellow fever virus
ZIKV	Zika virus

Dankwoord

Alweer meer dan zes jaar zijn voorbij gegaan sinds ik voor het eerst als MSc student bij Virologie in Wageningen kwam binnenlopen. Ik heb tijdens deze jaren met veel plezier onderzoek gedaan, achtereenvolgens als MSc student, junior onderzoeker, en PhD kandidaat. En nu nog steeds ben ik bij Virologie te vinden, als postdoc. Samenwerken vind ik één van de leukste dingen van onderzoek doen, en ik ben blij dat ik daar tijdens mijn PhD zoveel mogelijkheid toe heb gehad. Nu dit proefschrift er ligt, is het tijd om iedereen te bedanken die hierbij een rol heeft gespeeld, want een proefschrift fabriceren, dat doe je zeker niet alleen.

Als eerste wil ik graag **Gorben** bedanken voor de goede begeleiding tijdens mijn promotietraject. Jouw colleges over tropische virussen, diva's en doodgeslagen muggen maakten mij als student meteen enthousiast over het onderzoek bij Virologie. Ik ben heel blij met jou als begeleider, want je geeft me goed advies wanneer het nodig is, maar ook de volledige vrijheid om mijn eigen projecten vorm te geven. Jouw optimisme werkt aanstekelijk, je bent altijd enthousiast over nieuwe ideeën en onverwachte onderzoeksresultaten. Verder weet je mijn Noord-Hollandse directheid te waarderen, en dat is iets wat ik ook zeer op prijs stel. Ook draag je in belangrijke mate bij aan de leuke sfeer in de Arbo groep, waar ook het af en toe ter beschikking stellen van tuin en zwembad natuurlijk een rol bij speelt. Onze samenwerking eindigt hier gelukkig niet en ik kijk uit naar meer wetenschappelijke discussies in de toekomst!

Monique, bedankt voor je interesse in m'n onderzoek, voor je oog voor detail tijdens het nakijken van de manuscripten, en voor je snelle reacties op elk moment dat er iets geregeld moest worden. Ik vind het leuk dat jij naast het besturen van een hele leerstoelgroep, ook gewoon de tijd neemt om te vragen hoe het met iemand gaat op persoonlijk vlak. Al jouw ervaring gecombineerd met jouw makkelijke benaderbaarheid maken jou een goede promotor.

Toen ik aan het begin van m'n promotietraject stond, wist ik nog niet veel meer over muggen dan dat je ze kan doodslaan. Gelukkig kwam daar snel verandering in met Sander als co-promotor. Bedankt, **Sander**, voor je uitleg over hoe een muggenlarve eruit ziet, voor jouw hulp met het veldwerk opzetten in Lelystad, voor het lezen van m'n muggenmanuscripten, en voor heel veel meer. Naast het delen van jouw kennis over allerlei muggensoorten was je ook nooit te beroerd om mijn algemene kennis over de fauna in Lelystad bij te spijkeren, en heb ik dankzij jou ook bijgeleerd over roeipootkreeftjes, watermijten, spinnen en andere kleine diertjes waarvan ik de namen inmiddels alweer vergeten ben.

Haidong, it was a pleasure to collaborate with you. Our joint efforts resulted in a lot of data, and I am especially thankful that you helped me in Lelystad many times to locate and empty the mosquito traps. No matter what happened, being it extremely rainy weather, or a collapsed tree on top of mosquito traps, or the appearance of dozens of hungry Asian bush mosquitoes specifically interested to feed on your Asian blood, you were always there to help me out. I also really enjoyed our many talks in the office and lab, as well as the dinners at Eastern Express. I wish you good luck with establishing your own research group in China!

Tijdens het organiseren van het Virologie lab uitje in 2017 samen met Corinne en Marleen, wist ik al wie ik als paranimfen zou vragen voor tijdens mijn verdediging. Corinne en Marleen zijn niet alleen allebei een ster in het organiseren en regelen van eigenlijk alles, maar ook nog eens heel gezellig! **Corinne**, vanaf mijn eerste dag in het Virologie lab ben je betrokken geweest bij mijn onderzoek. Jij hebt me leren kloneren en vaccins zuiveren, en je hebt me getraind in het BSL3 lab. Ook zorg je dat mensen zich thuis voelen in de Arbo groep en organiseer je vrijwel alle Arbo activiteiten en borrels, dank voor dat alles. **Marleen**, een student die terugkwam van een stage zei eens tegen mij over een minder goed georganiseerd lab: 'Ze hadden er geen Marleen'. Veel dank voor jouw inzet om het lab zo goed georganiseerd te houden! Ook heb jij veel gepipetteerd in het lab en muggen verzameld in het veld om te helpen mijn projecten tot een goed einde te brengen. Daarnaast was het heel gezellig om vaak samen het eerste stuk vanaf Radix richting huis te fietsen, en nog even bij te praten over van alles en nog wat, ook bedankt daarvoor.

En dan zijn er nog heel veel meer Arbo mensen om te bedanken. **Jelke**, inmiddels heb je de gezelligste hoek van Radix verruild voor een heus kantoor, maar het was leuk om je meerdere jaren als buur te hebben. Jij bent altijd geïnteresseerd om een nieuw wetenschappelijk idee te testen, en samenwerken met jou is erg efficiënt en productief. Bedankt voor al je hulp, en ik weet zeker dat het Fros lab het ver zal brengen! **Giel**, jij hebt mij geleerd hoe je muggen de poten en vleugels uit moet trekken, dat zal ik uiteraard niet snel vergeten. Ook denk ik met plezier terug aan onze narnavirus brainstorm sessies. Bedankt voor de prettige samenwerking tijdens de eerste twee jaar van m'n PhD. **Tessy**, jij hebt energie voor tien en bent één van de drijvende krachten achter de Arbo feestcommissie. Jouw PhD is al een eind op weg, en ik wens je veel succes met de laatste loodjes! Ik weet zeker dat dat wel goed komt. **Miao**, we started our PhDs around the same time and it was nice to share our experiences and visit the PE&RC weekend together. **Lisa**, leuk dat jij van Nema naar Viro bent gekomen en het narnavirus onderzoek een vervolg gaat geven. Ik ben dankbaar voor jouw goede hulp met praktische zaken tijdens de laatste fase van m'n PhD. **Gwen,** zonder jouw hulp had ik de vaccinzuiveringen nooit afgekregen, erg

bedankt! **Jerome**, **Joyce**, **Linda** en **Linda**, bedankt voor de goede gesprekken en de gezelligheid!

Bij Entomologie stond de deur altijd voor mij open, en zonder de inzet van vele entomologen was het mij nooit gelukt om het muggenonderzoek tot een succes te maken. **Tessa**, jouw hulp bij het organiseren van de human landing catches in Lelystad en het kweken van muggen in Wageningen heeft ontzettend veel bijgedragen aan het succes van mijn experimenten. Daarnaast ben je ook vaak beschikbaar voor een gezellig praatje in Radix, en het was leuk en nuttig om af en toe PhD ervaringen uit te wisselen tijdens een lunchafspraak. **Chantal**, jij hebt vooral in het eerste jaar van mijn PhD veel hulp geboden met het opstarten in het BSL3 lab en het aanleveren van muggen voor m'n experimenten, waardoor ik dankzij jou een goede start had. **Charlotte**, met plezier heb ik jou ingewijd in het druppel voeren van *Aedes japonicus* en het is leuk te zien dat dat jou allemaal prima afgaat. En bedankt voor je inzet voor de viroom studie. Verder wil ik graag **Julian** en **Tim** bedanken voor hun gezellige aanwezigheid binnen en buiten het BSL3 lab, **Hans** voor het maken van de mooie foto's van *Aedes japonicus*, **Pieter** en de andere insectenkwekers voor het kweken van héél veel muggen voor m'n experimenten, en alle andere entomologen die geholpen hebben met veldwerk of in het lab.

Bij een BSL3 lab komt veel regelgeving en onderhoud kijken. Graag wil ik alle mensen die hierbij betrokken zijn bedanken voor de inzet om ons lab draaiende te houden, met speciale vermelding voor **Dirk Jan**, **Reinoud**, **Carolien** en **Chris**.

I would also like to thank all former BSc and MSc thesis students who contributed to my work over the years, with special thanks to **Carlijn**, **Jet**, **Kirsten**, **Elise**, **Ties**, **Denise**, **Chris**, **Christina**, **Marjolein**, **Lex**, **Victor** and **Niek**. I enjoyed working together with all of you, and your efforts have contributed substantially to the progress of my research.

Jan, bedankt voor dat je me hebt geïntroduceerd in de elektronenmicroscopie. De kennis die ik daardoor heb opgedaan, heb ik nog vaak daarna tijdens m'n PhD kunnen toepassen. Dankzij jou zal Calimero voor mij nooit meer dezelfde zijn. En ook wil ik **Marcel** en **Jelmer** bedanken voor de assistentie als ik er even niet meer uitkwam met de TEM.

Jort en **Dirk**, bedankt dat ik jullie incubatoren mocht gebruiken als die bij Virologie te druk bezet waren, en voor jullie tips en hulp bij het produceren van de Zika vaccins.

I very much enjoyed the many national and international collaborations during my PhD research, and I would like to highlight a number of them here. **Barry**, **Marion**, **Noreen**, **Chantal**, **Byron**, **Eric**, thank you for the scientific discussions and your

useful input during my PhD project. **Jody,** thanks for the helpful emails, the nice talks at conferences, the fun time when you visited our lab, and providing lots of materials for my experiments. **Roy** and **Sonja**, it was great to show you around the reclaimed land in Flevoland and collect mozzies together. I remember the people in Lelystad were honoured to have visitors all the way from Australia to have a look at their veggie gardens. **João Paulo**, I am really happy that we joined our efforts to elucidate the *Aedes japonicus* virome, you are a great bioinformatician. Many thanks for your enthusiasm and the excellent collaboration. Also thanks to **Roenick**, **Eric** and **João** for your contributions and the fruitful scientific discussions. **Wilson**, **Natalie**, **Kexin** and **Andreas,** thank you for testing our VLP vaccines in your mouse models. Fingers crossed for the improved Zika vaccine, let's hope it will work out well! **Ricardo** and **António**, thank you for your help with the large-scale Zika VLP production. **Stefan**, bedankt voor het karakteriseren van de Zika VLPs, dat heeft ons erg vooruit geholpen.

Virology in Wageningen is a very pleasant place to work. I would like to thank all former and current members for making this possible, including **Melanie**, **Vera**, **Just**, **Emilyn**, **Richard**, **René**, **Dick**, **Dick**, **Els**, **Hanke**, **Dorothy**, **Cristina**, **Dennis**, **Astrid**, **Corien**, **Janna**, **Simone**, **Gabriela**, **Irene**, **Irene**, **Hannah**, **Ahmed**, **Melissa**, **Annamaria**, **Caroline**, **Jirka**, **Mandy**, **Sharella**, **Fengqiao**, **Min**, **André**, **Magda**, **Bob** and **Han**. And also thanks to **Judith**, **Erick** and **Jeroen** for being around in Wageningen now and then.

Dan de vriendinnen van de leukste studie in Wageningen. **Eline**, erg leuk dat jij ook in Wageningen bent gebleven. Bedankt voor de etentjes en Skype calls, en ik wens je veel succes met het afronden van je PhD! **Mirjam**, bedankt voor je nieuwsgierigheid naar de mugjes, je vrolijkheid, en je grappen (ook al snap ik ze niet altijd). **Hinke**, **Nadine**, **Marjolein** en **Laura**, jullie ook bedankt voor alle gezelligheid!

Valeria, thank you for the wonderful trips during the past years. I really enjoyed your visit to Amsterdam, and our many trips in England. I am looking forward to meet again soon.

Dennis, **Tosca** en **Aéyiondy**, bedankt voor jullie bezoekjes aan Wageningen. We zijn heel verschillend maar met jullie is het altijd lachen en ik hoop dat we dat in de toekomst nog heel vaak zullen doen!

En dan zijn we aangekomen bij **mijn ouders**. Het maakte niet uit hoe vaak ik als kind een grote toren van boeken uit de bibliotheek meenam, of jullie bedolf onder 'Waarom ...' vragen, jullie hebben altijd mijn interesses aangewakkerd. Heel erg bedankt voor alles! **Manon** en **Lars**, jullie ook bedankt voor de interesse in m'n onderzoek en het zo nu en dan doorbreken van de Wageningse bubbel.

Lieve **Nico-Jan**, heel erg bedankt voor jouw steun tijdens het gehele PhD proces. Jouw relativeringsvermogen en handige IT skills waren onmisbaar de afgelopen jaren, maar bovenal wil ik je bedanken voor de leuke tijd samen, ik zie onze toekomst met plezier tegemoet!

About the author

Sandra Riekje Abbo was born in Alkmaar, the Netherlands in 1993. After attending primary school in Bergen, Noord-Holland, she went to secondary school in Alkmaar (gymnasium, CSG Jan Arentsz) and graduated *cum laude* in 2011. She then started her study Biology at Wageningen University, where she completed her BSc degree *cum laude* in 2014 with a thesis on the microdiversity of bacteria in marine sponges at the Laboratory of Microbiology. She continued her studies at Wageningen University and obtained her MSc degree in Biotechnology *cum laude* in 2016. During her MSc internship, she worked on cancer cell metabolism at the MRC Cancer Unit of the University of Cambridge, United Kingdom, which resulted in a *Nature* publication in 2016. Her MSc thesis research on virus-like particle vaccines against arboviruses was carried out at the Laboratory of Virology at Wageningen University, where she received the Van der Want award for the best MSc thesis in Virology. Next, she was offered a research position at the Laboratory of Virology in Wageningen and continued her work on arbovirus vaccines in collaboration with a company.

In 2017, Sandra started a collaborative PhD project between the laboratories of Virology and Entomology at Wageningen University under supervision of Prof. Dr M.M. van Oers, Dr G.P. Pijlman and Dr C.J.M. Koenraadt. During her PhD research, she investigated the vector competence of Dutch mosquitoes for pathogenic arboviruses, studied the mechanisms underlying the vector specificity of mosquito-borne viruses, analysed mosquito viromes, and developed arbovirus vaccine candidates. She conducted experiments under biosafety level 3 conditions with cell lines and live mosquitoes, carried out field work in Lelystad, the Netherlands, designed, produced and purified vaccines, supervised 2 BSc and 9 MSc thesis students, and collaborated with a large number of national and international research partners. Her research resulted in various peer-reviewed publications. She presented her work at national and international conferences, and won the award for the best poster at the 2nd international conference on Zika virus in Tallinn, Estonia in 2018. Besides her research work, she also represented the PhD candidates and postdocs during staff meetings of the Laboratory of Virology at Wageningen University.

Sandra is currently working as a postdoctoral researcher on a collaborative project about virus-mosquito interactions at the Laboratory of Virology in Wageningen and the Radboud University Medical Center in Nijmegen, the Netherlands.

List of publications

Peer-reviewed publications

Sciacovelli M, Gonçalves E, Johnson TI, Zecchini VR, da Costa AS, Gaude E, Drubbel AV, Theobald SJ, **Abbo SR**, Tran MG, Rajeeve V, Cardaci S, Foster S, Yun H, Cutillas P, Warren A, Gnanapragasam V, Gottlieb E, Franze K, Huntly B, Maher ER, Maxwell PH, Saez-Rodriguez J, Frezza C. 2016. Fumarate is an epigenetic modifier that elicits epithelial-to-mesenchymal transition. *Nature* 537:544-547.

Göertz GP, **Abbo SR**, Fros JJ, Pijlman GP. 2018. Functional RNA during Zika virus infection. *Virus Res* 254:41-53.

Göertz GP, van Bree JWM, Hiralal A, Fernhout BM, Steffens C, Boeren S, Visser TM, Vogels CBF, **Abbo SR**, Fros JJ, Koenraadt CJM, van Oers MM, Pijlman GP. 2019. Subgenomic flavivirus RNA binds the mosquito DEAD/H-box helicase ME31B and determines Zika virus transmission by *Aedes aegypti*. *Proc Natl Acad Sci U S A* 116:19136-19144.

Abbo SR, Visser TM*, Wang H*, Göertz GP, Fros JJ, Abma-Henkens MHC, Geertsema C, Vogels CBF, Koopmans MPG, Reusken CBEM, Hall-Mendelin S, Hall RA, van Oers MM, Koenraadt CJM, Pijlman GP. 2020. The invasive Asian bush mosquito *Aedes japonicus* found in the Netherlands can experimentally transmit Zika virus and Usutu virus. *PLoS Negl Trop Dis* 14:e0008217.

Abbo SR, Vogels CBF, Visser TM, Geertsema C, van Oers MM, Koenraadt CJM, Pijlman GP. 2020. Forced Zika virus infection of *Culex pipiens* leads to limited virus accumulation in mosquito saliva. *Viruses* 12:659.

Pijlman GP, Grose C, Hick TAH, Breukink HE, van den Braak R, **Abbo SR**, Geertsema C, van Oers MM, Martens DE, Esposito D. 2020. Relocation of the attTn7 transgene insertion site in bacmid DNA enhances baculovirus genome stability and recombinant protein expression in insect cells. *Viruses* 12:1448.

Wang H, **Abbo SR**, Visser TM, Westenberg M, Geertsema C, Fros JJ, Koenraadt CJM, Pijlman GP. 2020. Competition between Usutu virus and West Nile virus during simultaneous and sequential infection of *Culex pipiens* mosquitoes. *Emerg Microbes Infect* 9:2642-2652.

Abbo SR, Visser TM, Koenraadt CJM, Pijlman GP, Wang H. 2021. Effect of blood source on vector competence of *Culex pipiens* biotypes for Usutu virus. *Parasit Vectors* 14:194.

Submitted / in preparation

Abbo SR*, Nguyen W*, Abma-Henkens MHC, van de Kamer D, Savelkoul NHA, Geertsema C, Le TTT, Tang B, Yan K, van Oers MM, Suhrbier A, Pijlman GP. A scalable, non-adjuvanted virus-like particle vaccine from insect cells protects mice against Mayaro virus infection. *Submitted.*

Abbo SR*, de Almeida JPP*, Olmo RP, Balvers C, Griep JS, Linthout C, Koenraadt CJM, Fros JJ, Aguiar ERGR, Marois E, Pijlman GP, Marques JT. The virome of the invasive Asian bush mosquito *Aedes japonicus* comprises highly prevalent novel viruses. *In preparation.*

Abbo SR, Prow NA, Yan K, Geertsema C, Hick TAH, Altenburg JJ, Nowee G, van Toor C, van Lent JW, Tang B, Nakayama E, Metz SW, Hobson-Peters J, Hall RA, Correia R, Roldão A, Martens DE, van Oers MM, Suhrbier A, Pijlman GP. Zika virus-like particle vaccines produced in insect cells. *In preparation.*

*These authors contributed equally.

PE&RC training and education statement

With the training and education activities listed below the PhD candidate has complied with the requirements set by the C.T. de Wit Graduate School for Production Ecology and Resource Conservation (PE&RC) which comprises of a minimum total of 32 ECTS (= 22 weeks of activities)

Review of literature (6 ECTS)
- Functional RNA during Zika virus infection

Writing of project proposal (4.5 ECTS)
- The risk of mosquito-borne Zika virus transmission for the Netherlands

Postgraduate courses (3.1 ECTS)
- Basic course transmission electron microscopy; Wageningen Electron Microscopy Centre, the Netherlands (2016, 2017)
- Rob Goldbach virology lecture and master class; Laboratory of Virology, Wageningen University, the Netherlands (2016, 2018)
- Biosafety for containment and handling of arthropods; European Biosafety Association, Copenhagen, Denmark (2018)
- DNA and RNA editing in virus evolution; University of Minnesota, Minneapolis, USA (2019)

Refresh courses (1.5 ECTS)
- Emergency response services (2017, 2018, 2019, 2020, 2021)

Laboratory training and working visits (1.2 ECTS)
- Arbovirus vaccine production; Mymetics, Leiden, the Netherlands (2016)
- Subgenomic flavivirus RNA; Leiden University, Leiden, the Netherlands (2017)
- Arbovirus vaccine production; ExpreS2ion, Hørsholm, Denmark (2018)
- Narnaviruses in mosquitoes; Leiden University, Leiden, the Netherlands (2019)

Invited review of journal manuscripts (3 ECTS)
- Emerging Microbes & Infections: mosquito vector competence for Zika virus (2018)
- Virology: mosquito vector competence for Usutu virus (2020)
- Journal of Invertebrate Pathology: iridescent virus in mosquitoes (2020)

Competence strengthening / skills courses (3.2 ECTS)
- Project and time management course; WGS (2017)
- Presenting with impact course; WGS (2018)
- Supervising MSc and BSc students course; WGS (2018)
- Writing propositions for your PhD course; WGS (2021)

Scientific integrity/ethics in science activities (0.1 ECTS)
- Ethics, philosophy and history of the life sciences course; Wageningen University (2013)
- Science integrity workshop; Wageningen University (2020)

PE&RC annual meetings, seminars and the PE&RC weekend (1.9 ECTS)
- PE&RC first year weekend (2017)
- PE&RC day (2017)
- Careers after PhD seminar (2017)
- PE&RC midterm weekend (2019)

Discussion groups / local seminars or scientific meetings (5.7 ECTS)
- Dutch arbovirus research network meeting (2016, 2017, 2018, 2019, 2021); oral presentation in 2019
- Dutch annual virology symposium (2017, 2018, 2019, 2021); oral presentation in 2021
- WEES seminar (2017)
- NEV entomologendag (2017, 2019); oral presentation in 2019
- ZikaRisk meeting (2017, 2019, 2020); oral presentations in 2017, 2019, 2020
- Vaccine symposium Utrecht (2018)
- NVT reproduction toxicology Zika virus meeting (2018); oral presentation
- Netherlands centre for one health annual meeting (2019); oral presentation
- Netherlands centre for one health science café (2019)
- International virtual seminars on arbovirus biology (2021)

International symposia, workshops and conferences (10.5 ECTS)
- International meeting on arboviruses and their vectors; poster presentation in 2017, oral presentation in 2019; Glasgow, UK (2017, 2019)
- International conference on Zika virus and *Aedes* related infections; poster presentation; Tallinn, Estonia (2018)
- ZIKAlliance annual meeting; oral presentation; Rotterdam, the Netherlands (2019)
- American society for virology annual meeting; poster presentation; Minneapolis,

USA (2019)
- IS BioTech spring meeting; oral presentation; online (2021)

Societally relevant exposure (0.2 ECTS)
- News item microbiology society website (2019)

Committee work (3 ECTS)
- PhD/postdoc representative during staff meetings of the Laboratory of Virology (2018, 2019, 2020)

Lecturing/supervision of practicals/tutorials (15.9 ECTS)
- Cell biology and health (2017)
- Frontiers in medical and veterinary biology (2017, 2018, 2019, 2020)
- Fundamental and applied virology (2018)
- Molecular virology (2018)
- Immunotechnology (2018, 2019, 2020)

BSc/MSc thesis supervision (2 BSc students and 9 MSc students; 25 ECTS)
- The role of subgenomic flavivirus RNA during persistent infections in mosquito cells
- The function of subgenomic flavivirus RNA during persistent infection in *Aedes* mosquitoes
- Increasing the upstream production yield of a virus-like particle vaccine against chikungunya virus
- Optimization of chikungunya virus-like particle vaccine production in the baculovirus-insect cell expression system
- Optimization of Zika virus-like particle vaccines by varying pH during production, and introducing a stabilized recombinant envelope protein
- Development and optimization of a virus-like particle vaccine against Mayaro virus
- Yield and size characterization of improved chikungunya virus-like particle vaccines
- Investigating the molecular determinant of Zika virus vector specificity by the use of chimeric viruses
- Optimization of protein production by baculoviruses
- The characterization of a newly discovered mosquito-associated narnavirus in the Asian bush mosquito, *Aedes japonicus*
- Characterization of newly discovered viruses in the Asian bush mosquito *Aedes japonicus*

The research described in this thesis was carried out at the Laboratories of Virology and Entomology at Wageningen University, the Netherlands, and was financially supported by the ZonMw project ZikaRisk ('Risk of Zika virus introductions for the Netherlands'; project number 522003001), the European Union's Horizon 2020 Research and Innovation Programme under grant number 734548 (project: ZIKAlliance), and a strategic fund award from the Graduate School Production Ecology & Resource Conservation.

Financial support from Wageningen University for printing this thesis is gratefully acknowledged.

Cover
The Asian bush mosquito *Aedes japonicus*
by Hans M. Smid (bugsinspace.nl), Tessa M. Visser, Sandra R. Abbo

Printed by Gildeprint on FSC-certified paper